The application of an Eulerian chemical and transport model (CMAQ) at fine scale resolution to the UK

Anna Pederzoli
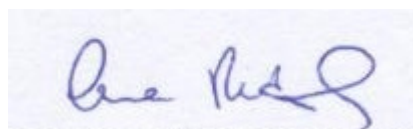
Doctor of Philosophy
The University of Edinburgh
2008

Declaration

This thesis has been composed by myself, and all work reported herein is my own work, except where otherwise stated.

Anna Pederzoli

May 2008

AKNOWLEDGEMENTS

TABLE OF CONTENTS

CHAPTER 1

The problem of acidifying pollutants in the UK: a general

CHAPTER 2

Introducing the Community Multi-scale Air Quality system

CHAPTER 3

Application of the 5th Generation Mesoscale Model (MM5) to the UK

Application of the 5th Generation Mesoscale Model (MM5) to the UK.. 49

CHAPTER 4

The Sparse Matrix Emission Processor (SMOKE) applied to the United Kingdom

The Sparse Matrix Emission Processor (SMOKE) applied to the United Kingdom.. 87

CHAPTER 5

Modelling pollutant concentrations over the United Kingdom using CMAQ

CHAPTER 6

Modelling wet deposition fluxes of pollutants over the UK: comparison between two atmospheric dispersion models on a 5 km scale resolution

ABSTRACT

The application of the Community Multi-Scale Air Quality System (CMAQ) to the United Kingdom.

Present-day numerical air quality models are considered essential tools for predicting future air pollutant concentrations and depositions, contributing to the development of new effective strategies for the control and the reduction of pollutant emissions. They simulate concentrations and depositions of pollutants on a wide range of scales (global, national, urban scale) and they are used for identifying critical areas, integrating measurements and achieving a deeper scientific understanding of the physical and chemical processes involving air pollutants in the atmosphere.

The use of comprehensive air quality models started in the late 1970s and since then their development has increased rapidly, hand in hand with the rapid increase in computational resources. Today more and more complex and computationally expensive numerical models are available to the scientific community. One of these tools is the Community Multi-Scale Air Quality System (CMAQ), developed in the 1990s by the US Environmental Protection Agency (EPA) and currently widely applied across the world for air pollution studies. This work focuses on the application of CMAQ to the United Kingdom, for estimating concentrations and depositions of acidifying pollutants (NO_X, NH_X, SO_X) on a national scale.

The work is divided into seven chapters, the first one describing the main issues related to the emission and dispersion in the atmosphere of acidifying species. It also includes a brief overview of the main international policies signed in the last thirty years in order to reduce the problem of acidification in Europe, as well as a brief description of some models mentioned in this thesis.

The second one describes the main features of CMAQ and addresses some issues such as the use of a nesting process for achieving temporally and spatially resolved boundary concentrations, and the implementation of the model on parallel machines, essential for reducing the simulation computing time. It also describes how this study is part of a wider context, which includes the application of CMAQ in the United Kingdom by other users with different scientific purposes (aerosols processes, air

quality in the urban area of London, contribution of UK power stations to concentrations and depositions etc.).

The third part of the thesis focuses on the application and evaluation over the United Kingdom of the 5th Generation Mesoscale Model MM5, used for providing 3D meteorological input fields to CMAQ. This study was performed assuming that an accurate representation of depositions and concentrations of chemical species cannot be achieved without a good estimate of the meteorological parameters involved in most of the atmospheric processes (transport, photochemistry, aerosol processes, cloud processes etc.).

The fourth part of the thesis describes the preliminary implementation of the Sparse Matrix Operational Kernel Emission System (SMOKE) in the United Kingdom. The processor provides input emissions to CMAQ. The use of SMOKE is usually avoided in CMAQ applications of outside America, and CMAQ input emission files are prepared by the application of other software. The reason is that the model requires radical changes for being applied outside Northern and Central America. Some of these changes have been made in this study such as the adaptation of the European emission inventory EMEP and the UK National Inventory NAEI to the modelling system for point and area sources, the introduction of new European emission temporal profiles in substitution of the American ones and the introduction of new geographical references for the spatial allocation of emissions.

In the fifth chapter the results of CMAQ application over the UK are discussed. The study focuses on NO_X, SO_2, NH_3 and NH_4^+. Maps of concentration are presented and modelled data are compared to measurements from two different air quality networks in the UK. An analysis of the performance of CMAQ over the UK is also performed.

In the final chapter an annual inter-comparison between CMAQ and the Lagrangian transport model FRAME is carried out. Maps of annual wet deposition fluxes of NH_X, NO_Y and SO_X for year 1999 are presented. The results of both models are compared to one another and they are also compared to values from the UK official data set CBED.

Finally, the last chapter suggests the work that has to be done in the future with CMAQ and it summarizes the conclusions.

CHAPTER 1
The problem of acidifying pollutants in the UK: a general introduction

SUMMARY

In the last 40 years the UK government has signed a series of international protocols in order to try to prevent damage to the environment caused by atmospheric acidifying pollutants (NH_x, SO_x, NO_x); even if this action contributed to reduce the emissions considerably, the problem is not yet solved and the effects caused by acid deposition still have a strong negative impact on sensitive ecosystems. Constant monitoring of both concentrations and deposition fluxes is therefore essential, as well as the development of regulatory policies for the control of emissions to the atmosphere. Measurements alone cannot provide a complete description of the temporal and spatial distribution of acidifying pollutants on a national scale. This chapter introduces dispersion models as tools for integrating measurements and for estimating acidifying pollutants for past and future scenarios, giving important information for new emission reduction and control strategies. The chapter contains a wide overview of the main acidifying pollutants, their properties and the damage they cause to the environment (acidification of soils and fresh waters, eutrophication, impact on climate change). The main differences between Eulerian and Lagrangian modelling approaches are briefly described and some models mentioned later in this work (STOCHEM, FRAME and CMAQ) are introduced. The last section of the chapter lays out the aims of this study and summarizes the content of the following chapters.

1.1 INTRODUCTION

The primary aim of this study is the description of the spatial distribution of deposition fluxes and concentrations of acidifying pollutants over the United Kingdom, by the application of a dispersion model at fine scale resolution (5 x 5 km^2).

The class of pollutants which is the object of this study mainly includes ammonia (NH_3), nitrogen oxides (NO_x) and sulphur oxides (SO_x) which are primarily emitted into the atmosphere, and their secondary products in form of ammonium (NH_4^+)

aerosols, such as ammonium sulphate ($(NH_4)_2SO_4$) and ammonium nitrate (NH_4NO_3).

The distribution of NH_3 emission sources across the UK is very widespread and most NH_3 comes from agricultural activities, primarily from the application of nitrogen based fertilisers and the volatilisation of livestock waste. NH_3 emissions over the UK have changed little since the 1970s (NEGTAP, 2001), maintaining a constant value of approximately 300 kt-N yr^{-1} (Figure 1-1). The major oxides in the family of SO_x are sulphur dioxide (SO_2) and sulphur trioxide (SO_3). The former is far more abundant in the atmosphere because the conversion of SO_2 to SO_3 occurs only slowly and also because, once formed, SO_3 reacts rapidly with water droplets in the air to form sulphuric acid (H_2SO_4). The main sources of sulphur dioxide (SO_2) are industrial processes, power production and residential heating. In many European countries including the UK SO_2 emissions have decreased by about 80% since the 1970s (Figure 1-1), mainly because of a general reduction in coal production and burning by industry over the same period (NEGTAP, 2001). Whereas emissions of sulphur dioxide have reduced in the last 40 years, nitrogen oxides ($NO + NO_2$) have seen a period of increase since the 1970s, with the highest peaks reached in the eighties (1984-1990). The main cause of anthropogenic NO_x emissions is the high temperature combustion of fossils fuels, mainly in motor vehicles, but also in ships and aircrafts. The growth registered in emissions can probably be associated to the increased road, sea and air traffic in the same decade. In the last twenty years NO_x emissions have started declining, mainly as a consequence of the introduction of catalytic converters in road vehicles (NEGTAP, 2001).
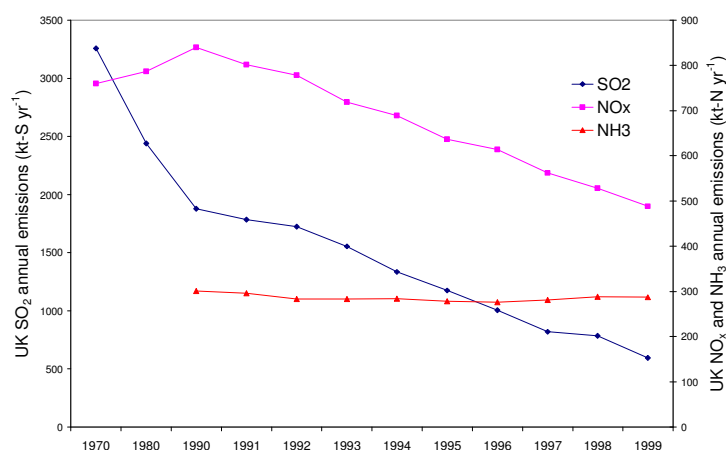
Figure 1-1. UK emissions of NH₃, NOₓ and SO₂ from 1970 to 1999. Source: adapted from NEGTAP (2001).

Even if NO_x and SO_2 emissions have considerably reduced in the last 20 years these two pollutants, together with NH_3, still have a strong negative impact on the environment in the UK. The main environmental damage caused by acidifying pollutants is related to the deposition process. Dry and wet deposition of ammonia and ammonium aerosols can lead to several environmental effects, such as the acidification of soil and fresh waters and the replacement, in ecosystems like moorland and heathland, of original vegetation by more competitive, nitrogen-rich species (grassland). Finally acidifying pollutants may have a global impact contributing to climate change by both direct and indirect radiative forcing.

For all these reasons the constant monitoring of NH_x, NO_x and SO_x primary emissions to the atmosphere as well as the development of new methods to estimate their concentrations and depositions fluxes are essential. However such a task can often be problematic. For example, the measurement of NH_3 concentrations on a national scale is a difficult challenge, because the primary emissions of NH_3 are extremely spatially variable and the samples are very sensitive to wind speed and therefore subject to biases (Tang et al., 2001). The measurement of acidifying pollutants can be affected by both spatial and temporal limitations in the air quality networks; even if the number of monitoring sites is high, they cannot cover the entire

territory and wide areas where stations are missing exist. Periods of malfunctioning during which the monitoring is interrupted also occur.

Therefore, in order to describe the spatial and temporal distribution of these pollutants accurately, it is necessary to integrate the available measured concentrations with "modelled" air concentrations, obtained by the application of atmospheric dispersion models over gridded domains. A further reason for considering dispersion models a complementary approach to measurements is the fact that they can be used to estimate UK deposition and concentration for past and future scenarios, giving crucial information for new emission reduction and control strategies. The same information may then be converted into regulatory policies, both on national and regional scales.

The use of detailed regional-scale air quality models started in the late 1970s with the development of several specific models for carbon monoxide studies, such as APRAC (Ludwig et al., 1970). The US Environmental Protection Agency (EPA) Reactive Plume Model (RPM) was the first model specifically developed for ozone in 1980, followed by the Reactive Oxidant Model (ROM) (Lamb, 1983a; 1983b) and by the Urban Airshed Model (UAM) (Morris et al., 1990). Attention to acid deposition issues was addressed in the 1980s with the development and evaluation of regional acid deposition models such as the Regional Acid Deposition Model (RADM) (Chang et al., 1987; 1990), the Acid Deposition and Oxidant Model (ADOM) (Venkatram et al., 1988), and the Sulfur Transport and Emissions Model (STEM) (Carmichael and Peters, 1984a; 1984b; 1991).

The main purpose of this work is to investigate the use, on a fine scale UK modelling domain (5 x 5 km^2 resolution), of the Community Multi-Scale Air Quality System (CMAQ), a dispersion model developed by the US Environmental Protection Agency (EPA) in the 1990s; the study has the goal of verifying if the model can be suitable for simulating acidification processes and for predicting the distribution of acidifying pollutants accurately over the United Kingdom. CMAQ is an Eulerian chemistry and transport model: its complexity gives the chance of simulating the chemistry and dynamics processes with a high level of detail, using input meteorological and emission data both spatially (5 x 5 km^2) and temporally (1.e. one hour) resolved. CMAQ was chosen because of its reliability (the model has been extensively applied

and evaluated in the US) and its flexibility in the choice of the meteorological driver, the chemical mechanisms and the parameterization schemes of advection and diffusion of pollutants, as well as its well known capabilities for conducting simulations of air quality issues including acid deposition. The existence of a wide user community in the US is a further reason for choosing CMAQ: the support of experienced users makes the initial implementation of the model easier and it helps to sort computational problems out.

The modelling domain is a high resolution grid and the dynamics equations are solved at each time step (12 min) in every grid cell of the domain. This methodology differs from the one adopted in a wide range of Lagrangian models which advect individual particles or air volumes along selected trajectories.

Section 1.1 of this chapter considers the issues concerning acidifying pollutants and the main damage they cause to the environment (acidification, eutrophication, contribution to climate change). Section 1.2 introduces the main differences between the Lagrangian and Eulerian modelling approaches and it includes a brief description of some Eulerian and Lagrangian models mentioned in this work (FRAME, STOCHEM, CMAQ). Finally, Section 1.3 summarizes the content of the upcoming chapters and the main goals of this study.

1.1.1 Environmental impacts of acidifying pollutants

The release of sulphur dioxide and nitrogen oxides into the atmosphere and the consequent reaction with oxidants such as OH radical, ozone (O_3) and hydrogen peroxide (H_2O_2) leads to the formation of sulphuric acid (H_2SO_4) and nitric acid (HNO_3). In dry air, the gas-phase oxidation of SO_2 to H_2SO_4 is given by the following reactions (eq. 1.1-1.3):

$$SO_2 + OH + M \rightarrow HOSO_2 + M \tag{1.1}$$

$$HOSO_2 + O_2 \rightarrow HO_2 + SO_3 \tag{1.2}$$

$$SO_3 + H_2O \rightarrow H_2SO_4 \qquad\qquad (1.3)$$

where M is an air molecule (typically N_2 or O_2). Inside clouds, the absorption of SO_2 in water results in the following equations (Seinfeld and Pandis, 1998):

$$SO_2\,(g) + H_2O \leftrightarrow SO_2 \cdot H_2O \qquad\qquad (1.4)$$

$$SO_2 \cdot H_2O \leftrightarrow H^+ + HSO_3^- \qquad\qquad (1.5)$$

$$HSO_3^- \leftrightarrow H^+ + SO_3^{2-} \qquad\qquad (1.6)$$

In daylight, the oxidation of nitrogen dioxide can also occur:

$$NO_2 + OH \rightarrow HNO_3 \qquad\qquad (1.7)$$

While at night:

$$NO_2 + O_3 \rightarrow NO_3 + O_2 \qquad\qquad (1.8)$$

$$NO_2 + NO_3 \rightarrow N_2O_5 \qquad\qquad (1.9)$$

$$N_2O_5 + H_2O \rightarrow 2HNO_3 \qquad\qquad (1.10)$$

The gas phase oxidation of NO_2 is about ten times faster than the gas phase oxidation of SO_2 (UK Review Group on Acid Rain, 1990). Ammonia can neutralise the oxidation products of both NO_2 and SO_2; the process leads to the formation of

ammonium aerosols such as ammonium nitrate (NH_4NO_3), ammonium hydrogen sulphate (NH_4HSO_4) and ammonium sulphate (($NH4$)$_2SO_4$) (eq. 1.11-1.13):

$$NH_3 + HNO_3 \longleftrightarrow NH_4NO_3 \qquad\qquad (1.11)$$

$$NH_3 + H_2SO_4 \longrightarrow NH_4HSO_4 \qquad\qquad (1.12)$$

$$NH_4HSO_4 + NH_3 \longrightarrow (NH_4)_2SO_4 \qquad\qquad (1.13)$$

Reaction (1.12) tends to be irreversible, whereas ammonium nitrate can decompose back to ammonia and nitric acid (Hov et al., 1994).

The removal of acidifying pollutants from the atmosphere may occur by dry deposition (direct uptake by surfaces and vegetation) or wet depostion (also called "acid rain"). Because ammonia is mainly emitted by ground level sources and its atmospheric lifetime is short, much of the deposition occurs in areas close to the emission sources (Sutton et al., 1995b). Major sinks of ammonia are regions covered by semi–natural vegetation like moorland and forests (Sutton et al., 1993b). According to Sutton et al. (1993a) ammonia has a very short residence time in the atmosphere (about 1 day), but its secondary products have a longer life time (order of several days) and can be subject to long range transport; deposition can also occur in areas up to 1000 km from the point of emission (Barret et al., 1995). This means the possibility of crossing national borders and causing damage to ecosystems in European countries neighbouring the UK, transforming an ecological issue into a political one. The main international agreements taken in order to reduce this problem are mentioned in Section 1.1.2.

The effects of acid deposition are essentially two-fold: the acidification and the eutrophication of ecosystems. The first process is defined as the build-up of acidic elements in soil and fresh waters. These elements include the oxidation products of NO_2 and SO_2 as well as hydrogen ions (H^+) released in the following reactions:

$$SO_2 + 2OH \rightarrow SO_4^{2-} + 2H^+ \tag{1.14}$$

$$NO_2 + OH \rightarrow NO_3^- + H^+ \tag{1.15}$$

A further contribution can be given by the oxidation of NH_4^+ to NO_3^- by micro-organisms:

$$NH_4^+ + 2O_2 \rightarrow NO_3^- + H_2O + 2H^+ \tag{1.16}$$

The change in acidity can alter the type of ecosystem in sensitive habitats and can contribute, by the action of acid rain, to the corrosion of buildings, monuments and materials.

Eutrophication is the increase of the level of fixed nitrogen in the soil. Many semi-natural ecosystems such as moorland and heathland are adapted to low levels of fixed nitrogen. The process may cause the alteration of land use by the replacement of nitrogen poor vegetation by nitrogen rich vegetation (grassland). It may also increase the level of N in plant leaves. This influences biochemical processes and it changes tissue cell structures, making plant cuticle and epidermis more sensitive to insects, bacteria and virus attacks.

Finally, a further impact on the environment by acidifying pollutants can be identified in the close link with climate change. Anthropogenic aerosols including sulphate and nitrate have a strong influence on climate, acting both directly (by scattering and absorbing radiation) and indirectly (modifying the optical properties of clouds). Direct and indirect total aerosol radiative forcings are estimated to be about -0.5 Wm^{-2} and -0.7 Wm^{-2} respectively (IPCC, 2007) (Figure 1-2); the net climatic effect of all anthropogenic aerosols therefore results in the cooling of the Earth's surface by a radiative forcing of -1.2 Wm^{-2} (Figure 1-2). The role of nitrogen oxides in the global mean radiative forcing is complicated. On the one hand, anthropogenic NO_x emissions significantly contribute to increase the levels of tropospheric ozone

(O_3) which gives a positive contribution to the Earth's radiative forcing of +0.35 Wm^{-2} (IPCC, 2007). On the other hand NO_x are also involved in the formation of the radical OH which leads to a reduction in methane (CH_4) (Stevenson et al., 2004), the second main greenhouse gas after carbon dioxide (CO_2). The main greenhouse gasses, other than CO_2, O_3 and CH_4, are halocarbons (HFCs) and nitrous oxide (N_2O). Because CH_4, N_2O and NH_3 have common sources in agriculture, the abatement of one of these gases may have an impact on emissions of the others (Brink et al., 2001a). Recent studies (Brink et al., 2001b) indicate that in Europe, reducing agricultural emissions of NH_3 may cause an increase of N_2O emissions from the same sector of up to 15% compared to the case with no NH_3 control. According to the same study the effect of NH_3 abatement on CH_4 emissions is instead negligible.

Climate change may influence acidification processes. For instance, the increase of global temperature may enhance the process of mineralization of nitrogen. This can lead to a further enhancement of nitrogen leaching in the soil (Mol-Dijkstra and Kros, 2001). Secondly, according to Sanderson et al. (2006), for oxidized N species climate change increases the amount of nitric acid (HNO_3) produced and deposited to soils. For reduced N species it contributes to convert more ammonia (NH_3) to ammonium sulphate (reactions 1.12-1.13) which in turn may result in further acidification of soils. This increased conversion is due to the increased aqueous phase oxidation of SO_2 to H_2SO_4 (reactions 1.1-1.3).
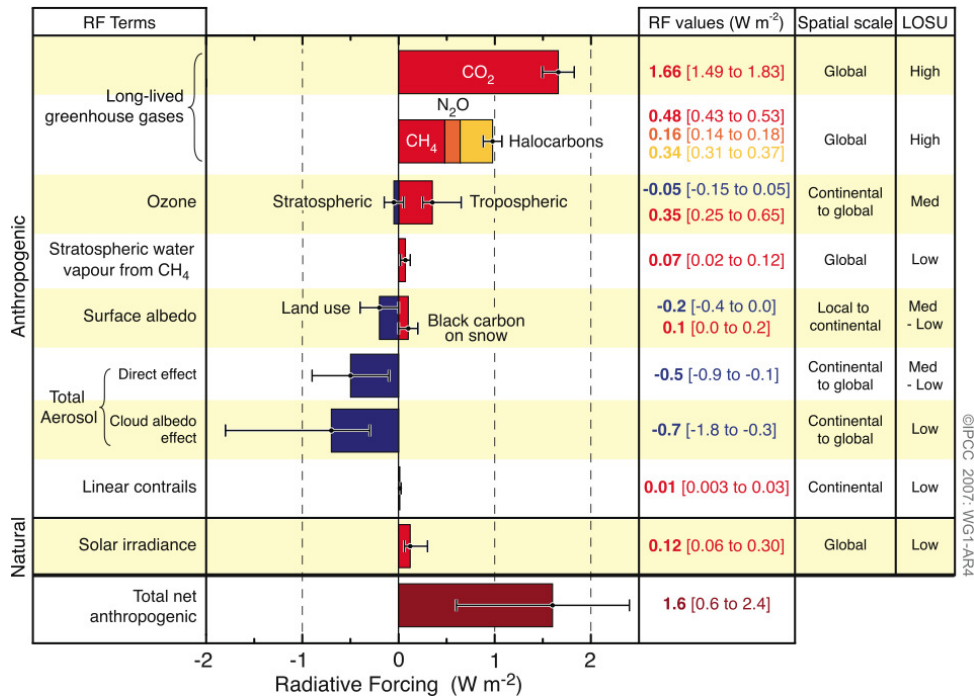
Figure 1-2. Global mean radiative forcing (RF*) of the climate system for the year 2005. The spatial scale indicates the geographical extent of the forcing and LOSU is the assessed "level of scientific understanding" of the forcing. Source: IPCC report (2007), Working Group I, Summary for Policy Makers, Figure 2.*

1.1.2 International policies

The "critical load concept" is a policy tool used to assess the damage caused by acidifying pollutants to the environment. It was introduced first in Canada in the 1980s and subsequently widely used in Europe. According to the definition given by the United Nations Economic Commission for Europe (UNECE), the critical load is a "quantitative estimate of exposure to one or more pollutants below which significant harmful effects on sensitive elements of the environment do not occur according to present knowledge" (UN, 1994). In other words it is a threshold value above which sensitive damage to ecosystems may occur. Whereas critical loads for sulphur are considered simply in terms of acidification effects, critical loads for N are less easily calculated since N may acidify but can also be a nutrient in soils and

waters. In this case critical loads must be calculated for both acidity and nutrient effects and the lower value of the two should be used.

In order to reduce the primary emissions of acidifying pollutants the UK government has signed a number of international agreements over the last 30 years. The problem of long range transport of pollution was discussed for the first time in 1979 during the United Nations Economic Commission for Europe (UNECE) Convention on Long-Range Transboundary Air Pollution (CLRTAP) (Tarrason et al., 1999). The Convention has been extended in the following years by eight protocols, the latest being the Gothenburg Protocol, signed in 1999 in order to abate acidification, eutrophication and ground-level ozone (UN/ECE, 1999). Annex II of the Protocol sets annual emission targets for ammonia, nitrogen oxides and sulphur oxides which should be met by 2010. According to these targets, NH_3, NO_x and SO_2 emissions in UK must be reduced by 12%, 41% and 63% respectively by 2010 compared to the 1990 emissions. Annex IX contains a number of duties for the countries signing up to the Protocol, such as the obligation of distributing an advisory code of good agricultural practice to control ammonia emissions and limiting the use of urea-based fertilisers (UN/ECE, 1999).

The EC Directive on Integrated Pollution Prevention and Control (IPPC) of 1996 also forces extensive pig and poultry rearing to take measures to reduce emissions of a range of pollutants including ammonia (EC, 1996).

More recently (November 2002) the National Emission Ceilings Directive 2001/81/EC (EU NECD) became law in the UK. It targets the same air pollutants as the Gothenburg Protocol and sets the same limit on ammonia emission per year (297 kt yr^{-1}), which has to be met by 2010 (EU NECD, 2001)

The international agreements have contributed to the reduction of emissions in the last 40 years (Figure 1-1). According to the UK Department for Environment, Food and Rural Affairs (DEFRA) ammonia emissions have reached a value of approximately 336 kt in 2004, not far from the limit imposed by the Gothenburg protocol and by the EU NECD. Total emissions of sulphur dioxide have also seen a drastic decrease: they fell by 77% between 1990 and 2004 to 833 kt (DEFRA, 2006). The UK is committed to further reductions to 585 kt by 2010 under the EU NECD. Total NO_x emissions declined by 45% between 1990 and 2004. In 2004 emissions

were estimated around 1621 kt, not far from the ceiling fixed by the EU NECD (1167 kt by 2010). Figure 1-3 shows the NO_X, SO_2 and NH_3 2004 emissions as well as the targets imposed by the EU NECD for year 2010.
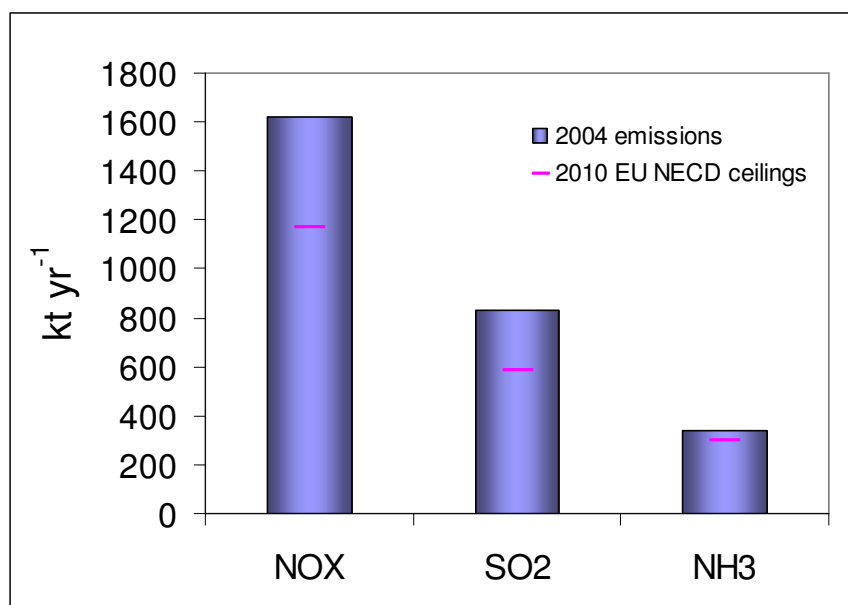
Figure 1-3. 2004 emissions of NH_3, SO_2 and NO_x and targets for 2010 set by the EU NECD. Source: adapted from "Provisional 2005 UK climate change sustainable development indicator and 2004 air pollutant emissions", DEFRA (2006).

1.2 CHEMISTRY AND TRANSPORT MODELS

1.2.1 Classification of models

The criteria for the selection of the most appropriate atmospheric model for a specific study are usually the following: the class of pollutants which is object of the study, the spatial and temporal scale of the atmospheric processes involving these pollutants, and the orography of the area of interest.

Atmospheric models can be classified according to the spatial scale of atmospheric processes. Microscale models are usually selected for studying phenomena at less than 1 km scale resolution, such as, for example, the turbulence in an urban street

canyon. Mesoscale models aim at quantifying the concentration and deposition of acidifying pollutants such has sulphur and nitrogen and photo-oxidants such as ozone at regional and national scale (from few km up to hundreds of km). These models also consider heavy metals, organic pollutants and particulate matter. They are developed for both policy-making and research purposes. Finally global models are applied to study phenomena on a continental or global scale (from hundreds to thousands km), like the long range transport of pollutants and their interaction with climate. They cannot resolve short-range aspects of the dispersion such as the influence of a building or small-scale terrain effects near to a source.

A further distinction is based on the temporal scale: short-term models are usually applied for simulating short-term (multi-day) episodes characterised by unusual high levels of air pollution, whereas long term models perform long term (i.e. 1-year) simulations in order to provide an estimate of indicators such as percentile or annual average to be compared to air quality standards.

If the orography is not complex (flat terrain) Gaussian plume models can also be used. They have been widely applied for regulatory purposes historically. The dispersion parameterization is usually based on empirical coefficients (Pasquill or Gifford stability categories) and it is straightforward. These models need few essential input meteorological data and limited computational resources. If the scenario is more complex, the use of 3-D Lagrangian and Eulerian models (Section 1.2.2) is usually preferred.

1.2.2   Eulerian and Lagrangian approach

Chemistry and transport models are also divided into two classes: Eulerian models and Lagrangian models. Pollutant concentrations in an Eulerian model are represented by a spatial distribution on a fixed three-dimensional grid of points, whereas Lagrangian models simulate the evolution of air parcels or columns driven by the flow. In other words, in the Eulerian approach the dynamics equations are solved in every grid cell of the modelling domain, whereas in the Lagrangian one the meteorology is used to advect individual particles or air volumes in each time step along selected trajectories. Lagrangian models can be extremely fast (i.e. the execution time for a 1-year simulation with the Lagrangian model FRAME is usually

of the order of minutes) and they are mostly used to achieve long-term results (i.e. estimates of annual concentrations/depositions). Eulerian models like CMAQ solve the chemistry and dynamics equations at each time step at each grid point. They need meteorological input and emission values both spatially (values for each grid cell) and temporally (i.e. hourly values) resolved. On the one hand this approach permits very detailed results because it includes all relevant chemical and physical processes, on the other hand this detail makes the computational performance worse. The computing time can be very long (range is typically from days to weeks for one year's simulation) and consequently these models are usually used only to simulate shorter periods of time (i.e. multi-day episodes). An estimate of the computing time in CMAQ is given in Table 2-5.

Because of the constant development of new and more complex models, also due to the rapid increase in computational resources, it is difficult to assess the exact number of Eulerian and Lagrangian models currently available to the scientific community for air pollution studies. Some examples of models which have been used over the last decade are listed in Table 1-1.

Model name	Institution	Model category	domain	Simulation period	Chemistry
CALGRID	Earth Tech, California	3D-Eulerian	Local to regional	Episodes (1 day-1 week)	Photochemical model; it includes SAPRC90 and CB4 chemical schemes
CMAQ	Enviromantel Protection Agency (EPA), US	3D-Eulerian	Local to regional	Episodes (1 day-1 week)	It includes SAPRC99, RADM2 and CB4 chemical schemes
DHEM-REGINA	NERI (National Enviromental Research Institute, Denmark)	3D-Eulerian	Northern emisphere	Episodes (1 day-1 week)	EMEP extended chemical scheme with 60 species and 150 reactions
EMEP	Norvegian Meteorological Institute (DNMI)	3D-Eulerian	EUROPE	Monthly-annual	Two sulphur components, linear chemistry
MERCURE	Electricité de France (EDF)	3D-Eulerian	Local to regional	Episodes (1day-1week)	Not included
CHIMERE	Institute P. Simon Laplace, Paris University	3D-Eulerian	Local to regional	Episodes (1 day-1 week)	Not included
MINNI	ARIANET, ENEA (Italy)	3D-Eulerian	National	Episodes (1 day-1 week)	It includes EMEP chemical scheme and SAPRC90
RAMS	National Oceanic & Atmospheric Administration (US. NOAA)	3D-Eulerian	Local to regional	Episodes (1 day-1 week)	Not included
CAMx	ENVIRON (US)	3D-Eulerian	Sub-urban to continental US	Episodes (1 day-1 week)	It includes SAPRC99 and CB4 chemical schemes
REMSAD	ICF International Systems Applications (US)	3D-Eulerian	Continental US	Annual	Mercury chemistry, SOA treatment, micro-CB gas phase chemical scheme
2-D OSLO	University of Oslo	2D-Eulerian	Global	Monthly-annual	44 chemical species, 126 chemical reactions
FRAME	CEH Edinburgh, University of Edinburgh	3D-Lagrangian	Local to regional	Annual	Treatment of sulphur and oxidised nitrogen
STOCHEM	UK Met Office	3D-Lagrangian	Global	Monthly-annual	50 species, 16 photolytic reactions, 90 chemical reactions
GRAL	Graz University of Technology	3-D Lagrangian	Urban	Annual	Not included
NAME	UK Met Office	3-D Lagrangian	Global	Monthly-annual	Sulphate and nitrate chemistry
HARM	UK Met Office, University of Edinburgh, University of Hull	2D-Lagrangian	Europe	Annual	9 components, coupled sulphur and nitrogen

Table 1-1. Examples of Eulerian and Lagrangian models. Adapted from EEA report: Ambient air quality, pollutant dispersion and transport models-Appendix A1 (http://reports.eea.eu.int), 1999. Further information is from the EPA web site: http://www.epa.gov/epahome/models.htm.

1.2.3 Examples of Lagrangian and Eulerian models

The next paragraphs briefly introduce some chemistry and transport models used or mentioned in this study: the Eulerian model CMAQ, the global 3D model STOCHEM and the Lagrangian model FRAME. STOCHEM is used in this study for providing boundary and initial concentrations to CMAQ, whereas FRAME has been

used for comparing annual wet deposition fluxes of several pollutants to CMAQ results.

1.2.4   The CMAQ model

The Community Multi-Scale Air Quality System (CMAQ) is an Eulerian dispersion model developed by the US EPA in the 1990s. It is coupled with several modelling systems such as the 5th Generation Mesoscale model MM5 and the Sparse Matrix Operator Kernel Emission system (SMOKE) which pre-process meteorological and emission fields respectively. Initial Conditions and Boundary Conditions pre-processors (ICON, BCON) provide concentration fields for all chemical species for the beginning of a simulation and for the grids surrounding the modelling domain respectively. The main processes considered by CMAQ are chemistry, cloud and aerosol processes, advection, wet and dry deposition. Because a nesting process is required for running the model, a high resolution (5 x 5 km^2) UK domain is nested into a lower resolution grid (45 x 45 km^2) covering the British Isles and part of Europe (Figure 5-1). CMAQ is run with 15 vertical levels in σ- coordinates (Phillips, 1957; Gal-Chen and Somerville, 1975) ranging from the surface to 13700 metres. Output concentrations from the global model STOCHEM are used as boundary fields for the outer grid. The CMAQ model provides output concentrations (Figure 1-4), wet and dry deposition fluxes of more than 60 gaseous species including NH_3, SO_2, NO_X and about 30 aerosols. A detailed description of CMAQ is given in Chapter 2.
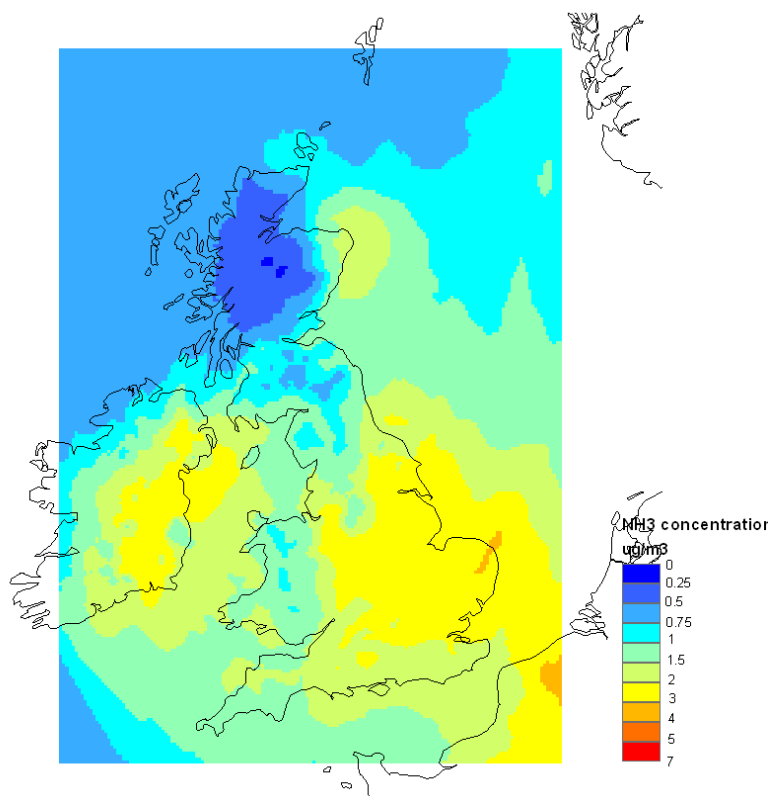
Figure 1-4. Example of CMAQ output. Map of NH₃ concentration for June 1999. Units are $\mu g\ m^{-3}$.

1.2.5 The STOCHEM model

STOCHEM is a 3D chemistry transport global model which adopts the Lagrangian approach; the atmosphere is divided into 50000 to 100000 air parcels advected every three hours (Stevenson et al., 1998). Meteorological data from the UKMO Unified Model are used for driving the model (Johns et al., 1997). Between advection time steps, parcels are mapped onto an Eulerian grid of 5 x 5 degrees horizontal resolution. The model vertical resolution is 9 levels from 950 hPa to 150 hPa with 50000 air parcels or alternatively 19 levels from the surface to 50 hPa with 100000 air parcels. The chemical scheme is based on the one adopted in the EMEP model (Simpson, 1991; 1992) and it includes 70 species and 174 chemical reactions of which 16 are photochemical reactions with diurnal dependence (Collins et al., 1997). Further than the tropospheric chemistry, other processes treated in STOCHEM are convective transport and dry and wet deposition. Emissions from several sources are

also implemented, including anthropogenic sources, biomass burning, lightning and input from the stratosphere.

STOCHEM is currently used for studying the long range transport of pollutants on a global scale, for quantifying global scale budgets of ozone, and for studying interaction of some pollutants (mainly O_3) with climate (Derwent et al., 2006; Stevenson et al., 2005; 2006). An example of STOCHEM application is shown in Figure 1-5. STOCHEM has also been used for studying the impacts of climate change on global patterns of sulphur deposition (Sanderson et al., 2006).
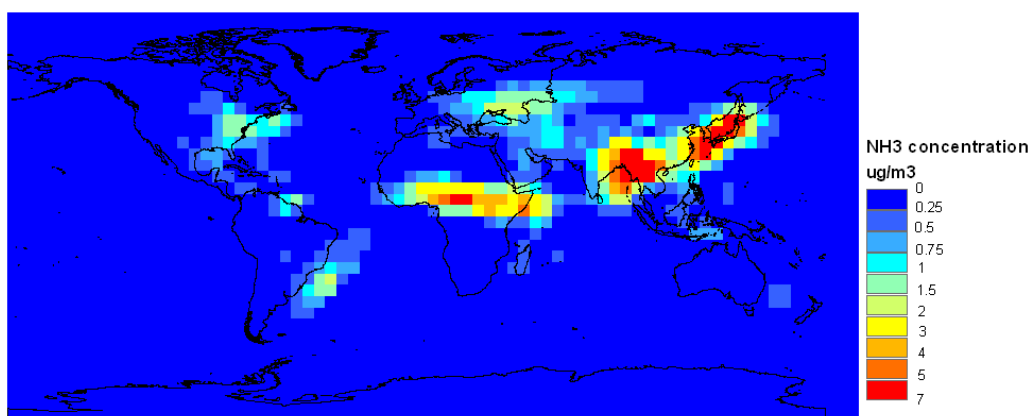

Figure 1-5. Example of STOCHEM output: distribution of global surface NH$_3$ concentration (annual mean) for year 1990. Units are $\mu g \ m^{-3}$.

1.2.6 The FRAME model

Up to now, Lagrangian models have mainly been used for acidification studies in the UK. In particular, the Lagrangian model framework FRAME (Fine Resolution Atmospheric Multi-pollutant Exchange) is one of the models used to assess the long-term deposition and concentration of sulphur and nitrogen species over the UK.

The model domain is a 172 x 244 cells grid covering the United Kingdom and Eire with a 5 x 5 km^2 resolution. The vertical column extends from the surface to a height of 2.5 km divided into 33 layers, with a thickness varying from 1 m (bottom layer) to 100 m (top layer). Every air column (5 x 5 x 2.5 km^3) is advected along parallel straight line trajectories using a specific wind rose (Dore, 2006). General features, application and evaluation of FRAME can be found in Singles et al. (1996), Fournier et al. (2002) and Vieno (2006). An example of FRAME output is given in Figure 1-6.
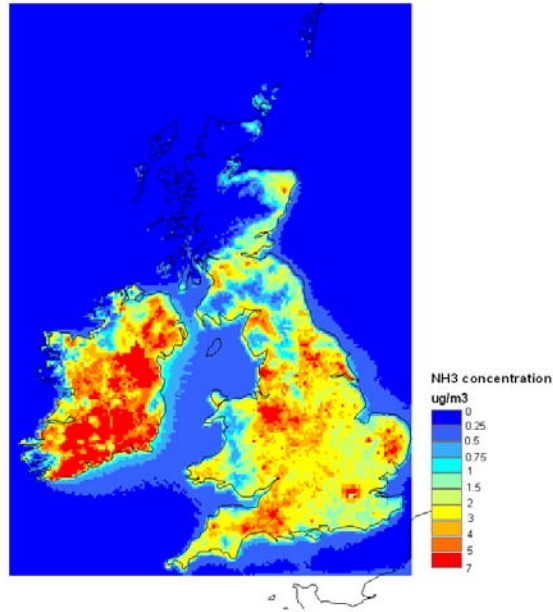
Figure 1-6. Example of FRAME output: NH₃ surface concentration for year 1999. Units are $\mu g\ m^{-3}$. Source: Centre for Ecology and Hydrology (CEH) of Edinburgh.

1.3 CONTENTS OF THE THESIS

The aim of this study is to predict NH_X, NO_Y and SO_X concentrations, wet and dry deposition fluxes over the United Kingdom accurately. To achieve this goal, the use of the Community Multiscale Air Quality System (CMAQ) has been investigated.

The thesis is divided as follows:

Chapter 2. General description of CMAQ with main focus on photochemistry, aerosol processes, cloud processes and wet deposition.

Chapter 3. Application and evaluation of the meteorological model MM5 over the UK. Predicted values of rainfall, surface temperature and wind speed are compared to observations from several meteorological stations across the UK. A statistical analysis is also performed.

Chapter 4. Implementation of the emission model SMOKE in the UK. Because this model has been specifically developed for working in Northern and Central America, its application outside these countries is not straightforward. The chapter describes a preliminary adaptation of SMOKE to the European context and to the United Kingdom in particular.

Chapter 5. Application of CMAQ to the UK. The chapter contains the results of two CMAQ simulations for June and February 1999. Modelled concentrations are compared to observations from several UK air quality monitoring sites. An analysis of the performance of CMAQ over the UK is also performed.

Chapter 6. Comparison between CMAQ and FRAME. An annual inter-comparison between the two models has been performed. Annual wet deposition fluxes of SO_X, NO_Y and NH_X as modelled by both models are compared to each other and compared to observations from the UK official dataset CBED.

Chapter 7. Conclusions, summary and suggestions for future work.

CHAPTER 2
Introducing the Community Multi-scale Air Quality system (CMAQ)

SUMMARY

This chapter is an introduction into the use of the Community Multi-scale Air Quality System (CMAQ). It contains a wide overview of the processes treated by CMAQ, with particular focus on the gas phase chemistry, aerosol processes and wet deposition. The first section briefly introduces the general structure of the model, describing every module inside CMAQ and its specific task. The pre-processors for Boundary and Initial Concentrations (ICON and ICON) are also presented, as well as the tool for calculating photolysis rates (JPROC). Meteorology and emissions processors are not taken into consideration in this chapter, because described apart in Chapters 3 and 4 respectively.

The chapter addresses some important issues concerning the model's application, such as the use of a nesting process (Section 2.2.6) for achieving realistic boundary concentrations as well as the implementation of the model on parallel machines (Section 2.2.7), essential for reducing the simulation computing time. The chapter makes the user familiar with the CMAQ model thus it is a good starting point for introducing the main issues included the next chapters, focused on the model implementation and application over the UK. It also describes how this study is part of a wider context, which includes the application of CMAQ in the United Kingdom by other users with different scientific purposes (aerosols processes, air quality in the urban area of London, contribution of UK power stations to concentrations and deposition fluxes).

2.1   INTRODUCTION

The Community Multi-Scale Air Quality System (CMAQ) is a multi-pollutant, multi-scale air quality model that contains sophisticated parameterization schemes for simulating the main atmospheric processes that affect the concentration and deposition of atmospheric pollutants on both regional and urban scales (Ching et al., 1998). It was developed by the US. Environmental Protection Agency (EPA) in 1990 and released to the scientific community for the first time in June 1998. Until then, most air quality models in the US typically treated individual pollutant issues separately. However, the limitation of this approach was evident: pollutant concentrations and deposition fluxes are sensitive to specific mixtures of different

chemical compounds in atmosphere: as a consequence, when pollutant issues are treated in isolation, the resulting control and reduction strategies may solve one set of problems but may lead to unexpected aggravation of other related pollutant issues. For example, processes affecting oxidants, acid deposition and particulate matter are too closely related to be treated separately. A new strategy became necessary.

CMAQ was designed and developed starting from this assumption: the influence of interactions at different dynamic scales and among multi-pollutants cannot be ignored (Byun et al, 1998). The new approach adopted in CMAQ was called "a one atmosphere perspective" and according to it the range of temporal and spatial scales of multi-pollutant interactions is considered simultaneously. In other words, many relevant processes influencing the evolution of pollutants in the atmosphere are included and modelled in a system that operates on a large range of temporal scales (covering minutes to days to weeks) and spatial (ranging from local to continental) scales. CMAQ is today considered a state-of-the-science, "one-atmosphere" air-quality model and it is daily used in regulatory and research applications.

In the last decade the model was updated many times and several specific versions were developed. Some examples are CMAQ MADRID (Model of Aerosol Dynamics, Reaction Ionization and Dissolution) which provides an alternative, sectional treatment for simulating the formation and deposition of particulate matter (PM) in the atmosphere (Pun et al., 2005), and CMAQ-Hg (Bullock and Brehme, 2002) a modified version of CMAQ for simulating the emission, transport, transformation and deposition of atmospheric mercury (Hg).

The increasing development of computational capabilities is gradually making it easier to use CMAQ for longer term simulations on finer scales (i.e. up to 1 x 1 km^2 resolution). However, despite this rapid development, its application in Europe still remains limited. The main reason is that some modules of the CMAQ system (in particular the emissions processor) are developed taking into account the inventory formats and geographical references of the United States. This is an obstacle for its application in other countries and it needs a considerable amount of work in order to adapt many subroutines of the model to the European context.

Compared to the one in the US, the CMAQ user community in the UK is still small and the development and application of the model are still on a preliminary stage.

Further information about the UK projects recently developed involving the use of CMAQ can be found in Section 2.3.

The following sections provide a brief description of CMAQ architecture; further details can be found in Novak et al. (1998), Ching et al. (1998) and Byun et al. (1998b).

2.2   DESCRIPTION OF THE MODEL

2.2.1   Structure

The architecture of the CMAQ system is shown in Figure 2-1. A main model feature is undoubtedly its modularity. This means it is not made by a single subroutine or by group of subroutines but rather by a well defined sequence of modules, each one with a specific task: chemistry, emissions, meteorology, boundary and initial concentrations. All the input data of CMAQ are output fields of other modelling systems and interface processors.

The meteorological modelling system can be replaced with alternative processors chosen by the user. The model also gives the chance of selecting different chemical schemes and different parameterizations for horizontal and vertical advection and diffusion.

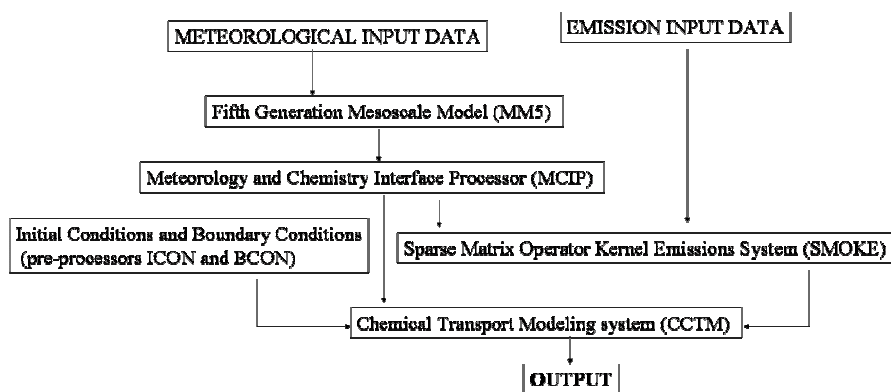*Figure 2-1. Schematic diagram of CMAQ structure. The model is a well defined sequence of linked modules. The arrows show the flow of data between the modules. The output data are concentrations and wet and dry deposition fluxes of gaseous and aerosol chemical species.*

As shown in Figure 2-1, the CMAQ Chemical Transport Modeling system (CCTM) is the core of the model, as it solves the chemistry and dynamics equations every

time step. CCTM contains the parameterizations of atmospheric processes affecting transport, transformation (chemistry), and deposition of all pollutants species. CCTM main features are described in Section 2.2.2.

The MM5/MCIP meteorological modelling system provides 3D meteorological input fields for CCTM. Chapter 3 describes in detail the scientific aspects (data assimilation process, input processing, parameterizations) of the Fifth Generation Mesoscale Model (MM5), and it includes the evaluation of the model over the United Kingdom. MM5 is coupled with the Meteorology and Chemistry Interface Processor (MCIP) which converts meteorological data from MM5 for use in CCTM and calculates surface and boundary layer parameters not provided by the mesoscale model.

Initial conditions and boundary conditions pre-processors (ICON and BCON) provide concentration fields for all chemical species for the beginning of a simulation and for the grids surrounding the modelling domain respectively.

Finally the Sparse Matrix Operator Kernel Emissions System (SMOKE) provides hourly gridded speciated emissions for CCTM. As SMOKE was developed taking into account all inventories and geographical references of the Northern and Central America, a new method for implementing SMOKE in the United Kingdom was introduced. Chapter 4 describes in detail this new methodology.

2.2.2 The CMAQ Chemical Transport Model (CCTM)

As explained in Section 2.2.1, the CMAQ Chemical Transport Model (CCTM) can be considered as the main part of CMAQ, as it simulates the relevant atmospheric chemistry, transport and deposition processes involving pollutants in the atmosphere. All processes treated in CCTM are described in the next paragraphs.

2.2.2.1   <u>Governing equations</u>

Pollutant concentration in an Eulerian model is represented by the spatial distribution on a fixed three-dimensional grid of points. The mass conservation equation for species i in Cartesian coordinates can be written as:

$$\frac{\partial \varphi_i}{\partial t} = -\varphi_i \, div(\vec{v}) - \vec{v} \nabla \varphi_i + D\nabla^2 (\varphi_i) + \frac{\partial}{\partial x}\left(K_{xx} \frac{\partial \varphi_i}{\partial x} \right) + \frac{\partial}{\partial y}\left(K_{yy} \frac{\partial \varphi}{\partial y} \right) + \frac{\partial}{\partial z}\left(K_{zz} \frac{\partial \varphi}{\partial z} \right) + Q_{\varphi_i} + R_{\varphi_i} + W_{\varphi_i} \qquad (2.1)$$

  (a) (b) (c) (d) (e) (f) (g)

a)   Time rate of change of pollutant concentration

b)   Advection

c)   Molecular diffusion

d)   Terms for eddy diffusion

e)   emissions

f)   Production or loss from chemical reactions

g)   Deposition

φ_i = mean concentration in density units (e.g., kg m^{-3})

D = constant diffusion coefficient in air (equal to $0.8 \; 10^{-5}$ m^{2}s^{-1} at Pressure = 1 Atm and Temperature= 25 $^\circ$C)

$\vec{v}$ = wind speed vector (ms^{-1})

Q_{φ_i} = Emission term (moles s^{-1} or g s^{-1} for Particulate Matter)

R_{φ_i} = Chemical reaction term

W_{φ_i} = Deposition term (kg ha^{-1})

K_{xx}, K_{yy}, K_{zz} = eddy diffusivities (m^{2}s^{-1}).

Equation (2.1) as written inside CCTM (generalized coordinates), is reported in Appendix A. Further details about the generalized coordinate system used in CCTM can be found in Byun et al. (1998).

2.2.2.2 <u>Gas phase chemistry</u>

The CCTM system currently includes three optional base chemical schemes with different tasks, as illustrated in Table 2-1. The three schemes are mutually exclusive.

Name	$N^{\underline{o}}$ gas phase reactions	$N^{\underline{o}}$ chemical reactions	Main species	Main task
RADM2	57	157	NH_x, HNO_3, HNO_4, NO_x	Acidification processes
CB4	36	93	NO_x, O_3	Photochemical processes
SAPRC99	400 (VOCs)	290	VOC, NO_x	Ozone impacts (reactivities) of VOCs emitted in atmosphere

Table 2-1 Main features of the Statewide Air Pollution Research Center Chemical Mechanism (SAPRC99), the Regional Acid Deposition Model (RADM2) and the Carbon Bond IV (CB4) chemical schemes.

For modelling sulphur and nitrogen deposition and for describing the acidification process in detail a specific acid deposition chemical scheme is needed. The best choice for this work is the scheme implemented in the US EPA's Regional Acid Deposition Model (RADM), considered as one of the most comprehensive and widely applied schemes currently available for atmospheric chemistry modelling (Grell et al., 2000). It includes state-of-the-science representations of the physical and chemical processes leading to the formation and deposition of acidic species over multi-state geographic areas (Chang et al. 1987). The version of RADM currently used in this work is RADM2 (Stockwell et al., 1990) evolved from the

original RADM1 mechanism (Stockwell, 1986). The RADM2 chemical mechanism implemented into CCTM contains 57 model species and 157 reactions.

Variants of this chemical scheme are also available within the CMAQ system to provide the necessary links to the aerosol and aqueous chemistry processes (RADM2_AE). RADM2 has also been modified to create a new variant that includes enhanced isoprene chemistry representations (RADM2_CIS).

The chemical species treated in RADM2 are both organic and inorganic. The Volatile Organic Compounds chemical category (VOCs) contains some hundreds of compounds that are important for modelling photochemical reactions in the atmosphere. Most of dispersion models including RADM2 cannot take into account the full set of chemical reactions involving every single VOC, but act on a small number of categories having similar chemical behaviour. This grouping process is known as "lumping" of VOC. In RADM2, 10 species represent groups of organic compounds aggregated together ("lumped") on the basis of their reactivity with the hydroxyl radical (OH) and their emission magnitudes. The aggregation factors for the most emitted VOCs can be found in Middleton et al. (1990). The 10 groups are shown in Table 2-2.

1	OLN	*Higher organic peroxides*
2	KET	*Ketones*
3	ALD	*Aldehydes*
4	OLT	*Terminal alkynes*
5	OLI	*Alkenes and terpenes*
6	CSL	*Cresols and phenols*
7	TOL	*Aromatics*
8	XYL	*Naphthalenes*
9	ORA2	*Higher organic acids*
10	ORA1	*Formic acid*

Table 2-2. "Lumped" groups of VOCs in RADM2

Five organic compounds are explicit: Ethane (ETH), Methane (CH4), Ethene (OL2), Isoprene (ISO), Formaldehyde (HCHO).

The inorganic chemistry module in RADM2 contains most of the oxidised nitrogen species that are considered in this study, such as nitrogen dioxide (NO_2), nitrogen monoxide (NO), and nitric acid (HNO_3). It includes 21 inorganic compounds, and 28 inorganic reactions (Table 2-3).

1	$O(^3P) + O_2 + M \rightarrow O_3$
2	$O(^3P) + NO_2 \rightarrow NO$
3	$O(^1D) + N_2 \rightarrow O(^3P)$
4	$O(^1D) + O_2 \rightarrow O(^3P)$
5	$O(^1D) + H_2O \rightarrow 2.0* HO$
6	$O_3 + NO \rightarrow NO_2$
7	$O_3 + HO \rightarrow HO_2$
8	$O_3 + HO_2 \rightarrow HO$
9	$HO_2 + NO \rightarrow NO_2 + HO$
10	$HO_2 + NO_2 \rightarrow HNO_4$
11	$HNO_4 \rightarrow HO_2 + NO_2$
12	$HO_2 + HO_2 \rightarrow H_2O_2$
13	$HO_2 + HO_2 + H_2O \rightarrow H_2O_2$
14	$H_2O_2 + HO \rightarrow HO_2$
15	$NO + HO \rightarrow HONO$
16	$NO + NO + O_2 \rightarrow 2.0*NO_2$
17	$O3 + NO_2 \rightarrow NO_3$
18	$NO_3 + NO \rightarrow 2.0*NO_2$
19	$NO_3 + NO_2 \rightarrow NO + NO_2$
20	$NO_3 + HO_2 \rightarrow HNO_3$
21	$NO_3 + NO_2 \rightarrow N_2O_5$
22	$N_2O_5 \rightarrow NO_2 + NO_3$
23	$N_2O_5 + H_2O \rightarrow 2.0*HNO_3$
24	$HO + NO_2 \rightarrow HNO_3$
25	$HO + HNO_3 \rightarrow NO_3$
26	$HO + HNO_4 \rightarrow NO_2$
27	$HO + HO_2 \rightarrow H_2O + O_2$
28	$HO + SO_2 \rightarrow SULF + HO_2$

Table 2-3. Inorganic reactions in RADM2. Unreactive products (e.g. O_2, H_2O) are not listed

For simulating a gas phase chemical reaction the following equation must be solved. If C_i is the concentration of pollutant i, the rate of change of C_i for a single grid cell is given by:

$$\frac{dC_i}{dt} = P_i - L_i C_i \qquad (2.2)$$

where P_i is the production rate of the species i, over all reactions:

$$P_i = \sum_{l=1}^{m_i} v_{i,l} r_l \qquad (2.3)$$

and L_i is the loss rate:

$$L_i C_i = \sum_{l=1}^{n_i} v_{i,l} r_l \qquad (2.4)$$

$v_{i,l}$ is the stochiometric coefficient for species i in reaction l, and r_l is the rate of reaction l. The sum $l = 1...m_i$ is over all reactions in which species i appears as a product, and the sum $l = 1...n_i$ is over all reactions in which species i appears as a reactant. Equation (2.2) can be rewritten as a system of non linear ordinary differential equations:

$$\frac{dC_i}{dt} = P_i(\vec{c}, t) - L_i(\vec{c}, t) C_i \qquad i = 1, N \qquad (2.5)$$

with the initial condition

$$\vec{c}(t_0) = \vec{c}_0 \qquad (2.6)$$

where $\vec{c}$ is the vector of species concentrations and N is the total number of species. The system is non linear because the terms of loss and production include second and third-order reactions. In order to find a solution to equation (2.2) specific numerical

procedures are used. These numerical methods, also known as "numerical solvers", are developed for providing accurate solutions in a computationally efficient way. It is important to emphasize that the numerical solver is the portion of CMAQ that is most computationally expensive: it consumes 50% to 90% of the total CPU time used in a model simulation (Gipson and Young, 1999).

Four numerical solvers have been implemented in CCTM: SMVGEAR (implicit Sparse-Matrix Vectorized Gear algorithm, Jacobson and Turco, 1994), EBI (Euler Backward Iterative method, Hertel et al., 1993), ROS3 (Rosenbrock solver, Sandu et al., 1997), and MEBI (Modified Euler Backward Iterative method, Huang and Chang, 2001). In this work the MEBI scheme is used. The choice of the chemical solver was limited to SMVGEAR, ROS3 and MEBI. EBI was in fact excluded because it is coupled just with the CB4 family of mechanisms and it cannot therefore be used in RADM2. Concerning the other three schemes, the choice was made considering computational efficiency as the main factor. Several tests (Huang et al., 2001) indicate that in terms of accuracy the Rosenbrock solver (ROS3) is significantly better than MEBI and SMVGEAR but its computational efficiency is worse. For most applications MEBI should give the best computing performance. SMVGEAR is based on the algorithm originally described by Gear (1971a, 1971b) and then modified by Jacobson and Turco (1994) which incorporate special sparse matrix techniques to improve computational performance. The Gear algorithm is part of a class of methods referred to as Backward Differentiation Formulae (BDF). CMAQ ROS3 solver is based on the s-stage Rosenbrock algorithm as described in Sandu et al. (1997). Finally MEBI uses functional iteration to obtain a solution to the implicit Euler backward approximation.

More details of the numerical solvers implemented in CCTM can be found at http://www.cmascenter.org/help/model_docs/cmaq/4.4/CHEM_SOLVER_NOTES.txt.

2.2.2.3 **Aerosol processes**

The method adopted in CCTM for describing the particle size distribution in aerosol processes is called the "modal approach". In this representation the particle size distribution is described as the superposition of three lognormal distributions (Withby, 1978), named "modes": Aitken mode (*i-mode*), Accumulation mode (*j-mode*) and Coarse mode (*c-mode*). The smaller distribution, called Aitken mode, represents fresh particles either from nucleation or from direct emissions, while the Accumulation mode represents aged particles. Primary emissions may also be distributed between these two modes. The two modes interact with each other through coagulation. The Coarse mode species include sea salt, wind-blown dust and other unspecified material of anthropogenic origin. Each mode may grow through condensation of gaseous precursors or shrink by evaporation and is subject to wet and dry deposition. Assuming the particles as spheres of diameter D_p (Seinfeld et al., 1998) the three modes can also be identified as the fraction of particles with $D_p < 0.1$ μm (Aitken), the fraction of particles with 0.1 μm $< D_p < 1$ μm (Accumulation) and the fraction of particles with $D_p > 1$ μm (Coarse).

CCTM solves a set of prognostic equations for three integral properties of the particle size distribution, namely the total particle number concentration, the total surface area concentration and the total mass concentration of the individual chemical components in each mode. The number distribution is typically unimodal, with a maximum value of D_p around 0.01 μm. The surface area distribution can be unimodal or bimodal, with a first maximum around a D_p of 0.2 μm. Finally the mass distribution (Figure 2-2) typically shows maximums around D_p values of 0.01μm, 0.3 μm and 10 μm. According to Seinfeld and Pandis (1998) these distributions can also vary depending on the origin of particulate matter (highly polluted urban area, rural area, free troposphere).

The main advantage of the modal approach is the limited number of variables which helps to improve the computational performance. On the contrary, the sectional approach adopted in most models describes particle behavior using a set of bins of increasing size. It therefore requires a large numbers of variables (equal to the

product between the number of size bins and the number of chemical components) and this makes the sectional representation numerically less efficient.
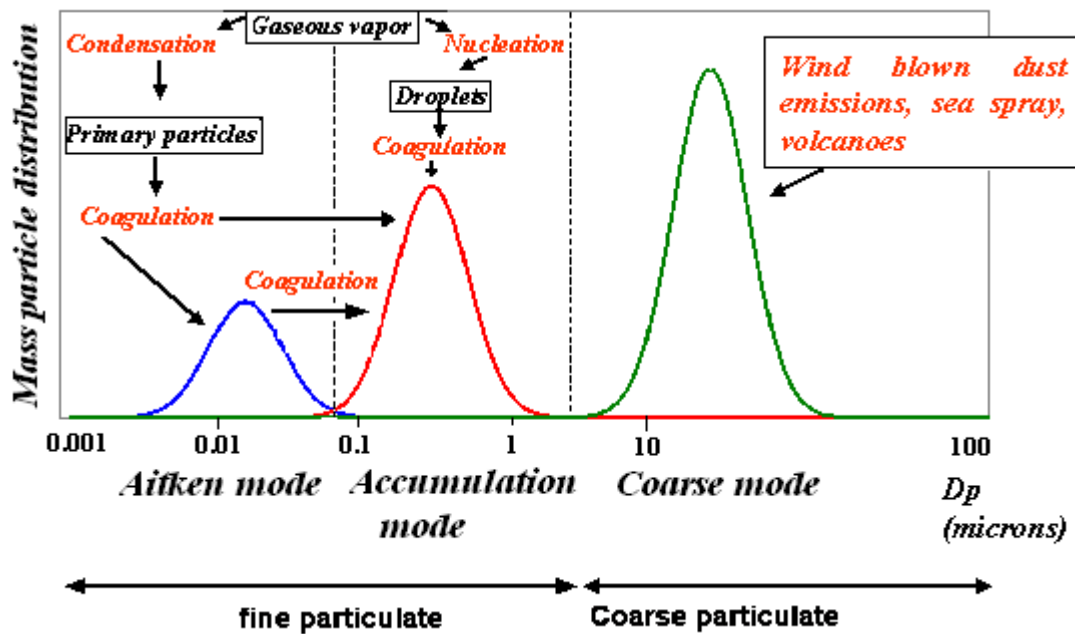

Figure 2-2. Schematic diagram of the mass particle distribution with respect to the diameter D_p. Aitken, Accumulation and Coarse mode are indicated in blue, red and green respectively. The maximum values of the distributions are typically 0.01 μm for the Aitken distribution, 0.3 μm for the Accumulation mode and 10 μm for the Coarse mode. Source: adapted from US-EPA Visibility Monitoring Guidance Document (1999).

The main aerosol processes treated in CCTM are condensation/evaporation as described by Whitby (1991), nucleation of the H_2O-H_2SO_4 system applying the method of Kulmala et al. (1998), production of SOA (secondary organic aerosols) applying the method of Pankow et al. (1994a, b) and coaugulation using numerical quadratures accurate to six decimal places (Whitby at al., 1991). Kulmala et al. (1998) predict the rate of increase of the number of particles by the nucleation from sulfuric acid vapour. In order to predict the rate of increase of new mass, following work by Weber et al. (1997), the new particles are assumed to be 3.5 nm in diameter. About secondary organic aerosols, the method of Pankow et al. (1994a, b), based upon laboratory experiments, calculates the yield of SOA as a function of the amount

of organic material already in the particle phase. More details about the description of aerosol processes in CCTM can be found in Binkowski (1998).

CCTM calculates concentrations and depositions of 26 species, divided in 21 mass distributions, two surface distributions and three number distributions. The list of species is reported in Table 2-4.

		AITKEN	ACCUMULATION	COARSE
ASO4	Sulphate mass	X	X	
ANH4	Ammonium mass	X	X	
ANO3	Nitrate mass	X	X	
AORGA	Anthropogenic secondary organic mass	X	X	
AORGPA	Primary organic mass	X	X	
AORGB	Secondary biogenic organic mass	X	X	
AEC	Elemental carbon mass	X	X	
A25	unspecified anthropogenic mass	X	X	
ACORS	Unspecified anthropogenic mass			X
ASEAS	Marine mass			X
ASOIL	Soil-derived mass			X
AH2)	Water mass	X	X	X
NUM	Number of particles	X	X	X
SRF	Surface area	X	X	X

Table 2-4. Aerosol species treated in CCTM. The "X" in each box indicates that the corresponding mode is calculated by the model. CCTM also calculates the total number of particles in all three modes (NUMCOR, NUMACC, NUMATKN) and the total area for Aitken and Accumulation modes (SRFATKN, SRFACC).

2.2.2.4 **Transport processes**

In Eulerian models, advection and diffusion processes are modelled using numerical algorithms. These numerical schemes must satisfy two important requirements. They must conserve mass and they must be convergent. Convergence means the solution approaches the true solution of the corresponding partial differential equation when the time step (ΔT) and the grid spacing (Δx) tend to zero. Thus, in theory a convergent numerical scheme can provide a solution as accurate as desired within finite bounds by reducing ΔT and ΔX indefinitely. In practice computational limitations make it necessary to set a minimum value for these parameters, with the consequent introduction of numerical errors. This condition, also known as Courant-Friedrichs-Lewy (CFL) condition (Courant et al., 1967), is given by (in a one-dimensional case):

$$\frac{\Delta T}{\Delta X} < C \qquad\qquad (2.7)$$

where C is a constant depending on the equation to be solved. The CFL condition imposes a limit to the reduction of the time step ΔT. It is therefore essential that the numerical transport algorithms minimize numerical errors due to the CFL condition. The scheme adopted in this work for the parameterization of the advection process is the Piecewise Parabolic Method (PPM), described in Colella and Woodward (1984) which assumes the concentration distribution to be parabolic in any given grid cell. For computing eddy diffusion in convective conditions the Asymmetric Convective Model (ACM) (Pleim and Chang, 1992) is applied. It is based on the non-local closure scheme by Blackadar (1978) but with a different scheme for downward mixing in the convective boundary layer (CBL). Horizontal diffusion is modelled using a constant eddy diffusion coefficient. A detailed description of the transport processes implemented in CMAQ can be found in Byun et al. (1990).

2.2.2.5   Cloud processes

The accurate description of clouds is extremely important in modelling concentrations of atmospheric pollutants. Clouds influence photochemical reactions, as they reflect and absorb solar UV radiation, and they also have strong influence on wet deposition, contributing to the removal of soluble pollutants from the atmosphere. Clouds also affect aqueous-phase chemistry reactions and mixing processes. The rate of change in pollutant concentrations (m_i) due to cloud processes is therefore a function of the mixing, scavenging, aqueous chemistry and wet deposition of a "representative cloud" within the grid cell:

$$\frac{\partial m_i}{\partial t} = f(mixing, scav, aqchem, wetdep) \tag{2.8}$$

Two schemes may be applied for simulating cloud processes in CCTM, called "sub-grid cloud model" and "resolved cloud model" respectively. The first scheme includes parameterizations of convective clouds (precipitating and non precipitating) and it is applied on coarse resolution domains, when the size of the cloud is smaller than the model grid size. The maximum resolution permitted is 8 x 8 km^2; for smaller scales the resolved cloud model is employed. In the second case (resolved cloud model) the cloud horizontally covers the whole area of the grid cell and it has already been "resolved" by the meteorological model (MM5) which includes stratus, cumulus and cirrus type clouds. The following paragraphs briefly describe the features of both schemes.

a) Sub grid cloud model

The current sub-grid cloud scheme implemented in CMAQ was derived from the diagnostic cloud model in RADM2 (Dennis et al., 1993; Walcek and Taylor, 1986;

Chang, et al., 1987; Chang et al., 1990). Precipitating clouds are simulated by the sub grid cloud model when the meteorological mesoscale model MM5 indicates precipitation over that grid cell. The convective cloud contains air transported vertically-from below the cloud, entrained from above the cloud (for precipitating clouds), and entrained from the sides of the cloud. The average pollutant concentration over the cloud volume is given by:

$$\overline{m}_i^{cld} = \frac{\int\limits_{z_{base}}^{z_{top}} \overline{m}_i^{cld}(z) W_C(z) dz}{\int\limits_{z_{base}}^{z_{top}} W_C(z) dz} \tag{2.9}$$

where $W_c(z)$ is the liquid water content and $\overline{m}_i^{cld}(z)$ is the concentration of pollutant i for each layer z of the cloud, function of the above and below cloud concentration and of the fraction of entraining air coming from the side of the cloud. The processes of mixing, scavenging, aqueous chemistry can now be modelled. Details about the algorithms used to model these processes can be found in Roselle and Binkowski (1999).

The wet deposition algorithms in CMAQ were taken from RADM (Chang et al., 1987). Deposition is accumulated over 1-hour increments before being written to the output file. The wet deposition amount of chemical species i depends on the precipitation rate (P_r) and the cloud water concentration (m_i^{cld}):

$$wet\_dep_i = \int\limits_0^{\tau_{cld}} \overline{m}_i^{cld} P_r dt \tag{2.10}$$

b) Resolved cloud model

If the grid size is less than 8 x 8 km^2 the resolved cloud scheme is applied; a resolved cloud horizontally covers the entire grid cell and vertically extends over the whole depth of the layer. The average liquid water content W_c in a model layer z for the resolved cloud is given by:

$$\overline{W}_C(z) = \left[Q_G(z) + Q_C(z) + Q_R(z) \right] \rho(z) \qquad (2.11)$$

where $Q_C(z)$ is the cloud water mass mixing ratio (kg kg^{-1}), $Q_R(z)$ is the rain water mass mixing ratio (kg kg^{-1}), $Q_G(z)$ is the graupel mass mixing ratio (kg kg^{-1}) and $\rho(z)$ is the air density (kg m^{-3}). All these quantities are calculated by MM5.

Precipitation amounts for resolved cloud layers, $P_r(z)$, are derived applying to the MM5 non-convective precipitation amounts (R_n) a specific vertical profile:

$$P_r(z) = R_n \left(\frac{\overline{W}_C(z)}{\int \overline{W}_C(z) dz} \right) \qquad (2.12)$$

Using this new quantity the resolved cloud model then simulates the wet deposition process using equation (2.10).

2.2.3 The Photolysis rate PROCessor (JPROC)

Photodissociation is defined as the conversion of solar radiation into chemical energy to activate and dissociate chemical species. Examples of species that photodissociate include many important trace constituents of the troposphere such as NO_2, O_3, formaldehyde (HCHO), acetaldehyde (CH_3CHO), nitrous acid (HONO) and hydrogen peroxide H_2O_2. It is therefore important to estimate photodissociation accurately in order to predict effects of air pollution properly. The module JPROC was developed as a tool for calculating photodissociation reaction rates.

The photodissociation reaction rate (or photolysis rate), also called J-value, is defined as:

$$J_i = \int_{\lambda_1}^{\lambda_2} F(\lambda) \sigma_i(\lambda) \Phi_i(\lambda) d\lambda \qquad (2.13)$$

where λ is the wavelength of the solar radiation (nm), $F(\lambda)$ is the actinic flux (photons cm^{-2} s^{-1} nm^{-1}), $\sigma_i(\lambda)$ is the absorption cross section for the molecule undergoing photodissociation (cm^2 molecule^{-1}) and $\Phi_i(\lambda)$ the quantum yield of the photolysis reaction (molecules photon^{-1}).

Absorption cross sections and quantum yields are functions of λ, and they may also be temperature and pressure dependent. Actinic flux $F(\lambda)$ is the spectral radiance integrated over all solid angles per unit area. It therefore depends on longitude, latitude, altitude, season and time of the day (sun angle). It is also strongly affected by Earth's surface albedo as well as by atmospheric scatterers and absorbers.

For solving equation (2.13) the actinic flux, absorption cross section, and quantum yield must be determined as a function of λ. The delta-Eddington two-stream radiative transfer model (Joseph et al., 1976; Toon et al., 1989) is used for computing the actinic flux. Absorption cross section and quantum yield data are specified by the user through input files. The original sets of cross section/quantum yield data published with the Regional Acid Deposition Model RADM2 are available for use in JPROC. Output files are tables containing clear-sky photolysis rates, one for every simulation day. J-values are calculated for 6 latitudes (10N, 20N, 30N, 40N, 50N, and 60N), 7 altitudes (0 km, 1 km, 2km, 3 km, 4 km, 5 km, and 10 km), and ±9 hours from local noon (0 h, 1 h, 2 h, 3 h, 4 h, 5 h, 6 h, 7 h, and 8 h).

Photolysis rates as calculated by JPROC for individual grid cells are then interpolated in the subroutine PHOT. PHOT also uses a parameterization to correct the clear-sky photolysis rates for cloud cover. The parameterization was taken from RADM (Chang et al., 1987; Madronich, 1987). The correction depends on whether the location is below, above, or within the cloud.

Below cloud photolysis rates will be lower than the clear-sky values due to the reduced transmission of radiation through the cloud. The below cloud photolysis rate (J_{below}) is calculated as:

$$J_{below} = J_{clear}(1 + cfrac(1.6t_r \cos(\theta) - 1) \tag{2.14}$$

where *cfrac* is the cloud coverage fraction (interpolated from hourly data for each grid cell), θ is the zenith angle and t_r is the cloud transmissivity:

$$t_r = \frac{5 - e^{-\tau_{cld}}}{4 + 3\tau_{cld}(1 - f)} \tag{2.15}$$

where f is scattering phase function asymmetry factor (assumed to be 0.86) and τ_{cld} is the cloud optical depth. This is calculated using the empirical formula from Stephens (1978):

$$\log(\tau_{cld}) = 0.2633 + 1.7095 \ln(\log(L)) \tag{2.16}$$

L is the liquid water path where $L = W\Delta z$ (g m^{-2}); W is the averaged cloud liquid water content (g m^{-3}), and Δz is the cloud thickness.

The above cloud photolysis rate is calculated as:

$$J_{above} = J_{clear}\left[1 + cfrac(\alpha_t(1 - t_r)\cos(\theta))\right] \tag{2.17}$$

J_{above} will be greater than J_{clear} because of the additional reflected radiation from the cloud.

Within the cloud, the correction factor is a simple linear interpolation of J_{below} at cloud base to J_{above} at cloud top. Once computed, the below, above, and within cloud rates are used to scale the clear sky photolysis rates to account for the presence of clouds.

2.2.4   Pre-processors for boundary and initial concentrations

BCON and ICON are processors for computing boundary (BCs) and initial (ICs) concentrations respectively. The ICON processor generates species concentrations for every cell in the model domain, whereas the BCON processor generates species

concentrations for the cells immediately surrounding the grid. It is not necessary for ICON and BCON to produce ICs and BCs for all species included in RADM2. If a species is not found on BCON and ICON output files, CCTM will automatically set its ICs and BCs to a minimum threshold limit (i.e., a nominal zero).

The main role of BCON and ICON is to allow for the influence of a wider domain on the inner high resolution grid. The process, known as "nesting", is explained in Section 2.2.6. As illustrated in Figure 2-3, a nested model simulation of CMAQ is performed using specific constant profiles for the outer low resolution domain. These profiles contain species concentrations as a function of height and they are spatially independent for the ICON processor and only minimally spatially dependent for the BCON processor. More precisely, BCON requires, for every layer, only four values for four directions: "North", "South", "East" and "West".

Only one value for every layer is required in the ICs input file. In both cases profiles are time independent. North, South, East, West and initial concentration values of NH_3, SO_2 and NO_x in the first vertical level for June 1999 are reported in Table 5-3. BCON and ICON do not perform any horizontal interpolation for generating the ICs and BCs from these profiles. They just project the East, West, South and North profiles onto the four sides of the outer domain (BCs) (Figure 5-3) and the spatially independent ones inside the grid (ICs) for every layer. A CMAQ simulation is then performed over the outer domain using the output files from BCON and ICON application as BCs and ICs. More details about the profiles used for the application of CMAQ over the UK can be found in Chapter 5.

The model results (CCTM concentration files) of the CMAQ simulation for the coarser grid are both temporally (i.e. hourly) and spatially resolved (5 x 5 km^2 resolution). These data are again used as input to either ICON or BCON for generating ICs and BCs onto the "small" domain (a nested modelling domain that has a finer resolution than the coarser, outer domain) (Figure 5-4). Horizontal interpolation is performed in this case. The horizontal mapping is done on the basis of cell proximity. The ground-level latitudes and longitudes at the centre of each vertical column of cells are first calculated for both the input and output domains. These computed values are then used to find which input column is closest to each output column (Gipson, 1998). It is important to add that, if the boundaries of the

outer domain are far enough from those of the inner domain, the lack of spatial resolution in the constant profiles lead to a negligible influence in the results of the second simulation. Figure 2-3 summarizes the entire procedure for generating BCs and ICs.
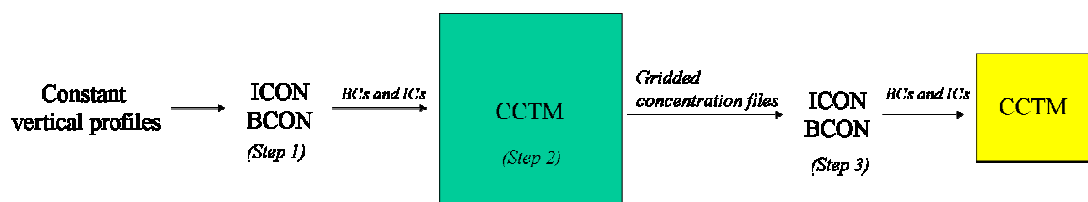

Figure 2-3. Scheme for the use of BCON and ICON in a nesting process. The procedure can be divided into 3 steps. BCON and ICON re-project the BCs profiles onto the 4 sides of the outer domain (in blue) and the ICs profiles inside the domain (step 1). The output files from BCON and ICON application are now used as BCs and ICs for a CMAQ simulation over the outer grid (step 2). The output gridded concentration files are now re-interpolated (step 3) onto the inner high resolution grid (in yellow) by ICON and BCON for providing both spatially and temporally resolved BCs and ICs to CCTM.

2.2.5   The meteorology - Chemistry Interface Processor (MCIP)

The Meteorology-Chemistry Interface Processor (MCIP) is a computational interface which links meteorological mesoscale models like MM5 with the Chemical Transport Model (CCTM). MCIP deals with issues like conversion of units and reconstruction of meteorological data on different horizontal grids and vertical structures. More specifically, when meteorological data on a finer resolution grid than that simulated in MM5 are required, MCIP interpolates data using a bilinear interpolation. It can also perform a mass-weighted average of data in the vertical direction (21 MM5 vertical layers are aggregated into 15 layers to be used in CCTM). MCIP also converts the output files from MM5 in the format used into CCTM (IO/API format). Some parameters not available from the meteorological

model are also estimated with appropriate diagnostic algorithms. The most important are the computation of dry deposition velocities and boundary layer height.

Two methods are implemented in MCIP for estimating the deposition velocity of chemical species: the RADM method (Wesely, 1989) and the M3DDEP method (Pleim, 1996). The first is the one used in this study. For a stable atmosphere, the boundary layer height is calculated using the Zilitinkevich's formula (Zilitinkevich, 1989). In unstable conditions, it is calculated using the Richardson number and the vertical profiles of potential temperature with an equation similar to the one reported in Holtslag et al. (1995). More details about MCIP features and structure can be found in Otte et al. (1999).

2.2.6 **Nesting process**

A nesting process is a technique commonly used in environmental modelling combining different grids to drive high resolution simulations. Inside CMAQ, finer grids are "nested" inside outer coarser grids and the spatially and temporally resolved concentrations from a simulation over the bigger domain are used as initial and boundary concentrations for the finer inner domain.

IN CMAQ the resolution and the dimensions of the domains are set up by the user before the run and they remain fixed throughout the all simulation. In the study a 5 x 5 km^2 resolution grid covering the British Isles is nested within an outer lower resolution grid (45 x 45 km^2 resolution) (Figure 5-1). The features of both domains are summarized in Table 5-1. Nesting in CMAQ is used only in a one-way mode: this means there is no feedback from the inner domain to the outer one. In a two-way nesting concentrations over the coarser grid are updated by the concentrations over the finer grid in the cells which overlap. The use of a nesting process is essential for providing "realistic" 3D concentrations on the boundaries, reducing uncertainties in air pollution studies.

2.2.7 **Parallel performance**

On the one hand the Eulerian approach adopted in CMAQ permits very detailed results because it includes the parameterization of many relevant chemical and

physical processes, but on the other hand this high level of detail makes the computational performance worse (the simulation time is typically from days to weeks). For reducing this problem in December 2004 CMAQ was installed at the Centre for Ecology and Hydrology in Edinburgh on Nemesis, a 60 node dual-processor system running a derivative of Red Hat 7.2 Linux. The use of a multi-parallel processor system reduces the actual time required by the model, in particular when it is used for high resolution domains and for simulations of long periods of time. An estimate of the computational performance of CMAQ on Nemesis is shown in Table 2-5.

Simulated time period	4 days	1 month
Data size	1.69 Gb	12 Gb
Computing time	3 hours	24 hours

Table 2-5. Estimate of the computing time and the output data size of CMAQ on Nemesis. These performance results were achieved running the model with 20 processors on a modelling domain of 240x170 cells with a grid resolution of 5x5 km^2 nested in a coarser 45 x 45 km^2 wider domain.

While it is generally agreed that shorter processing times can be achieved using multi-processors, it is not true that the computing time decreases linearly with the increase of the number of processors used. The optimal number of processors for a given application depends in fact on a number of factors such as the parallelization method, the size of the data sets and the data transfer limitations between processors (Bresnahan et al., 2005). A useful parameter for quantifying the efficiency of a multi-parallel system is the scalability (Tonse, 2006):

$$Scalability = \frac{Time_{serial}}{Time_{parallel} * N_{processors}} \qquad (2.18)$$

where $N_{processors}$ is the total number of processors and $Time_{serial}$ and $Time_{parallel}$ are the computing times for the model running on a single processor and on parallel respectively.

If, for example, the increase in the number of processors is from 1 to 4 but the speed up is only a factor two, scalability is 50%. Tonse (2006) points out how the choice of the numerical chemical solver in CCTM plays a major role in the computing performance. Table 2-6 shows total simulation time and scalability of two parallel simulations using SMVGEAR and EBI respectively.

	Time (hour)	Scalability (%)
EBI	0.78	49%
SMVGEAR	5	78%

Table 2-6. Scalability and total simulation time with SMVGEAR and EBI solvers. 18 processors are used. The domain is a 96 x 117 grid with a 4 x 4 km^2 resolution. Adapted from Tonse et al. (2006)

2.3 THE USE OF CMAQ IN THE UK

2.3.1 Mesomaq

Several UK institutions including universities, government bodies and private companies have been carrying out projects involving the use of CMAQ for estimating pollutant concentrations and depositions across the country. Many of them have agreed to be part of Mesomaq (Mesoscale Modelling Air Quality group), a national network created in 2005 in collaboration with the National Centre of Atmospheric Science (NCAS) with the purpose of improving the knowledge and the activity in the fields of atmospheric chemistry modelling and numerical weather prediction. Through Mesomaq all modellers, including CMAQ users, can interact using a list server (http://www.ncas.ac.uk/mailman/listinfo/mesomaq) set up by the

British Atmospheric Data Centre (BADC). This facilitates the dialogue and the exchange of information among the different institutions and makes the use of the model easier for new users. More information about Mesomaq can be found at http://ncasweb.leeds.ac.uk/mesomaq/. In the next section some of the studies currently going on in the UK involving the use of CMAQ are briefly listed.

2.3.2   CMAQ applications in the UK

At University of Manchester the Atmospheric Science research group is currently applying CMAQ MADRID, a model developed in 2002 as an alternative version to the "standard" CMAQ for the study of aerosol processes. Its peculiarity is that it implements a sectional approach (2 or 8 size bins) for describing the mass distribution of aerosol particles instead of the modal approach adopted in the "standard" version. A comparison between CMAQ and CMAQ MADRID model predictions and between modelled data and measurements has been performed. Three nested grids are used for running the model: the first one covering North West Europe with a 108 x 108 km^2 resolution, the second one covering the whole UK at 36 x 36 km^2 and the inner one covering England and Wales at 12 x 12 km^2. The research group is also involved, together with the University of Hertfordshire, in the validation of "UM_MCIP", a new interface released in autumn 2006 by the Universities Weather Research Network (UWERN). The interface processes the output data from the Met. Office Unified Model (UM), making them usable for CMAQ. The interface gives the chance of using the UM as an alternative to the mesoscale models currently coupled with CMAQ (MM5, WRF).

The Atmospheric Science Research Group in the Science and Technology Research Institute of the University of Hertfordshire is running CMAQ for simulating air pollution episodes in urban areas. Sokhi et al. (2006) applied the suite MM5/CMAQ over the urban area of London on a 1 × 1 km^2 resolution grid. Specific periods during summer 2002 have been simulated and predicted hourly concentrations of O_3 have been compared to several urban background stations in London. Elizabeth Somerwell at University of Hertfordshire is currently implementing the UM-CMAQ modelling

system using three nested grids (12 km, 4 km, 1 km) centred on London; she is also developing a new interface for using output concentrations from the global model GEOS-CHEM as boundary and initial concentrations for CMAQ.

An air quality study over urban areas is also currently being carried out by Andrea Fraser at the Imperial College of London. The study focuses on a 39 days simulation in June and July 2006, a period characterised by critical ozone and PM air quality episodes. CMAQ has been implemented in the UK on three nested grids: a European scale grid, a North European grid, and a South East England grid. Meteorological data from the UK Met Office Unified Model (UM) are used. Studies of emissions sensitivity analysis have been carried out to evaluate the model performance with respect to VOC, NO_X, SO_2 and NH_3 emission reductions.

Not only universities but also two leading UK energy companies are carrying out studies with CMAQ in order to estimate the contribution of UK power stations to pollutant concentrations and deposition fluxes.

The Environmental Management Department of RWE Npower has been using CMAQ since its first release in the 1990s. In recent years several studies based on 1-year simulations have been carried out, mainly focused on acid deposition. The aim is to quantify the effects of individual coal and oil-fired power stations on several protected areas across the country. The outer domain covers Europe at 54 x 54 km^2 resolution and two inner domains at 18 x 18 km^2 and 6 x 6 km^2 resolution respectively cover the UK. Emissions are processed by SMOKE and meteorological input data are obtained by re-gridding the UK Met Office NAME-format files.

The technology centre of E.ON UK in Nottingham has also been using CMAQ since 1999. Initial studies were focused on the validation of the model by comparing model predictions to measured concentrations and wet depositions. Today the model is applied to study a wide range of environmental issues relevant to the power industry, including assessment of the contribution of UK power stations to $PM_{2.5}$ concentrations, the study of the deposition footprints of individual power plants for future emission scenarios and the assessment of population exposure to primary and secondary particulate matter from different European emission sectors.

2.4 CONCLUSIONS

The main features of the Community Multi-Scale Air Quality System (CMAQ) were presented, as well as the scientific aspects regarding the "one atmosphere" concept, at the base of the model development.

The chapter also emphasizes how the choice of the numerical solver may have strong influence on the computing performance, affecting the total simulation time and scalability in the model. A careful choice of the chemical scheme is also suggested, depending on the type of pollutants and gas/aerosol phase processes which form the subject of the study. The concept of nesting process is finally introduced, together with the procedure for achieving both spatially and temporally resolved boundary and initial concentrations.

The chapter provides a general introduction to the structure and main features of CMAQ thus it is a good starting point for the following chapters which are more focused on the implementation and application of the model to the UK.

CHAPTER 3
Application of the 5th Generation Mesoscale Model (MM5) to the UK

SUMMARY

Simulations of precipitation, wind speed and surface temperature are performed using the Mesoscale Model Generation 5 (MM5) developed by the Pennsylvania State University and National Center for Atmospheric Research (PSU/NCAR).

The model domain covers the British Isles with a horizontal grid resolution of 5 x 5 km^2. Year 1999 is selected for running the model. Two periods covering February 1999 and June 1999 are analysed in detail. MM5 is initialized using the meteorological parameters from the ERA-40 re-analysis of the European Centre for Medium-Range Weather Forecasts (ECMWF).

Modelled values of surface temperature, wind speed and rainfall in single grid cells are extracted and compared to observations from several meteorological stations across the UK. For every site, the main performance indicators are calculated. Vertical profiles of temperature and dew point temperature in the lower atmosphere are also presented. Modelled profiles are compared to typical day time profiles in Nottingham for several days in June 1999. A detailed analysis of rainfall distribution across the country is performed by comparing maps of monthly precipitation predicted by MM5 to climatology maps from the Climatic research Unit (CRU) dataset CRU TS 1.2 (http://www.cru.uea.ac.uk/cru/data/hrg.htm).

The results show a general tendency of MM5 in overestimating wind speed (+30%) and underestimating precipitation (between -10% and -20%) whereas there is generally a good agreement with observations for surface temperature. In terms of systematic error, the absolute bias for temperature is estimated approximately between -0.2 ºC and +0.1 ºC in June and between -0.5 ºC and +0.1 ºC in February.

3.1   INTRODUCTION

Meteorology plays a major role in many processes involving atmospheric pollutants, such as formation of aerosols, dry and wet deposition, transport and photodissociation of chemical compounds.

An accurate representation of deposition fluxes and concentrations of chemical species therefore requires a good estimate of meteorological variables such as air temperature, atmospheric pressure, wind speed, rainfall, relative humidity and cloud

coverage. Meteorological mesoscale models are developed with the specific purpose of weather forecasting but they can also be used for providing these meteorological parameters to atmospheric transport and dispersion models. The rapid improvement of computational capabilities in the last few years make more and more sophisticated meteorological models available for users. One of the most used and well known models is the Fifth-Generation Mesoscale Model (MM5) developed by the National Centre for Atmospheric Research (NCAR) and by the Pennsylvania State University (PSU).

Recent studies have investigated various aspects of MM5 evaluation. For example, Hanna and Yang (2000) focus on the evaluation of near surface wind speed and direction and near surface vertical temperature gradient on Eastern U.S. and Central California domains. In Jimenez et al. (2005) MM5 wind speed, wind direction and temperature have been evaluated over the Iberian Peninsula during a pollution event (13th -16th August 2000). A quantitative performance analysis of MM5 forecast rainfall was produced during the July 1998 episode of the Indian monsoon (Rakesh et al, 2006). Miao et al. (2007) validated the model over the Swedish west coast and Rantamaki et al. (2005) performed the evaluation of vertical temperature profiles and relative humidity over the Helsinki area for December 1995.

Altough the model has been extensively evaluated in the United States (Hanna and Yang, 2000; Hayes et al., 2002; Gilliam et al., 2004; Shafran et al., 2000) and in other countries over the recent years, few validation studies (Fragkou, 2005; Kukkonen et al., 2005; Lennard and Griffiths, 2005; Kitwiroon, 2006) have been conducted in the United Kingdom, and none on a national scale.

This paper attempts to address this issue by applying MM5 on a UK high resolution domain (5 x 5 km^2 resolution) covering the whole country. The results of this application are also used as input meteorological fields for CMAQ. MM5 evaluation focuses on near surface temperature, wind speed and total precipitation. The results of MM5 application for year 1999 are presented and discussed. Section 3.2 briefly describes the model and introduces the case study; Section 3.3 includes the results and Section 3.4 summarizes the conclusions.

3.2 CASE STUDY

3.2.1 The model

The MM5 model has evolved since its introduction in the early 1970s (Anthes and Warner, 1978). The enhancements in MM5 over the original version (MM4) include the option for non-hydrostatic physics, more detailed explicit moisture schemes, parameterizations of boundary layer processes and radiation processes. The major upgrades from MM4 to MM5 can be found in Dudhia et al. (1993).

As a first step the program horizontally interpolates the regular latitude-longitude terrain elevation, land use and coarse resolution meteorological data (e.g. from ECWMF analyses) provided as input onto the mesoscale grid chosen by the user. The model then performs a vertical linear interpolation of 3D meteorological variables from pressure levels to σ- coordinates (Phillips, 1957; Gal-Chen et al., 1975) with a vertical resolution of 23 σ-levels. It finally solves the dynamics and thermodynamics equations at every time step (15 minutes). When MM5 performs the time integration, a Newtonian relaxation method (Stauffer and Seaman, 1990; Stauffer et al., 1991) is applied. This technique, also known as "nudging", is an example of data assimilation (FDDA): it consists of adding specific forcing terms to the model dynamics equations which relax the model value towards observations or, in this case, to a given analysis. This technique improves the accuracy in the results, keeping the modelled values close to the gridded analysis throughout all the simulation period.

MM5 also includes parameterizations for cloud processes, surface layer processes, atmospheric radiation, microphysics and boundary layer processes. The schemes selected in this work are listed in Paragraph 3.2.4.

3.2.2 Model domain

Two months have been selected for testing MM5, one in summer (June 1999) and one in winter (February 1999). The boundaries of the model domain are shown in Figure 3-2. It is a 240 x 170 cells grid with a resolution of 5 x 5 km^2. The map projection is Lambert Conformal. Central latitude and longitude are 55 degrees N and 3 degrees E respectively.

3.2.3 Input data

Terrain elevation and land use input data come from the US Geological Survey (http://www.usgs.gov/). They cover the whole globe and they are available at 2 minutes (3.70 km) resolution. In the land use data set, 25 categories of vegetation coverage are available; the data consist of a percentage for every category at each of the lat/lon grid points.

The coarse resolution meteorological input is given by 3D meteorological fields from the ERA-40 re-analysis of the European Centre for Medium range Weather Forecasts (http://www.ecmwf.int/). An example of ECMWF map is shown in Figure 3-1. The data set contains surface and upper-air fields derived on pressure levels; data have six-hour frequency, with a global coverage on a 2.5 x 2.5 degrees resolution grid. Pressure levels are 1000, 925, 850, 775, 700, 600, 500, 400, 300, 250, 200, 150, 100, 70, 50, 30, 20, 10, 7, 5, 3, 2, 1 mbar.
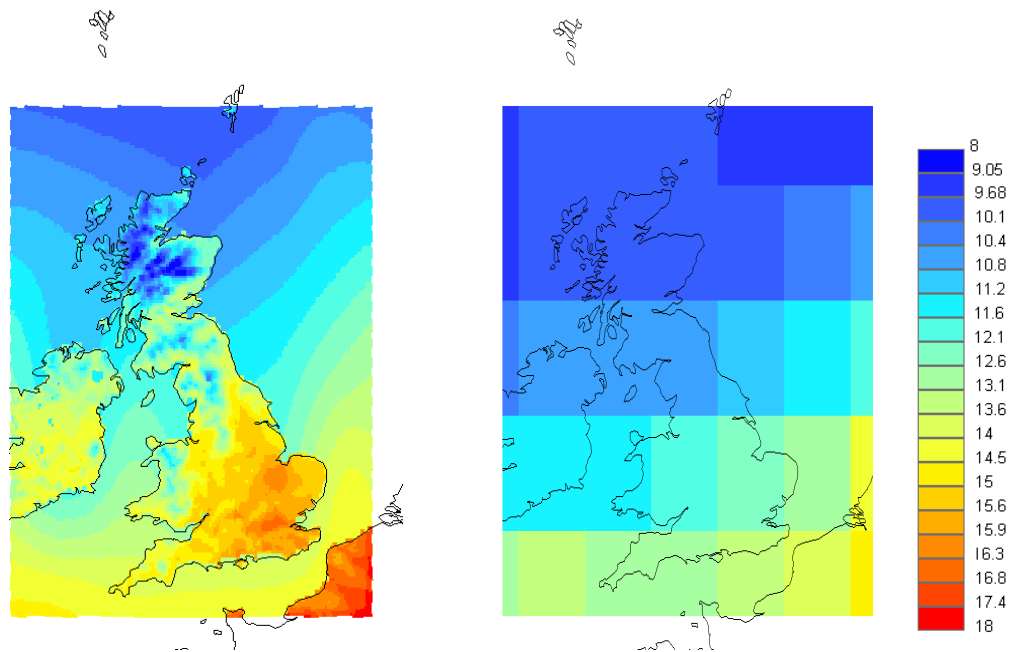
Figure 3-1. Monthly surface temperature as modelled by MM5 (left) and by ECMWF (right).

3.2.4 Parameterization schemes

Several optional parameterization schemes are available in MM5. For cloud processes, the cumulus parameterization scheme of Grell et al. (1994) is adopted. This is a simple single-cloud scheme with updraft and downdraft fluxes. There is no direct mixing between clouds and environmental air, except at the top and the bottom of the circulations. This scheme tends to allow a balance between the resolved scale rainfall and the convective rainfall (Grell et al., 1991; Grell, 1993). For grid-scale microphysics, a simple ice scheme (Dudhia, 1989) is used. It includes explicit treatment of cloud water, rainwater, ice and snow. Phase changes such as condensation and evaporation, freezing and melting are considered. This scheme does not include supercooled water and unmelted snow. The parameterization for the planetary boundary layer (*pbl*) process come from the Medium Range Forecast (MRF) model scheme (Hong and Pan, 1996) based on the parameterization described by Troen and Mahrt (1986). The scheme is a first–order vertical diffusion scheme. The planetary boundary layer height is determined using the bulk-Richardson approach. The profile of diffusivity is then specified as a cubic function of the *pbl* height. Surface layer processes are parameterized by the application of the 5-layer soil model (Dudhia, 1996). The soil temperature is predicted at layers of approximate depths of 1, 2, 4, 8, and 16 cm, with a fixed substrate below using a vertical diffusion equation. Finally, the atmospheric radiation scheme selected for this study is the Simple Cooling scheme (Dudhia et al., 1998). It sets the atmospheric cooling rate strictly as a function of temperature.

3.3 RESULTS

3.3.1 Comparison with observations

3.3.1.1 <u>Temporal series</u>

Modelled values of surface temperature, wind speed at 2 metres altitude and total precipitation in single grid cells are extracted and compared to observations from several meteorological stations across the UK. The sites initially selected should cover the main areas of the country (inland, East and West Coast, Scotland and Northern Ireland). The limited availability of data for the two months in 1999 reduced the number of sites to height, as shown in Figure 3-2. The time series have six-hour frequency. The trend over the period indicates a general overestimate of wind speed by MM5 for all stations. The over-prediction tends to be more pronounced for HiIlsborough station (Figure 3-3). Maximum and minimum daily values of temperature are well reproduced by MM5 for all sites (Figure 3-4). Time series of daily totals of precipitation are also presented (Figure 3-5). Observational data come from the UK Met Office MIDAS Land Surface Observation data set (http://www.badc.nerc.ac.uk/data/ukmo-midas/). ECMWF predictions have also been included in Figure 3-5 in order to show the improvement given by MM5 to the ERA-40 re- analysis (MM5 predictions of rainfall are closer than ECMWF to observations in both February and June).
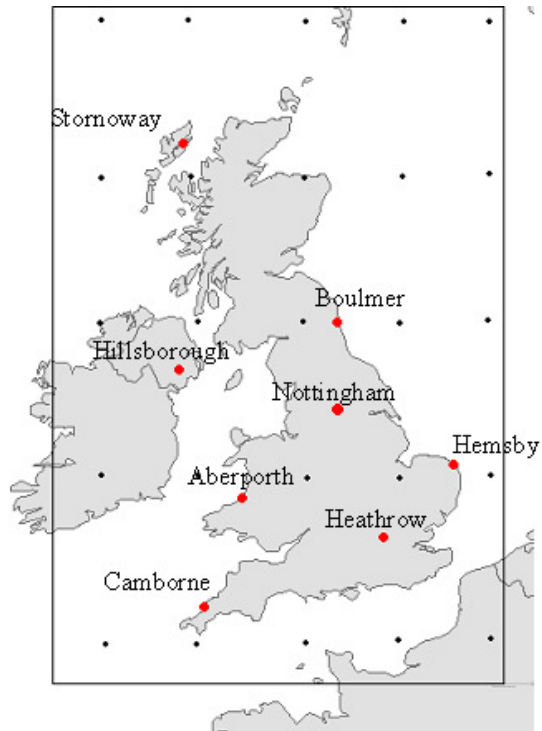
Figure 3-2. Boundaries of the modelling domain used for MM5 simulations. Red dots indicate the location of the meteorological stations selected for comparison with MM5. The black dots represent the centre grid points of the 2.5 x 2.5 degrees ECMWF grid.
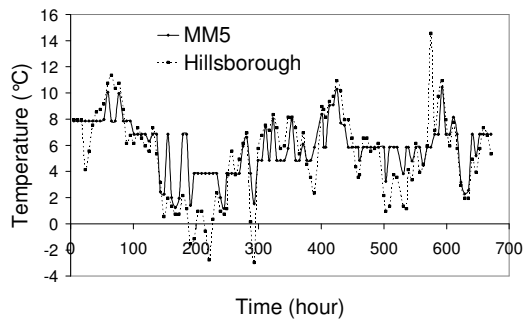
a)   February 1999
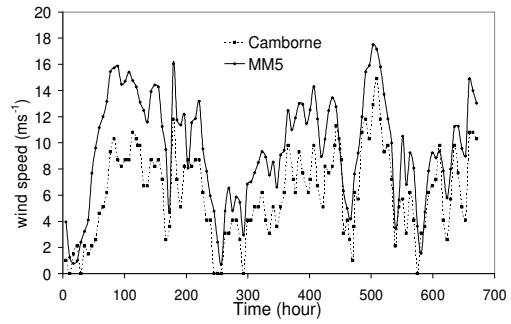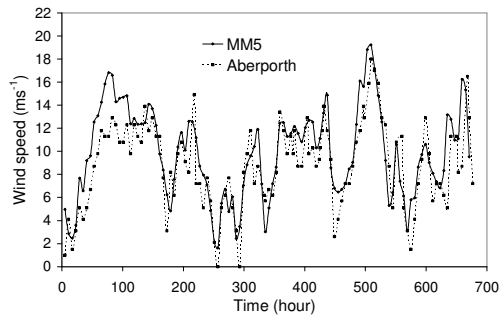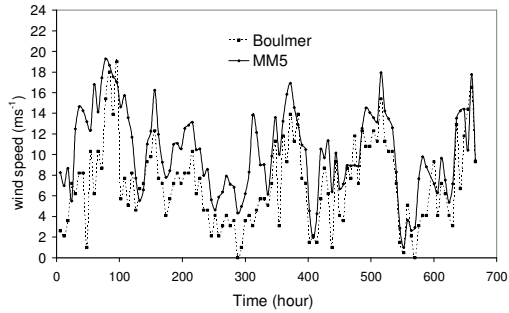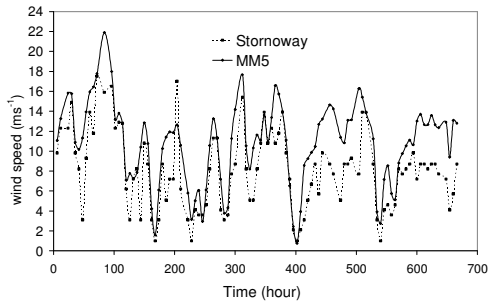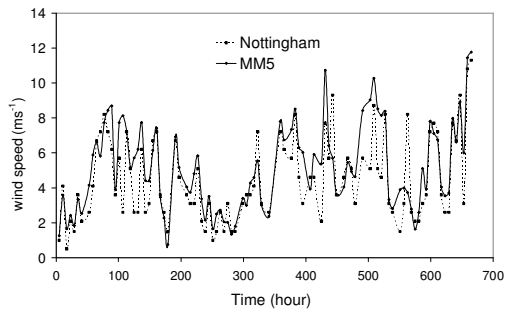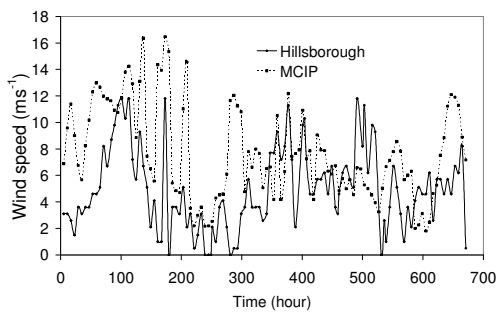
b) June 1999
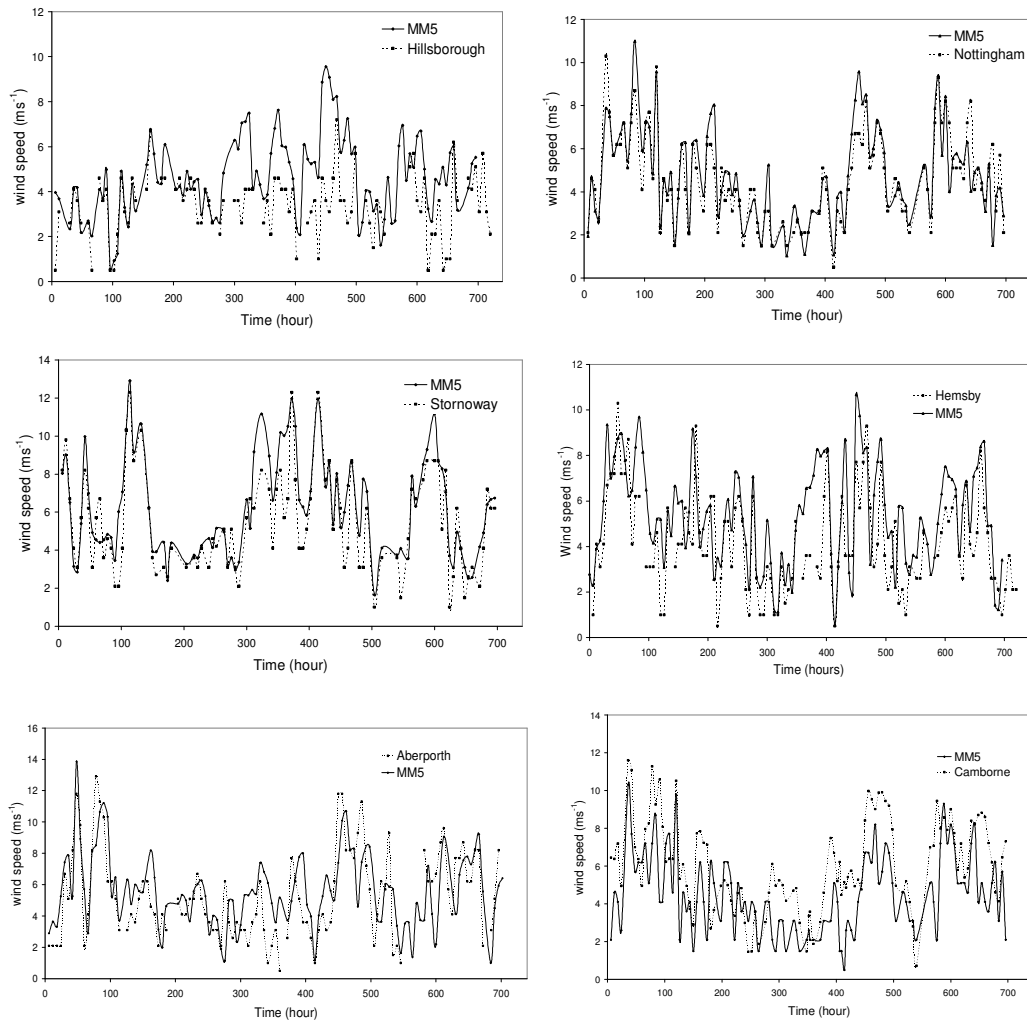
Figure 3-3. Time series of wind speed. Predicted values (black solid lines) are compared versus observations (dashed lines) every 6 hours. Two periods from a) the 1ˢᵗ February 1999 to the 28ᵗʰ February 1999 and from b) the 1ˢᵗ June 1999 to the 29ᵗʰ June 1999 are covered. Wind speed is in ms⁻¹.

a)   February 1999
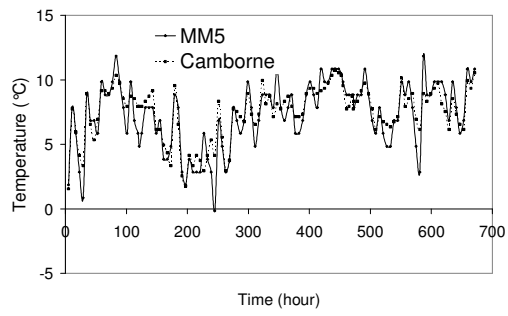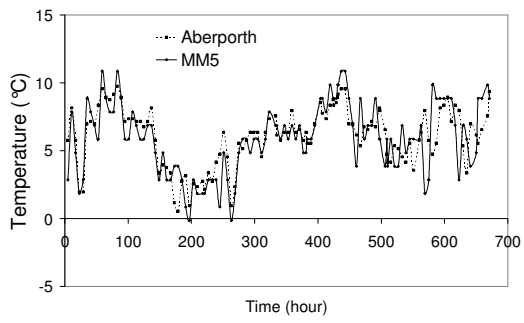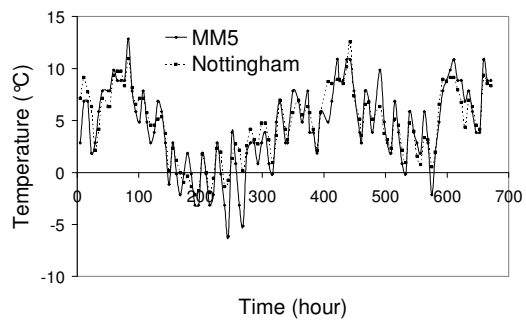
b)   June 1999
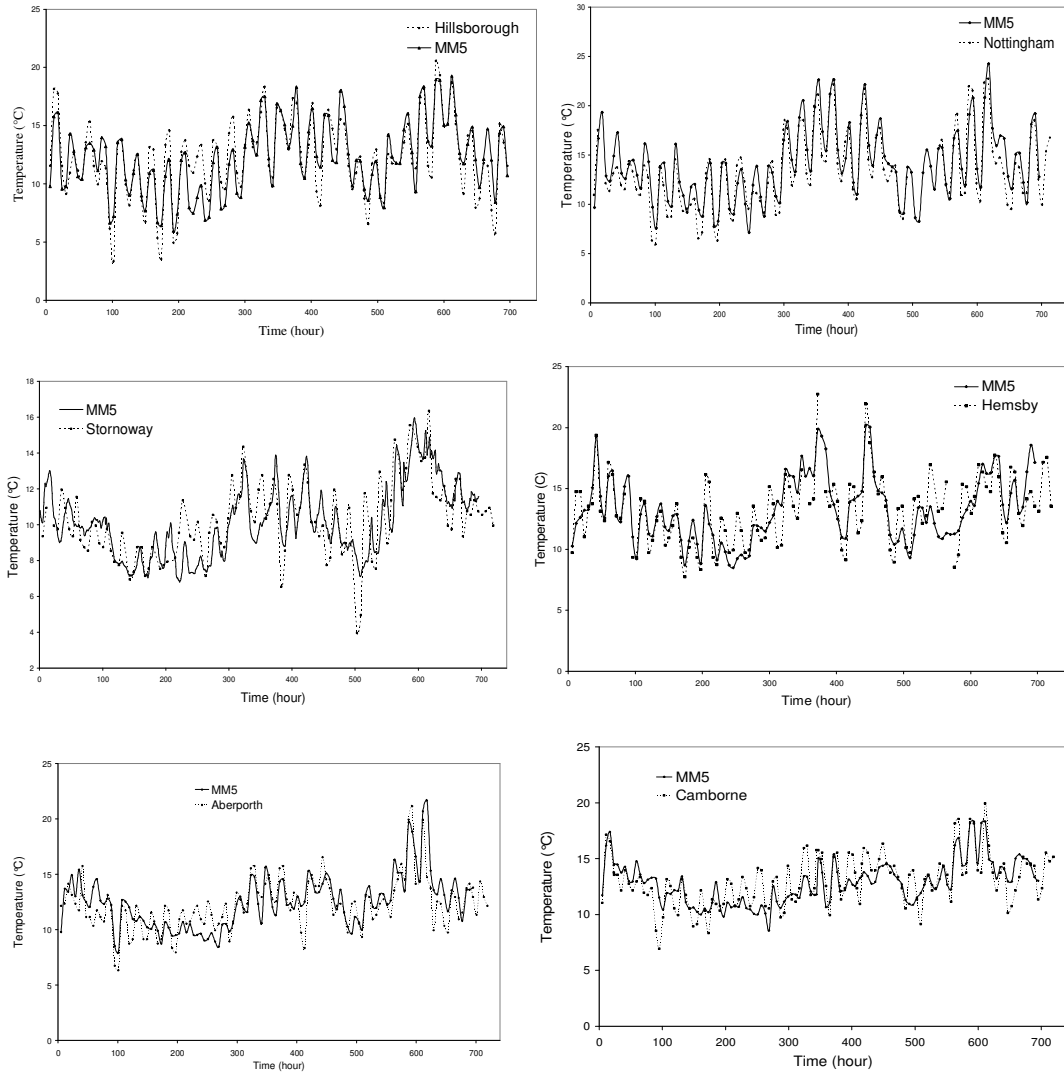
Figure 3-4. Temporal series of surface temperature (ºC) for a) February and b) June 1999. Maximum and minimum daily values are well reproduced by MM5 for all sites.

February 1999
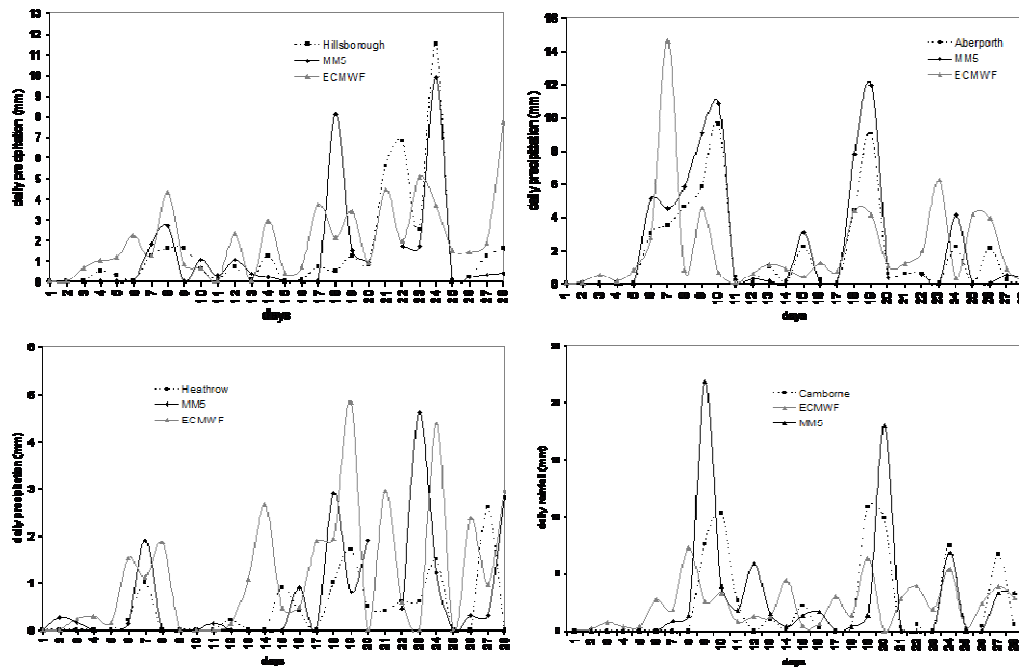
June 1999
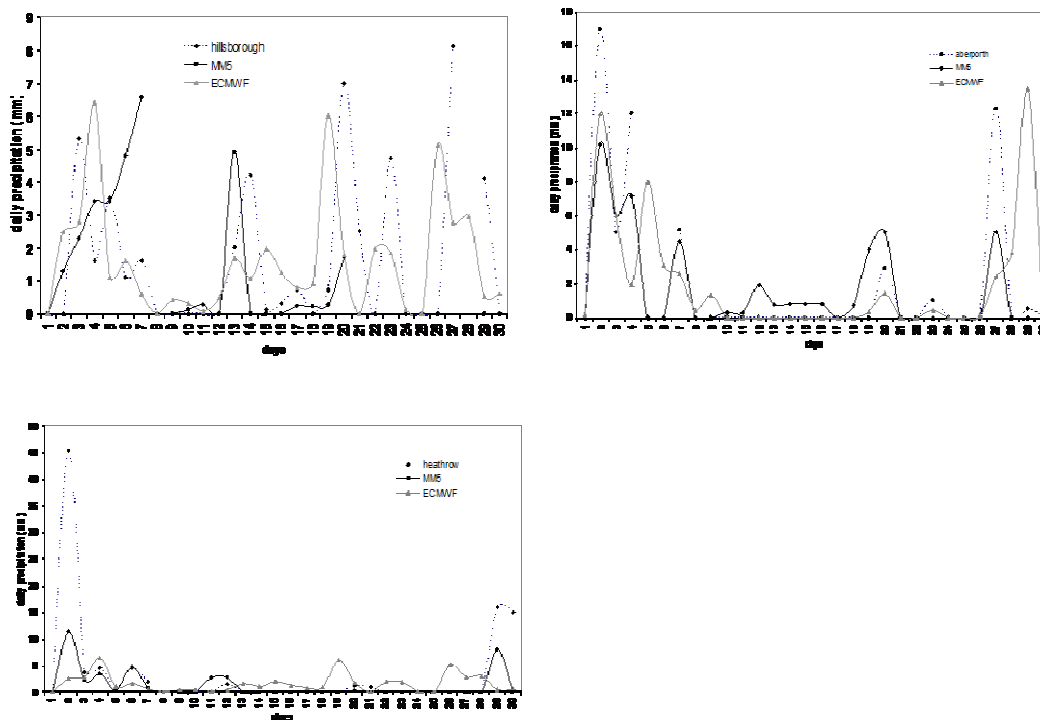
Figure 3-5. Total amount of precipitation (mm) over the hour periods for February 1999 (top) and June 1999 (bottom). Comparison with Hillsborugh (top left), Aberporth (top right), Heathrow (bottom left) and Camborne (bottom right). Data for Camborne are not available in June.

3.3.1.2 <u>Vertical profiles of temperature and dew point temperature</u>

Vertical profiles of temperature and dew point temperature in the lower atmosphere are presented (Figure 3-6). Modelled profiles are compared versus typical day time profiles in Nottingham for several days in June 1999. Observations are radiosonde soundings downloaded from the British Atmospheric Data Centre (http://badc.nerc.ac.uk/data/radiosglobe/). In the 13th and the 1st June the temperature inversion around 2400 m does not appear in the modelled profiles. The probable reason for the inability of MM5 to simulate the inversion is that the model's vertical resolution is only about 200 m at that height so the vertical profile can not be fully resolved. The contour plots of temperature in Nottingham (Figure 3-7) confirm the good performance of MM5, with a small difference between modelled and observed values (approximately between -5 °C and 0 °C). Only the last three days (27th, 28th and 29th) show higher differences (between +5 °C and +15 °C).
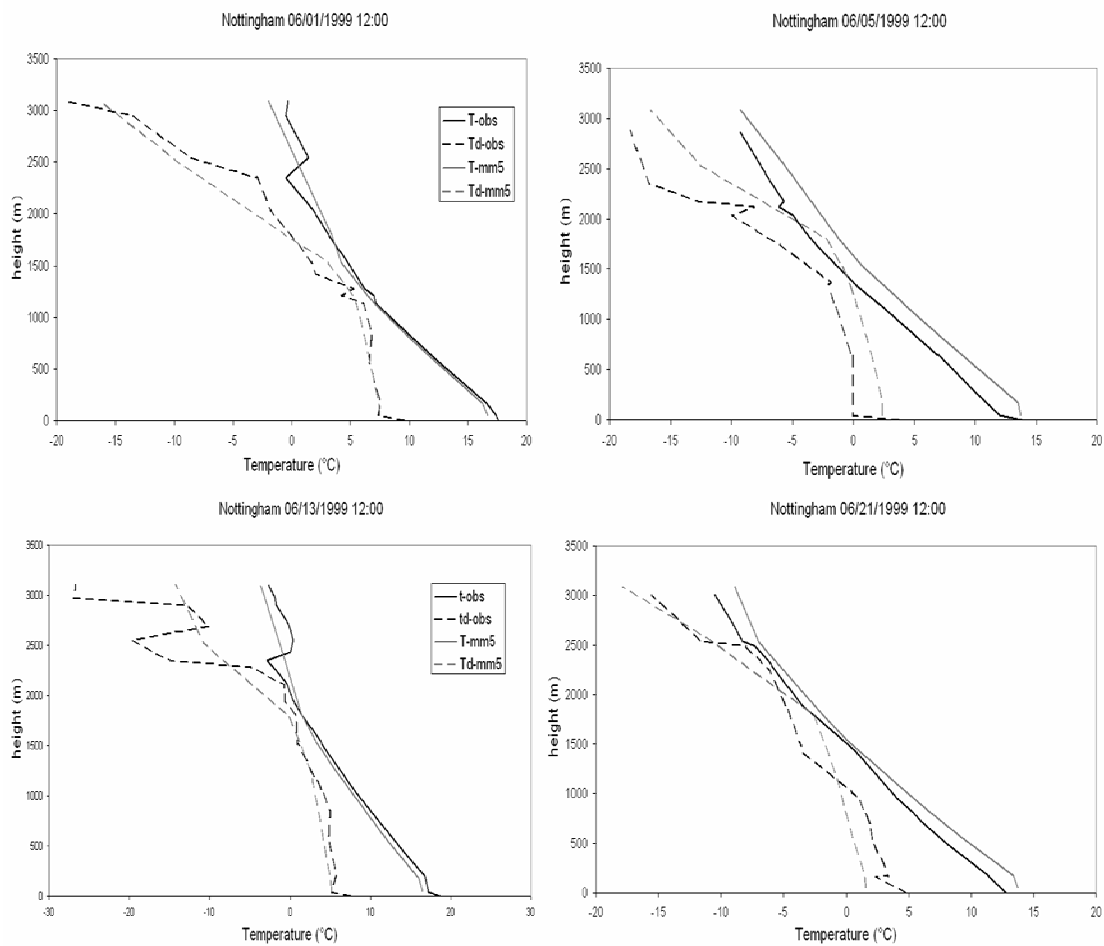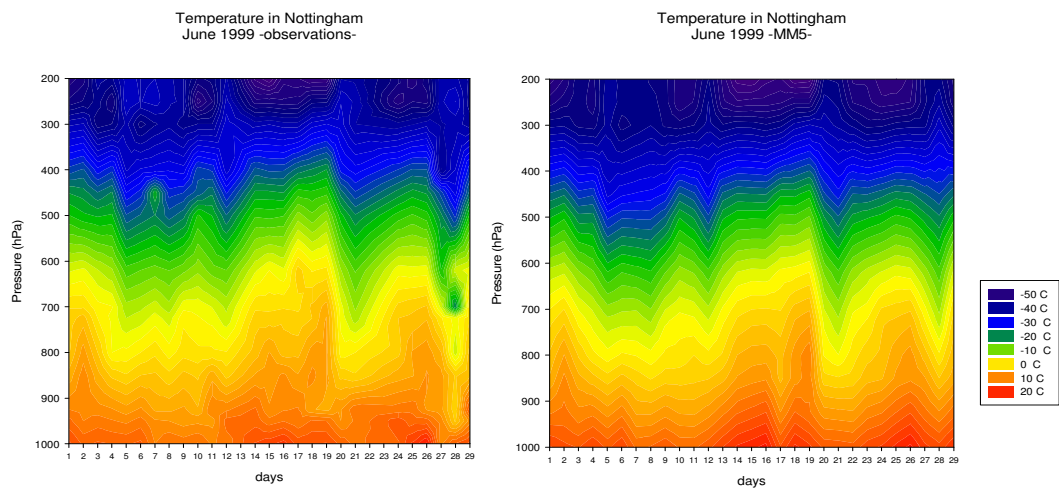
Figure 3-6. Vertical daytime profiles of temperature (T) and dew point temperature (T_d) in the lower atmosphere; modelled profiles (black) are compared with daytime profiles (grey) observed in Nottingham for days 1st, 5th, 13th, 21st June 1999 at noon local time.

Temperature in Nottingham
June 1999 -observations-

Temperature in Nottingham
June 1999 -MM5-

Difference between modelled temperature and observed temperature
Nottingham, June 1999
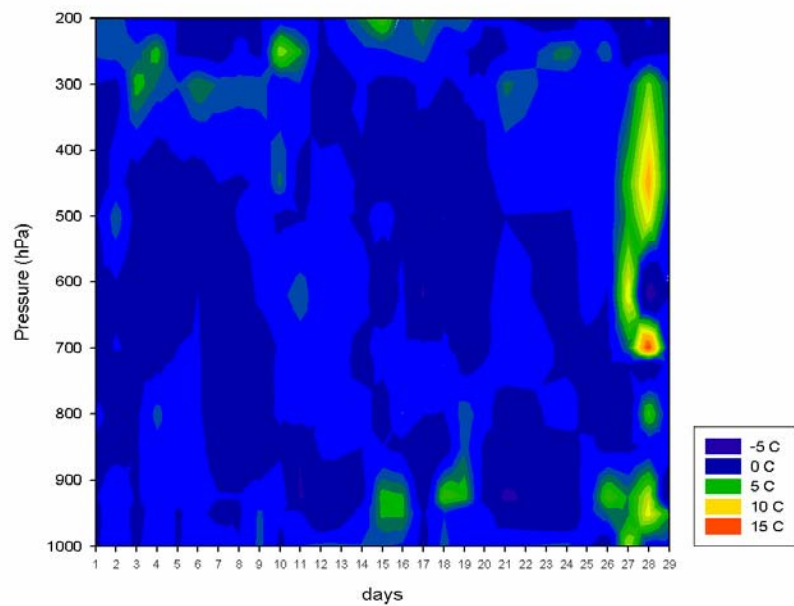
Figure 3-7. Vertical profiles of temperature in Nottingham, June 1999. Air temperature is plotted everyday at noon local time as function of pressure (hPa). The contour plot on the right contains MM5 temperature, the one on the left contains observations from radiosonde soundings. The third plot (bottom) contains the difference between predicted values and observed ones.

3.3.1.3   Surface temperature and precipitation spatial distributions

A comparison of surface temperature and precipitation distribution across the country is performed by comparing monthly maps as predicted by MM5 versus climatology maps from the CRU (Climate Research Unit) TS 1.2 dataset (http://www.cru.uea.ac.uk/cru/data/hrg.htm) (Figure 3-8, Figure 3-9). The dataset consists of monthly gridded observations for the period 1901-2002 covering the whole globe at 10 min. resolution (~ 20 km). Monthly grids were constructed using an "anomaly" approach (New et al., 1999) which attempts to maximize available station data in space and time. Angular distance-weighted (ADW) interpolation was used. This type of interpolation, as a function of latitude and longitude, ignores the influence of elevation (New et al., 2000). The CRU methodology is similar to the one used by Perris and Hollis (2005) for developing the UK Met Office monthly gridded datasets at 5 x 5 km^2 resolution (an example is given in Figure 6-3). In this case a multiple regression with inverse-distance-weighted interpolation was applied. Topographic and geographical factors such as terrain height, percentage of open water and percentage of urban land use were also considered.

MM5 precipitation and temperature have been interpolated from 5 km to the same resolution as CRU. Both MM5 and CRU can reproduce the effects of orographic enhancement of precipitation over hills and mountains in the Western UK. Precipitation is generally underestimated by MM5 of approximately 50 cm, with areas of larger under-prediction (between 120 and 200 cm) in the Western UK, Scotland and Western Ireland in both months. Surface temperature is well reproduced by MM5: the distribution is very similar to the CRU one, even if the model slightly overestimates (between 0 °C and 2 °C) in June and it underestimates in February (between -2 °C and 0 °C)
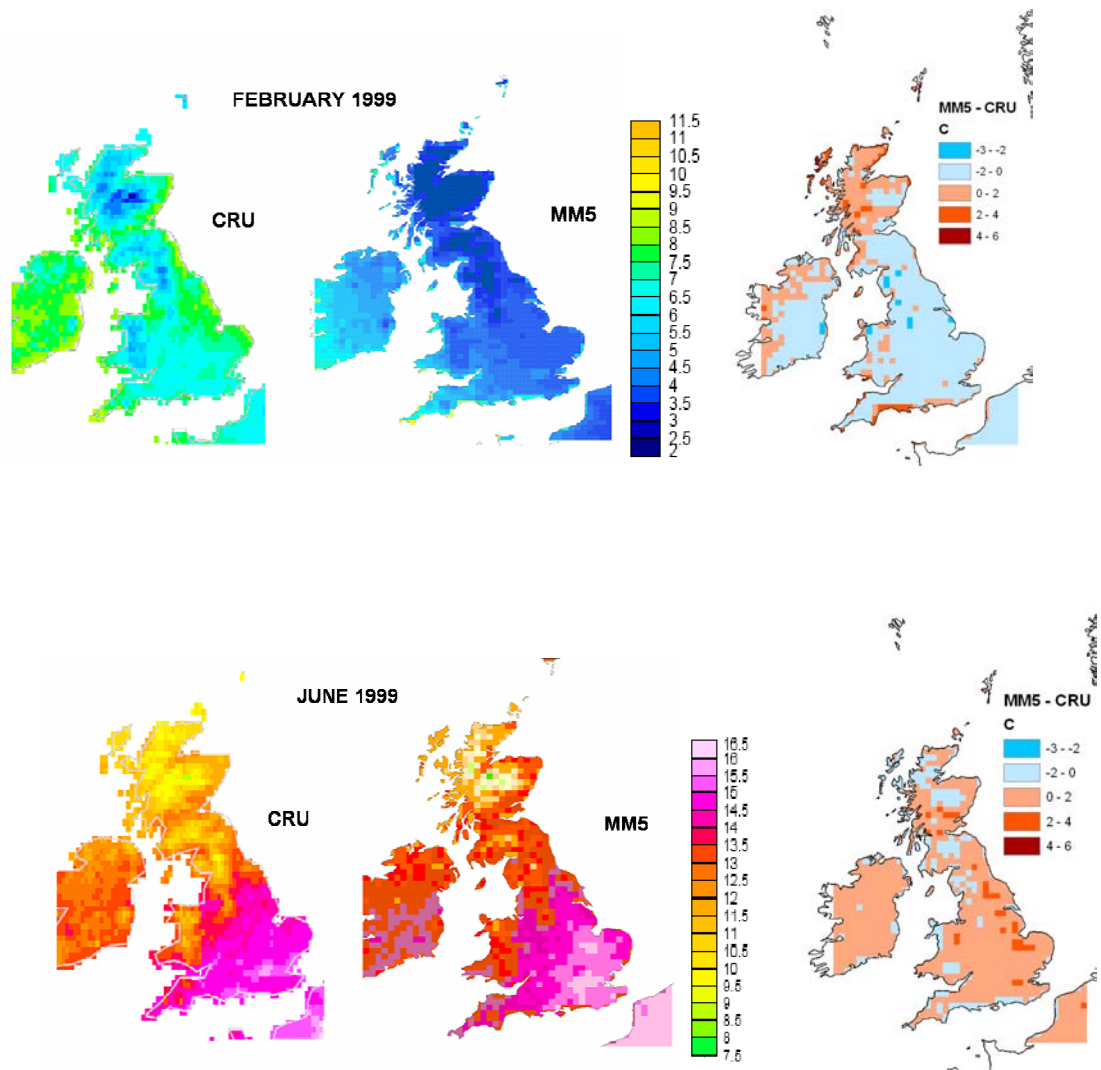
Figure 3-8. Maps of surface temperature over the UK for February 1999 (top) and June 1999 (bottom). Comparison between CRU images (left) and MM5 maps (centre).The third plot on the right represents the difference between MM5 and CRU in every grid cell. Temperature is in (C^o).
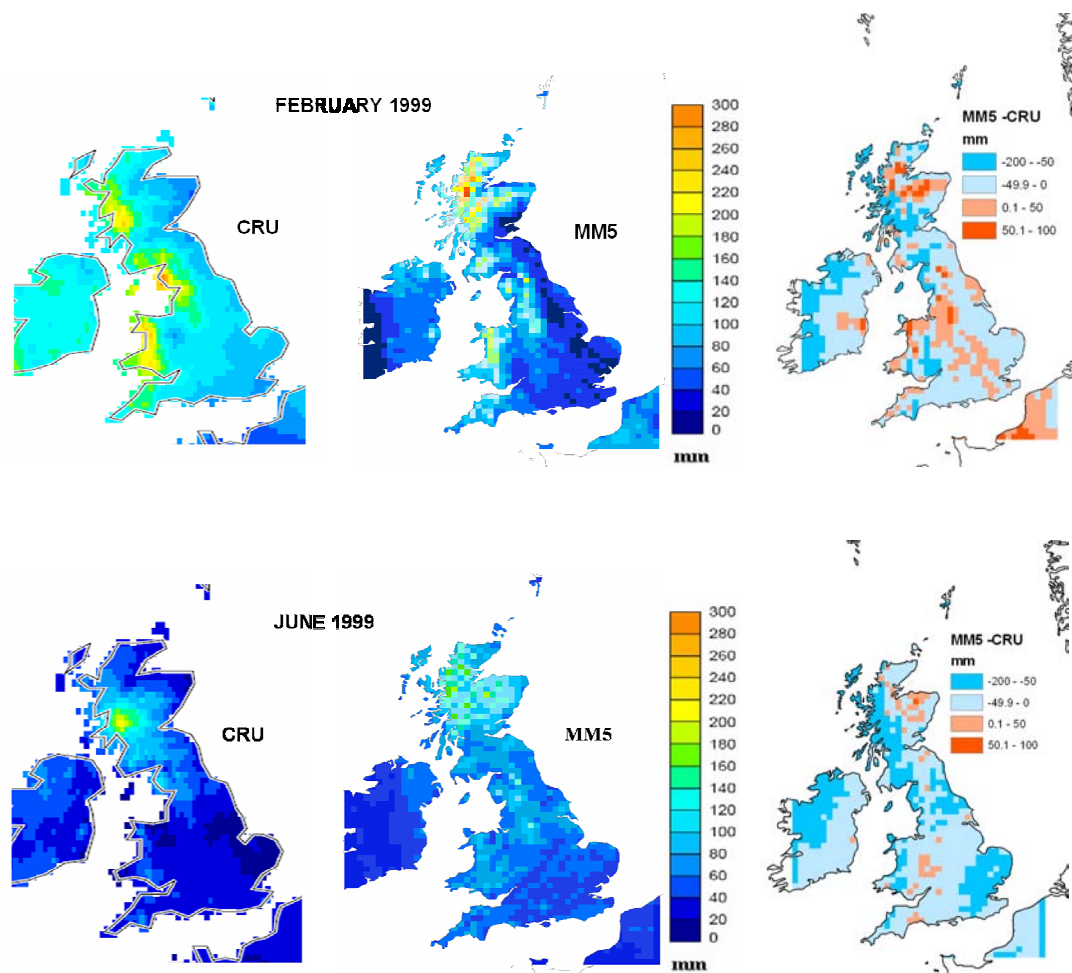
Figure 3-9. As Figure 3-8, but precipitation (mm).

3.3.2 Statistical Analysis

3.3.2.1 <u>Taylor diagrams</u>

For every station, the main performance indicators (Table 3-1) are calculated using 6-hourly (wind speed and temperature) and daily (rainfall) observations as described in Section 3.1.1.1. Taylor diagrams (Taylor, 2001) are used to visualize the standard deviation ratio (*SR*), correlation coefficent (*R*) and the Root Mean Square Error (*RMS*).

$$FB = \frac{\overline{C_o} - \overline{C_P}}{0.5\,(\overline{C_o} + \overline{C_P})} \qquad \text{fractional bias} \qquad 0$$

$$B = \overline{C_p} - \overline{C_o} \qquad \text{Bias} \qquad 0$$

$$RMS = \sqrt{\overline{(C_O - C_P)^2}} \qquad \text{root mean square error} \qquad 0$$

$$R = \frac{\overline{(C_O - \overline{C_O})(C_P - \overline{C_P})}}{\sigma_{C_P}\sigma_{C_o}} \qquad \text{correlation coefficient} \qquad 1$$

$$SR = \frac{\sigma_{C_P}}{\sigma_{C_o}} \qquad \text{Standard deviation ratio} \qquad 1$$

Perfect model

Table 3-1. Performance indicators used in MM5 evaluation. C_p and C_o are the predicted and the observed value respectively. Overbars signify time or space means. Fractional and absolute biases indicate only systematic errors, whereas RMS reflects both systematic and random errors. The correlation coefficient indicates the linearity between the two values. SR compares the standard deviation of the modelled data set (σ_{C_p}) with the one of the measured data set (σ_{C_o}). In other words SR describes the variability (dispersion) of the modelled data compared with the observed data.

On a Taylor plot (Taylor, 2001; example shown in Figure 3-10) a dot represents the ratio (*SR*) between the modelled standard deviation and the observed one. S*R* is proportional to the radial distance from the origin; better results will be given by points having *SR* close to 1 (reference dashed line). The degree of angular rotation from the horizontal *x*-axis indicates the correlation coefficient (*R*), whereas the dashed semi-circles represent the root mean square error (*RMS*). In many cases a model may have a good correlation with observations (points close to the *x*-axis) but the wrong spatial variability (points far from the reference dashed line). The perfect model would be represented by dots laying on the intersection between the horizontal *x*-axis and the dashed reference line (*SR* equal 1, *R* and *RMS* equal 0).
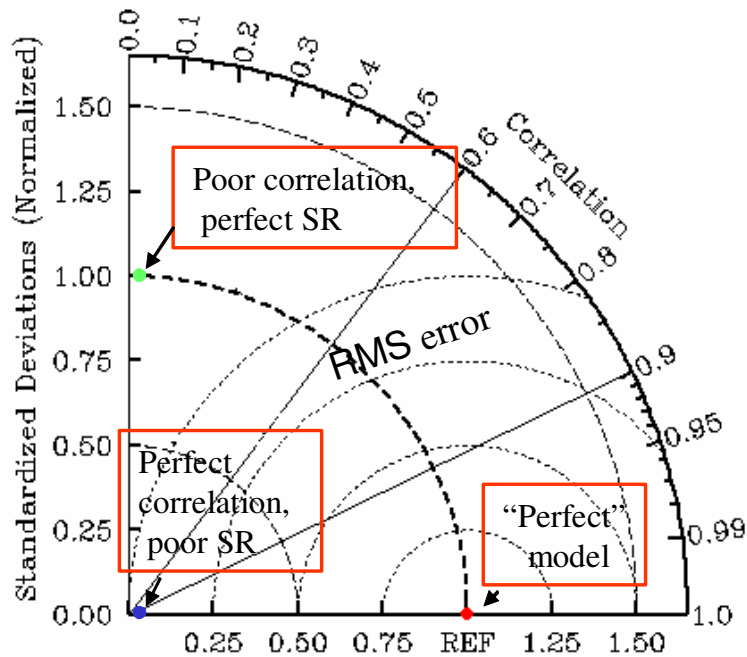
Figure 3-10. Sample Taylor diagram. The red dot represents the "perfect" model, the blue one a model having a good correlation with observations (points close to the x-axis) but the wrong variability (points far from the reference dashed line) and finally the green dot represents a model having poor correlation but the right standard deviation ratio.

Taylor plots for wind speed, rainfall and temperature are shown in Figure 3-11. These are based on 6-hourly data (Figures 3-3, 3-4) for wind speed and temperature and on daily data (Figure 3-5) for rainfall.

Wind speed

The analysis of the diagram for wind speed in June 1999 (Figure 3-11a) shows MM5 gives a better agreement than ECMWF for all stations but Camborne (5), where the SR is very close to the ECMWF one. The MM5 correlation coefficient is between 0.5 and 0.9 for all sites whereas the ECMWF correlation coefficients are lower. The best comparisons are with Nottingham (3) and Stornoway (4). The MM5 correlation coefficient is about 0.8 in both cases and SR is close to 1. The RMS (dashed lines) is about 2 ms^{-1}. In the comparison with Hillsborough both models have the poorest agreement: there is a high modelled variability (with a standard deviation of about 1.80 ms^{-1} compared to the observed value of 1.37 ms^{-1}) and the correlation coefficient is low (about 0.5).

In February (Figure 3-11b) the ratio between predicted and observed standard deviations is close to 1 in most cases, indicating a general good simulation from both ECMWF and MM5 in modelling wind speed variability in the winter period. In terms of correlation coefficient, MM5 performs better than ECMWF (all MM5 coefficients are higher than ECMWF ones, except for Hillsborough).

Surface temperature

Taylor diagrams for temperature (Figure 3-11c, Figure 3-11d) show in both months the correlation coefficient between modeled and observed temporal series is between 0.5 and 0.95 for both models. MM5 more accurately represents 6-hourly variability, especially in June.

Precipitation

In June (Figure 3-11e) MM5 performs better than ECMWF for Aberporth and Camborne. There is also a better correlation between MM5 values and Heathrow observations but *SR* is lower (0.6 compared to 0.9 for ECMWF). In February (Figure 3-11f) *RMS* and *R* present better values for MM5 compared to ECMWF, whereas the standard deviation ratio is close between the two.
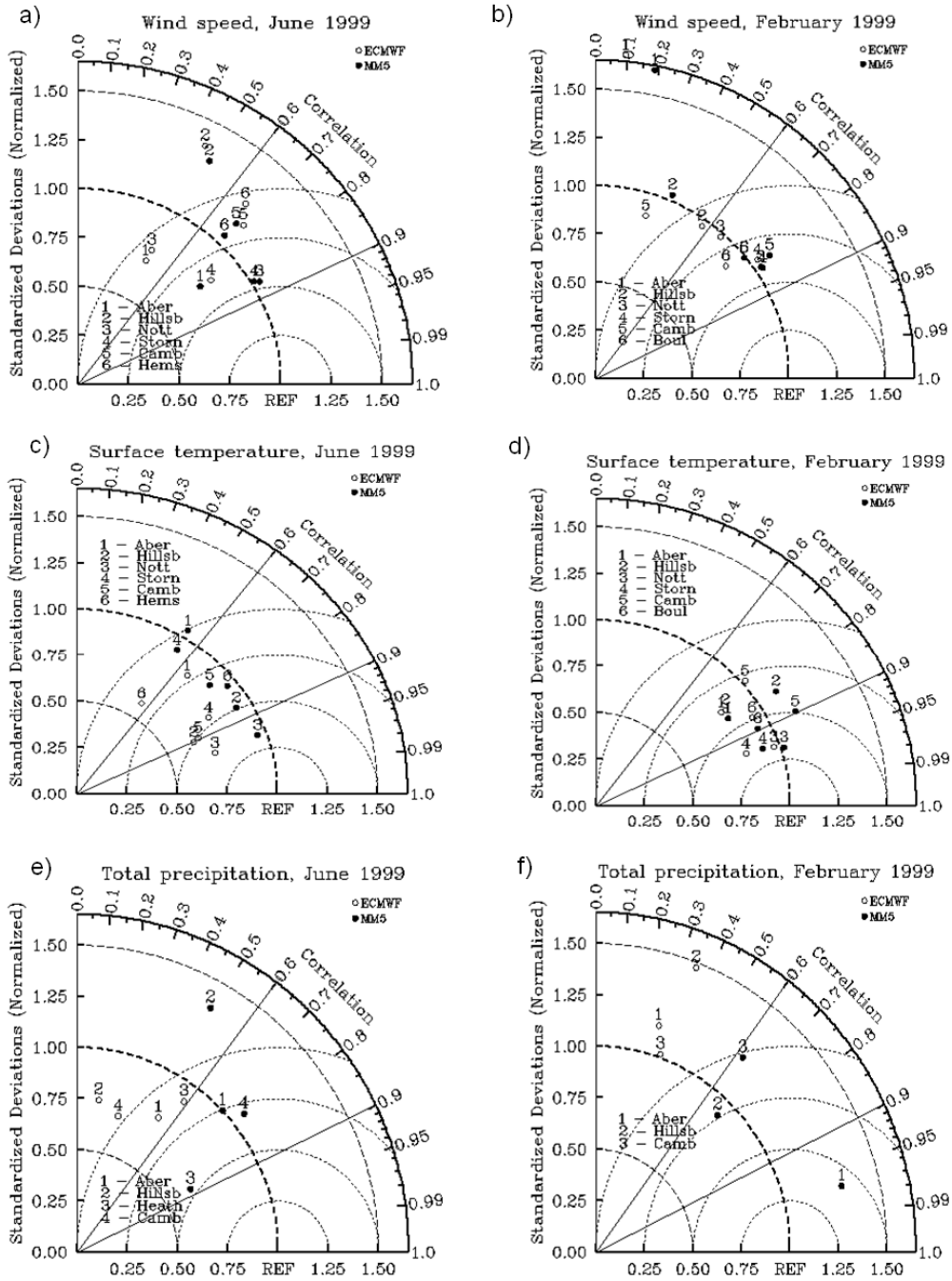
Figure 3-11. Taylor diagrams for June 1999 and February 1999. The dots represent the ratio between MM5 standard deviation and the observed one (black) and between ECMWF standard deviation and the observed one (white).

3.3.2.2 Systematic errors

In terms of absolute bias and fractional bias (Figure 3-12, Figure 3-13), the systematic error of all variables is generally lower for MM5. In June the fractional bias for rainfall (Figure 3-12b) is between 0.1 and 0.2 for MM5 and between 0.3 and 0.5 for ECMWF. In February (Figure 3-12a) rainfall is overestimated by MM5 with a fractional bias of approximately -0.3. Wind speed is overestimated by MM5 of approximately 30% in both months. The absolute bias on MM5 for temperature is approximately between -0.2 ºC (excluding Nottingham station) and 0.1 ºC in June and between -0.5 ºC and 0.1 ºC in February.
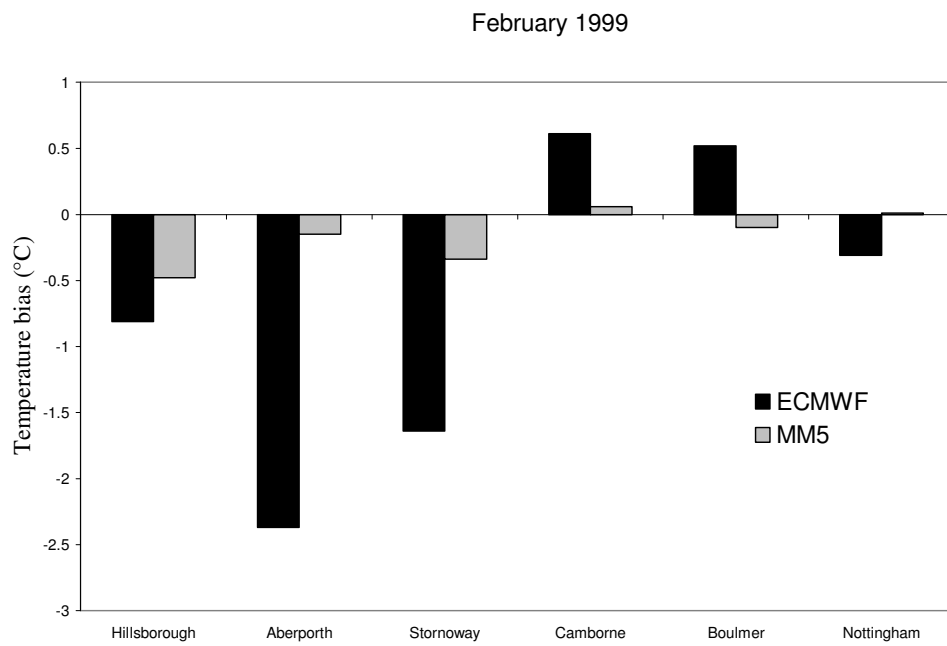
a)

February 1999

b)

June 1999
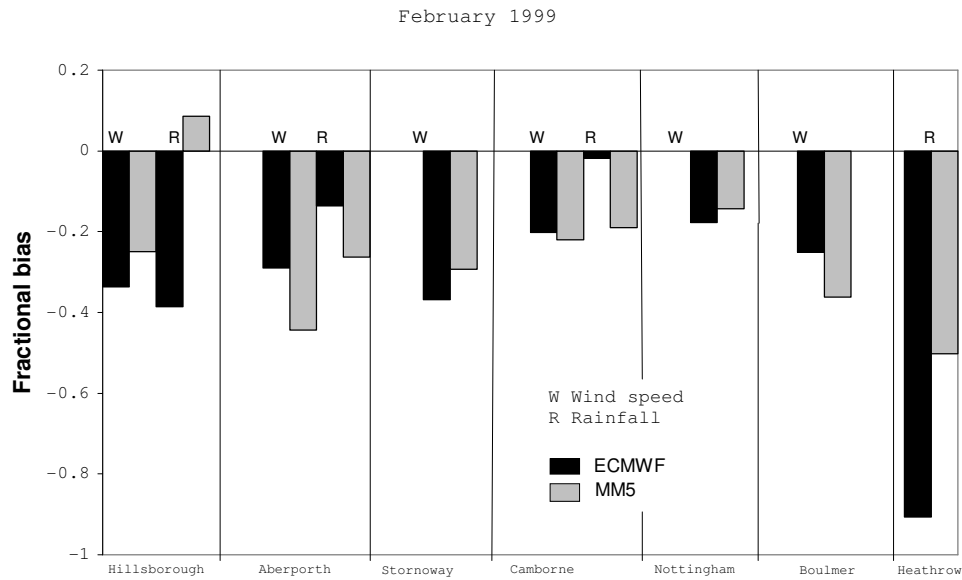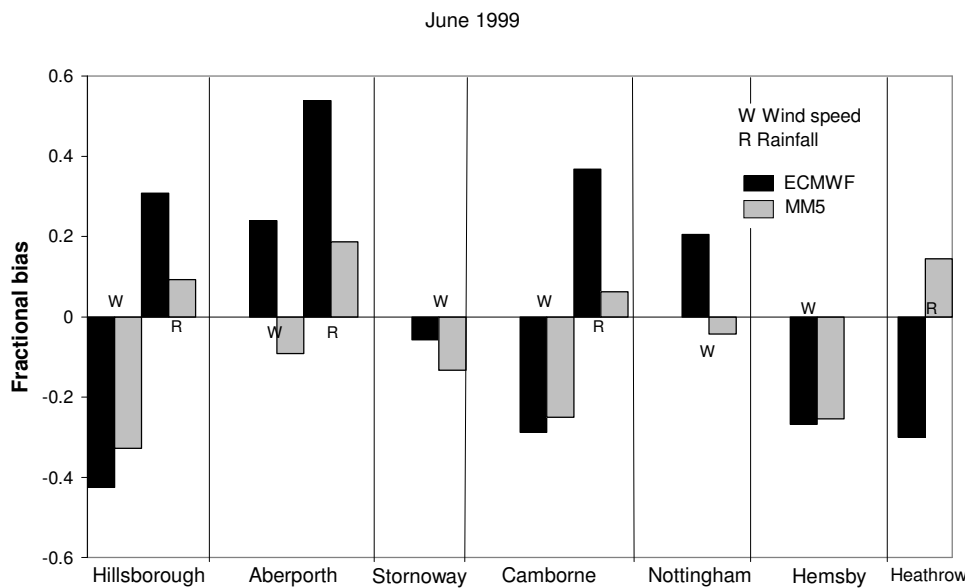
Figure 3-12. Fractional bias values of rainfall (R) and wind speed (W) for ECMWF (black) and MM5 (grey) in June and February 1999.

a)

February 1999
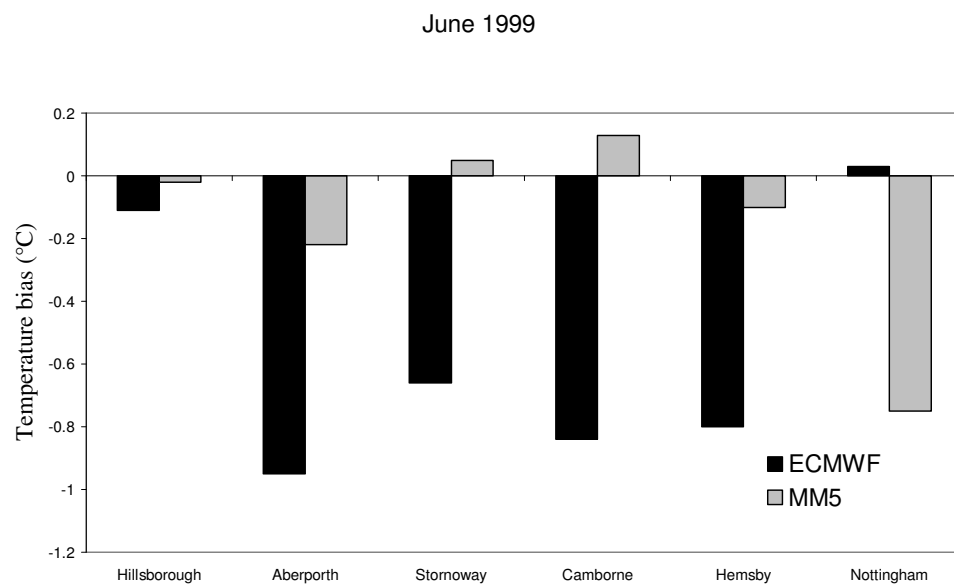

b)

June 1999

Figure 3-13. Absolute bias values of temperature (ºC) for ECMWF (black) and MM5 (grey) in a) June and b) February 1999.

3.3.2.3 Scatter plots

The improved correlation between MM5 and observations (compared to ECMWF) is also confirmed by the scatter plots (Figure 3-14, Figure 3-15) of temperature and wind speed 6-hourly data. The graphs also show a slight overestimation of wind speed by MM5 for most of the sites, whereas the model clearly overestimates temperature for low values (below ~14 ºC) and underestimates it for high values (above ~20 ºC).
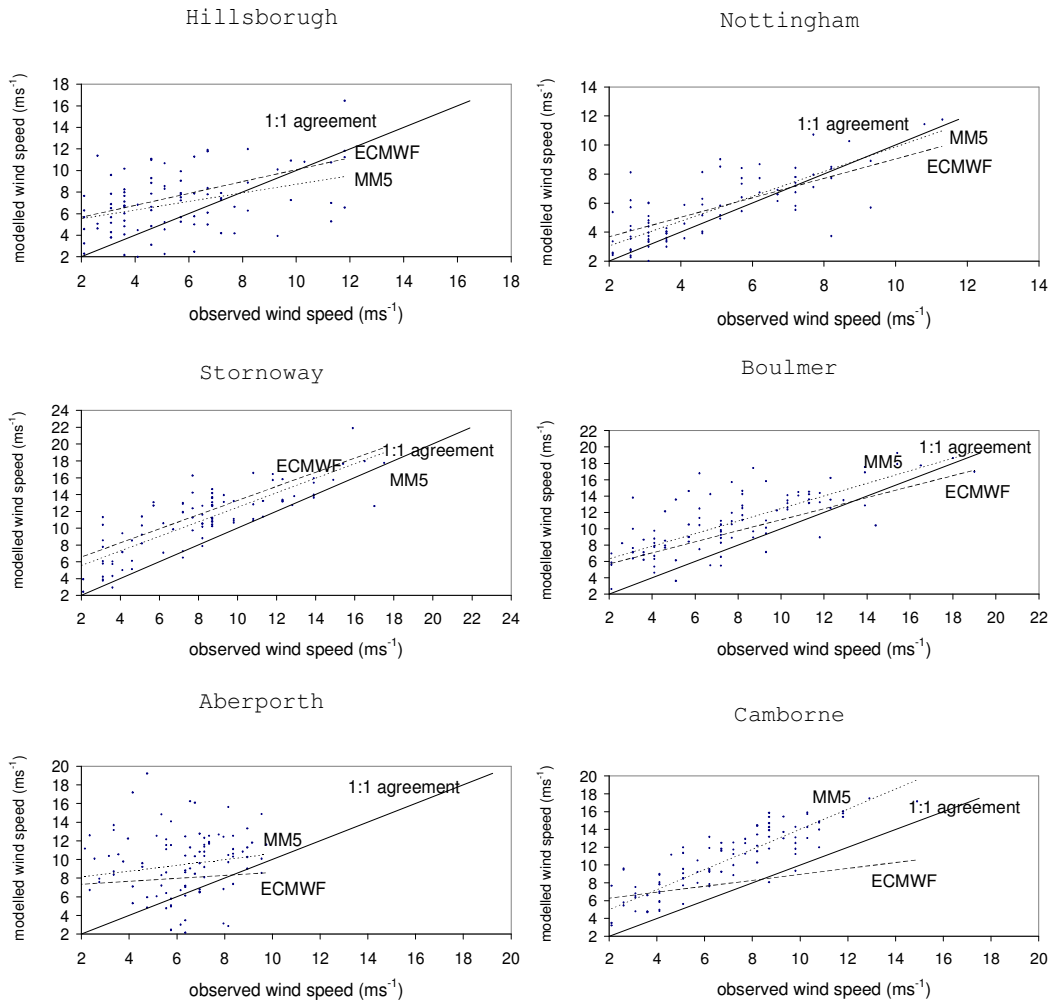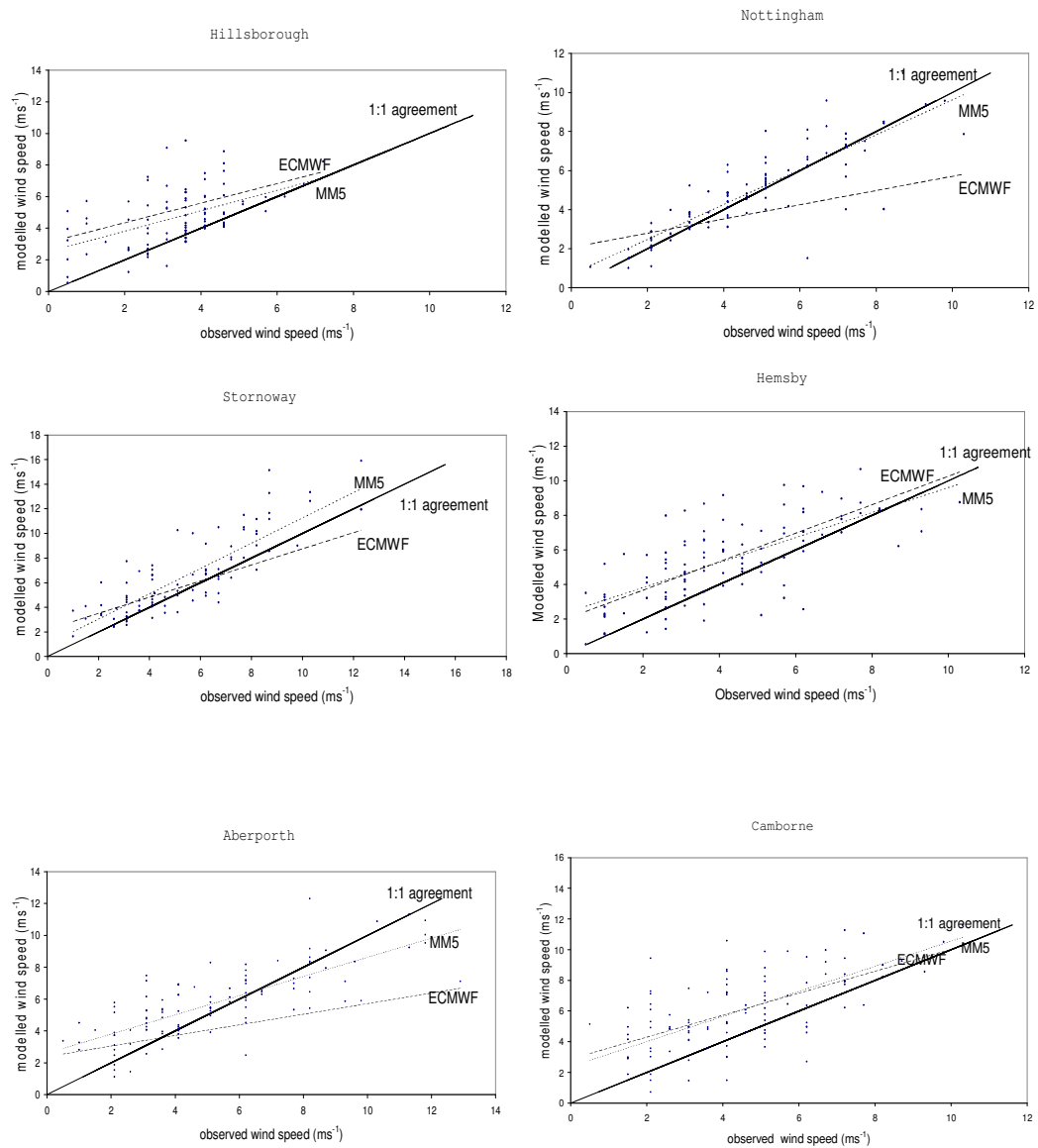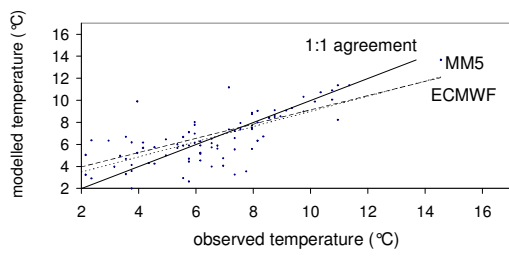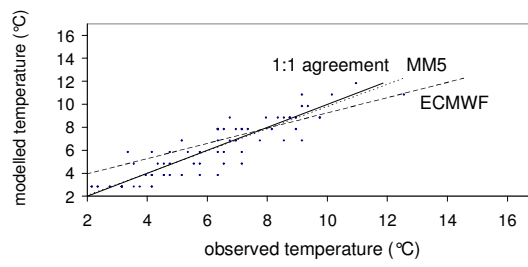
February 1999

June 1999

Figure 3-14. Scatter plots of modelled and observed 6-hourly wind speed at 6 sites in February and June 1999. The solid line indicates a 1:1 agreement between observed and modelled values. The dotted line represents the best linear fit between measured values and MM5 predictions. The scatter plots highlight the better correlation between MM5 predictions and observations, compared with the ECMWF best linear fit (dashed line). The graphs also show a slight overestimation of wind speed by MM5 for most of the sites.
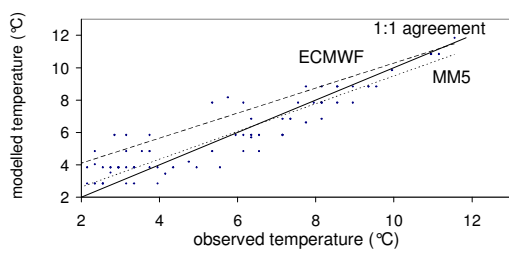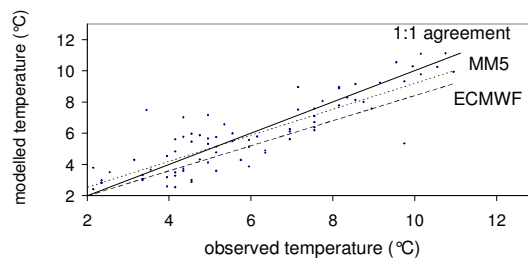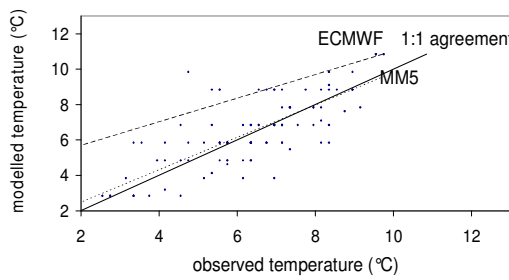
February 1999

Hillsborough

Nottingham
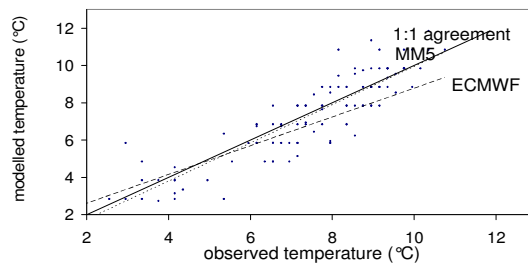

Stornoway

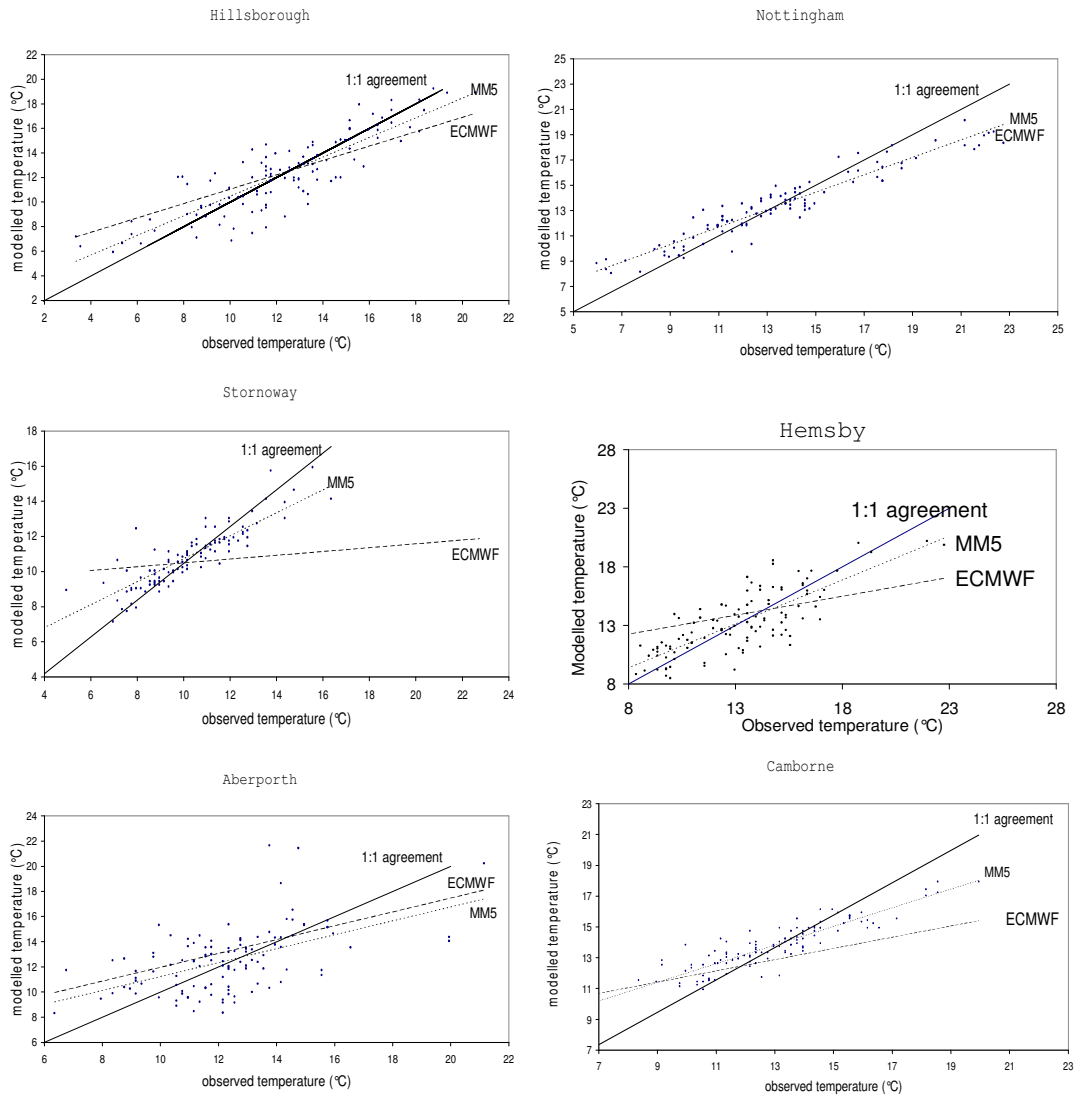### Boulmer

Aberporth

Camborne

June 1999

Figure 3-15. As for Figure 3-14, but for surface temperature in February and June 1999 at 6 stations.

3.3.3   A One-year Simulation with MM5

Even if this work mainly focused on two specific months (those selected for performing air pollution studies with CMAQ), a 1-year simulation with MM5 was also performed. This helps to confirm or disprove the monthly results and it permits to achieve more solid conclusions in MM5 evaluation. Temperature and wind speed for the whole year were compared every 24 hours versus daily observations in several points of the domain (Figure 3-16, Figure 3-17). The annual trends confirm the good agreement as observed in the monthly analysis with a correlation coefficient between 0.7 and 0.9 for temperature temporal series (Table 3-2) and between 0.6 and 0.9 for wind speed temporal series (Table 3-3). MM5 generally performs better than ECMWF. The long term run also confirms the tendency of MM5 in overestimating temperature for low values and underestimating it for high values (Figure 3-18).

The scatter plots in Figures 3-19 and 3-20 show the total annual precipitation and the surface temperature as predicted by MM5 versus CRU data for all the points of the domain; the best MM5 linear fit (black dashed line) in Figure 3-20 indicates rainfall is underestimated. The areas of larger under-prediction (between 120 and 200 cm) mainly involve the western area of the UK and Ireland (Figure 3-21). Regions of lower temperature (between 1 ºC and 2 ºC) are also visible in England and Ireland (Figure 3-22). The difference between MM5 and CRU surface temperature is close to zero in the other areas of the UK.

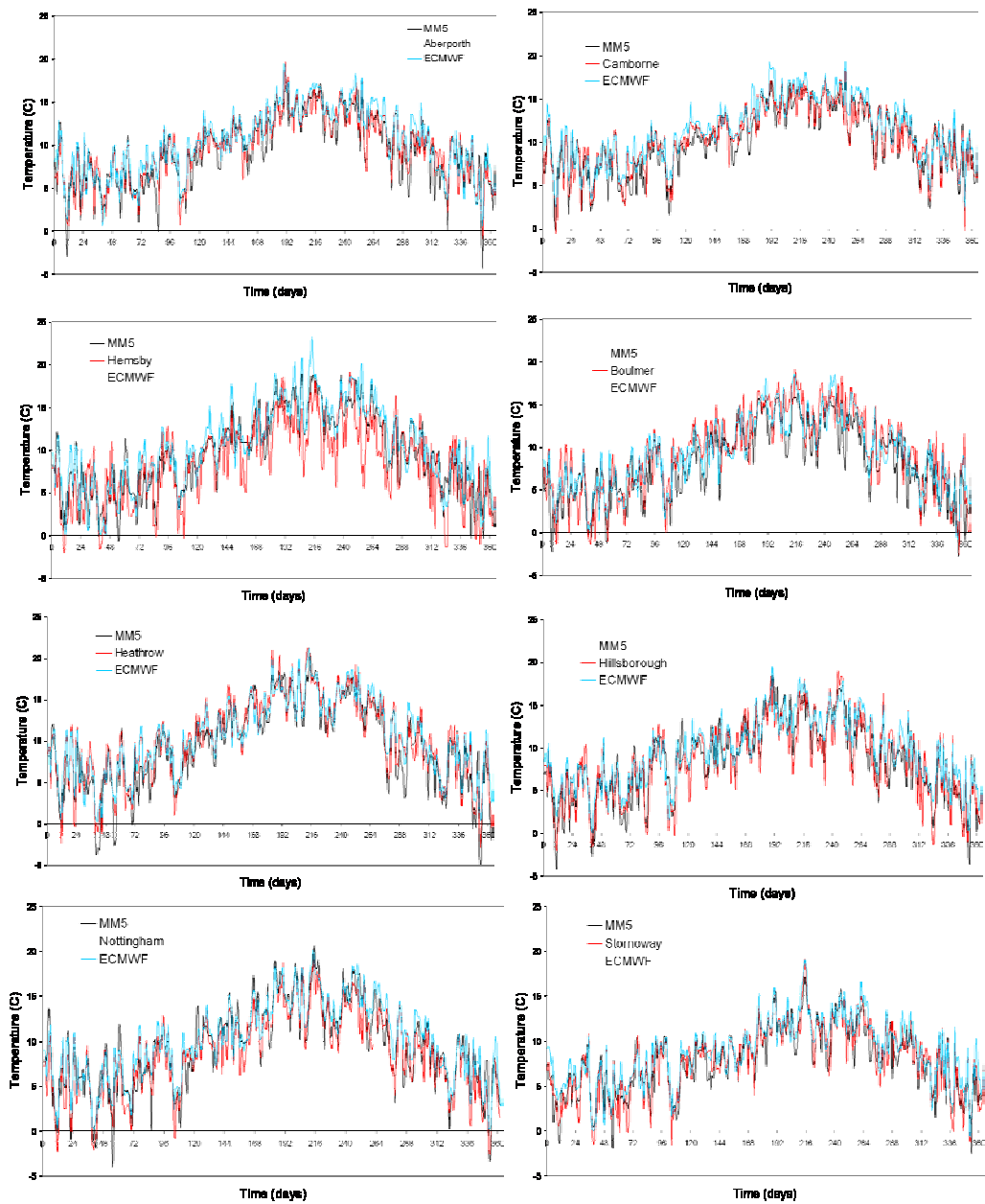*Figure 3-16. Temporal series of temperature for the whole year. Daily observations (red) of surface temperature are compared to MM5 temperature (black) and ECMWF (blue). Units are ºC.*
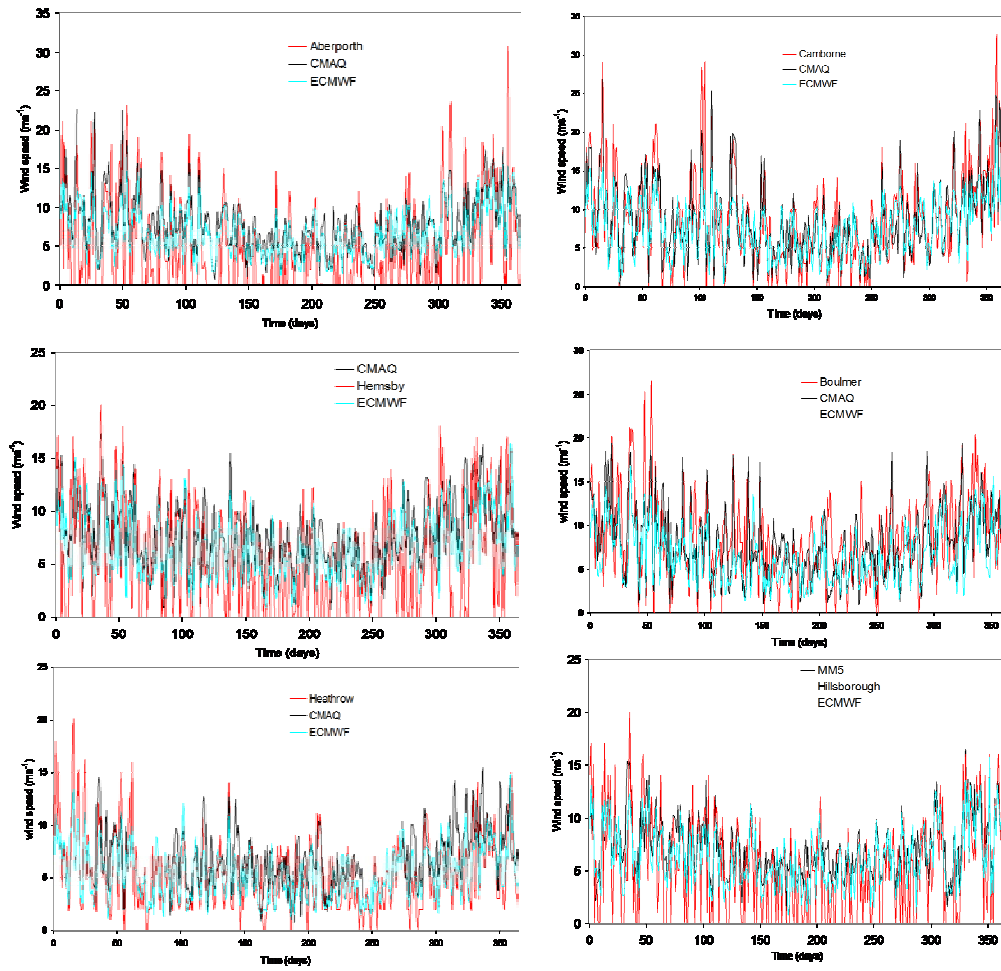
Figure 3-17. As Figure 3-16, but wind speed (ms^{-1})
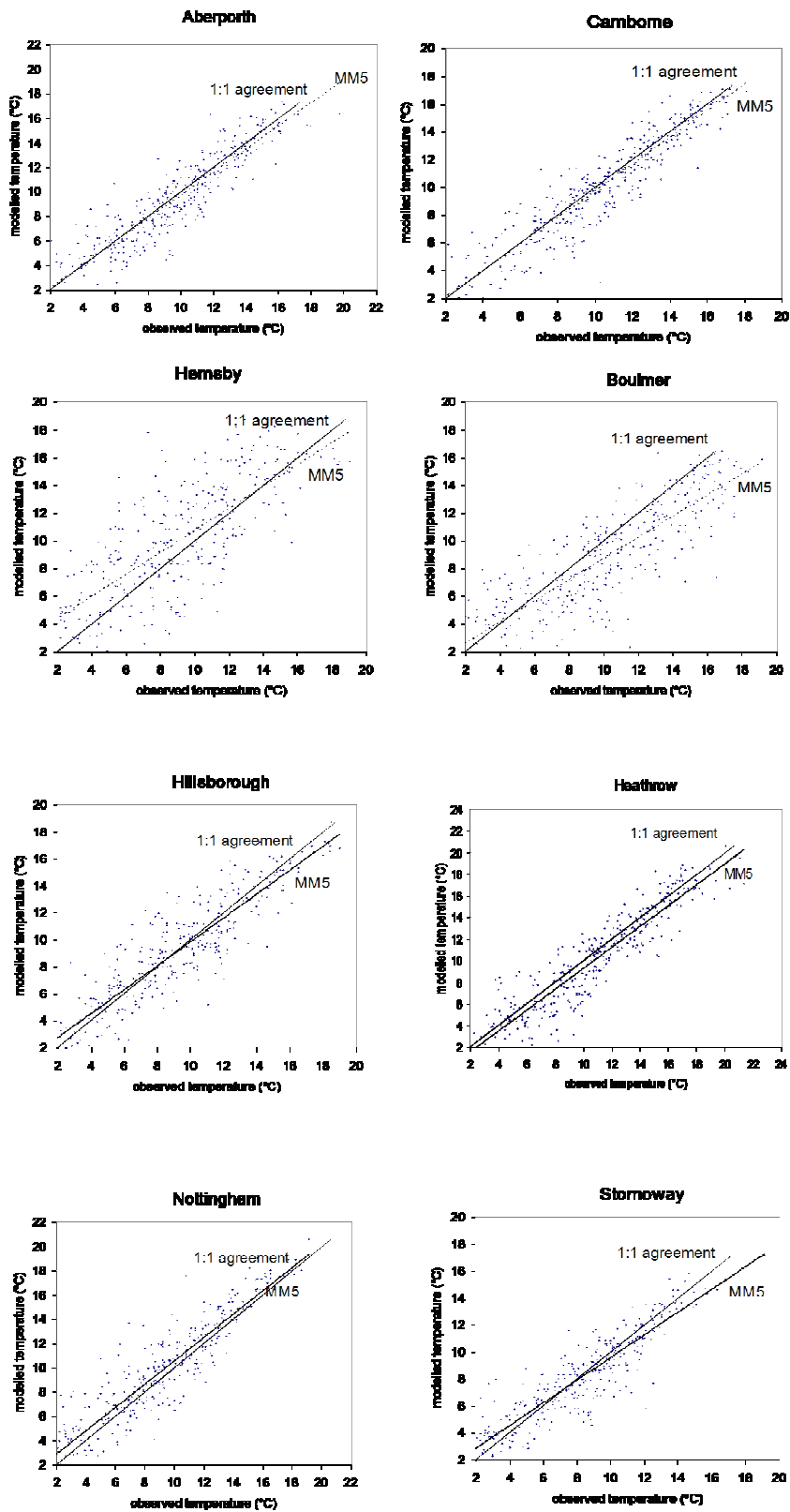
Figure 3-18. Scatter plots of modelled temperature versus observed temperature. MM5 tends to underestimate maximum values of temperature and to overestimate the minima.

	Aberporth	Camborne	Boulmer	Hillsborough	Hemsby	Nottingham	Heathrow	Stornoway
R	0.950	0.923	0.882	0.904	0.774	0.923	0.931	0.912
Intercept	0.237	0.137	0.904	0.945	2.777	0.885	-0.423	1.104
Slope	0.955	0.959	0.787	0.889	0.794	0.968	0.971	0.847

Table 3-2. Results of the best linear fit between measured and observed surface temperature temporal series. Data are compared every 24 hours for year 1999.

	Aberporth	Camborne	Boulmer	Hillsborough	Hemsby	Heathrow
R	0.803	0.852	0.456	0.813	0.665	0.828
Intercept	3.067	3.971	5.372	4.929	6.296	4.820
Slope	0.354	0.426	0.232	0.408	0.276	0.394

Table 3-3. As Table 3-2, but wind speed (ms^{-1})
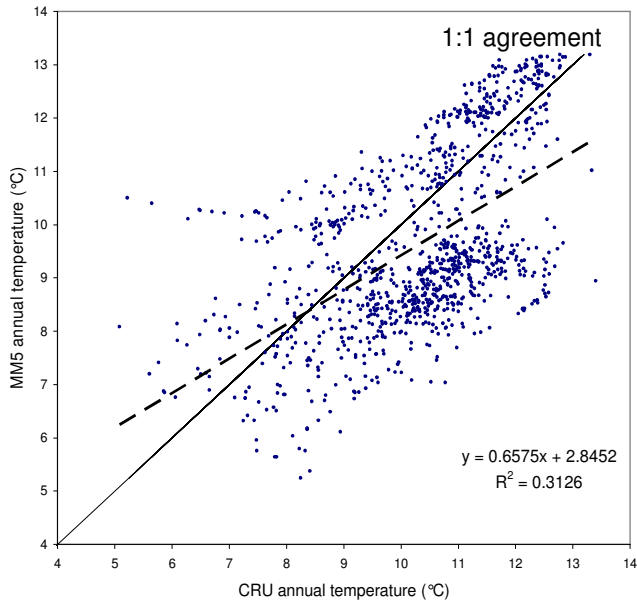
Figure 3-19. Scatter plot of average annual temperature as modelled by MM5 versus CRU data. The dashed line represents the best linear fit. Grid cells over the sea have been excluded.
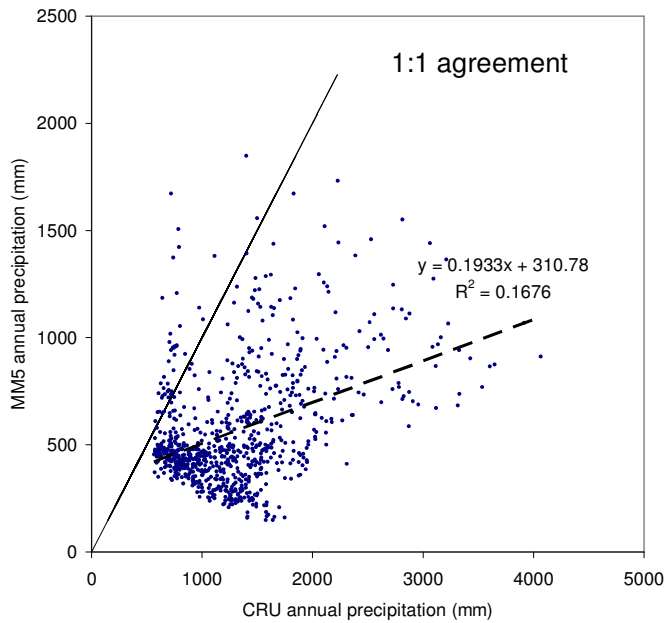
Figure 3-20. As Figure 3-19,, but average annual precipitation (mm).
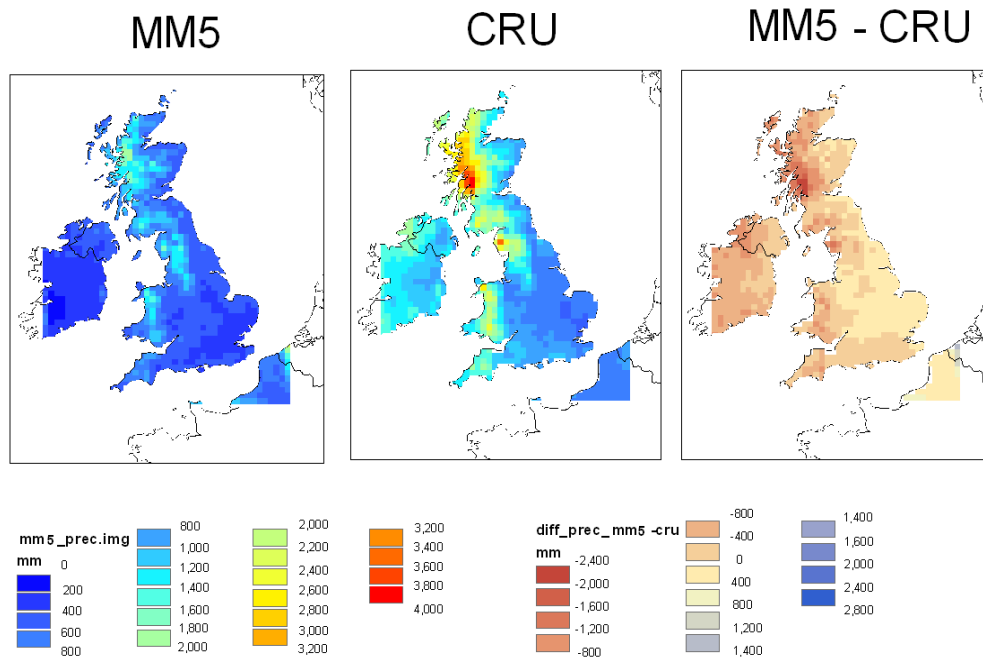
Figure 3-21. MM5 precipitation minus CRU precipitation, year 1999. Areas where MM5 under-predicts precipitation are in red whereas the areas of over-prediction are highlighted in blue. Units are mm. Grid cells over the sea have been excluded.
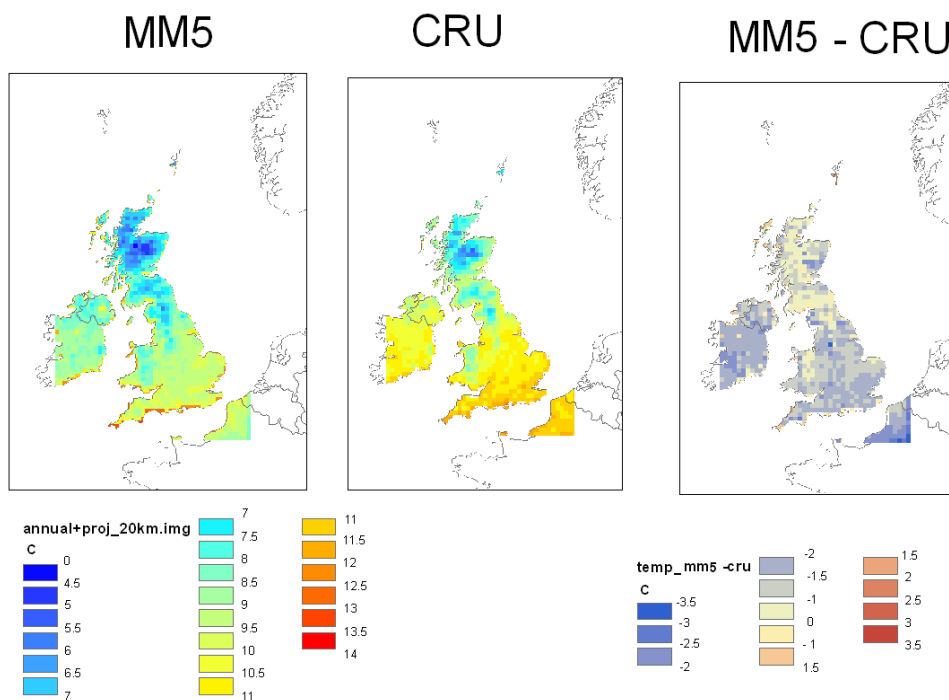
Figure 3-22. *MM5 surface temperature minus CRU precipitation, year 1999. Areas where MM5 under-predicts temperature are in blue red whereas the areas of over-prediction are highlighted in red. Units are (ºC). Grid cells over the sea have been excluded.*

3.4 CONCLUSIONS

A detailed analysis of MM5 performance versus observations was presented.
The study focused on the capability of the model to reproduce rainfall, near surface wind speed and temperature temporal series in specific grid points in two months in 1999. The results show a general tendency of MM5 in overestimating wind speed (+30%), underestimating precipitation in summer (between -10% and -20%) and overestimating it in winter (+30%), whereas there is generally a good agreement with observations for surface temperature even if the model tends to overestimate it for low values (below ~14 $^{\circ}$C) and underestimate it for high values (above ~20 $^{\circ}$C). The evaluation study shows MM5 generally performs better than ECMWF re-analysis in terms of standard deviation and correlation coefficient. A 1-year simulation with MM5 was also performed in order to confirm or disprove the monthly results. The annual trends confirm the good agreement as observed in the monthly analysis with a correlation coefficient between 0.7 and 0.9 for temperature temporal series and between 0.6 and 0.9 for wind speed temporal series. MM5 generally performs better than ECMWF. The long term run also confirms the tendency of MM5 in overestimating temperature for low values and underestimating it for high values. The surface temperature spatial distribution is generally well reproduced by MM5. Regions of under-prediction (between 1 $^{\circ}$C and 2 $^{\circ}$C) are visible in England and Ireland. The study shows that the spatial distribution of total rainfall is also underestimated. The areas of larger under-prediction (between 120 and 200 cm) mainly involve the western area of the UK and Ireland. The overestimate of wind speed and the underestimate of rainfall need to be taken into account when air quality studies are carried out using atmospheric dispersion models (i.e. CMAQ) because it may affects the processes of transport (advection) and removal of atmospheric pollutants, resulting in a systematic error in concentrations and deposition fluxes estimates.

CHAPTER 4
The Sparse Matrix Emission Processor
(SMOKE) applied to the United Kingdom

SUMMARY

The Sparse Matrix Operator Kernel System (SMOKE) developed by the MCNC-North Carolina Supercomputing Centre in the 1990s, is a tool for processing emission data for air quality models including the Community Multiscale Air Quality System (CMAQ). Because this software has been specifically developed to work in Northern and Central America, its application outside these regions is a difficult task. This chapter describes the attempt to adapt the modelling system to the European case and to the United Kingdom in particular. The implementation has the goal of making future air pollution studies with the Community Multiscale Air Quality System (CMAQ) easier in the UK. Because the emission databases used in this study are the National Atmospheric Emissions Inventory for the UK (NAEI) as well as the EMEP database (Co-operative programme for monitoring and evaluation of long range transmission of air pollutants in Europe) a specific methodology to adapt these inventories to SMOKE was introduced. The new method is presented together with the results of SMOKE application for a specific month (June 1999). Point and area sources have been considered in this preliminary study: further work needs to be done in the future for a more detailed treatment of mobile emissions.

4.1 INTRODUCTION

Fine scale air quality modelling requires the use of high resolution emission input data sets. Emissions must be properly spatially distributed over the grid domain and sufficiently temporally resolved (i.e. 1 hour time frequency). A correct grid distribution at high resolution is necessary for capturing the spatial variability of pollutants in the lower atmosphere whereas the temporal resolution is essential for reproducing the diurnal cycles of photochemical pollutants such as O_3 and its precursors (e.g. NO_X). A detailed chemical and granulometric speciation of the

primary Particulate Matter (PM) emitted into the atmosphere is also required as well as the aggregation process ("lumping") of Non Methane Volatile Organic Compounds (NMVOC).

Emission inventories are usually provided by national governments on an annual basis and they do not contain this level of information. For achieving the detail required by chemistry models specific emission tools are therefore applied. They perform the chemical, temporal and spatial speciation of emissions providing model-ready emission input data at high resolution.

Several European emission models have been successfully developed in recent years such as THOSCANE (Monforti and Pederzoli, 2004) and POEM-PM (Carnevale et al., 2005). Both these process annual emissions of the European CORINAIR (CORe INventory of AIR emissions) database and they have been applied for air pollution studies in Northern Italy. Parra (2004) developed a specific emission tool (EMICAT2000) for estimating emissions of primary air pollutants over the Catalonia area in year 2000. Symeonidis et al. (2004) implemented an Emission Inventory System for Transport (EIST) in Greece. In the United States several models have also been developed including SMOKE (Houyuox et al., 2002), EPS2.5 (Causley et al., 1990), and EMS (Judson and Janssen, 2001). The Sparse Matrix Operator Kernel System (SMOKE) is one of the most widely used pieces of software currently available for emission modelling in the US. It is coupled with several air quality models such as the Community Multi-Scale Air Quality System (CMAQ), the Regulatory Modelling System for Aerosols and Deposition (REMSAD) and the Urban Airshed Model (UAM-V). SMOKE, created by MCNC-North Carolina Supercomputing Centre in the 1990s, has been developed taking into account the inventory formats and geographical references of Northern and Central America (US, Canada, Mexico, Cuba, Haiti, Bahamas, Dominican Republic). The application of this tool to other countries is therefore a difficult challenge, because it requires the modification of several sub-routines inside the model in order to read and process the new inventories. Some input data specific for the American continent like stack parameters for point sources, emission temporal profiles and spatial surrogates also need to be substituted with some more specific for Europe, making the work difficult.

Few studies have tried to adapt SMOKE to the European contest. One example is Borge et al. (2003), who implemented the model over Spain for year 2000. This chapter describes the preliminary adaptation of the modelling system to the United Kingdom, making the model usable for air pollution studies with CMAQ. The emission databases used in this study are the National Atmospheric Emission inventory for the UK (NAEI) and the Co-operative programme for monitoring and evaluation of long range transmission of air pollutants in Europe (EMEP) database; a specific methodology to adapt these inventories to SMOKE was needed. This chapter describes this new method in detail (Section 4.2) and presents the results of SMOKE application for a specific month (June 1999) (Section 4.3). Finally Section 4.4 summarizes the conclusions and highlights the advantages and limitations of SMOKE applicability in regions outside America.

4.2 METHODOLOGY

4.2.1 Structure of the model

SMOKE was originally conceived in the 1990s at North Carolina Supercomputing Center (MCNC) as an idea by Coats et al. (1996). Main contributions to the development of the model were then given by Houyoux et al. (1999) and by Seppanen et al. (2005). More recent upgrades and the development of new versions of the model are described by Baek et al. (2006). Most of the general information about the model structure and features can be found in Houyoux et al. (2002). SMOKE can process gaseous pollutants such as CO, NO_X, VOC, NH_3, SO_2 and Particulate Matter (PM) as well as a large number of toxic pollutants including CH_4.

The transformation of the inventory data set into detailed emission input data is performed by SMOKE through several steps (Figure 4-1). Single groups of sub-routines inside SMOKE are responsible for each task. The inventory import performs operations like assigning pollutant names to data input by code numbers, assigning point source locations to area sources, filling in and checking stack parameters. The spatial processing combines the grid specification for the CMAQ model domain with source locations from the SMOKE inventory file, whereas the temporal processing

applies monthly, weekly and diurnal profiles to annual emissions. The chemical speciation addresses issues such as pollutant-to-pollutant conversions as well as the conversion of the input emissions pollutants to the model species used in CCTM. Not all processes are considered in this first stage study, as shown in Figure 4-1. Those processes which required changing before being applied in the UK are outlined in red in Figure 4-1 and they are fully explained in the sections 4.2.2 and 4.2.3.
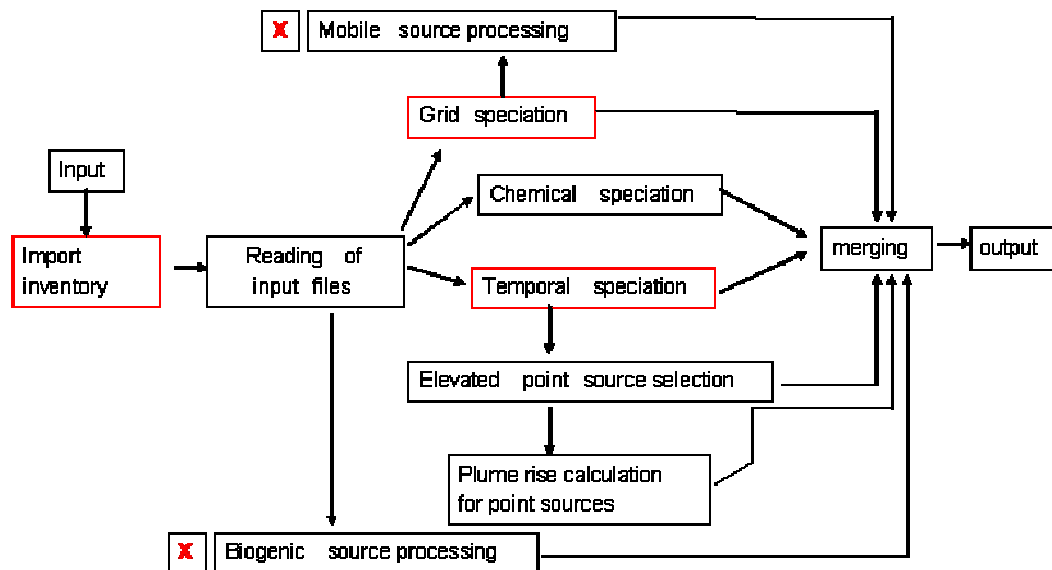
Figure 4-1. Schematic diagram of SMOKE processes. The red cross indicates that the corresponding processes are not considered at this stage. The red boxes required changes for the application to the UK.

4.2.2 Import inventory

4.2.2.1 Emission types

Five emitted pollutants have been selected for this study: ammonia (NH_3), nitrogen oxides (NO_X), sulphur dioxide (SO_2) and particulate matter less than 10 μm (PM_{10})

and less than 2.5 μm ($PM_{2.5}$). SMOKE emissions are classified in four categories: area, point, mobile and biogenic emissions. As shown in

Figure *4-1* only area and point emissions have been included in this preliminary approach. Area sources are classified as those which cover a uniform spatial region; in this work NH_3 and Particulate Matter are considered emitted by area sources only. Point emissions come from Large Point Sources (LPS) which mainly represent power plants, large metal smelters, district heating plants, large industrial boilers and oil refineries and they are identified by single points. Many models including SMOKE treat emissions from LPS separately, because these sources present features with regard to atmospheric transport and chemistry which make them substantially different from the other sources. For example, LPS typically release gaseous pollutants through tall smokestacks or chimneys, so the emissions enter the atmosphere at a greater altitude than emissions from ground-level (i.e. area) sources. Emissions are strongly influenced by stack parameters (stack height and diameter, gas exit temperature and velocity, flow rate etc.) and fuel details (type, annual consumption, sulphur content). Emissions control solutions are also often available (and cost-effective) for LPS that are not as applicable to other emissions sources (Vallack and Rypdal, 2007).

It is important to consider the contribution given by *LPS* to acidifying pollutants emissions. It is estimated that between 75% and 90% of anthropogenic emissions of sulphur in Europe come from a few thousand point sources, and about a hundred of them are alone responsible for more than 40% of the total (Barrett and Protheroe, 1995; Barrett, 2000). In this study NO_X and SO_2 are considered emitted by both area and *LPS* sources.

4.2.2.2 <u>Emission inventories</u>

Emissions for all pollutants are provided by the EMEP database; EMEP annual emissions are distributed on a 50 x 50 km^2 grid in Polar Stereographic Projection (Figure 4-2). The estimated total EMEP emissions for the UK in 1999 are reported in

Table 4-1. The National Atmospheric Emissions Inventory for the UK (NAEI) is used for providing NO_X and SO_2 *LPS* emissions (Figure 4-3). This data set is calculated on a yearly basis and it covers the UK mainland and Northern Ireland. The data are provided in coordinates of the British National Grid reference system. Stack information and geographical location of every point were provided by the Centre for Ecology and Hydrology (CEH) of Edinburgh. Table 4-1 shows that the addition of *LPS* emissions to NO_X and SO_2 EMEP emissions makes the total annual estimates close to those provided for year 1999 by the National Expert Group on Transboundary Air Pollution report (NEGTAP 2001).

It is important to remember that the total emissions estimates for each source category are usually hard to quantify as they are affected by high uncertainty. Uncertainties for UK emissions are included in Table 4-1. NO_X and SO_2 uncertainties derive from NEGTAP whereas PM and NH_3 estimates come from the e-Digest of Environmental statistics report (2004). For pollutants primarily emitted by production and combustion processes, the uncertainty is mainly due to the lack of information concerning the fuel, the combustion conditions and technical characteristics of the power stations. Few indications are available. According to the CORINAIR guidebook (http://reports.eea.eu.int/technical_report_2001_3/en) the uncertainty for production of fossil fuels is estimated at +/- 25% whereas for solvent use it is a factor 1.25 to 2.

The same document also indicates a margin of error for ammonia emissions from the agriculture sector of +/- 50%, showing a discrepancy with the e-Digest report which indicates a value around ±20% (Table 4-1).

The same e-Digest report suggests NO_X and SO_2 uncertainties may also be overestimated by NEGTAP (±8% for NO_x and ±3% for SO_2, compared to NEGTAP percentages of ±30% and ±10-15% respectively). Parrish (2005) shows how the difficulty in estimating emissions correctly is not limited to the European inventories: in the US NO_X traffic emissions for years from 1989 to 2004 differ by at least 10-15%, suggesting a significant uncertainty in the estimates. This inter-annual variability is mainly due to highly variable factors influencing emissions such as the kind of vehicle, the average speed and the vehicle conditions (Parrish, 2005).
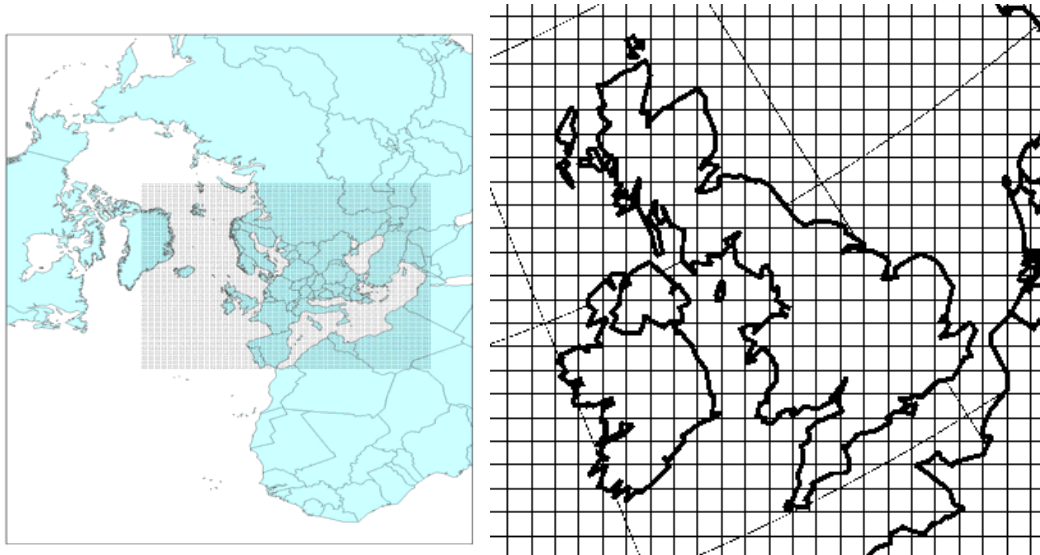
Figure 4-2. 50 x 50 Km^2 European EMEP grid (left) and The United Kingdom as included in the EMEP grid (right). Source: EMEP
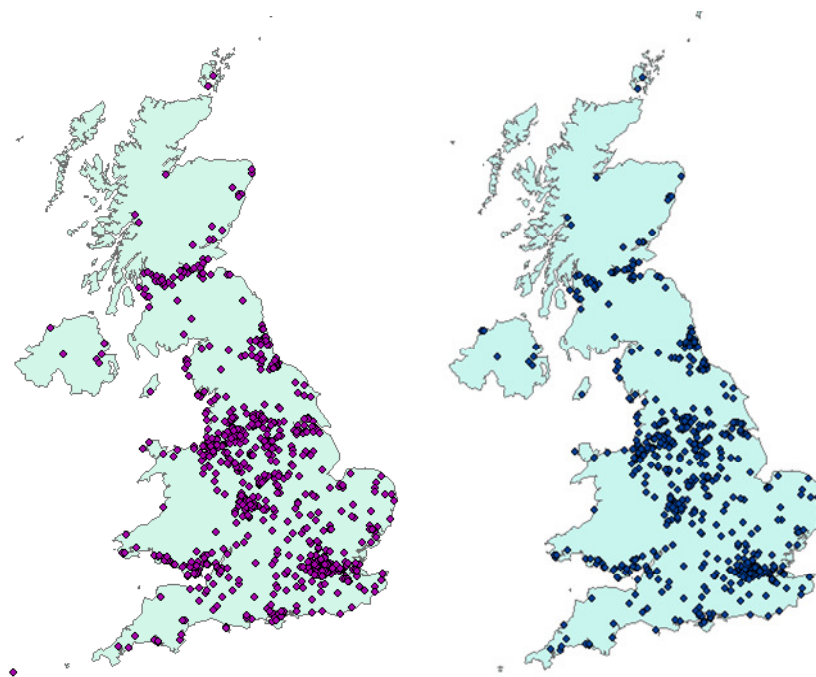

Figure 4-3. Geographical location of NO$_X$ point sources (left) and SO$_2$ point sources (right) in the UK.

	NH_3	PM	SO_2	NO_X
EMEP	358	199	1201	1936
CEH/NAEI	-----	------	21	616
EMEP+CEH/NAEI	-----	------	1222	2552
NEGTAP	348	186	1188	2649
Uncertainty	±20%	-20% to 50%	±10-15%	±30%

Table 4-1. Estimated total UK emissions and estimated uncertainties for year 1999. Units are Gg yr^{-1}.

4.2.2.3   Identification of source categories

Inventory databases usually consider primary pollutants as emitted by a limited number of source categories. Both NAEI and EMEP inventories use the UNECE (United Nations Economic Commission for Europe) classification in 11 sectors (Table 4-2). Because the source categories are identified in SMOKE by the 10-digit US EPA Source Classification Code (SCC), a correspondence between UNECE sectors and SCC sectors was introduced (Table 4-2). The 1999 emission sectors are also shown in Figure 4-4.

UNECE sector	UNECE name	EPA-SCC sector	EPA - SCC name
S1	Energy Production and Transformation	2101001000	Stationary source fuel combustion-electric utility
S2	Commercial, Institutional and Residential Combustion	2103001000	Stationary source fuel combustion-commercial
S3	Industrial Combustion	2102001000	Stationary source fuel combustion-industrial
S4	Production processes	2302000000	Industrial processes
S5	Production and Distribution of Fossil Fuels	2510501000	Storage and transport-petroleum
S6	Solvent use	2401001000	Solvent utilization
S7	Road Transport	2294000000	Mobile sources
S8	Other Transport and machinery	2515000060	Storage and transport
S9	Waste Treatment and Disposal Energy	2601000000	Waste disposal, treatment and recovery
S10	Agriculture	2801000000	Agriculture production
S11	Nature	2701001000	Natural sources

Table 4-2. Correspondence between UNECE sectors and EPA source categories
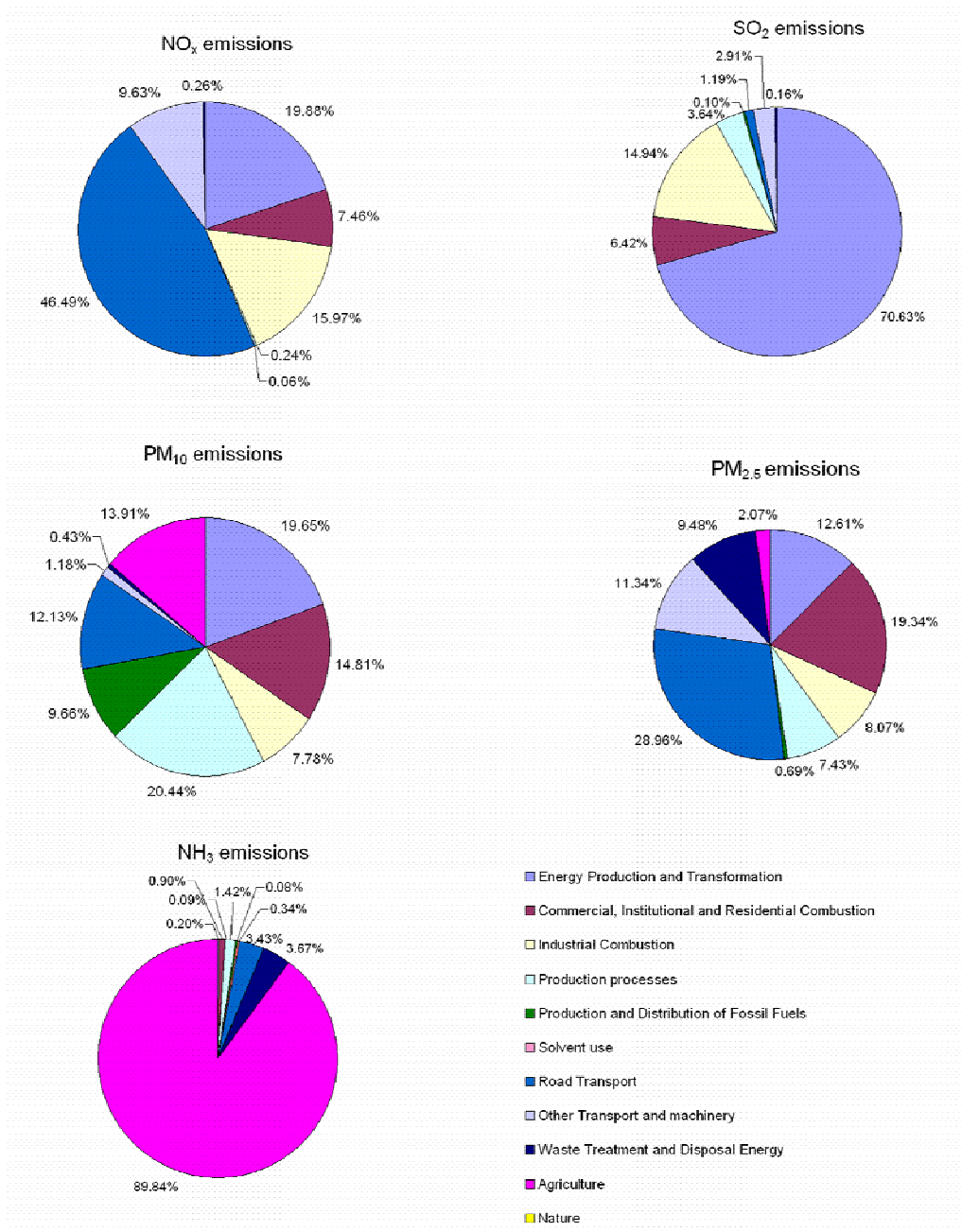
Figure 4-4. Sources of NH₃, NOₓ, SO₂ and PM in the UK. Source: EMEP

4.2.2.4 <u>Spatial allocation</u>

All SMOKE input files must contain county-level emission data. This means the geographical position of each area source is identified by a well defined Country/State/County code. It is a 6-digit number in the format "*C/SS/ccc*" where the first digit *C* identifies the Country, the following two digits *SS* identify the State and the last three digits *ccc* represent the subdivision of States into Counties. The basic original *Country/State/County* classification implemented in the model is American (the US Federal Implementation Planning Standards (FIPS) state and county codification) and therefore not applicable to the UK. A new classification was therefore introduced. The geographical reference chosen for the UK is a hierarchical scheme with 3 levels (Table 4-3) with a subdivision in Regions, Counties and Local Authorities. Every geographical area in the UK is identified by a six digit *Region/County/Authority* code which replaces the previous Country/State/County code (Figure 4-5). The new scheme is an adaptation of the European administrative classification provided by the European Statistical Office (http://epp.eurostat.cec.eu.int). The nomenclature was also derived from the UK National Statistics geography webpage (www.statistics.gov.uk/geography/) and from the national site of the Government Offices for the English Regions (http://www.gos.gov.uk/national/). The European Administrative Classification was considered as the most appropriate for this work even if a 3-levels subdivision causes a mismatch between the UK and the American spatial scale (i.e. many US states have almost the same size of the entire United Kingdom).

LEVEL	American units	American total	UK units	UK total
0	Countries	7	Government Office Regions	12
1	States	633	Counties	38
2	Counties	5984	Local Authorities	133

Table 4-3. US original classification and new UK classification for spatial allocation in SMOKE

Figure 4-5. Left: Subdivision of the UK into 12 Government Office Regions (level 0). Shetland and Orkney islands (top left boxes) are considered part of Scotland Region. Centre: Subdivision of Government Office Regions into 38 Counties (level 1). Right: Subdivision of UK Counties into 133 Local Authorities (level 2).

4.2.2.5 <u>Creation of SMOKE input files</u>

A GIS software package (ARCMAP) was used for projecting the EMEP grid onto the UK (Figure 4-6) and for calculating, inside each EMEP cell, the fraction of emissions belonging to every UK local Authority. If the size of the local Authority is smaller than the EMEP cell (so that the local Authority is entirely inside the 50 x 50 square) the total emission in that EMEP cell is given by the sum of the emission of the same local Authority plus the amounts of emissions belonging to the fractions of local Authorities surrounding that one. Figure 4-7 shows an example result from ARCMAP application: the distribution of total NH_3 emissions in the 133 Local Authorities for year 1999.

SMOKE input files containing point and area emissions were then generated in the format required by SMOKE (*ascii* "IDA" files) by the application of subroutines specifically written in Fortran90 by the author. The new files contain annual emission data for point and area sources respectively. Emissions are spatially allocated by the new classification in *Region/County/Local Authority* codes (Section 4.2.2.4). The correct source categories based on the correspondence of Table 4-2 are also introduced. Point emission input files also contain information about stack parameters (height, diameter, gas exit velocity and temperature).

Figure 4-6. EMEP grid covering the 133 UK local Authorities.

Figure 4-7. Example of spatial allocation in SMOKE. NH$_3$ annual emissions for all 133 UK Local Authorities. Units are 10^{-3} Gg day^{-1}.

4.2.3 Temporal variability

Specific temporal profiles (monthly, weekly and daily profiles) are applied to convert SMOKE input files from an annual basis to an hourly basis. The approach adopted in SMOKE is the one described in Stella (2002). Each emission sector must be associated to a 12-element monthly profile (M_i, with $i = 1,\ldots,12$), a 7-element weekly profile (W_j, with $j = 1,\ldots,7$) and a 24-elements daily profile (H_k with $k = 1,\ldots,24$). The amount of pollutant emitted in the i-th month E_i is derived from total annual emission E as:

$$E_i = E\left(\frac{M_i}{\sum\limits_{i=1}^{12} M_i}\right) \tag{4.1}$$

Daily average emission in the j-th weekday in the i-th month E_{ij} is computed as

$$E_{ij} = 7E_i \frac{12}{365}\left(\frac{W_j}{\sum\limits_{j=1}^{7} W_j}\right) \tag{4.2}$$

Finally, hourly emissions E_{ijh} are computed as

$$E_{ijk} = E_{ij}\left(\frac{H_k}{\sum\limits_{k=1}^{24} H_k}\right) \tag{4.3}$$

Temporal profiles initially included in SMOKE are specific for the US. New emission profiles have been introduced for each of the UNECE categories. Several sources have been used for creating emission profiles more suitable for the European case. General guidance for introducing new monthly and weekly profiles was taken from the CORINAIR guidebook-3rd edition

(http://reports.eea.eu.int/technical_report_2001_3/en). Information about monthly factors for the Agricultural sector (UNECE category 10) were also taken from Gyldenkaerne et al. (2005). Hourly factors for daily profiles were derived from Maffeis et al. (2002). Monthly and weekly profiles are assumed to be dependent only on the source category (Figures 4-8, 4-9); daily profiles can also vary based on the pollutant (Figure 4-10).
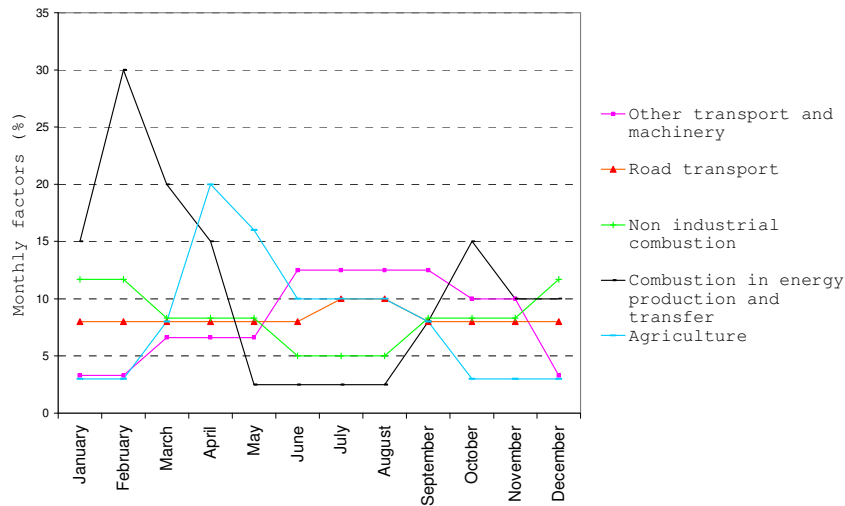

Figure 4-8. Monthly factors used for SMOKE application to the UK. Every profile is specific for one of the 11 UNECE sectors. Monthly profiles are assumed not to be dependent on the pollutant. Sectors with no monthly variation are not plotted.
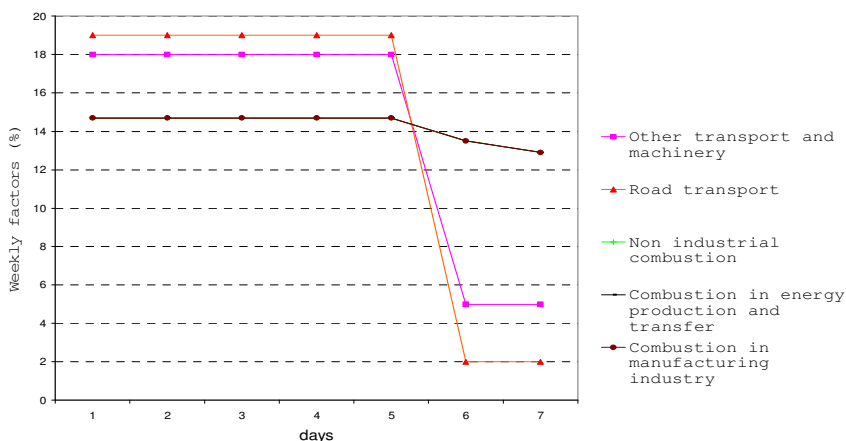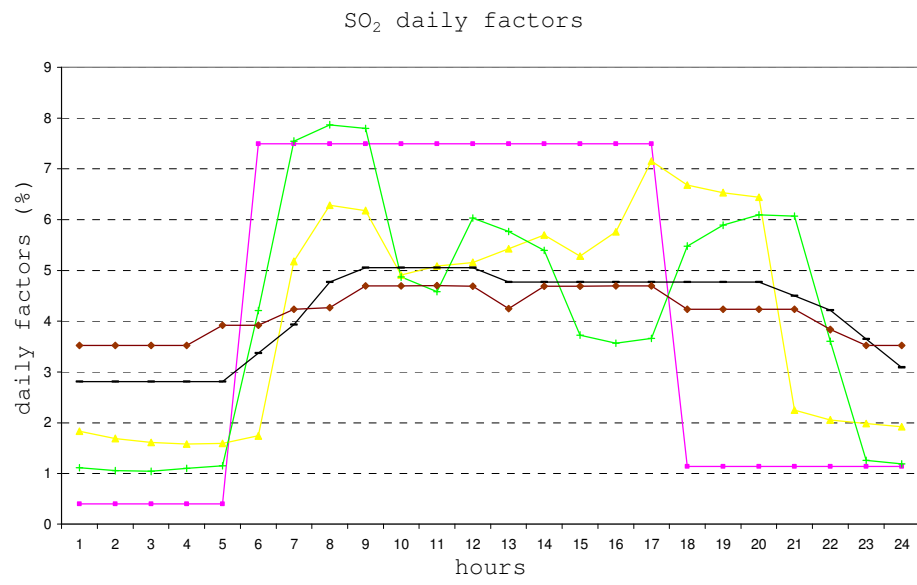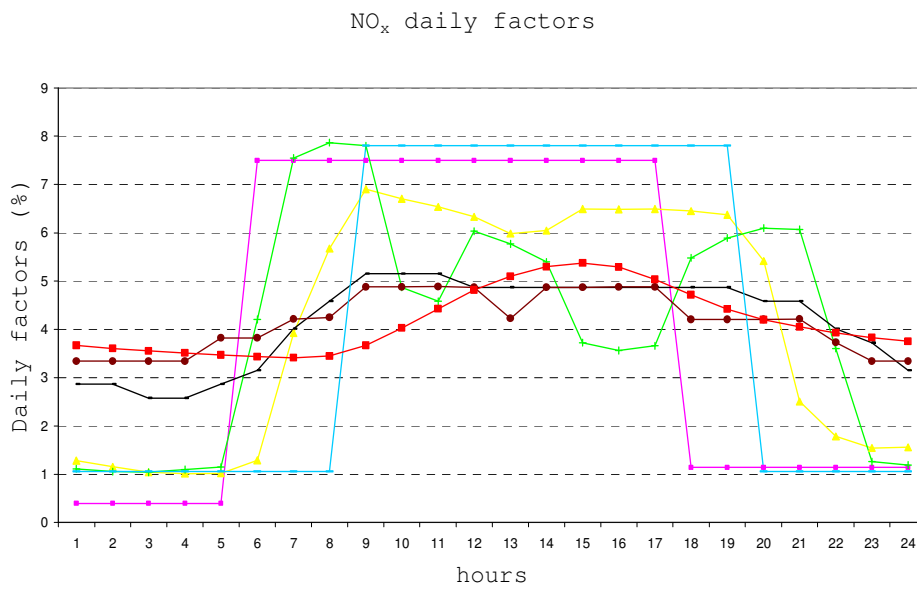

Figure 4-9. Weekly factors used for SMOKE application to the UK. Sectors with no weekly variation are not plotted. Weekly profiles are assumed not to be dependent on the pollutant.

a)

SO$_2$ daily factors

b)

NO$_x$ daily factors

c)

PM$_{10}$ and PM$_{2.5}$ daily factors

d)

NH$_3$ daily factors
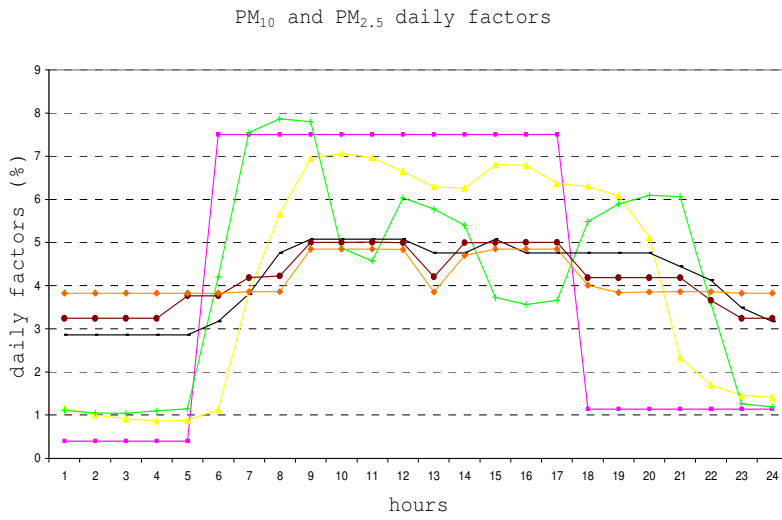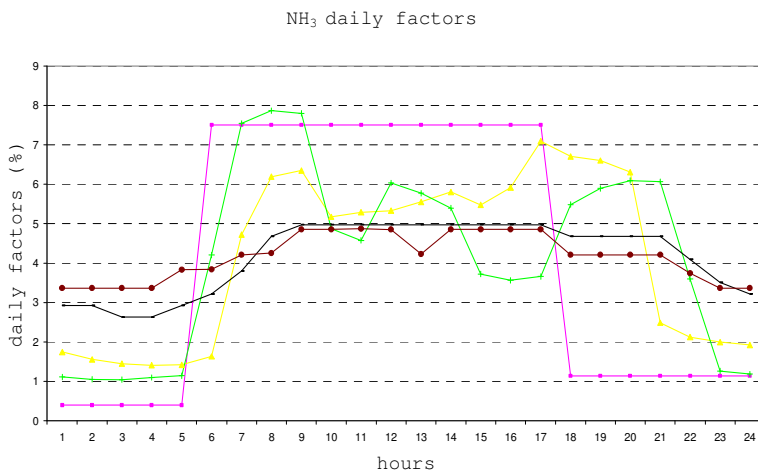
Other transport and machinery

Road transport

Non industrial combustion

Combustion in energy production and transfer

Combustion in manufacturing industry

Use of solvents

Agriculture

Other sources

Figure 4-10. Daily factors for SO$_2$, NO$_x$, NH$_3$, PM$_{10}$, PM$_{2.5}$ by source sector. Sectors/species with no diurnal variation are not plotted.

The temporal trends (Figures 4-8, 4-9 4-10) show how the main industrial and production processes are almost constant throughout the year, 24 hours per day with a slight decrease during the week-ends; the agricultural sector has a peak between March and June mainly due to fertilizer application during spring time (Figure 4-8). Emissions from this sector are lower in the cold season also because livestock is usually confined in housing units. According to Pinder et al. (2004) high temperatures in summer may also increase the volatilization of ammonia contributing to increased emissions. On a daily basis (Figure 4-10d) NH_3 is mostly emitted during the day, because agriculture is mainly a daytime activity. The emissions from combustion in energy production are clearly higher during winter rather than summer, according to a major use of heating systems during the cold season. Emissions due to road transport are substantially constant throughout the year, with a slight increase during summer, mainly due to the increase of road traffic in the holiday period (July-August) (Figure 4-8). On a weekly basis (Figure 4-9), the transport sector shows a drastic reduction of emissions in the week-ends: NO_X are estimated approximately 30% lower on Saturdays and Sundays than weekdays (Marr and Harley, 2002) because of a large decline in heavy-duty diesel track activity. The highest peaks in NO_x daily emissions (Figure 4-10b) from the traffic sector are in the morning (around 9 am) and in the evening (between 5 pm and 7 pm), corresponding to the beginning and the end of the daily working activity.

4.2.4 Grid speciation

Because air quality models require emissions over gridded domains, the *Region/County/Local Authority* emission data obtained by spatial allocation must be split by SMOKE onto the regular projection grid covering the model domain. The domain used in air quality studies with CMAQ is a 240 x 170 cells grid with a resolution of 5 x 5 km^2 covering the British Isles (Figures 4-11, 4-12). The map projection is Lambert Conformal. Central latitude and longitude are 55 degrees N and 3 degrees E respectively.
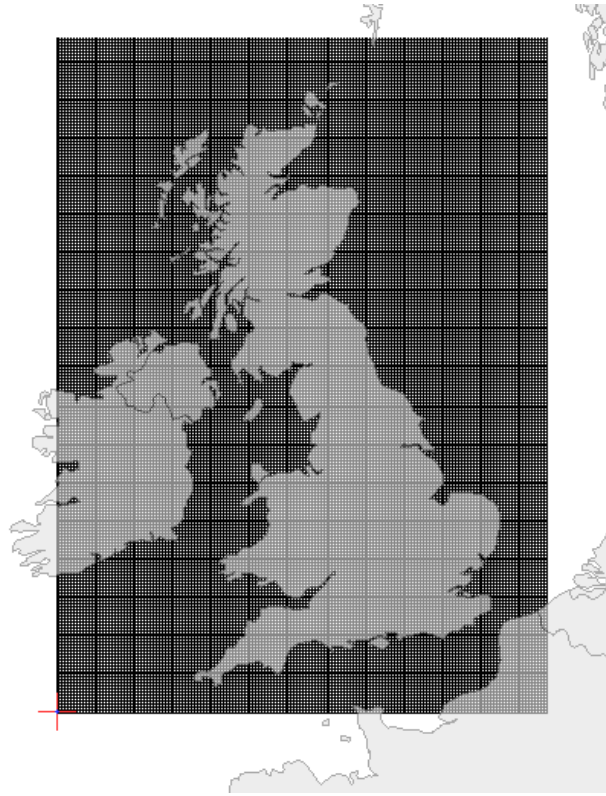
Figure 4-11. Modelling domain used for grid speciation.
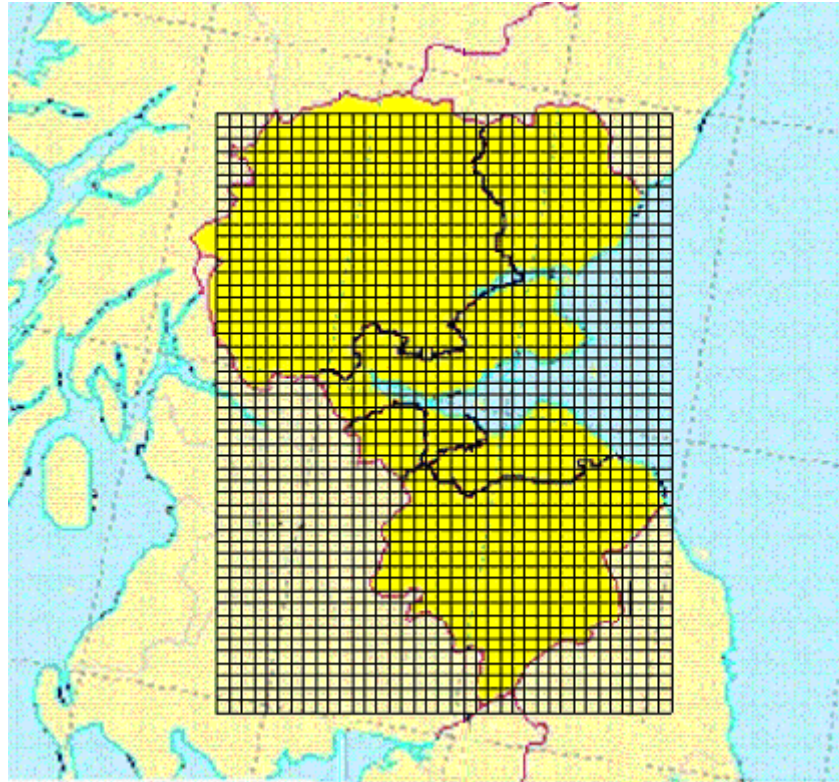
Figure 4-12. Zoom in the 5 x 5 km^2 resolution grid covering the South Eastern Scottish Local Authorities.

Instead of a simple uniform spread of emissions over the grid, a "weighting process" based on spatial surrogates has been used for a more specific allocation. An emission surrogate is a value between zero and one. It indicates the fraction of emissions in a region that must be allocated to a particular grid cell. The surrogate *srg* for the region of interest (i.e. a Local Authority) *C* and the grid cell *G* is given by (Eyth and Hanisak, 2003):

$$srg(C,G) = \frac{W(C \cap G)}{W(C)} \qquad (4.4)$$

where $W(C \cap G)$ is a weight attribute in the intersection between the region *C* and the cell *G*, while *W(C)* is a weight attribute in the entire region *C*. The emission in the grid cell *G* is therefore given by:

$$E(G) = srg(C,G) * E(C) \qquad\qquad (4.5)$$

The weight attributes in equation (4.4) may be points (ports, towns, airports), lines (railways, roads, rivers) and areas (national and regional parks, urban areas). The weight attributes for the geographical characterization of the UK are listed in Table 4-4. They are included in a data set called Bartholomew data set (http://www.bartholomewmaps.com) and they are provided as "shapefiles", a GIS industry format. An example is shown in Figure 4-13.

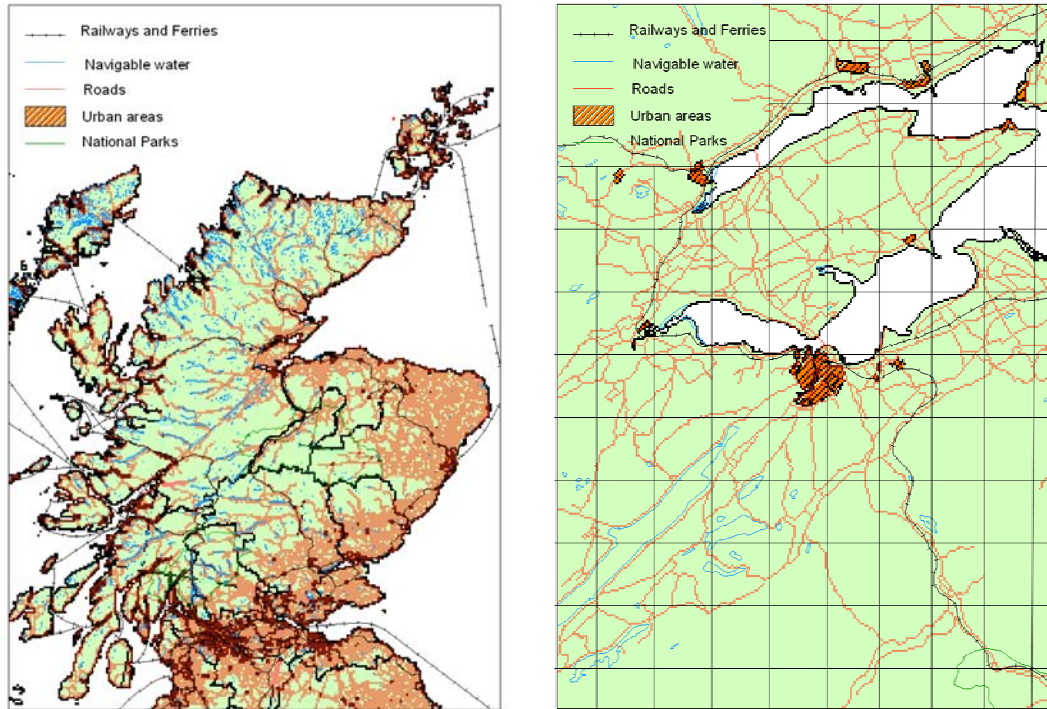| *W(C)*	*TYPE*
Airports	*Point*
Railways	*Line*
Urban Areas	*Area*
Navigable water	*Line*
Roads	*Line*
National Parks	*Area*

Table 4-4. Weight attributes used to calculate UK spatial surrogates.

Figure 4-13. Distribution of weight attributes W(C) over the Scottish Local Authorities (left) and 5 x 5 km² grid covering the weight attributes in the Invernessshire Local Authority (right).

For generating UK spatial surrogates *srg(C, G)* the Multimedia Integrated Modelling System Allocator (MIMS) was used; this tool was developed by the University of North Carolina (http://www.cep.unc.edu) in 2002. Because MIMS was originally written for generating American surrogates, (application only to the US, Canada and Central America) the original version of the code could not be applied to the UK. Several changes were therefore made in the program, and a new script named "generate_surrogates_4UK" was written in substitution of the original script. This new script can read the shapefiles of the Bartholomew data set, it solves equation (4.4) and it generates spatial surrogates based on the weight attributes listed in Table 4-4.

The introduction of new suitable spatial surrogates allows a more realistic grid speciation of emissions and consequently better results in SMOKE.

4.3 EMISSIONS MAPS

Figure 4-14 shows the distribution of emissions over the UK in June 1999. Monthly maps of NH_3, NO_x, SO_2 and Particulate Matter are presented and compared to maps of EMEP emissions over land for 1999 in order to show the improvement given by SMOKE to the original emission data set. The SMOKE emission estimate has a resolution of 5 x 5 km^2 whereas EMEP resolution is 50 x 50 km^2. The projection is Lambert Conformal. The units are moles sec^{-1} km^{-1} for NH_3, NO_X and SO_2 and g sec^{-1} km^{-1} for Particulate Matter. The high resolution maps show that high NH_3 emissions are spread all over the country, with areas of higher emissions mainly in East Anglia, the East Midlands, Northern Ireland and Eire, where livestock and agricultural activities are more extensive. Patterns of NO_x and SO_2 show pollutants are mainly emitted in the industrial areas of London and Yorkshire. The comparison shows the higher detail of SMOKE emission distributions compared to EMEP.

NH3 emissions

SMOKE
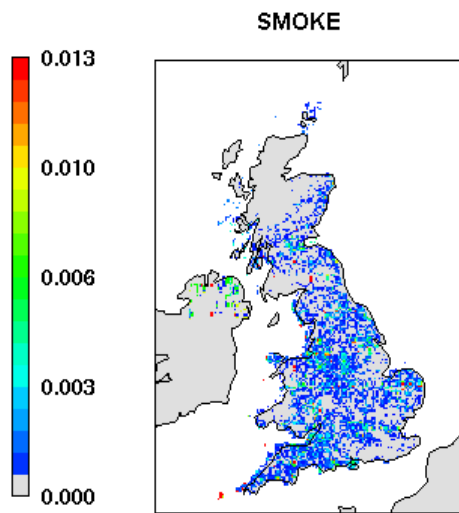
NH3 emissions
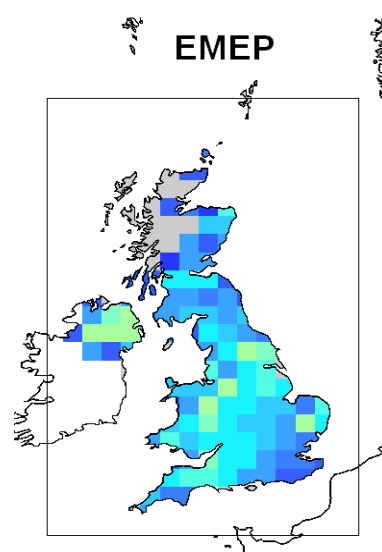
EMEP

NOx emissions
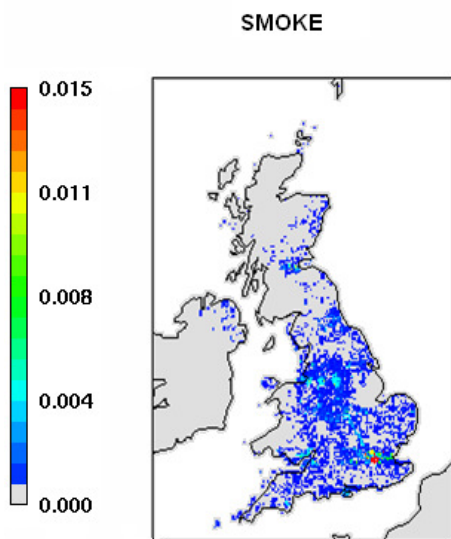
SMOKE
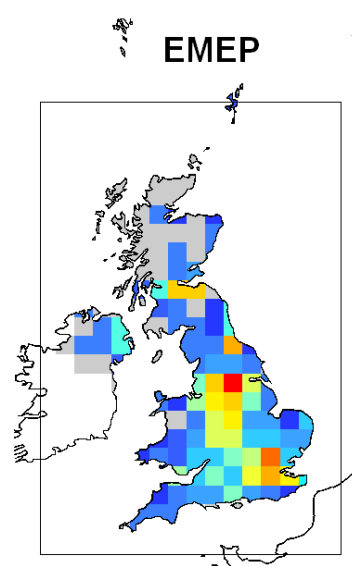
NOX emissions

EMEP

Figure 4-14. Maps of UK emissions for June 1999. The resolution is 5 x 5 km^2 for SMOKE emissions (left) and 50 x 50 km^2 for EMEP emissions (right). The projection is Lambert Conformal. Units are moles s^{-1} km^{-2} for NH$_3$, NO$_X$ and SO$_2$ and g s^{-1} km^{-2} for PM.
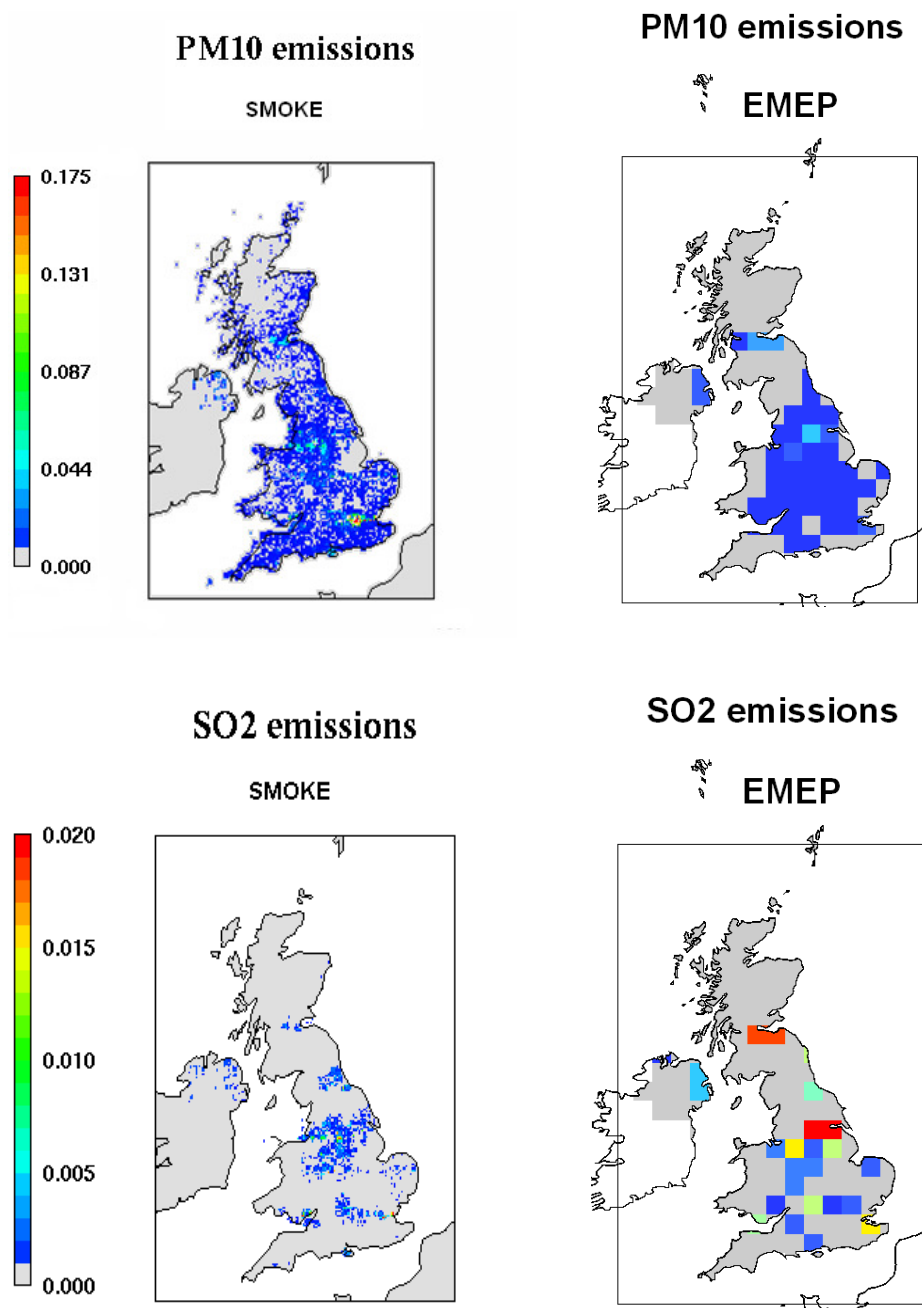
4.4 CONCLUSIONS

The chapter attempts to test the applicability of the American emission tool SMOKE to the European context and to the UK in particular. The implementation of SMOKE is a key factor for the future use of the chemistry model CMAQ in the UK. This preliminary study mainly focused on the implementation of three processes: import inventory, temporal disaggregation and grid speciation. New temporal profiles specific for the European contest have been introduced, as well as new geographical references and spatial surrogates which are more suitable for the UK area. The new temporal profiles show how emissions from industrial and production processes are almost constant throughout the year, 24 hours per day with a slight decrease during the week-ends. The agricultural sector shows a peak during spring time, when the fertilizer application enhances nitrogen emissions from the soil. During winter the contribution given by livestock to the total NH_3 emissions from this sector (mainly due to the volatilization of livestock waste) disappears because animals are confined in housing units. On a daily basis NH_3 is mostly emitted during the day. The SO_2 emissions from combustion in energy production are clearly higher during winter rather than summer, according to the intensive use of heating systems during the cold season. Emissions associated with road transport are substantially constant throughout the year, with a slight increase during summer, mainly due to the increase in vehicular traffic during summer holidays (July-August). On a weekly basis, this sector shows a drastic reduction of NO_X emissions in the week-ends compared to week-days because of a large decline in heavy-duty diesel track activity ("week end effect"). The highest peaks in NO_x emissions associated with the road transport sector are in the morning (around 9 am) and in the evening (between 5 pm and 7 pm), corresponding to the beginning and the end of the daily working activity.

Maps of emissions have been produced by SMOKE for NO_X, NH_3, SO_2 and PM_{10}. The application of SMOKE makes a positive contribution to the improvement of the distribution of emissions over the UK compared to the original emission dataset EMEP.

CHAPTER 5
Modelling pollutant concentrations over the United Kingdom using CMAQ

SUMMARY

The Eulerian dispersion model CMAQ (Community Multi-scale Air Quality system) is applied to calculate the concentrations of several acidifying pollutants (NH_x, NO_x and SO_2) over the United Kingdom. The model domain covers the British Isles with a horizontal grid resolution of 5 x 5 km^2. Two periods covering June and February 1999 respectively are selected for running the model. Modelled surface layer concentrations of NO_X, NH_X and SO_2 are compared to observations provided by several monitoring sites across the UK. The results indicate a better performance of CMAQ in February rather than in June for almost all pollutants. Significant over-predictions of NO_X concentration occur at urban sites. In both months the model cannot reproduce the diurnal cycle of pollutant concentrations, with correlation coefficients between measured and modelled data less than 0.5. Differences between modelled and observed NH_3 concentration vary approximately between -3 $\mu g\ m^{-3}$ and +1 $\mu g\ m^{-3}$, with a better performance in winter rather than in summer.

The Normalized Mean Error (NME) in June is around 50% for NO_X, NH_3 and SO_2. In February NME is approximately 36% for SO_2 and NO_2 and 50% for NH_3. In terms of systematic error the Normalized Mean Bias (NMB) is negative for NH_4^+ (-9%), NO_X (-25% and -40% in February and June respectively) and NH_3 (around -20%) and positive for SO_2 (4% and 27%).

5.1 INTRODUCTION

The atmospheric processes involving acidifying species like nitrogen oxides (NO_x), sulphur dioxide (SO_2), ammonia (NH_3) and ammonium (NH_4^+) can lead to a wide range of environmental effects on local, national and global scales, including damage to vegetation, acidification of both soil and fresh waters and formation of aerosols and tropospheric ozone. Currently one of the tools mainly used for acidification studies in the UK is FRAME (Fine Resolution Atmospheric Multi-pollutant Exchange), a Lagrangian Air Quality model with annual statistical meteorology (the

meteorological data set is a set of wind frequency roses and wind speed roses as shown in Figure 6-2) (Singles, 1996; Fournier, 2002; Vieno, 2005). In recent years the rapid increase in computational capabilities has created the opportunity of investigating the use of more computationally expensive Eulerian models including CMAQ and EMEP4UK (Vieno et al., 2006). A brief introduction to FRAME is given in Chapter 1, whereas a full description of CMAQ can be found in Chapter 2. This chapter has the aim of testing the ability of CMAQ to reproduce concentrations at high resolution (5 x 5 km^2) over the UK.

This study focuses on NH_3, NH_4^+, SO_2 and NO_x concentrations in June and February 1999. Section 5.2 consists of a brief description of the input data set (meteorological data, emissions, boundary and initial concentrations) and the modelling domain. The results of the application of CMAQ application over the UK, including maps of concentration, are presented in Section 5.3. Section 5.4 compares these results with results from previous applications of CMAQ. Section 5.5 finally summarizes the conclusions.

5.2 INPUT DATA

5.2.1   Modelling domain

A nesting procedure is used for running CMAQ over the United Kingdom. A 5 x 5 km^2 resolution grid covering the British Isles is nested within an outer lower resolution grid (45 x 45 km^2 resolution) (Figure 5-1). The features of both domains are summarized in Table 5-1. A description of the nesting process in CMAQ is given in Chapter 2.

	Outer grid	*Inner grid*
Resolution	45 x 45 km^2	5 x 5 km^2
Projection	Lambert Conformal	Lambert Conformal
Number of cells	45 x 45	237 x 167
Central latitude and longitude	55 °N, 0 °E	55 °N, -3 °E

Table 5-1. Features of the modelling domains used for the application of CMAQ over the UK.
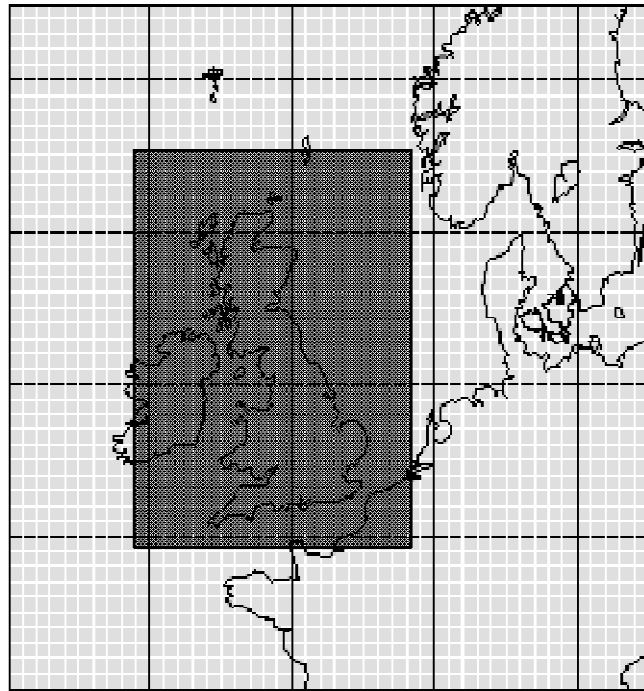
Figure 5-1. Inner 5 x 5 km^2 resolution grid (black) nested inside the outer 45 x 45 km^2 resolution grid (grey).

5.2.2 Boundary and initial concentrations

The procedure for the creation of CMAQ boundary and initial concentrations to be used in a nesting process is fully explained in Chapter 2. At each of the four edges (North, South, East, and West) of the outer 45 x 45 km^2 resolution domain a boundary condition is applied, comprising of single vertical profile of concentrations for each species. This profile remains fixed throughout a model run. Across the model domain, species concentrations are initialised to a single value at each vertical level. Monthly values of concentration from the global 3D Lagrangian chemistry transport model STOCHEM (Collins et al., 1997; Stevenson et al., 1998) are used for this purpose. A brief description of the STOCHEM model can be found in Chapter 1. Table 5-2 reports the STOCHEM chemical species included into CMAQ boundary

and initial concentration files for the outer grid as well as the six vertical pressure levels selected for creating the vertical profiles.

Species	Pressure levels (hPa)
NO_2,NO,O_3,N_2O_5,HNO_3,$HCHO$, NO_3,H_2O,CO,PAN,H_2O_2, SO_2,NH_3	950, 850, 750, 650, 550, 450

Table 5-2. STOCHEM output species included into CMAQ boundary and initial constant vertical profiles for the outer domain.

Figure 5-2 shows the CMAQ outer 45 x 45 km^2 resolution grid as nested into the 5 x 5 degrees STOCHEM grid. The STOCHEM grid squares in blue are those selected for representing "North", "East", "South" and "West" boundary concentrations in CMAQ profiles whereas those in yellow are used for calculating the initial concentrations. The values in the grid cells are averaged to give a single value for each one of the four directions (equations 5.1-5.4) and for the beginning of the simulation (equation 5.5). North, South, East and West concentration values are then re-projected onto the four sides of the outer grid (Figure 5-3) whereas the initial concentration ($C_{initial}$) is re-projected inside it. Values of NH_3, SO_2 and NO_x in the first vertical level for June 1999 are reported in Table 5-3. After CMAQ has run at the 45 x 45 km^2 resolution, output concentrations from the simulation over the outer domain are re-interpolated and high resolution boundary and initial concentrations are extracted. These concentrations are spatially (5 x 5 km^2 resolution) and temporally (hourly values) resolved and they are used for the simulation over the inner 5 x 5 km^2 grid. An example is given in Figure 5-4.

$$C_{South} = \frac{\sum_{S=a}^{S=g} C_S}{6}$$ (5.1)

$$C_{East} = \frac{\sum_{E=k}^{E=h} C_E}{4}$$ (5.2)

$$C_{North} = \frac{\sum_{N=l}^{N=q} C_N}{6}$$ (5.3)

$$C_{West} = \frac{\sum_{W=t}^{W=u} C_W}{4}$$ (5.4)

$$C_{initial} = \frac{\sum_{i=1}^{i=24} C_i}{24}$$ (5.5)
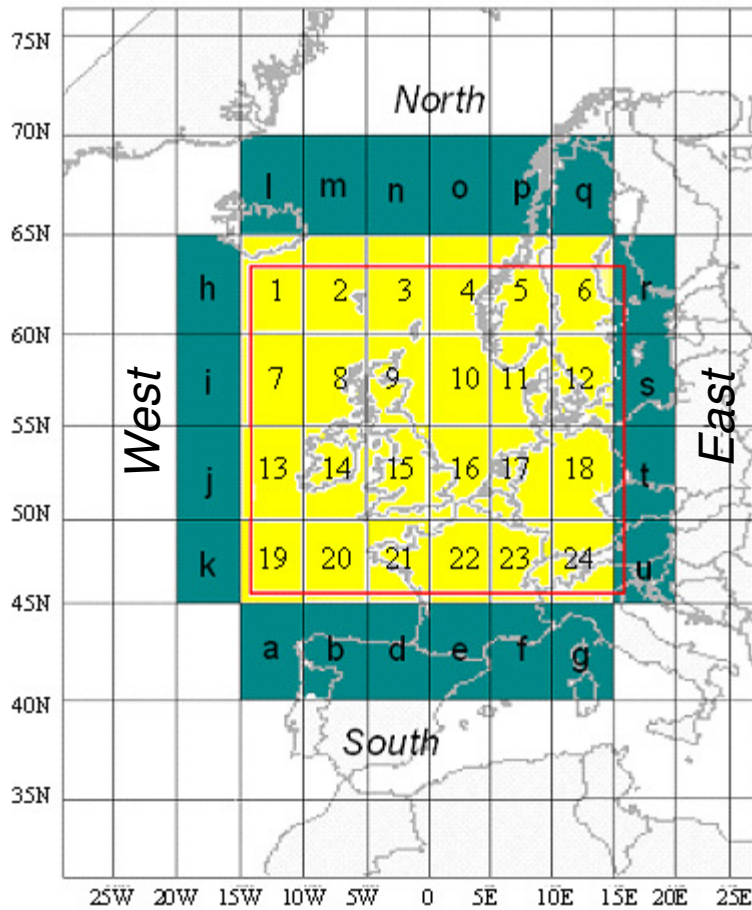
Figure 5-2. CMAQ 45 x 45 km² domain (red box) overlain onto the 5° x 5° STOCHEM grid. The cells in blue and yellow are those selected for calculating CMAQ boundary and initial concentrations respectively, using equations 5.1-5.5.

	NORTH	*EAST*	*WEST*	*SOUTH*	*INITIAL*
SO$_2$	5.98	8.49	5.04	9.36	86.55
NO$_X$	2.92	37.79	2.92	74.19	114.34
NH$_3$	0.31	9.43	0.31	0.31	5.57

Table 5-3. North, South, East, West and initial concentration values of NH$_3$, SO$_2$ and NO$_x$ in the first vertical level for June 1999. Units are μg m^{-3}
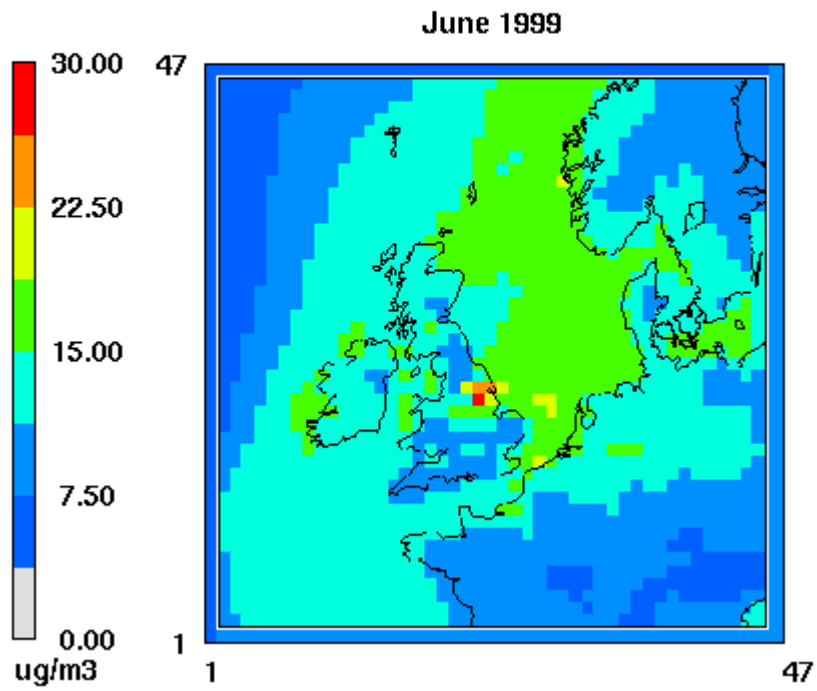
Figure 5-3. North, South, East and West concentration values as re-projected onto the four sides of the outer 45 x 45 km^2 resolution grid. Example of SO_2 boundary concentration in the first vertical level for June 1999. The values inside the grid represent the average monthly concentration for SO_2.

NH3 boundary concentration
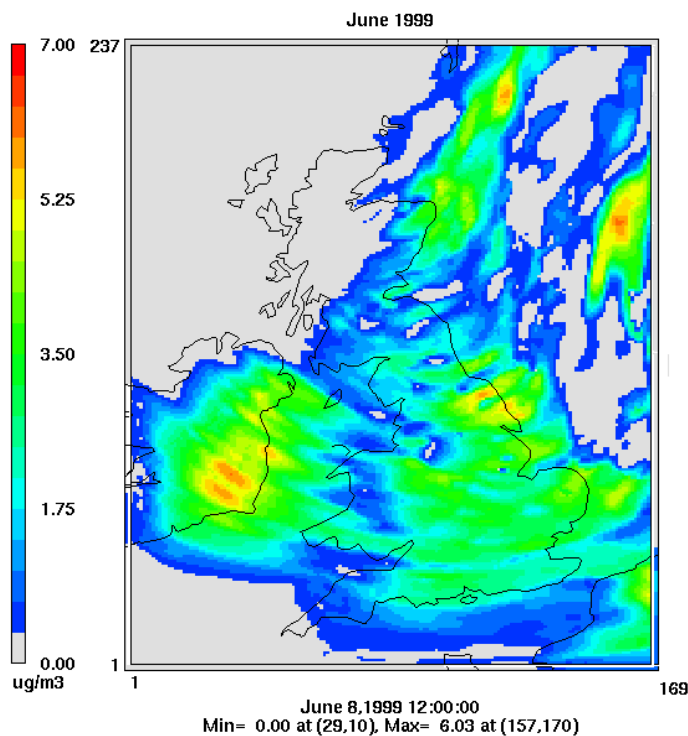
Figure 5-4. Value of hourly NH$_3$ concentration on the 8th of June at 12 am inside the 5 x 5 km^2 domain and hourly gridded NH$_3$ concentration from the boundaries.

5.2.3 Meteorological input data

The 3D meteorological fields required as input by CMAQ are provided by MM5 which was integrated over both grids of Figure 5-1, for June and February 1999. A brief description of the model and the results of its application and evaluation over the 5 x 5 km^2 resolution grid can be found in Chapter 3. The output data from MM5 are post processed by the Meteorology-Chemistry Interface Processor (MCIP) (Otte et al., 1999). The program converts the output files from MM5 into the format used by CMAQ (IO/API format) and it calculates some parameters not computed by the mesoscale model such as dry deposition velocity. Some general details about MCIP features and structure can be found in Chapter 2. Monthly mean surface temperatures from MM5 are shown in Figure 5-5.

a)

Surface temperature

February 1999

b)

Surface temperature

February 1999

a)

Surface temperature

June 1999

b)

Surface temperature

June 1999
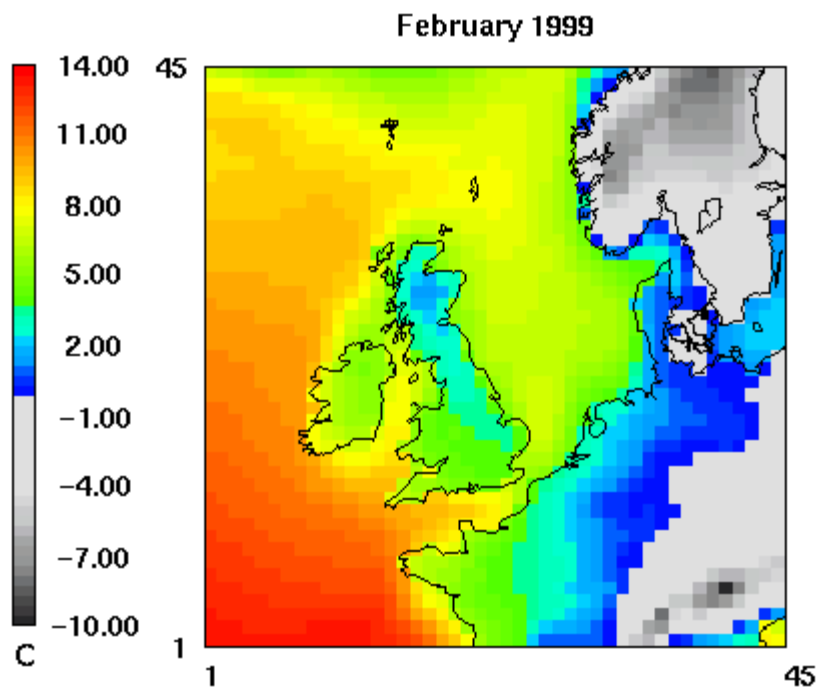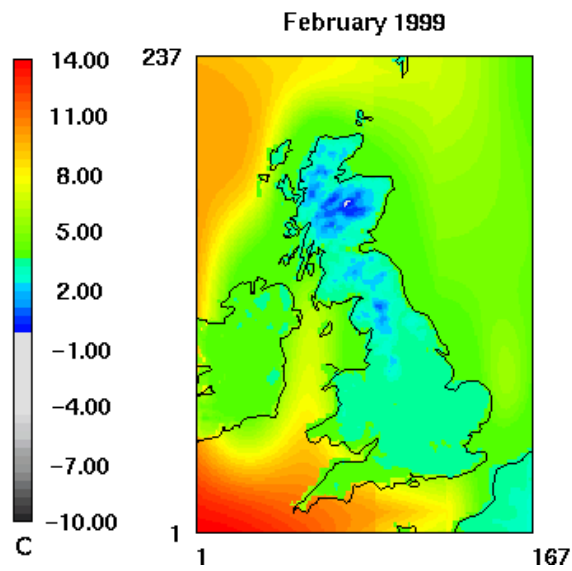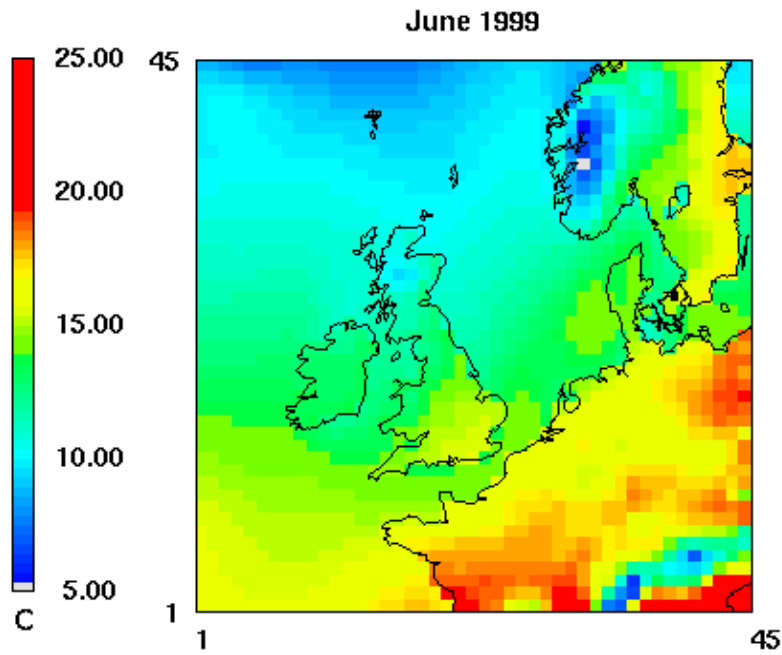
Figure 5-5. Examples of CMAQ meteorological input: monthly mean surface temperature for February (top) and June (bottom) 1999 a) over the outer 50 x 50 km² resolution grid and b) over the inner 5 x 5 km² resolution grid. Temperature is in ºC.

5.2.4   Emissions

Input emissions are required for both outer and inner domains. For the high resolution grid the Sparse Matrix Operator Kernel System (SMOKE) is applied. A detailed description of a preliminary SMOKE 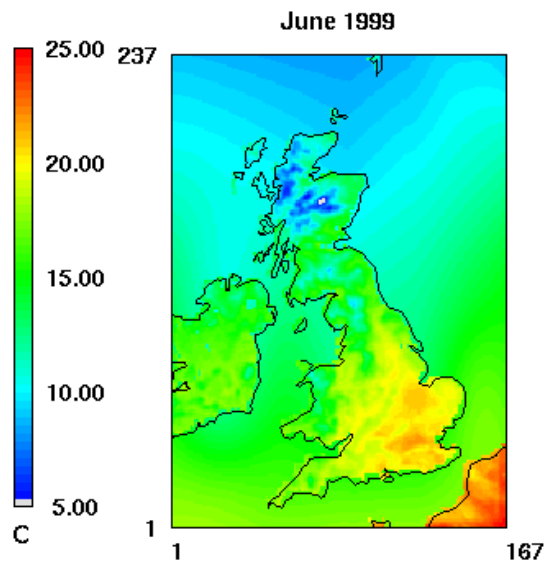implementation in the UK can be found in Chapter 4. For the coarser grid EMEP 50 x 50 km^2 resolution emissions are used. The data are interpolated from 50 x 50 km^2 resolution to 45 x 45 km^2 and re-projected from Polar Stereographic Projection to Lambert Conformal. The operations are performed by the application of a specific FORTRAN90 code named "EMEP2CMAQ" developed by Armin Aulinger at GKSS Research Centre. Because the basic version of the code does not include a proper temporal disaggregation of emissions, the program was modified for splitting annual emissions to hourly emissions by the application of specific temporal profiles. Monthly, weekly and daily emission factors used in this study can be found in Chapter 4. Monthly maps of NH_3, NO_X, SO_2 and PM emissions over the outer grid are shown in Figure 5-6. Because the application of SMOKE is limited to the UK only, and the inner CMAQ domain also covers part of Eire and France, non-UK emissions are needed. Eire and France emissions are derived from the EMEP inventory. EMEP emissions are converted to the Lambert Conformal Projection and interpolated from 50 km to 5 km (Figure 5-7). The same interpolation is also used for the emissions covering Northern Ireland, where the application of SMOKE does not provide a satisfying level of spatial detail (Figure 5-8). Table 5-4 shows the estimates, for June 1999, of total 5 x 5 km^2 resolution emissions and 45 x 45 km^2 resolution emissions, calculated over the same area (the one covered by the inner grid). Both grids show a similar distribution of emissions over the United Kingdom: NH_3 emissions are spread all over the country, with areas of higher emissions mainly in East Anglia, the East Midlands and Ireland, where livestock and agricultural activities are more extensive. Patterns of NO_x and SO_2 show pollutants are mainly emitted by power plants in the industrial areas of London and Yorkshire.
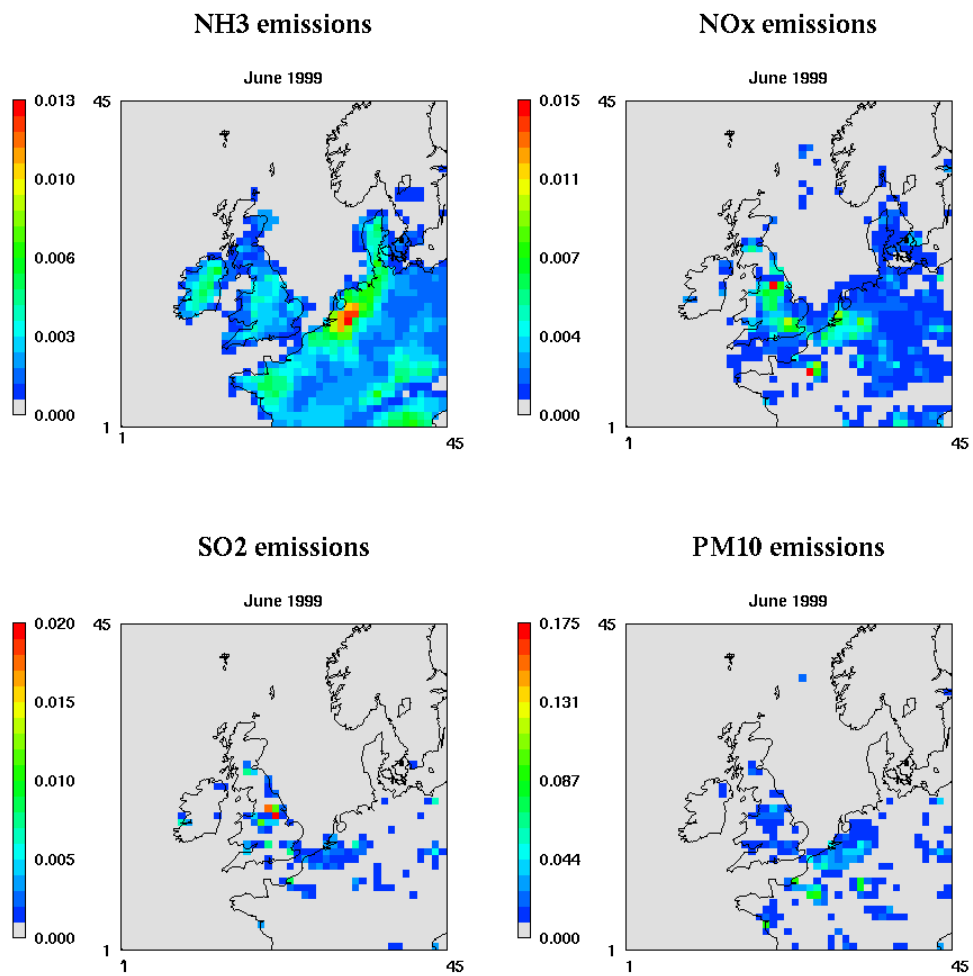
Figure 5-6. Examples of monthly emissions for NH₃, NOₓ, SO₂ and PM₁₀ for the outer 45 x 45 km² *resolution grid. Units are moles s⁻¹ km⁻²*

126
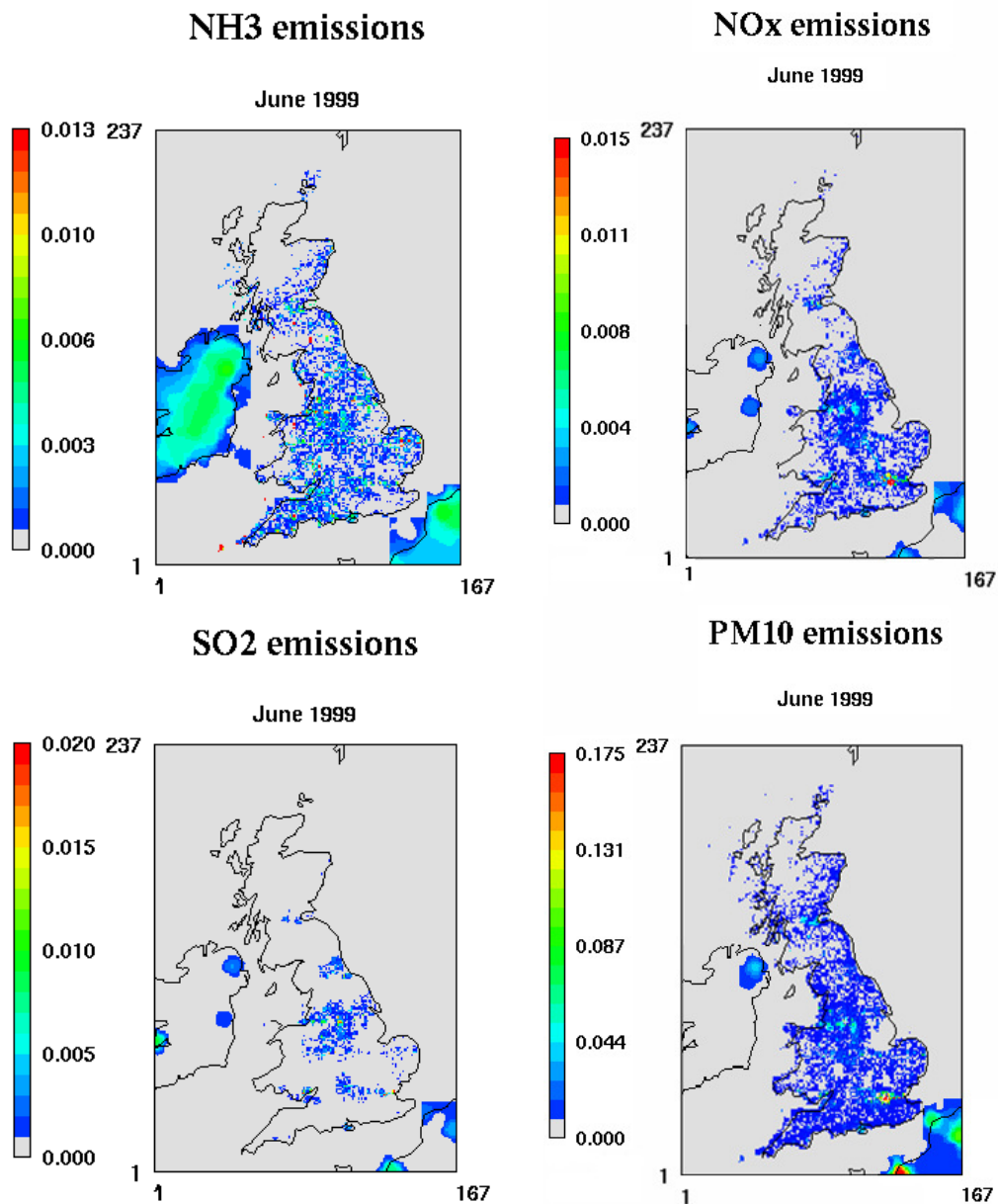
Figure 5-7. Examples of NH₃, SO₂, NOₓ and PM₁₀ monthly emissions over the inner grid (167 x 237 cells). Ireland, Northern Ireland and France emissions are interpolated from 50 x 50 km² to 5 x 5 km² resolution, whereas Great Britain emissions come from SMOKE application. Units are moles s⁻¹ km⁻² for NH₃, NOₓ and SO₂ and g s⁻¹ km⁻² for PM.
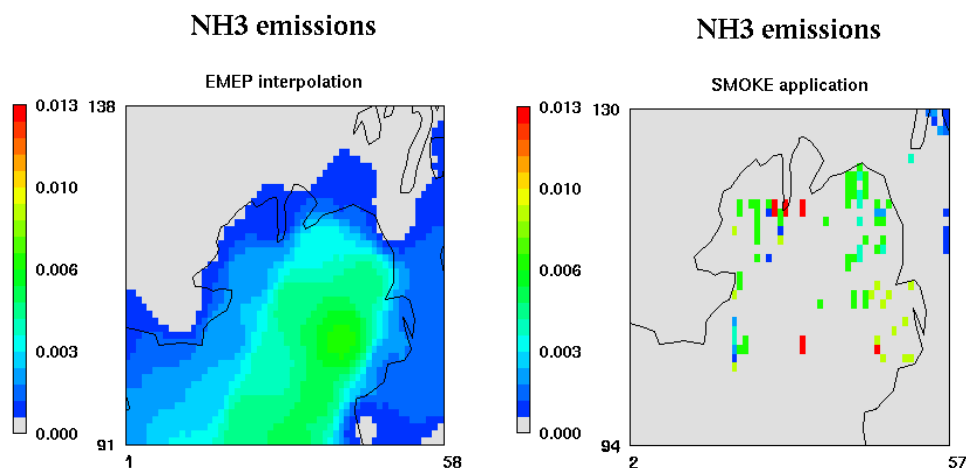
*Figure 5-8. Example of NH₃ EMEP emissions over Northern Ireland as interpolated at 5 x 5 km²
resolution (left) and as calculated by SMOKE (right) for June 1999. Units are moles s⁻¹ km⁻².*

	LOW RESOLUTION	HIGH RESOLUTION
NH$_3$	41.77	43.58
NO$_X$	155.30	100.55
SO$_2$	63.70	62.18
PM$_{10}$	6.99	10.21

*Table 5-4. Estimates of total emissions in June 1999 from the 5 x 5 km² resolution domain and the 45
x 45 km² resolution domain, calculated over the area covered by the inner grid. Units are Gg yr⁻¹*

5.2.5   Observations used for model validation

NO$_X$ and SO$_2$ concentrations measured at several monitoring sites across the UK are
used for comparison with concentrations modelled by CMAQ. The selected sites are
part of the National Air quality Archive Monitoring Network
(http://www.airquality.co.uk/archive) for the UK and the Air Quality Data Archive of
the Environmental Protection Agency (http://coe.epa.ie/air/) for Ireland.

Figure 5-9 shows the location of the monitoring sites selected for comparison; the choice of the stations is limited to background stations (urban, rural and remote stations). A background station is defined as a monitoring site "located such that its pollution level is not influenced by emissions from a nearby street, a single industrial source or industrial areas" (EC, 2001). Rural and remote stations are considered totally free from urban and industrial influence and therefore they are the most suitable for representing the air quality in the region surrounding the monitoring site (i.e. the entire 5 x 5 km^2 model grid cell). The limited number of data available from rural and remote stations for year 1999 made it necessary to include urban background stations for achieving a satisfactory spatial coverage of the UK. However in this case the comparison must be treated carefully; even if these sites are classified as background stations, they are located in populated areas where concentrations can be affected by the presence of a highway or an industrial plant not sufficiently far from the site. The additional contribution from these very local sources to air pollutant emissions needs to be taken into account when comparing observations from urban background stations with model predictions, and underestimates of concentration by the model should be expected.

Monthly NH_3 and NH_4^+ concentrations are compared versus concentrations measured by about 70 monitoring sites part of the Ammonia Monitoring Network (http://www.cara.ceh.ac.uk/). The location of the stations is shown in Figure 5-10. The sites are divided into three classes, based on the different methods applied for measuring NH_x concentrations. Red dots in Figure 5-10 represent stations using passive samplers, green dots represent sites implementing active denuders and blue dots indicate stations where both instruments are available.

The first method consists of sampling ammonia by molecular diffusion using a diffusion tube. This instrument is subject to systematic errors which can come from the incursion of wind eddies in the open ended-tubes and from the reaction of NO with O_3 within the sampler (Tang et al., 2001). This instrument tends to overestimate low concentrations (less than 1 $\mu g \ m^{-3}$) whereas it performs better for concentration values higher than 3 $\mu g \ m^{-3}$ (Tang et al., 2001; Sutton et al., 2001). Approximately 20 sites supplied with passive diffusion tubes and located in high concentration areas are included in this study. The second method consists of sampling air through two

glass tubes (denuders) coated on the inside with phosphoric acid, so that ammonia is captured by the internal tube walls. This method is more precise and sensitive than the previous one with a detection limit less than 0.1 μg m^{-3} (Sutton et al., 2001). Around 50 sites with active denuders are used in this study. In both cases sampling is on a monthly basis. More details about the ammonia monitoring network can be found in Sutton et al. (2001) and Tang et al. (2001).
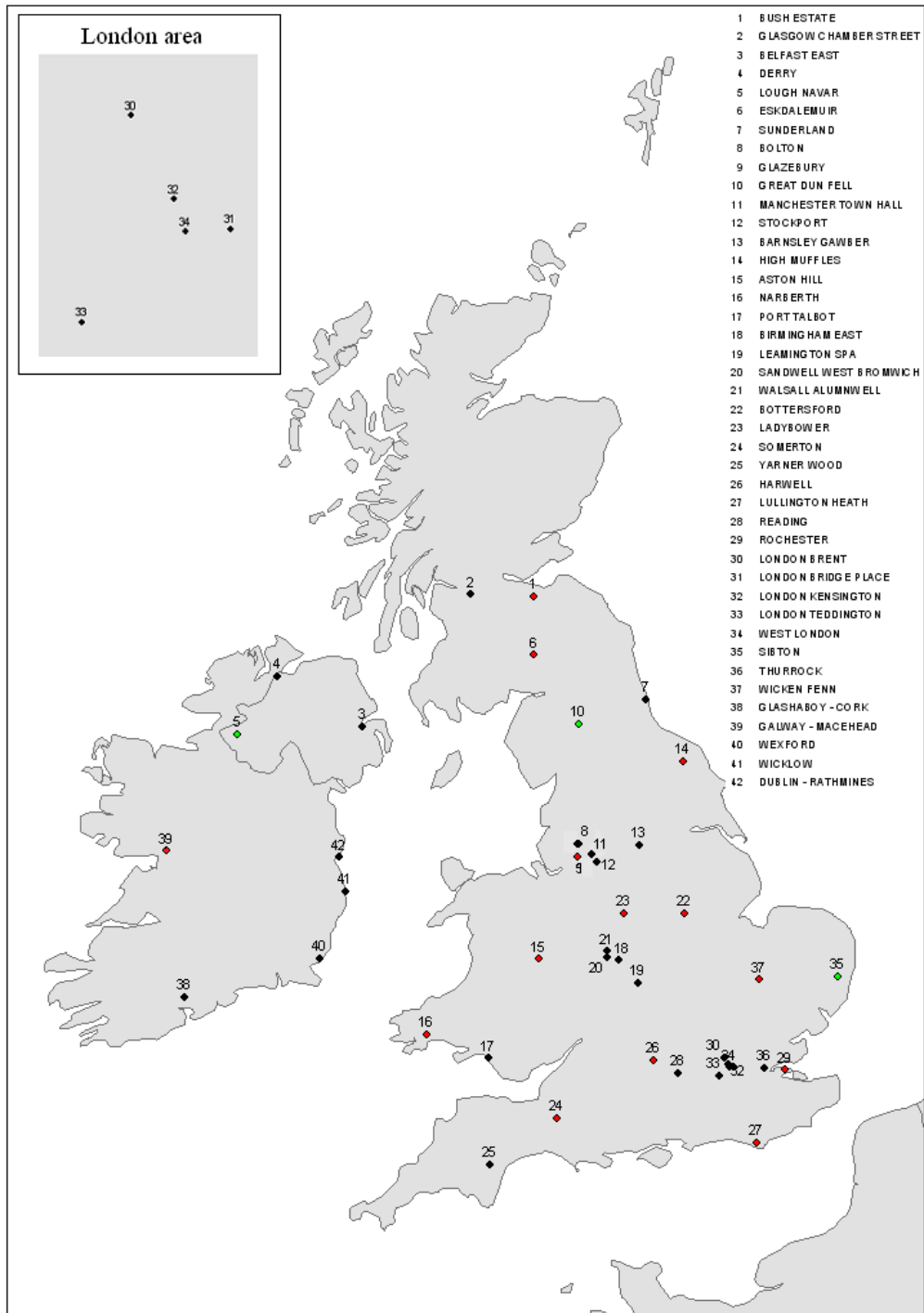
Figure 5-9. Location of the monitoring sites selected for comparison with SO_2 and NO_X modelled concentrations. Black, red and green dots represent urban background, rural and remote stations respectively. The sites are part of the UK Air Quality Monitoring Network and the Irish National Monitoring Network.
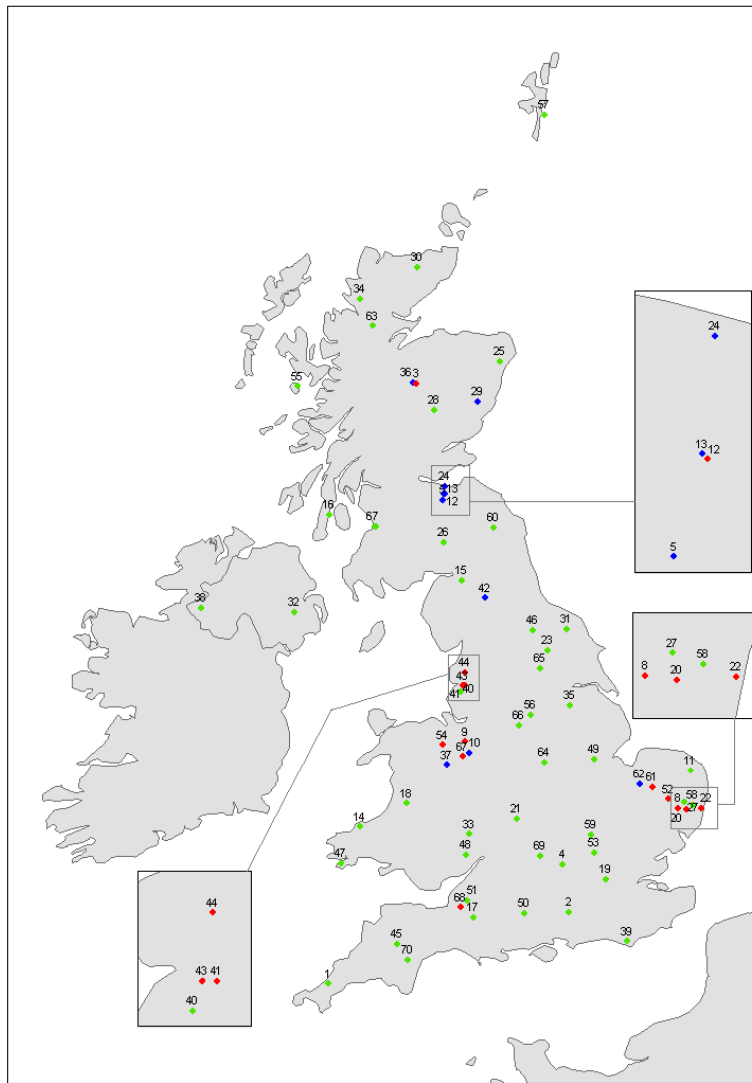
1 5 Acres	20 Dennington	39 Lullington Heath	60 Sourhope
2 Alice Holt	21 Drayton	40 Mere Sands Wood	61 Stanford
3 Allt a Mharcaidh	22 Dunwich Heath	41 Midge Hall	62 Stoke Ferry
4 Aston Rowant	23 Easingwold	42 Moor House	63 Strathvaich Dam
5 Auchencorth Moss	24 Edinburgh	43 Much Hoole	64 Sutton Bonington
6 Auchincruive	25 Ellon Ythan	44 Myerscough	65 Tadcaster
7 Auchincruive 2	26 Eskdalemuir	45 North Wyke	66 Wardlow Hay Cop
8 Bedlingfield	27 Fressingfield	46 Northallerton	67 Wem Moss
9 Bickerton Hill	28 Glen Shee	47 Orielton	68 Westhay Moor
10 Brown Moss NR 2	29 Glensaugh	48 Penallt	69 Wytham Woods
11 Bure Marshes	30 Halladale	49 Pointon	70 Yarner Wood
12 Bush Cabin	31 High Muffles	50 Porton Down	
13 Bush OTC	32 Hillsborough	51 Priddy	
14 Cardigan	33 Holme Lacy	52 Redgrave + Lopham	
15 Carlisle	34 Inverpolly	53 Rothamstead	
16 Carradale	35 Jenny Hurn	54 Ruabon	
17 Castle Cary	36 Lagganlia	55 Rum	
18 Cwmystwyth	37 Llynclys Common	56 Sheffield	
19 London, Cromwell R	38 Lough Navar	57 Shetland	

Figure 5-10. Location of the monitoring sites selected for NH$_3$ and NH_4^+ monthly comparison. The sites are part of the Ammonia Monitoring network. Green dots represent sites where active denuders are used, red dots where passive sampling is used and blue dots where both instruments are available.

5.3 RESULTS

5.3.1   Concentrations maps

Figure 5-11 show the modelled spatial distributions of NH_3, SO_2, NO_X and NH_4 concentration for June and February 1999 over the outer and the inner grid. The high resolution maps (Figure 5-11a) show that high NH_3 concentrations are spread all over the country, with areas of higher concentration mainly in East Anglia, the East Midlands, Northern Ireland and Eire, where livestock and agricultural activities are more extensive. Concentrations are also higher during summer rather than in winter (Figure 4-8), resulting from lower emissions in the cold season, when livestock is confined in housing units. High temperatures in summer may also increase the volatilization of ammonia contributing to increased emissions and concentrations (Pinder et al., 2004). Some differences appear between the 45 x 45 km^2 resolution and the 5 x 5 km^2 resolution map: NH_3 concentration over the UK is lower of approximately 1 $\mu g\ m^{-3}$ over the inner grid compared to the outer one: this might be due to a faster conversion of ammonia to ammonium (reactions 1.11 -1.13) at high resolution. This is consistent with the map of distribution of ammonium concentration (Figure 5-11b), which appears lower over the 45 x 45 km^2 resolution grid compared to the 5 x 5 km^2 resolution one.

Patterns of NO_x and SO_2 (Figure 5-11c, Figure 5-11d) show pollutants are mainly concentrated in the industrial areas of London and Yorkshire, with higher values in February rather than in June (SO_2 emissions are higher in the winter period due to a larger use of heating systems). The patterns for NO_x are very similar over the two domains, whereas SO_2 concentration is higher over the 45 x 45 km^2 resolution grid compared to the 5 x 5 km^2 resolution one. The highest differences (about 10 μgm^{-3} in June and 20 μgm^{-3} in February) are visible in the areas close to the main emission point sources. Possible reasons for the difference in SO_2 concentration between the two domains can be identified in a faster conversion of SO_2 to H_2SO_4 (reactions 1.1-1.3) or in a faster deposition process of SO_2 over the inner grid compared to the outer one.

a)

NH3 concentration
45 x 45 km^2 resolution grid
1−28 June 1999

NH3 concentration
45 x 45 km^2 resolution grid
1−28 February 1999

NH3 concentration
5 x 5 km^2 resolution grid
1−28 June 1999

NH3 concentration
5 x 5 km^2 resolution grid
1−28 February 1999

b)

NH4 concentration
45 x 45 km^2 resolution grid
1–28 June 1999

NH4 concentration
45 x 45 km^2 resolution grid
1–28 February 1999

NH4 concentration
5 x 5 km^2 resolution grid
1–28 June 1999

NH4 concentration
5 x 5 km^2 resolution grid
1–28 February 1999

c)

SO2 concentration
45 x 45 km² resolution grid
1−28 June 1999

SO2 concentration
45 x 45 km² resolution grid
1−28 February 1999

SO2 concentration
5 x 5 km² resolution grid
1−28 June 1999

SO2 concentration
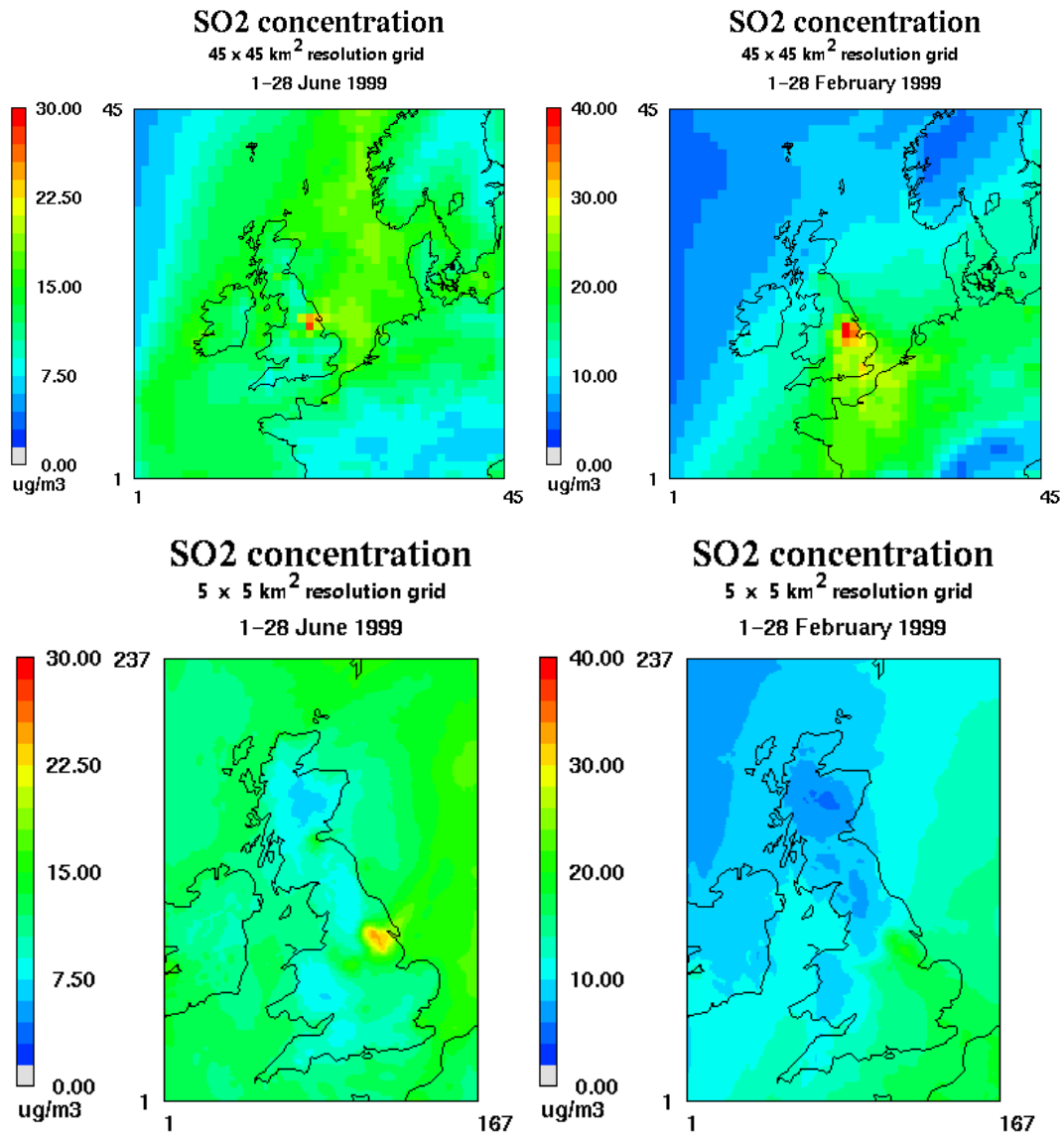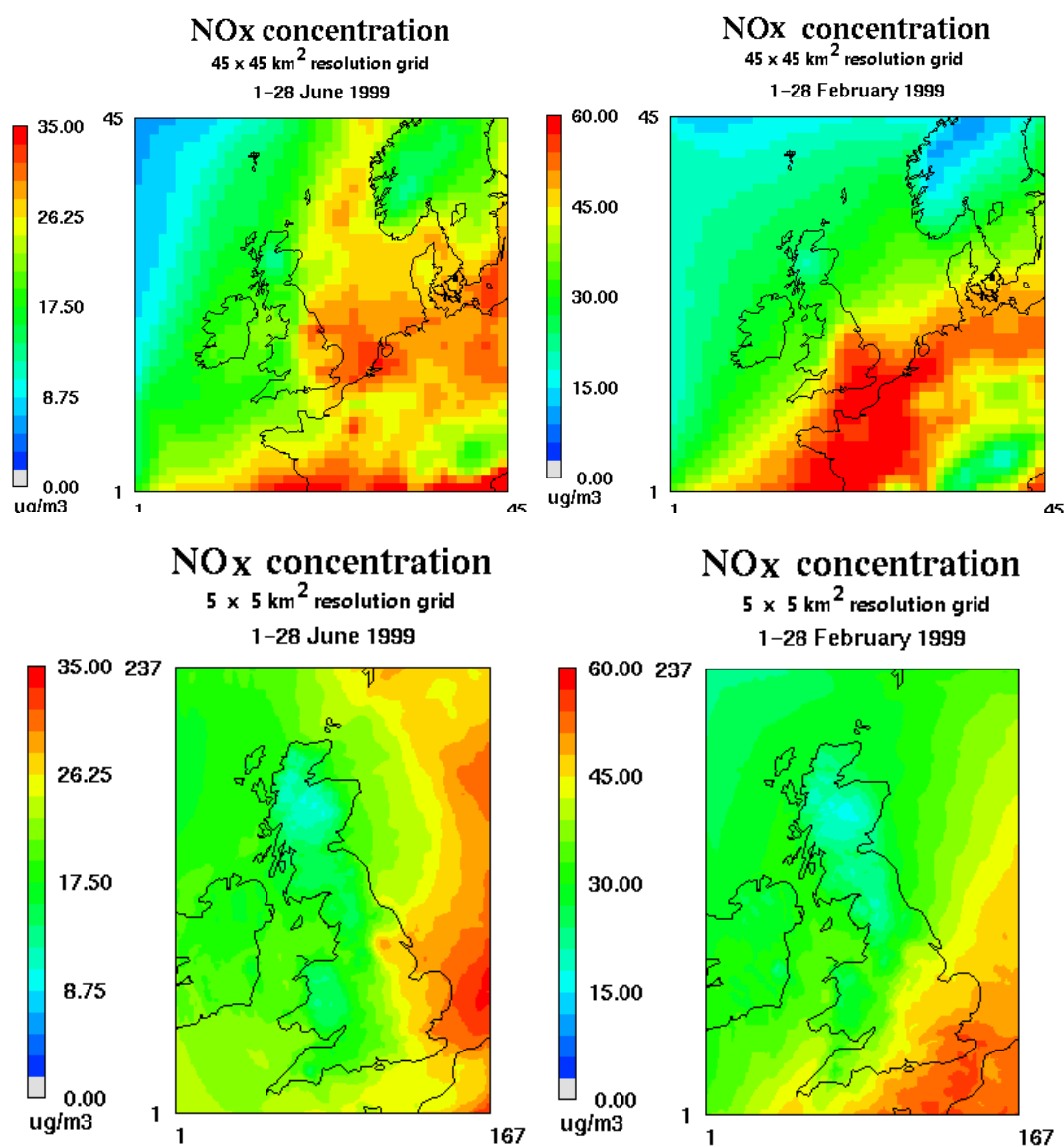**5 x 5 km² resolution grid**
1−28 February 1999

d)

Figure 5-11. CMAQ modelled concentrations for June and February 1999. Distribution of NH_3, NH_4, SO_2 and NO_X concentrations over the inner (5 x 5 km^2 resolution) and the outer (45 x 45 km^2 resolution) grid. Units are $\mu g\ m^{-3}$.

5.3.2   Temporal series of NO_X and SO_2 concentration

Temporal series of NO_X and SO_2 concentrations at specific points of the domain are presented (Figure 5-12). Six-hourly CMAQ concentrations are extracted and compared to concentrations measured by several monitoring sites part of the Air Quality Monitoring Network. Figure 5-12 shows four comparisons for both NO_x (Figure 5-12a) and SO_2 (Figure 5-12b) with two rural stations (Ladybower and Rochester) and two urban stations (Sandwell East and London Bridge) in June 1999. In all comparisons maxima and minima of CMAQ concentration are shifted respect to observations. Figure 5-13 shows the normalized monthly mean diurnal cycle of NO_X and SO_2 concentration in June 1999, averaged for rural and urban stations. The trend is clearly different for CMAQ and observations and this indicates that the model cannot reproduce the diurnal cycle of both pollutants properly.

This is also confirmed by the values of correlation coefficient between modelled and measured 6-hourly concentrations (Figure 5-14) always between 0.1 and 0.5 for most of the sites (r is between 0.1 and 0.5 for NO_X and between 0.1 and 0.4 for SO_2). A possible reason may be that the model's vertical resolution is insufficient to resolve the night time boundary layer. Another possible explanation can be identified in the uncertainty affecting the temporal profiles used for disaggregating annual NO_x and SO_2 emissions into hourly emissions. The creation of specific emission temporal profiles is a difficult task, because of the lack of information concerning the temporal variation of emissions from specific sources, especially from power stations. Important details including the rate of production of electrical power, the fuel consumption and the existence of breakdowns or periodic shut-downs due to planned maintenance are often unavailable. In addition, monthly and weekly profiles used in this work (Figure 4-8, Figure 4-9) are also assumed to be the same for all pollutants. Future introduction of pollutant-dependent emission factors in the weekly and monthly disaggregation may help to improve the quality of the results. In the future a study of sensitivity analysis also needs to be carried out in order to test how the model responds to the use of different types of emission factors. This will be help to identify the set of temporal profiles most suitable for UK emissions.

a)

b)
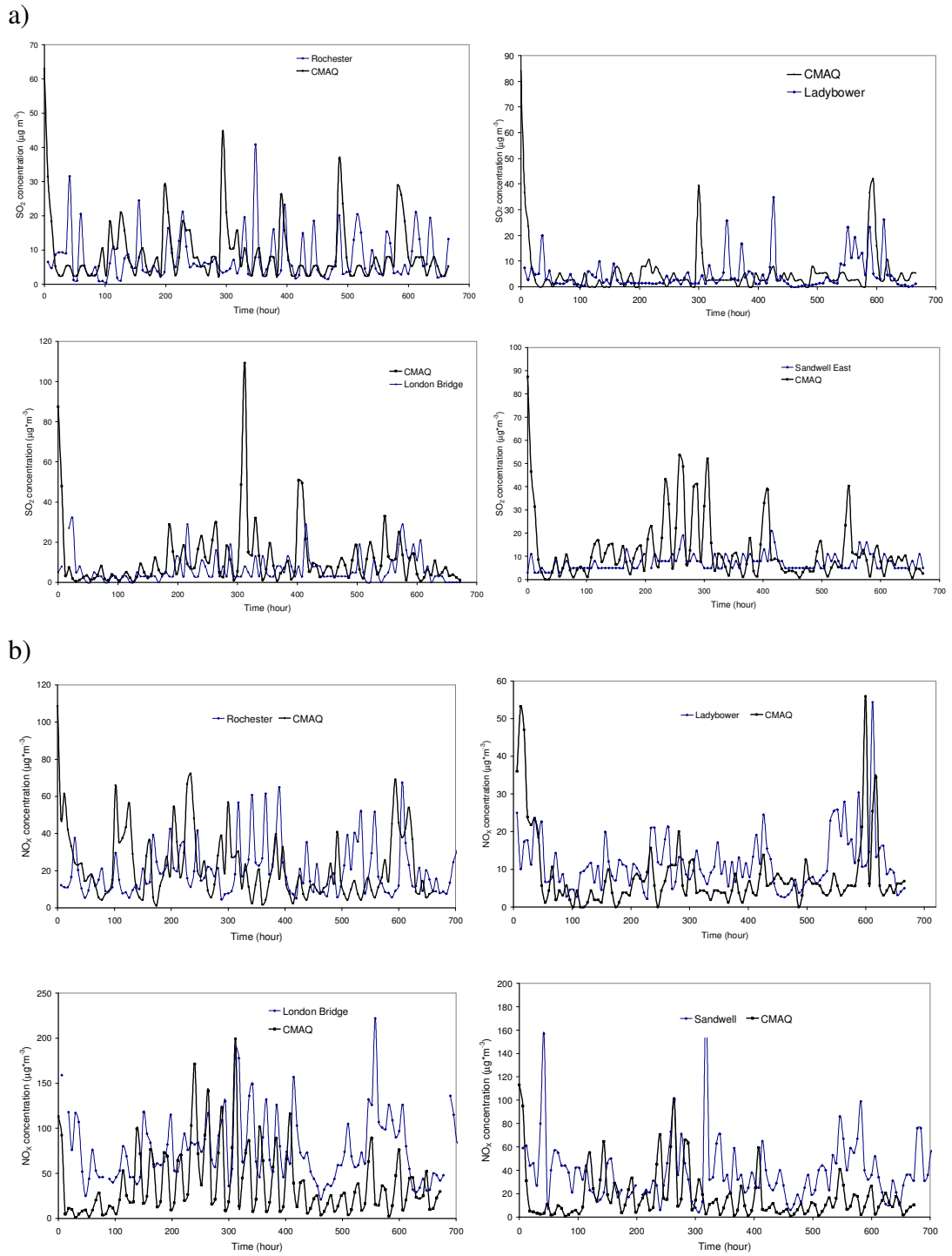
Figure 5-12. Examples of 6-hourly temporal series of SO$_2$ and NO$_X$ concentration for June 1999. Blue and black solid lines represent measurements and CMAQ predictions respectively. Two rural (Ladybower and Rochester) and two urban sites (London Bridge and Sandwell East) have been selected for comparison.

139
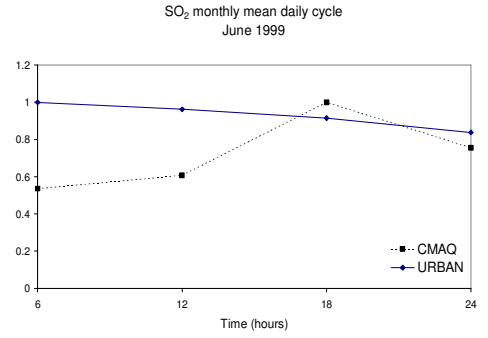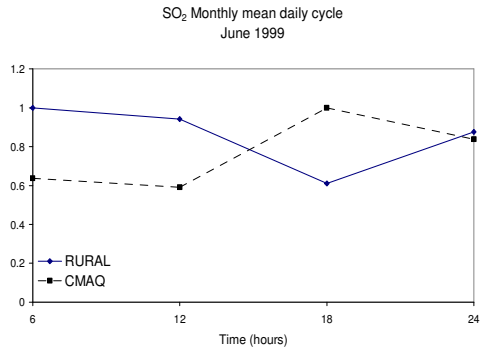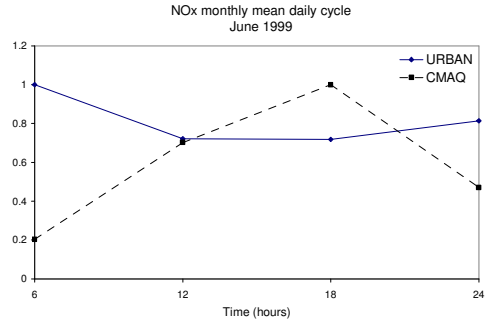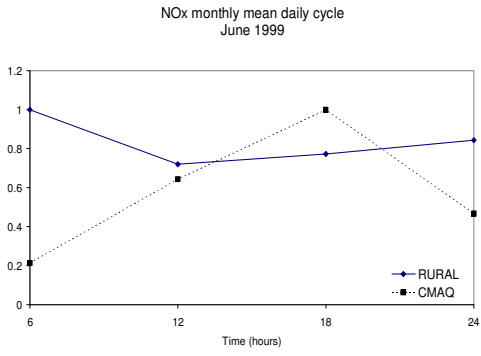
Figure 5-13. Normalized monthly mean diurnal cycle of NO$_X$ and SO$_2$ concentration in June 1999, averaged for rural (left) and urban stations (right).
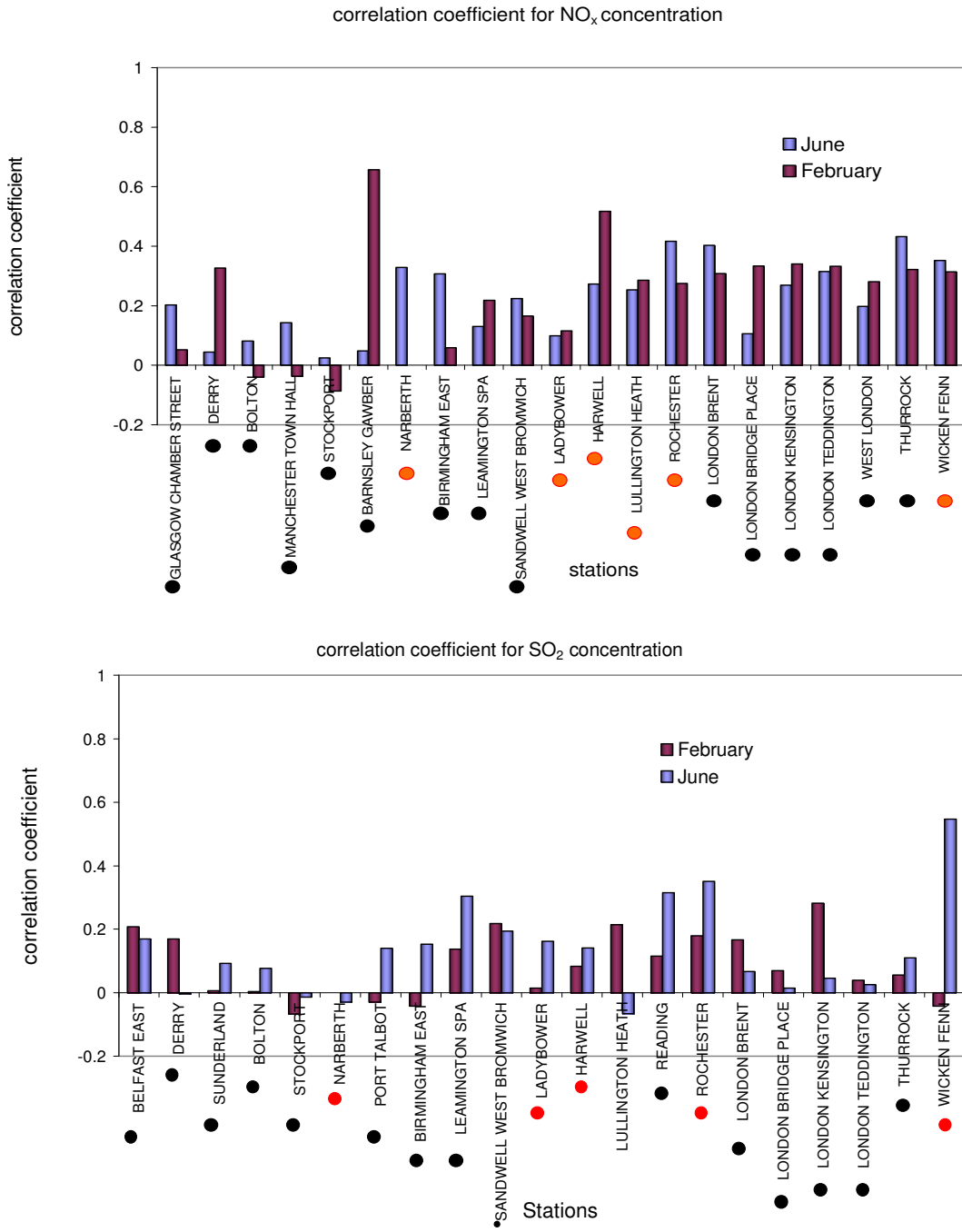
Figure 5-14. Correlation coefficient between modelled and measured 6-hourly concentrations, NO_X (top) and SO_2 (bottom). Red and black dots indicate rural and urban background stations respectively.

5.3.3 The weekend effect

The dependence of NO_X and SO_2 temporal series on the temporal variability of emissions can also be illustrated by the so called "weekend effect".

Figure 5-15 shows the monthly mean daily cycle of SO_2 and NO_X concentrations, averaged for urban and rural stations, for weekdays and weekends. In both months concentrations are lower during weekend rather than weekday. This phenomenon has been the topic of many research studies (Altshuler et al., 1995; Bronnimann and Neu, 1997; Jenkin et al., 2002; Pun et al., 2003 among others) and it is considered as very important especially for NO_X, because of the role of these pollutants in the photochemical production of photo-oxidants, tropospheric ozone (O_3) in particular. The reduction of NO_2 concentration is considered as one of the main causes of the increase of O_3 concentration on weekends (Blanchard and Tanenbaum, 2003; Heuss et al., 2003; Lawson, 2003; Marr and Harley, 2002a). From Monday to Friday, NO concentration is high, thus the titration of O_3 by NO_X ($NO+O_3 \rightarrow NO_2+O_2$) is strong, keeping O_3 concentration low. By contrast, at weekend NO_2 concentration declines thus the titration of O_3 by NO_X is weaker. The formation of new O_3 proceeds faster and O_3 concentrations increase. Thus on Saturdays and Sundays ground level ozone concentrations rise considerably above the typical weekdays values, despite the fact that its precursors are lower on the weekends compared to weekdays ("ozone weekend effect"). This increase in O_3 concentrations, typical of many urban areas, was first reported in the United States in the 1970s (Cleveland et al., 1974; Lebron, 1975).

The decrease in NO_X and SO_2 concentrations on weekends (Figure 5-15) is due to a reduction in emissions, mainly from traffic and combustion processes. Figure 5-16 shows the monthly mean weekly cycle of NO_X and SO_2 concentration in both June and February 1999, averaged for urban and rural stations. Weekly emission factors (Figure 4-9) have also been plotted for comparison. Both cycles are strongly dependent on the temporal emission profiles. Residential and industrial combustion in energy production is the dominant source (Figure 5-16a) of SO_2 emissions. This leads to a slight reduction of SO_2 concentration on Saturdays and Sundays, when many power plants partially reduce their production activity. Road vehicular traffic is

the dominant anthropogenic emission source of NO_X (Figure 5-16b) in both rural and urban areas. A reduction in NO_X concentration is visible on Saturday and Sunday; due to the decrease of heavy-duty diesel truck activity on highways in weekends compared to weekdays (Dreher and Harley, 1998).

a)
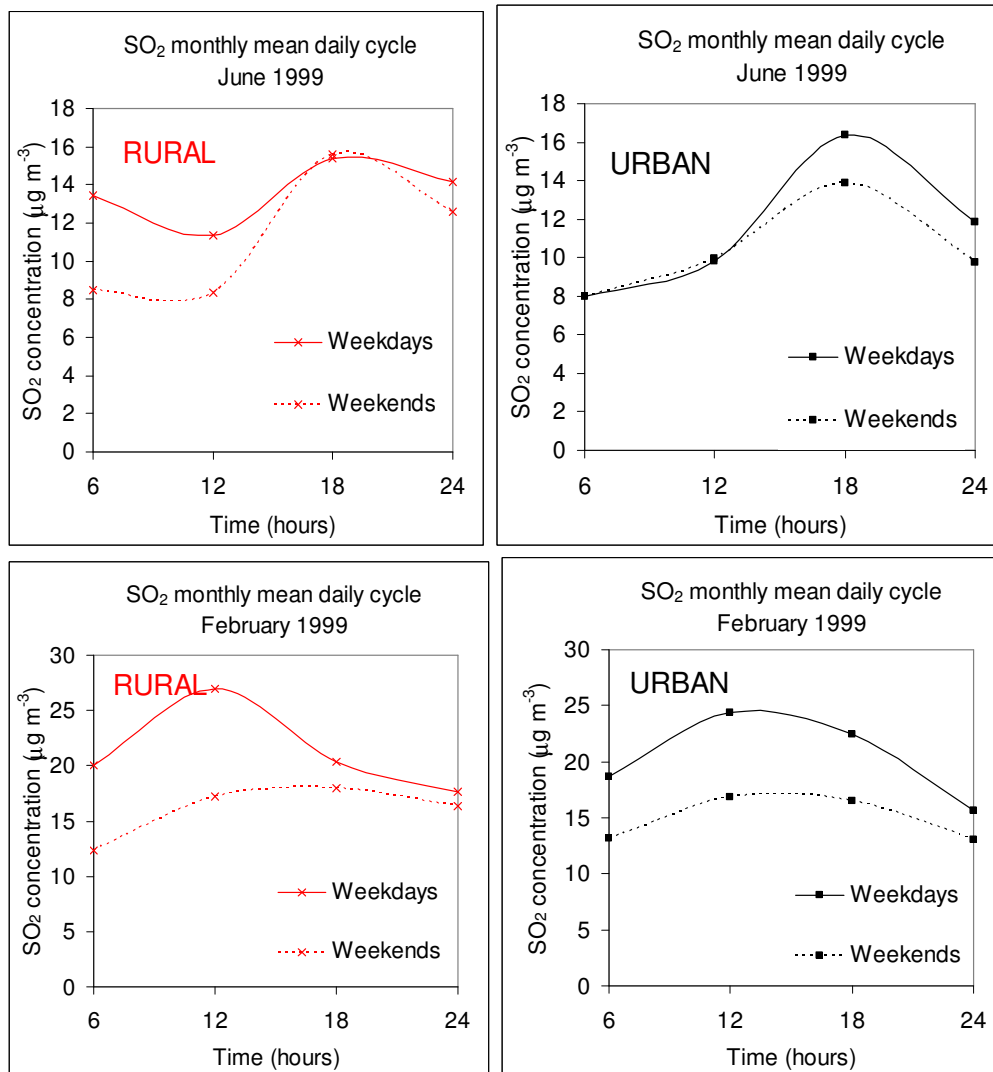
b)
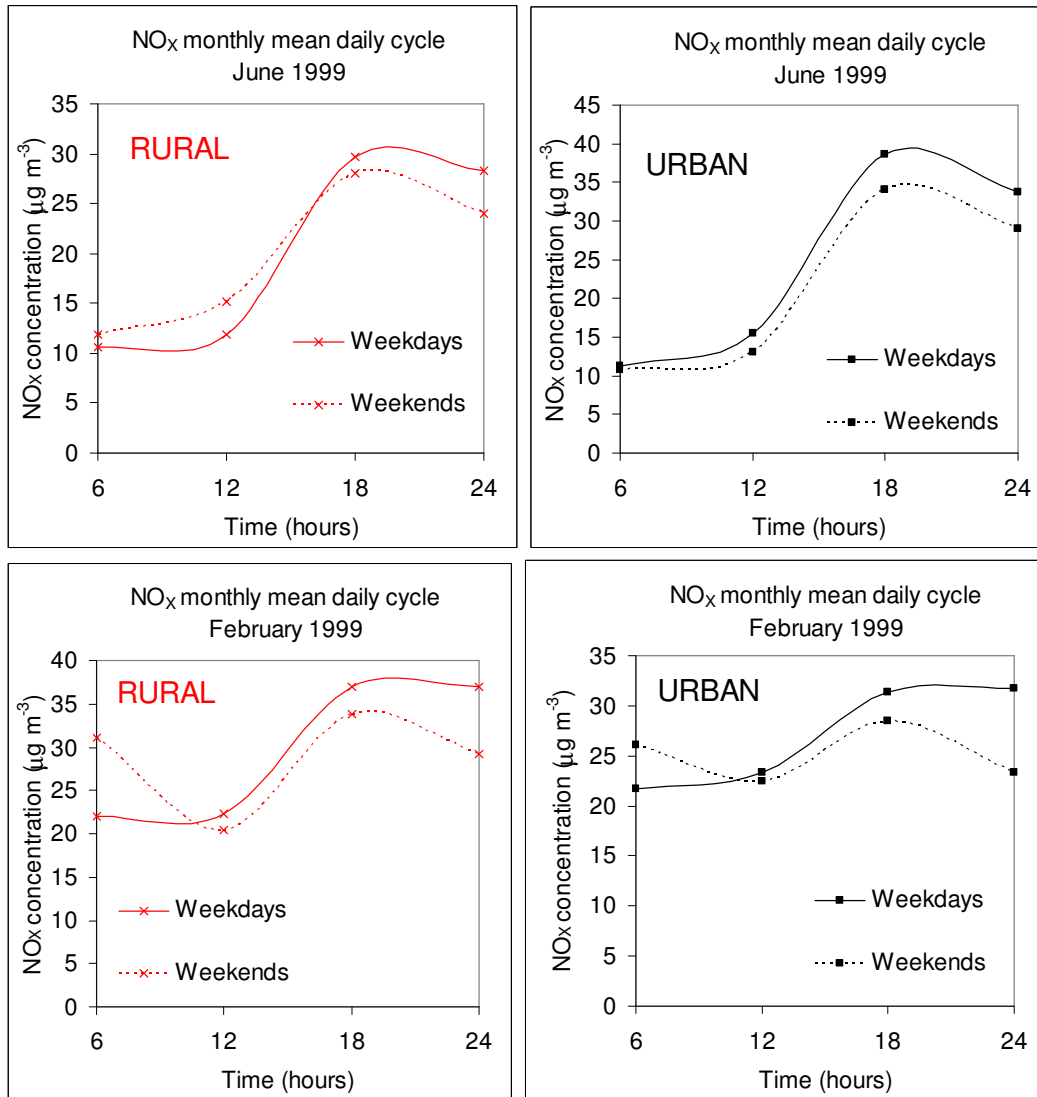
Figure 5-15. Monthly mean daily cycle of concentration for urban (black) and rural (red) stations in June and February 1999. a) SO_2 and b) NO_X cycles are plotted using solid and dashed lines, which represent averaged concentration in weekdays and weekends respectively. Units are $\mu g\ m^{-3}$.
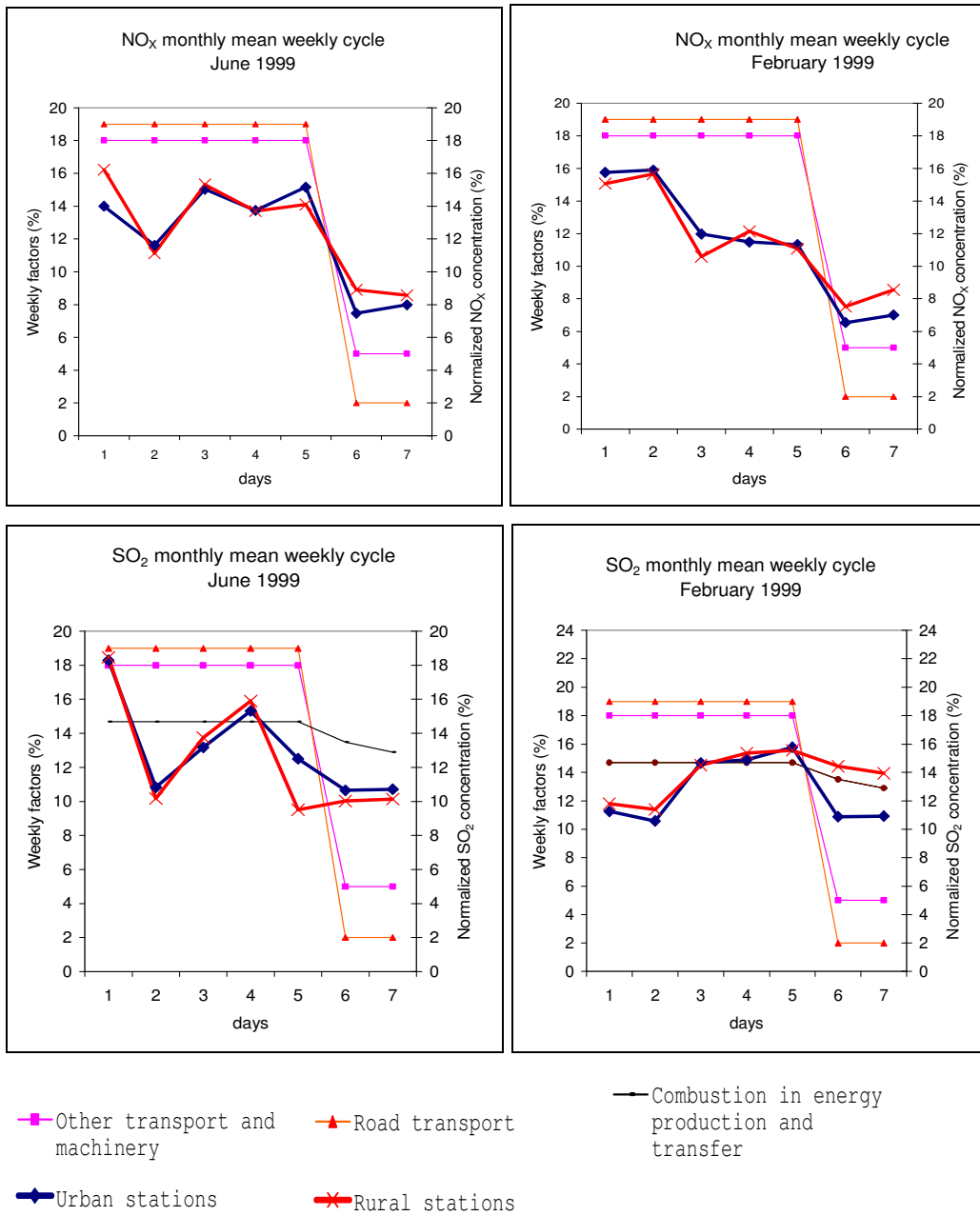
Figure 5-16. Weekly mean daily cycle of normalised concentration (%) for urban (blue) and rural (red) stations in June and February 1999. Weekly emission temporal profiles have been added for comparison.

5.3.4 Monthly concentrations

5.3.4.1 NO_X

On a monthly basis, some expected large discrepancies are observed at urban background sites, where the model under-predicts NO_X concentrations. In most of the rural stations measurements are close to modelled values in June whereas the model over-predicts NO_X concentration in February (Figure 5-17). The model under-predicts concentration mainly in the London area, Manchester, Bolton and Glasgow in both months. The scatter plot of NO_X predictions versus observations (Figure 5-18) shows a poor agreement (Table 5-5), with a correlation coefficient close to 0.2 for both June and February.
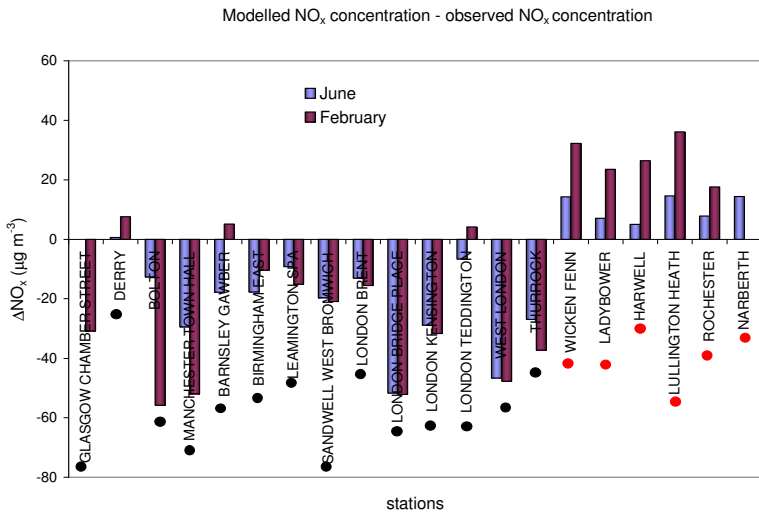
Figure 5-17. Difference between modelled and measured NO_X monthly concentrations. Red and black dots indicate rural and urban background stations respectively.

NO$_X$ scatter plot, all stations
June 1999
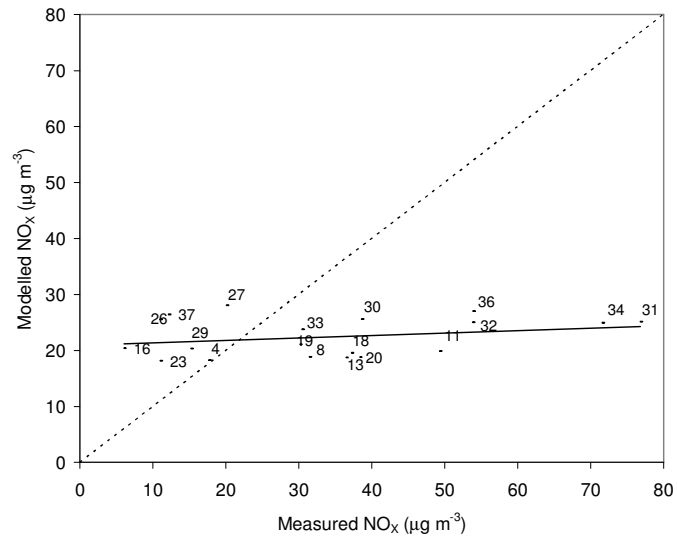
NO$_X$ scatter plot, all stations
February 1999
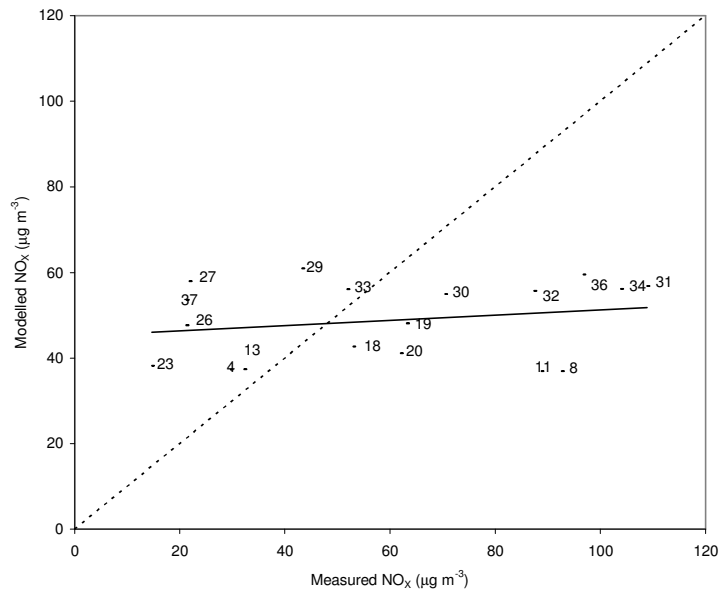
Figure 5-18. Scatter plots of modelled NO$_X$ concentrations versus observed concentrations. The numbers identify the stations of Figure 5-9. The dashed line indicates the 1:1 agreement. The black solid line represents the best linear fit. The results of the interpolation are reported in Table 5-5

147

5.3.4.2 SO₂

Figure 5-19 highlights the general tendency of CMAQ in overestimating SO_2 concentration, with significant over-predictions at rural sites. The results of the linear fit (Figure 5-20) are reported in Table 5-5. The large under-prediction in Belfast East can be explained considering that one of the major suppliers of natural gas in the UK is located in this area. This contributes to the increase of emissions and therefore concentrations of gaseous pollutants including SO_2 in the surroundings of the monitoring site. Because the grid point is not close enough to the monitoring site, CMAQ cannot predict SO_2 concentration correctly.
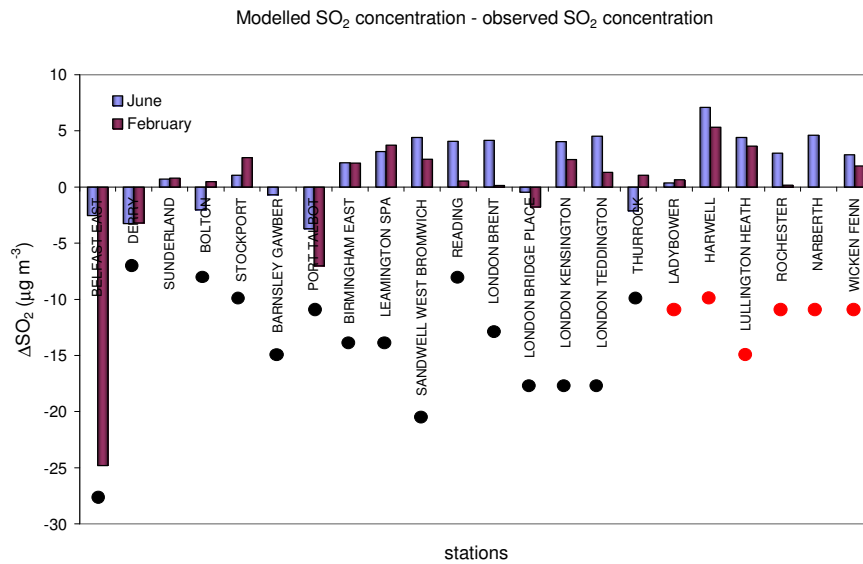
Figure 5-19. As Figure 5-17, but SO₂

SO$_2$ scatter plot, all stations
June 1999
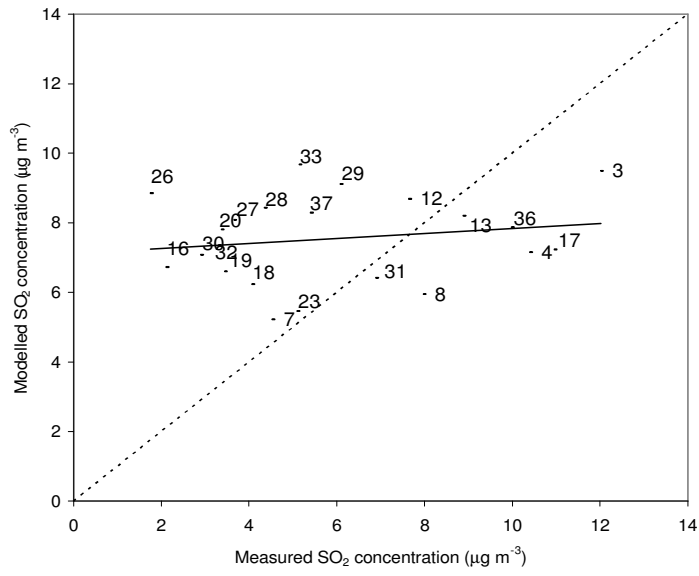
SO$_2$ scatter plot, all stations
February 1999
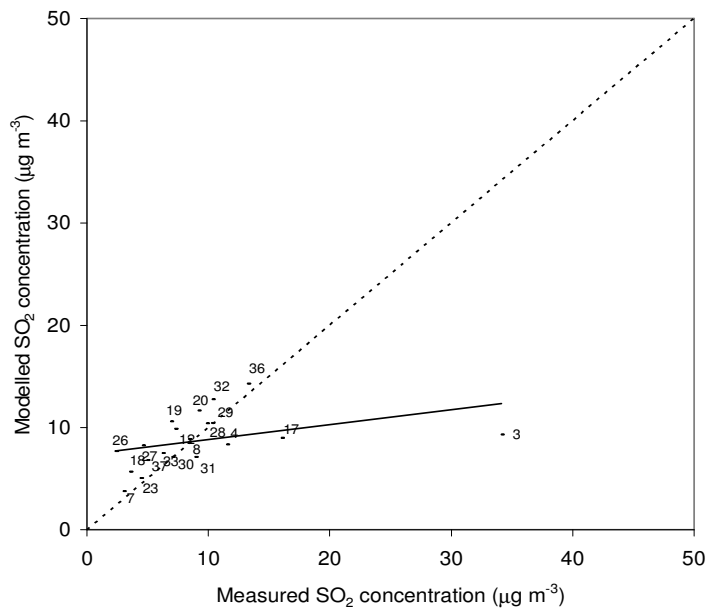
Figure 5-20. As Figure 5-18, but SO$_2$ concentration.

	SO_2		NO_X	
	June	February	June	February
R^2	0.029	0.150	0.069	0.047
Slope	0.071	0.145	0.044	0.061
Intercept	7.116	7.406	20.879	45.101

Table 5-5. Results of the linear fit between measured and modelled concentrations for SO_2 (left) and NO_x (right).

5.3.4.3   <u>NH$_3$ and NH$_4$</u>

The histograms in Figure 5-21 show the difference between modelled monthly ammonia concentrations and monthly measurements from the Ammonia Monitoring Network; it varies approximately between -3 µg m^{-3} and 1 µg m^{-3}. The scatter plots of modelled concentration versus observed concentration shows a better agreement in June rather than in February (Figure 5-22) with a correlation coefficient equal to 0.75 and an intercept close to 1 (Table 5-6). The model reproduces ammonium concentration well in June (Figure 5-23, Figure 5-24), with differences between modelled and measured data varying approximately between -0.2 and 0.2 µg m^{-3}. The correlation coefficient is about 0.5.
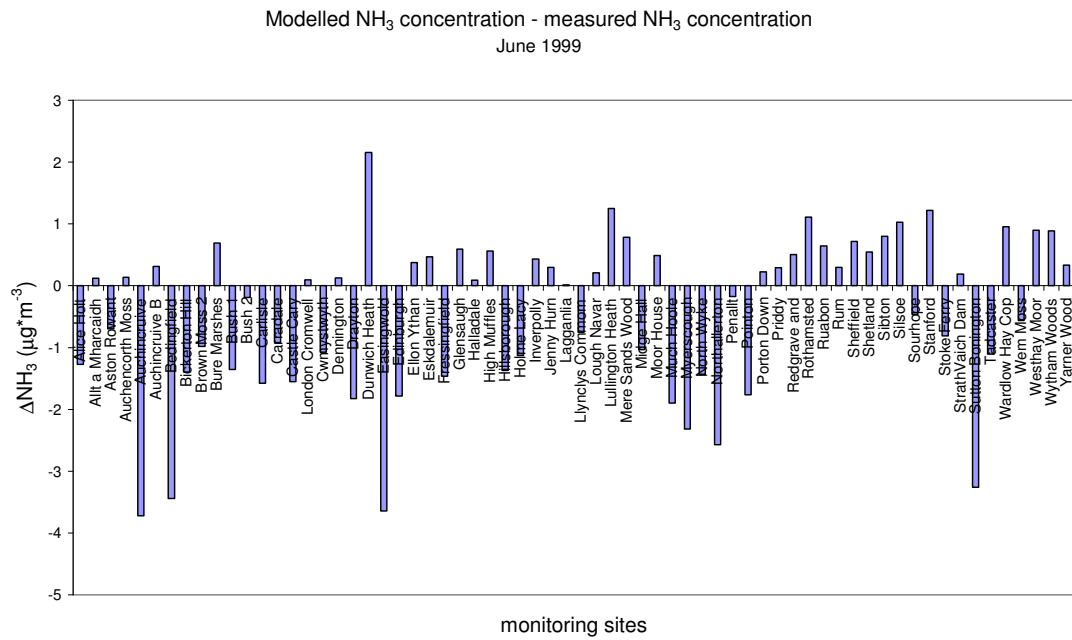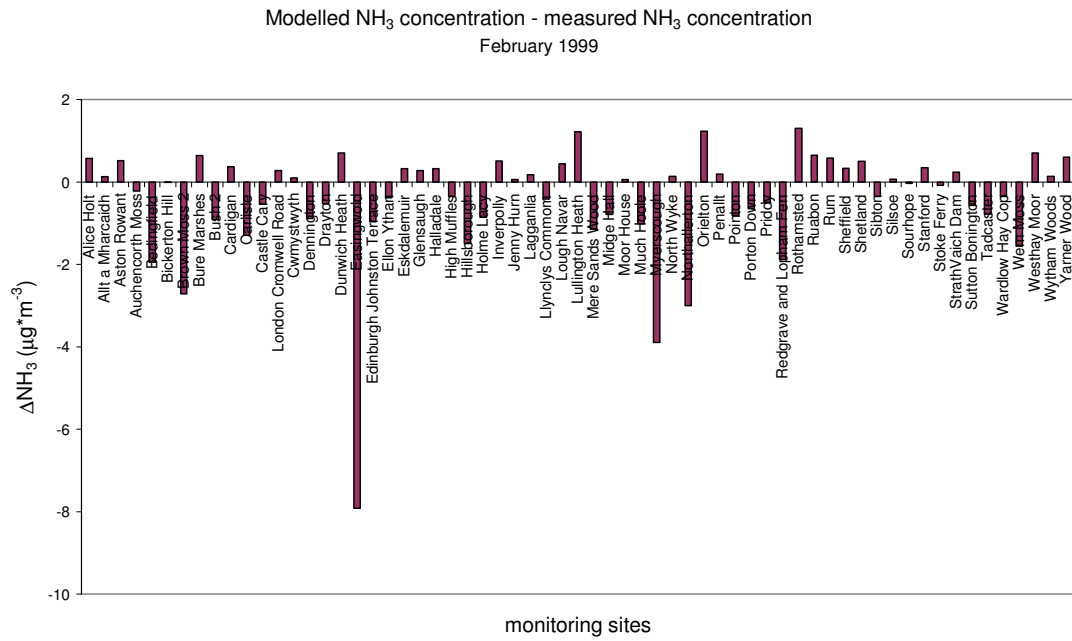
Figure 5-21. Difference between modelled and measured ammonia concentration in February (top) and June (bottom) 1999.
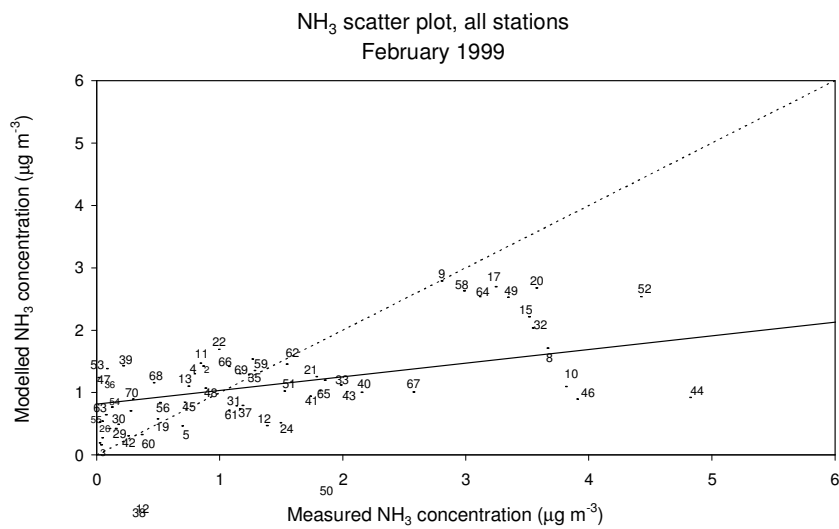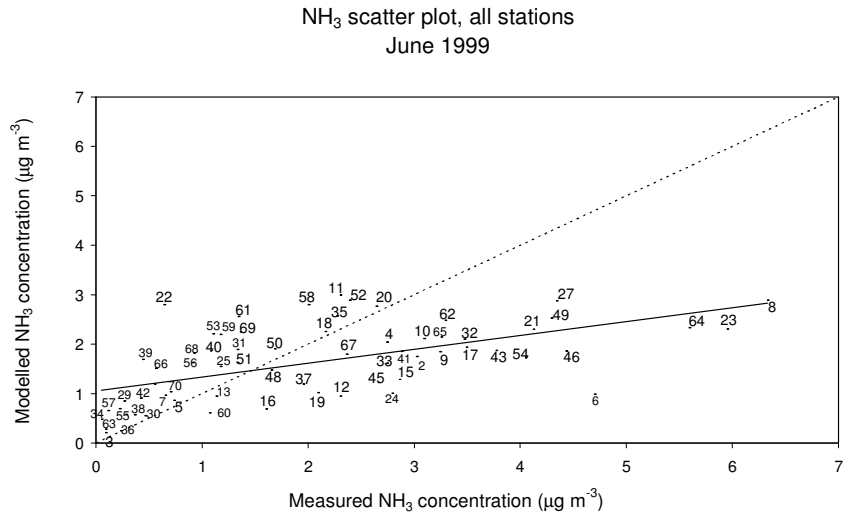
Figure 5-22. Scatter plots of modelled NH₃ concentration versus measurements for June 1999 (top) and February (bottom). The numbers identify the stations of Figure 5-10. The results of the linear fit (black solid line) are reported in Table 5-6.

	June	February
R^2	0.326	0.267
Slope	0.281	0.219
Intercept	1.053	0.816

Table 5-6. Results of the linear regression for ammonia concentration. The model performs slightly better in June rather than in February.

NH$_4$ concentration
June 1999
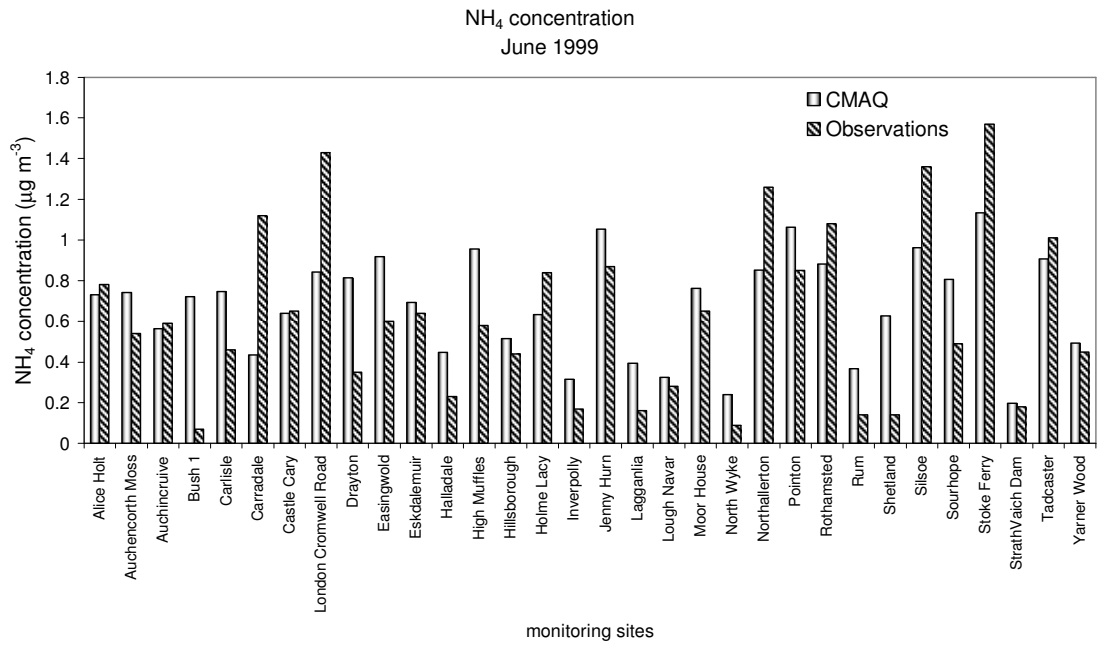
Figure 5-23. Concentrations of ammonium as modelled by CMAQ (grey) compared to monthly concentrations measured by the monitoring sites of the Ammonia Monitoring Network (black).

NH$_4$ scatter plot, all stations
June 1999
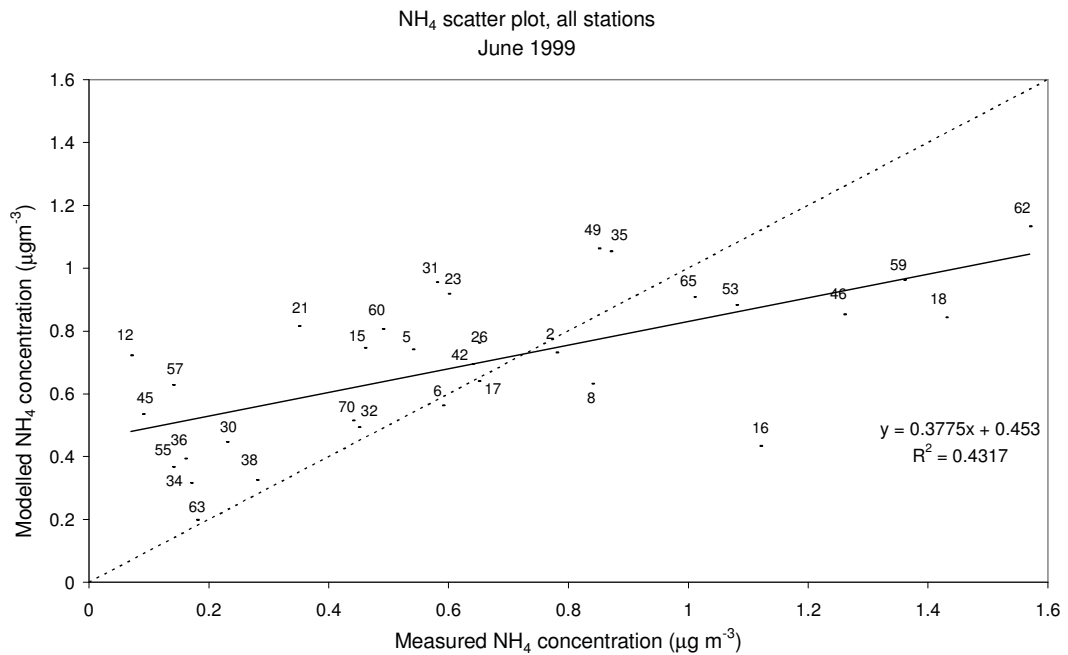
Figure 5-24. Scatter plots of modelled NH$_4$ concentration versus measurements for June 1999. The numbers identify the stations of Figure 5-10.

5.3.4.4 Statistics

The Normalized Mean Bias (NMB) and the Normalized Mean Error (NME) (Yu et al., 2006) are defined as:

$$NMB = \frac{\sum_{i=1}^{N}(M_i - O_i)}{\sum_{i=1}^{N} O_i} 100\% \qquad\qquad (5.6)$$

$$NME = \frac{\sum_{i=1}^{N}|M_i - O_i|}{\sum_{i=1}^{N} O_i} 100\% \qquad\qquad (5.7)$$

where M is the modelled value, O is the observed value and N is the number of observations. $|X|$ is the absolute value of X.

Estimates of Normalized Mean Bias (NMB) and Normalized Mean Error (NME) based on 6-hourly data are reported in Table 5-7. For NO_x the model performs better in winter rather than in summer. In June NME and NMB are around 55% and -40% respectively whereas in February NME is 47% and NMB is -24%. For NH_3 the response of the model is very similar in both months, with a NME close to 50% and a negative bias (around - 25%). For ammonium NME is approximately 40% in June, in agreement with Wu et al. (2005). NMB is negative and small for NH_4^+ (-10%), with a value close to the one provided for June 2001 by Gilliland et al. (2006) (around -7%). For SO_2 the model performs better in winter (NME of 37%) rather than in summer (NME of 50%) and SO_2 concentration is overestimated (NMB is 4% in February and 27% in June).

		NME (%)	*NMB (%)*
NO_X	June	55.56	-39.55
	February	46.47	-24.28
NO_2	June	53.93	-42.51
	February	35.83	- 4.16
SO_2	June	50.37	27.60
	February	36.36	4.36
NH_3	June	49.80	-20.49
	February	48.48	-25.76
NH_4	June	40.97	-9.97
	February	-----	-----

Table 5-7. Values of NMB and NME for monthly concentrations.

Taylor plots (Taylor, 2001) (Figure 5-25) are used for visualizing the correlation coefficient and the standard deviation ratio (Table 3-1) of NO_X and SO_2 6-hourly concentrations. Details about Taylor plots can be found in Chapter 3. In June the 6-hourly variability of NO_X is good (Figure 5-25a), with a standard deviation ratio between 0.9 and 1.6, excluding the stations of Barnsley, Narberth and Lullington Heath which present values above 2.5. The correlation coefficient is less than 0.5 in both months (Figure 5-25a,b). For SO_2 (Figure 5-25c,d) the plot highlights the poor performance of CMAQ with a correlation coefficient always less than 0.3 and a high dispersion (range between 0.5 and 3.5).

a)

NOX concentration, June 1999
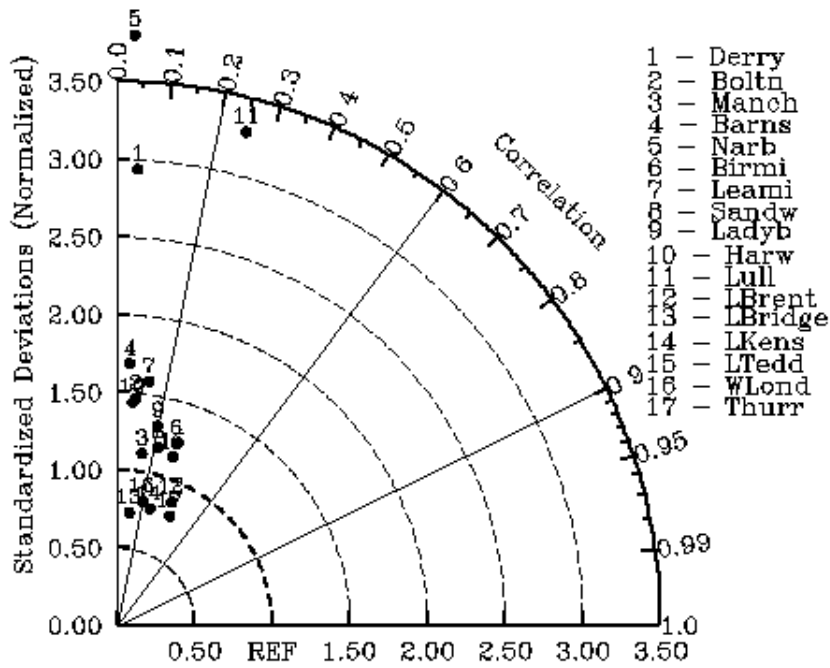
b)

NOX concentration, February 1999

156

c)
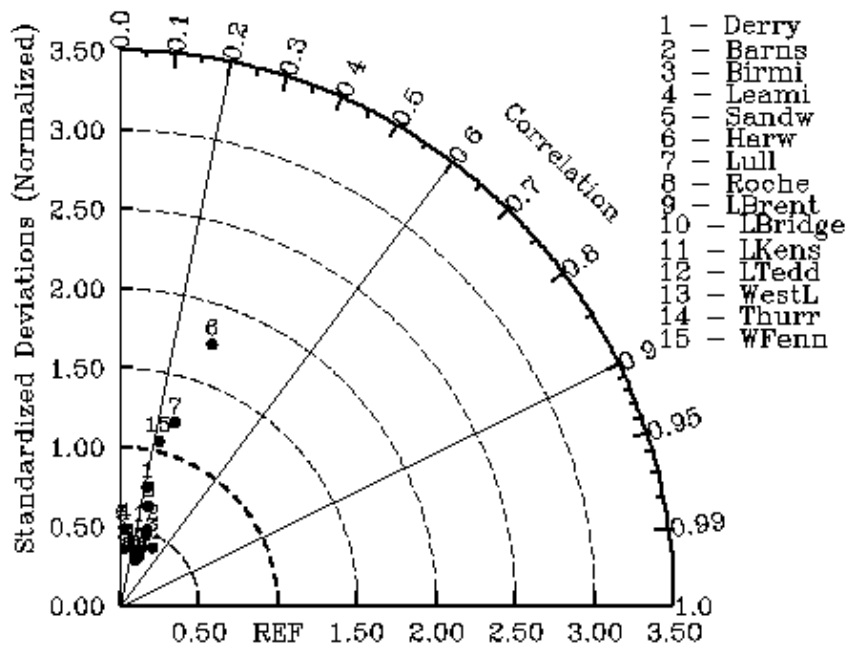
SO2 concentration, June 1999

d)
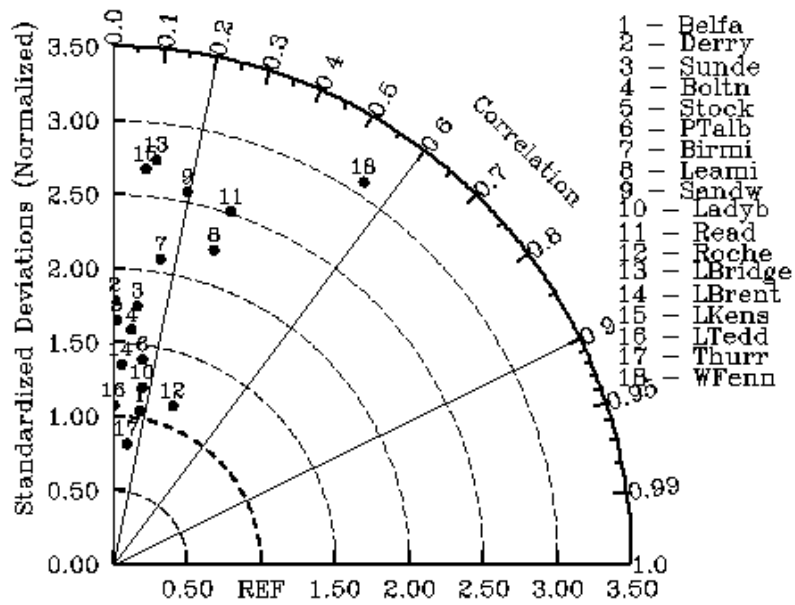
SO2 concentration, February 1999
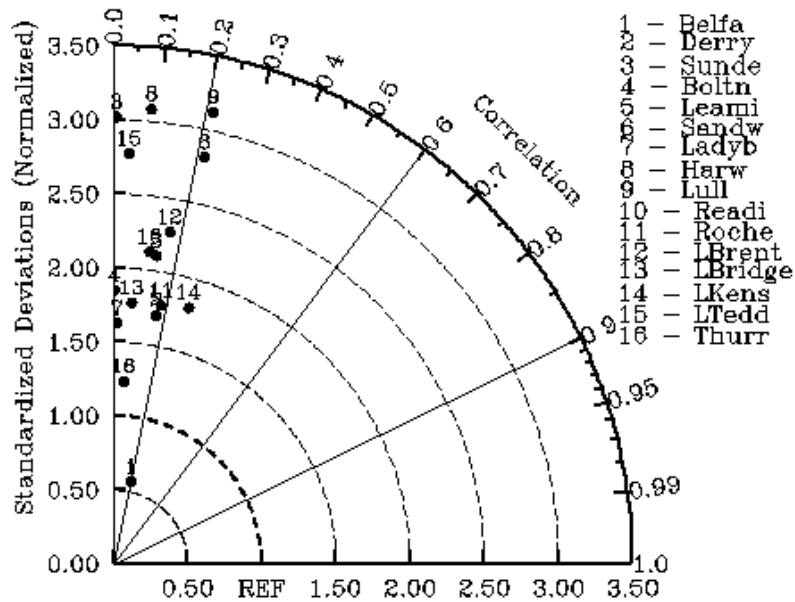
Figure 5-25. Taylor diagrams for June 1999 and February 1999. The black dots represent the ratio between CMAQ standard deviation and the observed one.

5.4 COMPARISON OF THESE RESULTS WITH OTHER CMAQ STUDIES

Table 5-8 and Table 5-9 list several CMAQ evaluation studies carried out in the US and East Asia between 2002 and 2006 and compare estimates of NMB and NME for various species. The results from this study are also presented; the version 4.4 of the model has been applied in both months (February and June 1999).

In addition to considering different geographical areas, the other studies applied CMAQ at a variety of different horizontal resolutions (4 km to 80 km) and used various model versions, driving meteorological models and chemical schemes. All these differences make direct comparisons with this work difficult, nevertheless they provide a useful context. Comparing the results of other studies with those presented in this study may help to assess the uncertainty in CMAQ concentrations, in a very general sense. For example, a possible agreement among all the studies for NMB values (all negative or all positive), may indicate a systematic tendency of the model in underestimating or overestimating concentrations.

Wu et al. (2005) performed a study with CMAQ on a 4 x 4 km^2 resolution grid over the Southern US using meteorological fields from MM5 and emissions from the National Emission Inventory for the US (NEI). NO_2 modelled data are compared to measurements taken in North Carolina from the North Carolina Department of Environment and Natural Resources Network (NCDEN) whereas SO_2 and NH_4^+ measurements were provided by the Clean Air Status and Trends Network (CASTNET), one of the main American networks consisting of approximately 90 sites across the eastern and western United States. According to Wu et al. (2005) NMB and NME are 40% and 70% respectively for modelled NO_2 in August 2002. Vijayaraghavan et al. (2006) used the same model version (CMAQ 4.4) and the same input sources (MM5 and NEI) to compare modelled tropospheric NO_2 columns over North America to satellite data (ERS/GOME) for January 2001 and August 2001. In August NME is approximately 40%, lower compared to the estimate provided by Wu et al. (2005). There is disagreement between the two studies for NMB. There are many potential reasons for this discrepancy: perhaps most importantly, the latter study concerns NO_2 columns, whereas the former focuses on surface NO_2, and

concentrations in the two cases can differ markedly (higher for the entire column); other contributing factors may be the different year of simulation and the different model domain (36 x 36 km^2 resolution grid over North America in the latter).

Over East Asia Zhang et al. (2005) indicate, for the same year, a NME value not far from Wu et al. (2005) (76%) whereas NMB was lower (26%) but these results were achieved on a different domain (80 x 80 km^2 resolution). A different meteorological driver (RAMS) was also used.

For SO$_2$ concentrations Wu et al. (2005) suggest NMB and NME values of 69% and 82% respectively using CASTNET. The EPA CMAQ Model Performance Evaluation for 2001 (2005), which also compares modelled data to CASTNET observations, provides lower estimates (53% for NME and 32% for NMB) for the summer period. The model is, in this case, version 4.5 of CMAQ and it is applied on a national scale at 36 km^2 resolution. The same domain and the same resolution are used in Eder et al. (2002) which performed a two-week evaluation study in 1999 (1-14 July) suggesting a NME of 186% and a NMB of 65%. In this case the model version is 4.2.1 (released in June 2002). In this study NMB is close to the one provided by the EPA report (27%). The four studies all provide a positive bias, which suggests a tendency of the model to overestimate SO$_2$.

For NH$_4^+$ concentrations, there is a general agreement for NME: Eder et al. (2002; 2006), in the evaluation studies for year 2001 and summer 1999, indicate values of 35% and 56% respectively. NME is assessed around 40% in both Wu et al. (2005) for August 2002 and in this study for June 1999. These results suggest a range for NME between 30% and 50%.There is an agreement for the systematic error: Eder et al. (2006) provide a NMB negative and small (-4%) and in Wu et al. (2005) NMB is also negative (-38%) for August 2002. In Gillinand et al. (2006) NMB is assessed in a wider range (between -30% and 66%) depending on the season. In August NMB is -23%. In this study NMB is also negative (-10%). The version of the model is 4.4 in all the evaluations. In almost all the studies NMB is negative in summer, which indicates a general tendency of CMAQ to underestimate ammonium during the warm season.

Few high resolution studies attempted to estimate ammonia concentrations using CMAQ. The high spatial variability of this pollutant, mainly due to its short lifetime in the atmosphere, makes it difficult to predict concentrations correctly even on a high resolution scale (order of 1 km). Daily variations of temperature, wind speed and relative humidity may also have a strong impact on ammonia concentrations (Phillips et al., 2004) contributing to increase the uncertainty in the estimates. Nowak et al. (2006) compared CMAQ NH_3 concentrations to measurements made in July and August 2002 using mass spectrometry techniques. They suggest that small-scale local sources like soil emissions, strongly influenced by soil temperature, pH and nitrogen content, may be responsible for further possible discrepancies between model results and measurements.

SOURCE	NETWORK	Period of simulation	Coverage	Resolution (km^2)	Version	METEO	EMISSIONS	CHEM. SCHEME
Wu et al. (2005)	CASTNET/ NCDENR	August 2002	Southern US	4	4.4	MM5	NEI	CB4
Eder et al. (2002)	CASTNET	1-14 July 1999	Continental US	36	4.2.1	MM5	NEI	SAPRC99
Eder et al. (2006)	CASTNET	2001	Continental US	36	4.4	MM5	NEI	CB4
EPA report (2005)	CASTNET	2001	Continental us	36	4.5	MM5	NEI	CB4
Gillinand et al. (2006)	CASTNET	2001	Continental us	36	4.4	MM5	NEI	CB4
Zhang et al (2005)	TRACE-P	February – April 2001	East Asia	80	?	RAMS	?	RADM2
Vijayaraghavan et al. (2006)	ERS/GOME	January and August 2001	Northern US	36	4.4	MM5	NEI	?
Evaluation over the UK (this study) (2008)	**UK AQMN**	**February and June 1999**	**United Kingdom**	**5**	**4.4**	**MM5**	**EMEP +NAEI**	**RADM**

Table 5-8. Evaluation studies performed between 2002 and 2008 using CMAQ

	NME (%)			NMB (%)		
SOURCE	SO$_2$	NO$_2$	NH$_4$	SO$_2$	NO$_2$	NH$_4$
Wu et al. (2005)	82	70	40	69	40	-38
Eder et al. (2006)			35			-4
Eder et al. (2002)	157		56	161		51
EPA report (2005)	53		28	32		-17
Zhang et al (2005)		76			26	
Gilliland (2005)						-23
Vijayaraghavan et al. (2006)		40			-7	
EVALUATION OVER THE UK (this study) (2008)	**50**	**54**	**41**	**27**	**-42**	**-10**

Table 5-9. Estimates of Normalized Mean Bias (NMB) (right) and Normalized Mean Error (NME) (left) in several studies which applied CMAQ over the United States, East Asia (TRACE-P) and the United Kingdom (this study). For the evaluation over the UK, the values refer to June 1999. NME and NMB estimates for February 1999 can be found in Table 5-7.

5.5 CONCLUSIONS

In this study the dispersion model CMAQ (Community Multi-scale Air Quality System) is applied to the United Kingdom on a high resolution scale (5 x 5 km^2) for estimating concentrations of acidifying pollutants (NH$_X$, NO$_X$, SO$_2$). Modelled values of concentration are compared to measurements provided by several monitoring networks in the UK.

The comparison reveals that the model tends to overestimate SO$_2$ concentration at rural sites. The model under-predicts NO$_X$ concentration in the urban areas of London, Manchester, Bolton and Glasgow in both months. The difference between modelled monthly ammonia concentrations and monthly measurements varies approximately between -3 μg m^{-3} and 1 μg m^{-3}. The model reproduces ammonium concentration well in June, with differences between modelled and measured data varying approximately between -0.2 and +0.2 μg m^{-3}. The model also cannot reproduce the diurnal cycle of NO$_X$ and SO$_2$ concentrations properly, with a

correlation coefficient between observed and modelled 6-hourly data of less than 0.5. Possible reasons can be identified in the uncertainty affecting the temporal profiles used for disaggregating annual emissions into hourly emissions or the model's vertical resolution not high enough to resolve the night time boundary layer. The Normalized Mean Error (NME) in June is assessed around 50% for NO_X, NH_3 and SO_2. In February NME is around 36% for SO_2 and NO_2 and 50% for NH_3. In terms of systematic error the Normalized Mean Bias (NMB) is negative for NH_4^+ (-10%), NO_X (-25% and -40% in February and June respectively) and NH_3 (around -20%) and positive for SO_2 (4% and 27%). A sensitivity analysis needs to be carried out in the future in order to assess the influence of different emission temporal profiles on the diurnal cycle of pollutant concentrations. The analysis of CMAQ concentrations also needs to be extended to a longer period (1-year simulation) in order to confirm or disprove the monthly results.

The analysis of the spatial distribution of pollutants over the UK reveals that the areas of highest concentration correspond to the areas of highest emissions (rural areas for ammonia and industrial areas for NO_X and SO_2). Concentrations are also dependent on the season (higher during summer rather than in winter for ammonia, opposite situation for NO_X and SO_2). Some differences in concentration between the 45 x 45 km^2 resolution and the 5 x 5 km^2 resolution map are visible: NH_3 concentration over the UK is lower of approximately 1 $\mu g \ m^{-3}$ over the inner grid compared to the outer one: this might be due to a faster conversion of ammonia to ammonium at high resolution. This is consistent with the map of distribution of ammonium concentration, which appears lower over the 45 x 45 km^2 resolution grid compared to the 5 x 5 km^2 resolution one. The patterns for NO_x are very similar over the two domains, whereas SO_2 concentration is higher over the lower resolution grid compared to the high resolution one. Possible reasons might be a faster conversion of SO_2 to H_2SO_4 or a faster deposition process of SO_2 over the inner grid compared to the outer one.

CHAPTER 6

Modelling wet deposition fluxes of pollutants over the UK: comparison between two atmospheric dispersion models on a 5 km scale resolution

SUMMARY

Two atmospheric dispersion models (FRAME and CMAQ) adopting the Lagrangian and the Eulerian approaches respectively have been applied on a high resolution domain (5 x 5 km^2) covering the British Isles. Annual wet deposition fluxes of SO_X, NO_Y and NH_X as modelled by both models are compared to each other and compared to deposition fluxes from the official UK dataset CBED. Both models can simulate the orographic enhancement of wet deposition over the western regions of the UK. CMAQ estimates of NH_X total wet deposition are significantly higher (+43%) than FRAME and CBED with the greatest differences over Scotland and Wales. In the other areas of the country the distribution patterns are very similar, with values slightly higher in FRAME compared to CMAQ. FRAME underestimates NH_X in Scotland by about -50%. For SO_X, CMAQ underestimates wet deposition by about -43%, whereas FRAME under-predicts by approximately -17%. This is mainly due to a negative bias over Scotland (-50%). Finally for NO_Y the CMAQ bias is close to zero (between -10% and +10%) for all the UK regions but England (-28%). CMAQ performs better than FRAME which over-predicts NO_Y wet deposition over England, Northern Ireland and Isle of Man (+30%) and under-predicts it over Scotland (-58%). The total estimates of NO_X boundary concentrations in CMAQ are about twice the ones in FRAME. This means an increased concentration of nitric acid which can be converted to ammonium nitrate. This may affect the amount of wet deposition of both NH_X and NO_Y as predicted by CMAQ. The future use of the same input sets in both models is therefore recommended in order to reduce inter-model differences.

6.1 INTRODUCTION

Lagrangian atmospheric transport models including FRAME (Singles et al., 1998; Fournier, 2003; Vieno, 2006), HARM (Metcalfe et al., 2001) and TRACK (Lee et al., 2000) have been applied for several years to describe the distribution of pollutant

concentrations and deposition fluxes in the United Kingdom. These models have the advantage of a short simulation time, which make them suitable for policy applications when a quick response to scientific issues is often required. The computing time for an annual simulation with FRAME is approximately 25 minutes using 100 processors on a Beowulf Linux Cluster (Dore et al., 2006). Using the same number of processors the execution time of CMAQ is significantly longer (approximately 1 week), which makes its use less straightforward for long term simulation studies. A strength of Eulerian models such as CMAQ is that they usually include a more detailed meteorology compared to the Lagrangian models previously mentioned, which adopt wind frequency roses for the transport of pollutants along selected trajectories. The input data set for CMAQ is represented by gridded 3D meteorological fields with a 6-hour frequency modelled by the Mesoscale model MM5.

In spite of the long computing time, a 1-year simulation with CMAQ has been performed for 1999 using a Beowulf Linux Cluster (Nemesis, CEH Edinburgh). The present study has the aim of verifying if CMAQ can also be considered a valid tool for simulating sulphur and nitrogen annual deposition fluxes in the United Kingdom. Maps of annual wet deposition fluxes of reduced nitrogen (NH_X), oxidised nitrogen (NO_Y) and oxidised sulphur (SO_X) for year 1999 from both FRAME and CMAQ are presented. The results of both models are compared to one another and they are also compared to the values provided by the UK official dataset CBED.

Section 6.2 introduces the two modelling systems, the input data sets and the parameterisation schemes of wet deposition adopted in both models; Section 6.3 presents the results of the comparison and the final section shows some conclusions.

6.2 CASE STUDY

6.2.1   CMAQ and FRAME

A detailed description of CMAQ can be found in Chapter 2. Results of its application over the British Isles are reported in Chapter 5. Some general information about FRAME can be found in Chapter 1 as well as in Singles et al. (1998), Fournier et al.

(2002) and Vieno (2006). The version of CMAQ used in this work is 4.4 whereas the FRAME version is 6.2.1.

6.2.2 Modelling domain

CMAQ is applied over the inner grid of Figure 5-1. Details about the model resolution and the grid projection can be found in Table 5-1. FRAME is run by the Centre for Ecology and Hydrology (CEH) of Edinburgh over a 244 x 172 cells grid in British National Grid projection. The resolution is the same in both models (5 x 5 km^2). In order to compare the output results from the two models, the CMAQ grid was re-projected from Lambert Conformal to National Grid using GIS software (ARCMAP). The two grids were then overlapped and the columns and rows in excess deleted. The resulting domain is a 166 x 234 cells grid shown in Figure 6-1.

Figure 6-1. Model domain used for the comparison of FRAME and CMAQ results. The domain is in British National Grid projection. The resolution is 5 x 5 km^2.

6.2.3   Boundary concentrations

FRAME boundary concentrations are calculated using FRAME-EUROPE, a European scale model which runs over an EMEP grid at 150 x 150 km^2 resolution (ApSimon et al., 1994). The model was initially developed to run a statistical model (a parameterised set of probability distributions) over Europe at 150 km scale resolution. CMAQ boundary concentrations are calculated using the global model STOCHEM (Collins et al., 1997; Stevenson et al., 1998). Details of the procedure followed for creating boundary concentrations from STOCHEM can be found in Chapters 2 and 5. Table 6-1 shows the total import of NH_X, NO_Y and SO_X in the FRAME and CMAQ model domains for year 1999.

	FRAME	CMAQ
NH_x	16	13
NO_X	55	128
SO_2	21	56

Table 6-1. Total imports of NH_X, NO_X and SO_2 in the FRAME and in CMAQ model domains for year 1999. Units are Gg N for NH_x and NO_Y and Gg S for SO_X. FRAME estimates are from Vieno (2005), page 50.

6.2.4   Meteorological input

The meteorological input for CMAQ is provided by the mesoscale model MM5. It consists of a set of 3D gridded meteorological fields with a 6-hour frequency. A full validation of MM5 over the United Kingdom for year 1999 can be found in Chapter 3. The meteorological variables used in CMAQ for the parameterisation of wet deposition are cloud and rain water mixing ratios (kg kg^{-1}) for each model vertical level as well as ground level precipitation (mm); these are computed by MM5 using the Grell cumulus parameterisation scheme (Grell et al., 1994). Some information about this scheme can be found in Section 3.2.4.

In FRAME the meteorological input data set consists of a set of wind frequency roses and wind speed roses (Figure 6-2) for the pressure level range 950-900 hPa (Dore et al., 2006). They are generated from a six hourly dataset of radiosonde data

from four stations in the British Isles (Valentia, Camborne, Hemsby and Stornoway) spanning the period 1991-2000, available at the British Atmospheric Data Centre (BADC) (Dore et al., 2006). Figure 6-2 shows the speed and frequency of winds blowing from 24 specific directions. Each concentric circle represents a frequency (or a speed) from zero at the centre to increasing values at the outer circles.

FRAME precipitation is provided by the UK Meteorological Office on a 5 x 5 km^2 resolution map covering the UK (Figure 6-3) and produced by interpolating measurements from their entire UK rain gauge network (Perry and Hollis, 2005). Both orographic and non orographic rainfall components are considered in FRAME. The first one is wind direction dependent and stronger for wind directions associated with humid air masses (Vieno, 2006). The second one has no directional dependence. Orographic enhancement of precipitation over hills and mountains is also included. Further details can be found in Fournier (2003). Maps of total annual rainfall used by FRAME and CMAQ are shown in Figure 6-3. Figures 6-3, 3-21 show that MM5 total rainfall is underestimated with areas of larger under-prediction mainly in the western UK and Ireland (Figure 3-21). The underestimate of rainfall by MM5 is consistent with many studies including Hall and Cratchley (2005a), Yang and Tung (2003) and Gallus (1999). Stensrud and Fritsch (1994b) suggest that the tendency in underestimating precipitation is due to the high sensitivity of cumulus parameterization schemes to the formulation of the trigger function (the complete set of criteria used to determine when and where deep convection occurs in a numerical model (Kain and Fritsch (1992)). Spencer and Stensrud (1998) also highlight the difficulties of these convective schemes to simulate the effects of deep, moist convection especially during the warm season, when a large fraction of precipitation is associated with mesoscale convective systems.
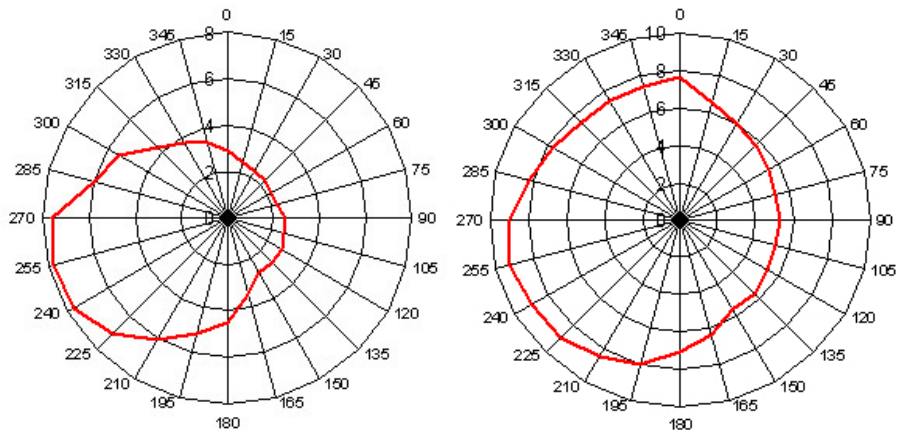
Figure 6-2. Wind speed rose (right) and wind frequency rose (left) used in the FRAME model. Red lines represent frequency of wind (%) and wind speed (ms⁻¹) as a function of wind direction. They are calculated from radiosonde data averaged for the period 1991-2000. Source: available at http://www.frame.ac.uk/documentation.htm
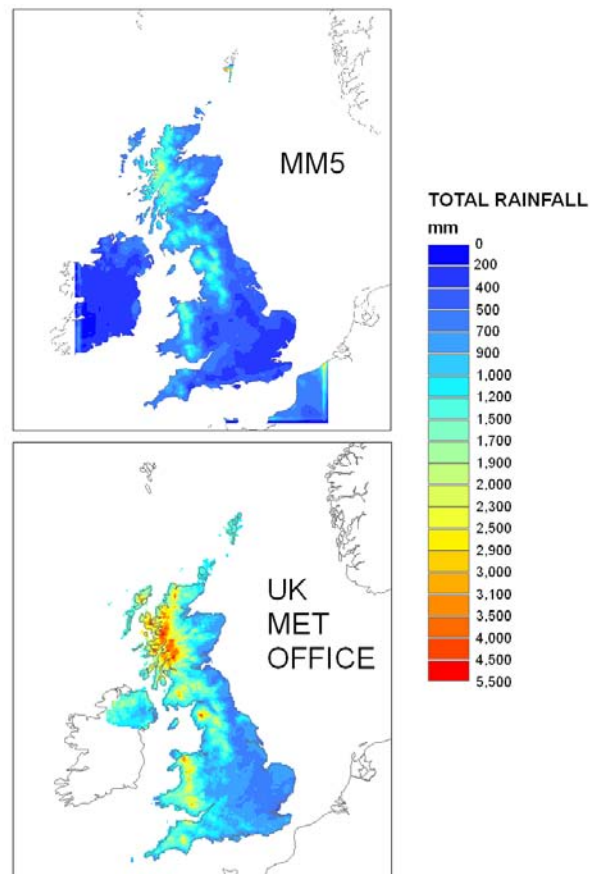
Figure 6-3. Total annual rainfall over land as modelled by the mesoscale model MM5 (top) and provided by the UK Met Office (bottom). Both maps are in the same projection (British National grid) and they have the same resolution (5 x 5 km²). Units are mm.

6.2.5 Emissions

In CMAQ the emission pre –processor SMOKE is used for providing hourly gridded emissions over Great Britain. For Ireland, Northern Ireland and France EMEP emissions are used. Further details can be found in Chapter 4. FRAME annual NO_x and SO_2 emissions are provided at 1 x 1 km^2 resolution by the National Emission Inventory (NAEI) for the UK. The ammonia emission inventory used in FRAME is described in Dragositis et al. (1998). Table 6-2 show the total estimates of NH_3, NO_X, and SO_2 emissions over the UK for the two models.

	FRAME	CMAQ	NAEI
NH_3	342	358	374
NO_x	1498	2552	2248
SO_2	1248	1222	1294

Table 6-2. Total anthropogenic input emissions over the UK for CMAQ and FRAME in 1999. Units are Gg yr^{-1}. FRAME emissions are from Vieno (2005), page 48. Emissions from the National Emission Inventory for the UK (NAEI) are included for comparison.

6.2.6 Chemistry

The chemical scheme part of the Regional Acid Deposition Model (RADM) (Stockwell et al., 1990) is used in CMAQ. Details about the chemical reactions and chemical species in RADM are reported in Chapter 2. The chemical scheme applied in FRAME is a simplified version of the one implemented in the EMEP acid deposition model (Barret et al., 1995). Details can be found in Singles et al. (1996) and Vieno (2006).

The RADM scheme is more detailed than the FRAME one primarily due to its more detailed treatment of organic chemistry. The photolysis rate parameters for the two mechanisms are also different. For RADM they are calculated by JPROC (Section 2.2.3) as a function of absorption cross sections and quantum yields. In contrast the EMEP mechanism uses parameterized photolysis rate parameters calculated on the basis of the data from Derwent et al. (1996, 1998) and Jenkin et al. (1997).

For NO$_X$, both models include the photolytic dissociation of NO$_2$, the oxidation of NO by O$_3$, the formation of PAN (peroxyacetyl nitrate) and the formation of nitric acid (HNO$_3$) (reactions 1.7-1.10). For SO$_X$, both schemes include the oxidation of SO$_2$ to H$_2$SO$_4$ (reactions 1.1-1.3). Conversion of ammonia in ammonium sulphate and ammonium nitrate (reactions 1.11-1.13) is also considered.

6.2.7 Terrain elevation

Orography plays a major role in the modelling of wet deposition fluxes. A correct representation of terrain elevation is needed in both models. FRAME uses a 5 x 5 km^2 resolution map provided by CEH Edinburgh whereas CMAQ terrain height comes from the US Geological Survey (http://www.usgs.gov/) (Figure 6-4). USGS data are provided at 2 minutes (3.70 km) resolution and they are interpolated to 5 km by MM5.
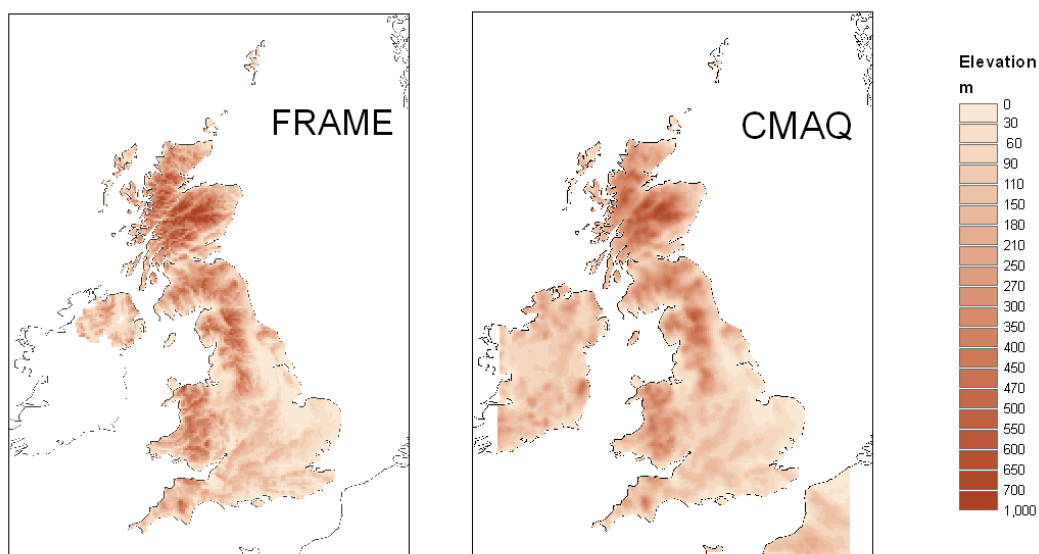
Figure 6-4. Maps of terrain elevation for FRAME (left) and CMAQ (right). Altitude is in meters.

6.2.8 Parameterization of wet deposition

The western regions of the United Kingdom are characterised by the presence of hills with an altitude varying between 300 and 1000 metres (Figure 6-4). These areas are

affected by the orographic enhancement of precipitation: rainfall rates are significantly greater over hills and mountains rather than low level regions because of the seeder-feeder effect (Bergeron, 1965) (Figure 6-5). The feeder cloud usually contains higher pollutant concentrations (sulphate, nitrate, ammonium) than the seeder cloud (Fowler et al., 1995). Therefore the enhancement of precipitation from the feeder cloud over upland areas is usually associated with an enhancement of wet deposition fluxes of pollutant ions over the same areas.

An accurate parameterization of wet deposition processes must take into account this process: both FRAME and CMAQ include parameterisation schemes of wet deposition which consider the influence of orography over rainfall distribution. In FRAME wet deposition is calculated as a function of the scavenging coefficients, the rainfall rates and the air concentration of the species (Fournier et al., 2003). The scavenging rate for the orographic component of rainfall is assumed to be twice the value used for the non orographic component (Dore et al., 1992). This enhanced scavenging rate is applied over those areas where rainfall exceeds 700 m (where this excess of rainfall is assumed to be due to altitudinal effects). Scavenging coefficients used in FRAME can be found in Dore et al. (2005) and Singles et al. (1998).

In CMAQ the precipitation rate $P_r(z)$ in a model layer z is calculated by the "resolved cloud model" applying a specific vertical profile (equation 2.11) to the ground level precipitation amount provided by MM5 (R_n). Wet deposition is computed as a function of the precipitation rate and cloud water and rain water mixing ratios (equation 2.10). A full description can be found in Chapter 2.
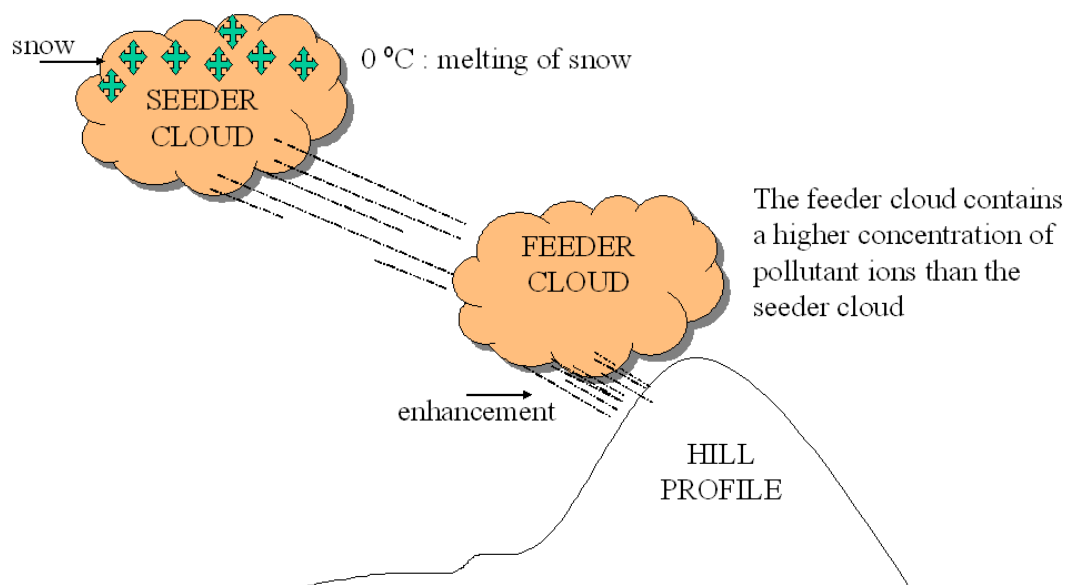
Figure 6-5. Schematic diagram of the seeder-feeder effect.

6.3 RESULTS

6.3.1 Maps of wet deposition

Totals of wet deposition for 1999 over the UK are reported in Table 6-3. Total estimates calculated using the concentration-based estimated deposition (CBED) approach (Smith et al., 2000; Smith and Fowler, 2001) are also included. This method is based on interpolation of measurements of wet deposition and estimates of dry deposition using observed gas concentrations (Vieno et al., 2006). The CBED data set is the official UK data set for estimation of exceedance of critical loads for acid deposition and nitrogen deposition. CBED estimates are compared to FRAME and CMAQ results in order to identify the main areas of under-prediction and over-prediction by both models. CBED values are preferred to observations provided by the monitoring sites of the UK Acid Deposition Monitoring Network (ADMN) because many sites are located in areas less than 300 meters high. Thus observations from these stations cannot take into account the effects of orographic enhancement in upland areas. On the other hand the same orographic enhancement is modelled in CBED using the ratios of ions concentrations measured in cloud and rainfall, as well as the estimate of the extra rainfall amount over hills (Smith et al., 2004). Predictions

from the Hull Acid Rain Model (HARM) are also reported in Table 6-3 for comparison. CMAQ estimates of NH_X are significantly higher than FRAME and CBED. The total amount of SO_X over the UK is lower in CMAQ compared to CBED and FRAME. Finally both FRAME and CMAQ underestimate the total amount of NO_Y wet deposition, but FRAME prediction is lower (the difference between CBED and CMAQ total amounts is +16 Gg N yr^{-1} whereas the difference between FRAME and CBED is +42 Gg N yr^{-1}).

It is important to analyse the distribution of the wet deposition fluxes all over the domain in order to identify the areas of main discrepancy. Maps of wet deposition fluxes in FRAME, CMAQ and CBED and the difference between the models at every grid point are shown in Figure 6-6. The effect of orographic enhancement of wet deposition is clearly visible over hills in the western regions of the UK. Both models reproduce the effect of enhanced precipitation in upland areas. For NH_X (Figure 6-6a) the main differences between the models concern Scotland, where CMAQ predicts higher values of wet deposition compared to FRAME despite the under-prediction of rainfall. The differences between CMAQ and CBED vary between 12 kg N ha^{-1} yr^{-1} and 24 kg N ha^{-1} yr^{-1}. Both models over-predict over Wales (between 6 kg N ha^{-1} yr^{-1} and 16 kg N ha^{-1} yr^{-1}). In the other areas of the country, the distribution patterns are all very similar, with values slightly higher in FRAME (approximately 3 kg N ha^{-1} yr^{-1}) compared to CBED over England. For SO_X (Figure 6-6b) CMAQ predicts lower values over England, Wales and Northern Ireland (between 4 and 6 kg S ha^{-1} yr^{-}). CMAQ and CBED distributions are very close in Scotland whereas FRAME under-predicts total SO_X wet deposition up to 12 kg S ha^{-1} yr^{-1}. Nitrate wet deposition (Figure 6-6c) is well reproduced by both models, with a spatial distribution very similar to the one provided by CBED. They both underestimate NO_Y of about 2 kg N ha^{-1} yr^{-1} across England, Wales and Northern Ireland. CMAQ performs better over Scotland, whereas FRAME underestimates NO_Y in a range between 4 and 8 kg N ha^{-1} yr^{-1}. Wet deposition over North Western Scotland is slightly over-predicted by CMAQ (the difference between CMAQ and CBED in this area is approximately between 4 and 6 kg N ha^{-1} yr^{-1}). Table 6-3 summarizes the total amounts calculated in every region of the UK. In general, CMAQ provides closer values to CBED than FRAME for NO_Y wet deposition.

CMAQ SO$_X$ totals are lower than CBED and FRAME in England, Wales and Northern Ireland. Over Scotland CMAQ performs better than FRAME, which underestimates SO$_X$ of about 50%. For NH$_X$ wet deposition, both models perform well, apart from Scotland where CMAQ total amount is almost three times higher than CBED.

	Wet deposition		
	NH$_x$	NO$_y$	SO$_x$
FRAME	121	64	112
CBED	111	106	139
HARM	103	110	---
CMAQ	159	90	78

Table 6-3. Total deposition predicted in CMAQ, FRAME, CBED and HARM over the UK. Units are Gg N yr^{-1} for NH$_x$ and NO$_y$ and Gg S yr^{-1} for SO$_x$. CBED estimates are measurement derived (1998-2000 averaged) and they are provided by CEH of Edinburgh. HARM estimates (1998-2000 averaged) are from Metcalfe et al. (2005).

a)

NH$_X$
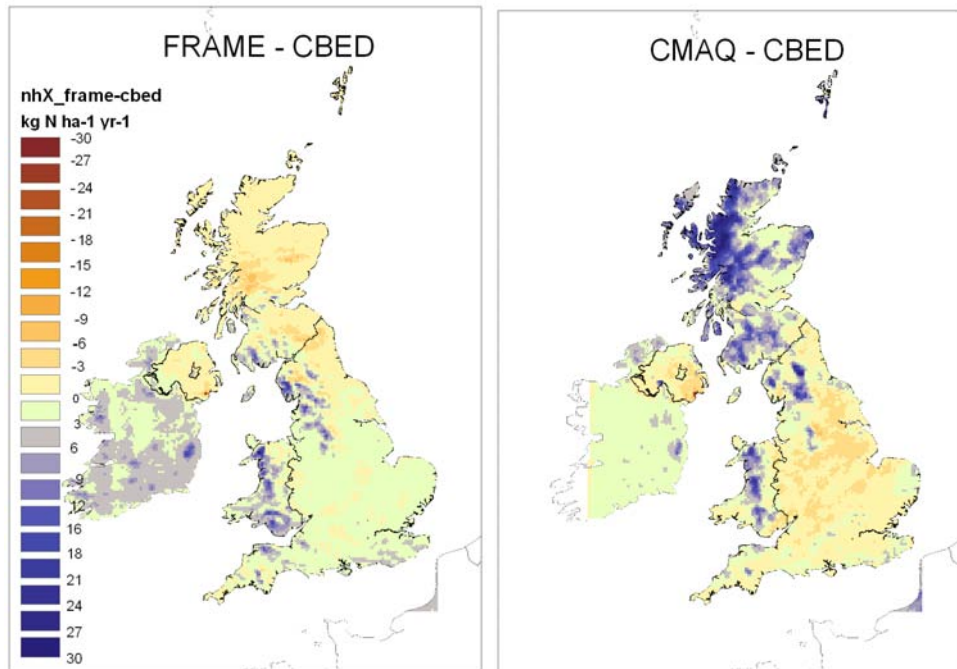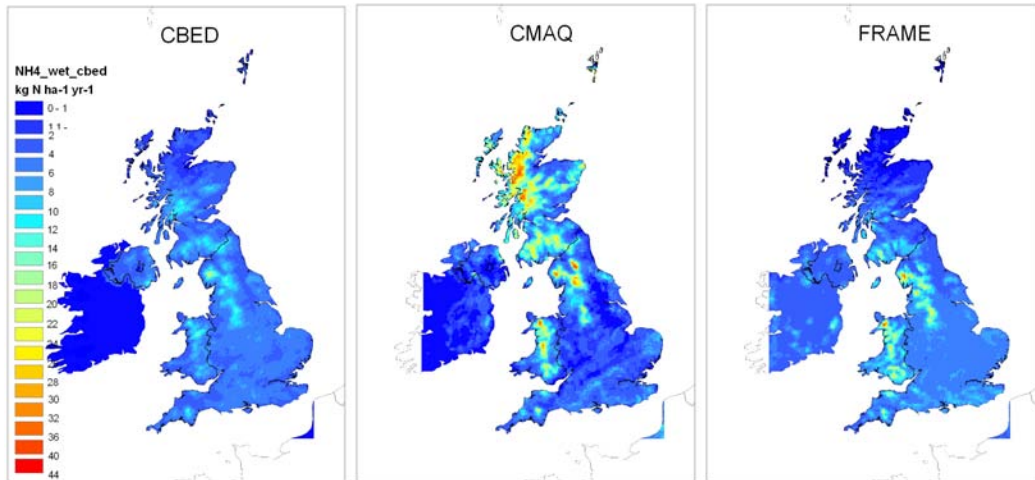
b)

SO$_X$
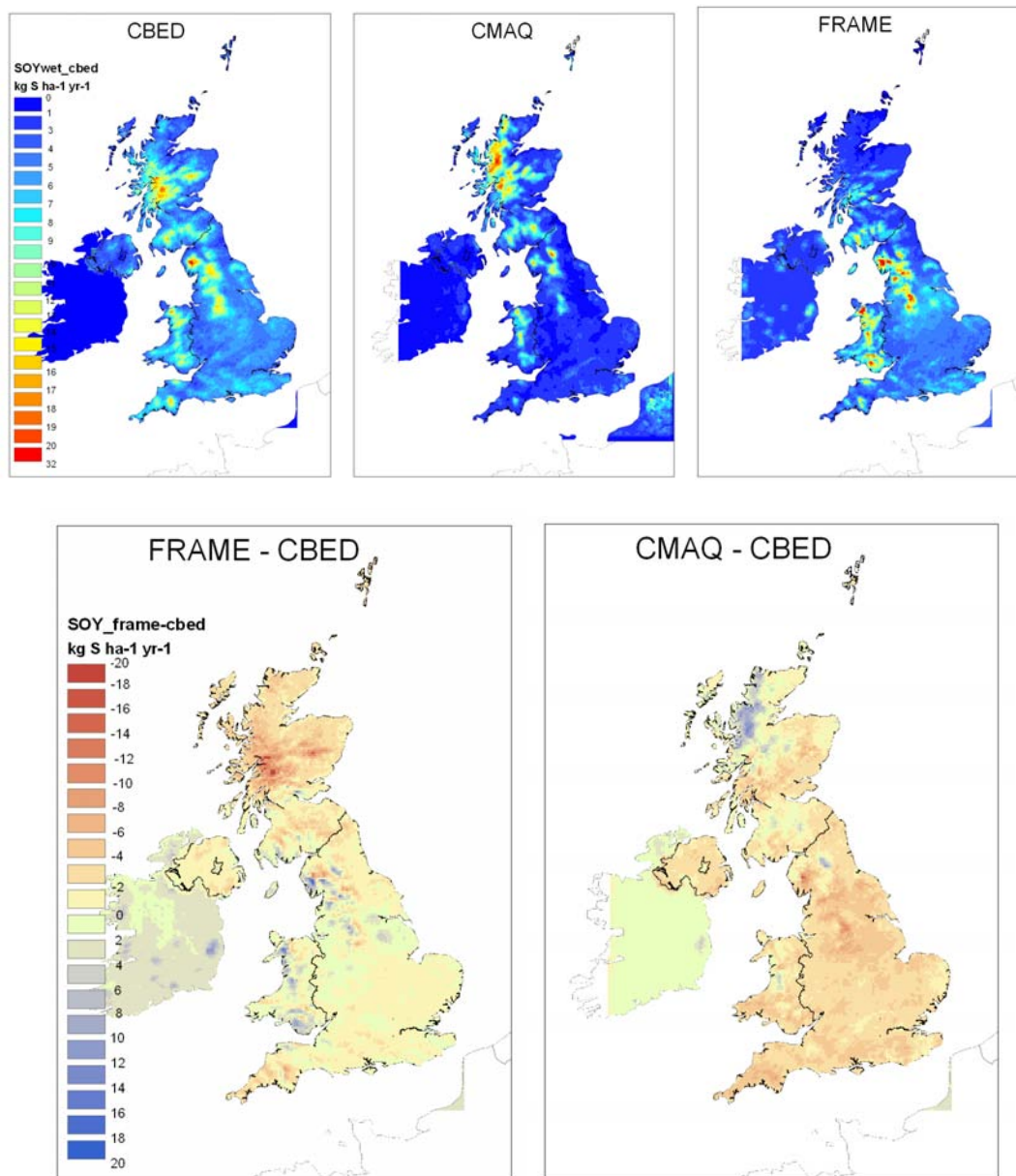
c)

NO$_Y$
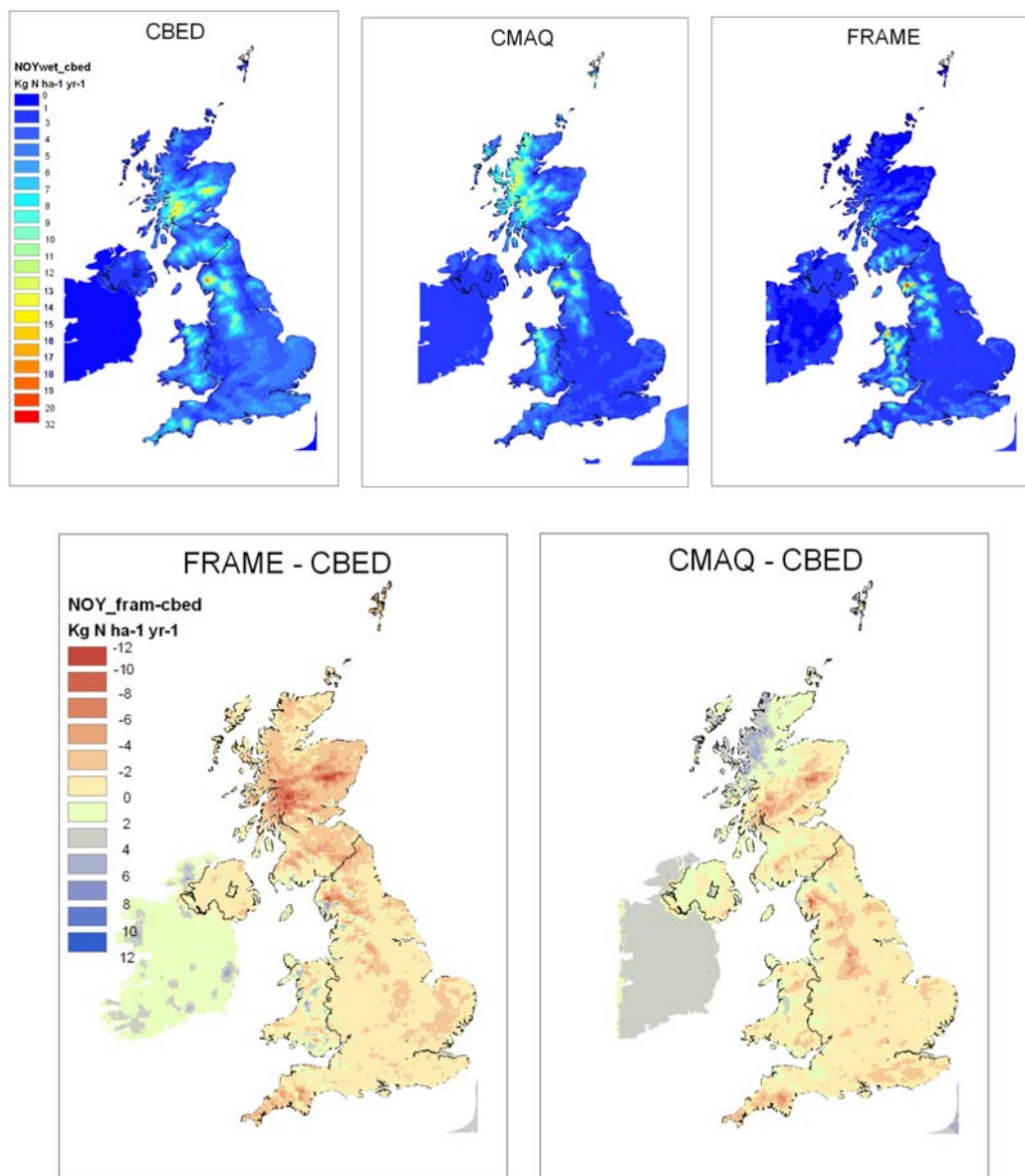
Figure 6-6. Maps of wet deposition of reduced nitrogen (a), oxidised sulphur (b) and oxidised nitrogen (c) as modelled by FRAME, CMAQ and CBED and the difference between the two estimates (CMAQ – CBED and FRAME – CBED) in every grid cell Units are kg N ha^{-1} yr^{-1} for NH$_X$ and NO$_Y$ and kg S ha^{-1} yr^{-1} for SO$_X$.

NH$_x$						
	Northern Ireland	Scotland	England	Wales	Isle of Man	**UK**
FRAME	4.78	21.06	76.80	18.59	0.37	**121**
CBED	5.64	30.46	63.86	10.72	0.22	**111**
CMAQ	3.56	84.83	54.54	15.83	0.23	**159**
FRAME – CBED	12.95	-9.4	12.94	-5.94	0.15	**10**
CMAQ- CBED	-2.08	53.97	-9.32	5.11	0.01	**48**

SO$_X$						
	Northern Ireland	Scotland	England	Wales	Isle of Man	**UK**
FRAME	3.74	23.31	69.16	15.60	0.32	**112**
CBED	5.24	46.35	73.64	13.22	0.21	**139**
CMAQ	1.54	41.23	27.73	7.48	0.09	**78**

NO$_Y$						
	Northern Ireland	Scotland	England	Wales	Isle of Man	**UK**
FRAME	2.43	15.20	37.16	9.00	0.18	**64**
CBED	3.44	36.69	56.07	9.27	0.14	**106**
CMAQ	3.52	37.39	40.16	8.51	0.16	**90**

Table 6-4. Totals of wet deposition predicted by CMAQ, FRAME and CBED for the UK regions. Units are Gg N yr^{-1} for NH$_x$ and NO$_Y$ and Gg S yr^{-1} for SO$_X$.

6.3.2   Average transects of wet deposition

Profiles of wet deposition from West to East across all the UK regions are shown in Figure 6-7. Wet deposition has been extracted from each 5 km grid square along horizontal transects (West to East trajectories).

The wet deposition has been calculated by averaging cell values of all transects (North-South direction) across Wales (2-37 grid cells), Scotland (1-83 cells), England (1-115 grid cells) and Northern Ireland (1-36 grid cells). Figure 6-7 highlights the effects of orographic enhancement in the Western regions of Scotland and in Wales and it gives a further indication about possible critical areas in the UK. All models show peaks of wet deposition in the uplands regions of Central England,

East Coast of Northern Ireland and Central Wales. Areas of high wet deposition also concern the West coast and the central regions of Scotland.

CMAQ SO_X wet deposition is lower almost everywhere in Wales, Northern Ireland and England (Figure 6-7a,b,d). CMAQ performs better than FRAME over Scotland (Figure 6-7c), even if it slightly over-predicts it in the North West (Figure 6-6).

For NO_Y, there is a good agreement between the models everywhere over Wales (Figure 6-7e). In the other areas of the country CMAQ performance is better than FRAME, which under-predicts over Northern Ireland and Scotland (Figure 6-7f,g). Both models predict lower NO_Y wet deposition in central and eastern England (Figure 6-7h). For NH_X, CMAQ overestimates all over Scotland (Figure 6-7k) with the highest peaks in the Western regions. CMAQ prediction is very close to CBED in Western Wales and Eastern Wales (Figure 6-7i), whereas both models over-predict in the central regions.

SO$_X$

a)

SO$_X$ WET DEPOSITION
Wales

b)

SO$_X$ WET DEPOSITION
Northern Ireland

c)

SO$_X$ WET DEPOSITION
Scotland

d)

SO$_X$ WET DEPOSITION
England

NO$_Y$

e)

NO$_Y$ WET DEPOSITION
Wales

f)

NO$_Y$ WET DEPOSITION
Northern Ireland

g)

NO$_Y$ WET DEPOSITION
Scotland

h)
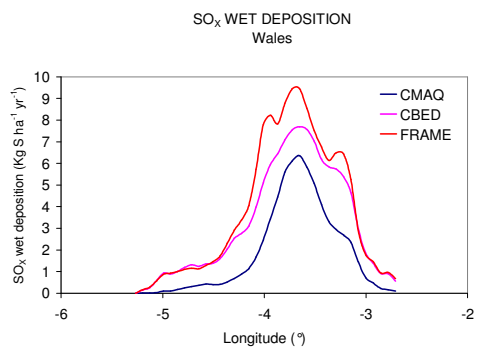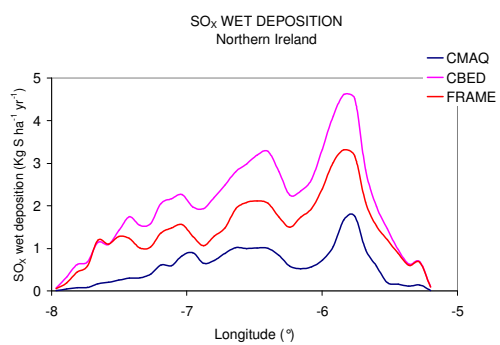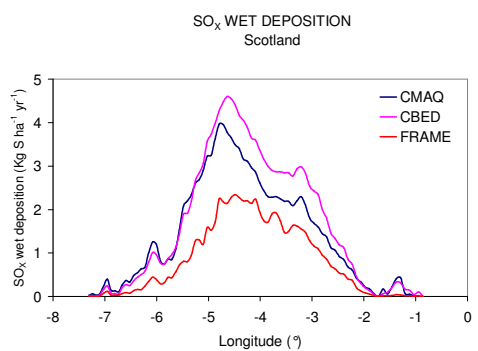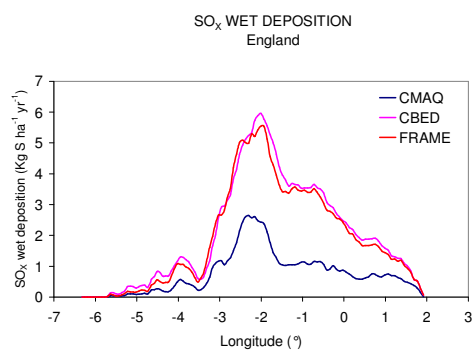
NO$_Y$ WET DEPOSITION
England
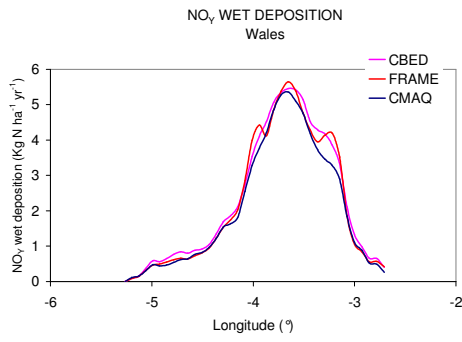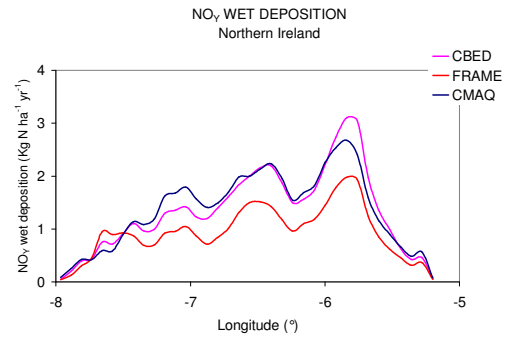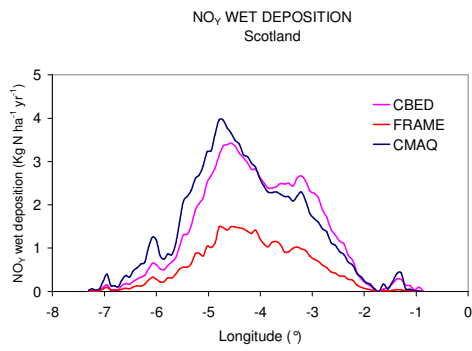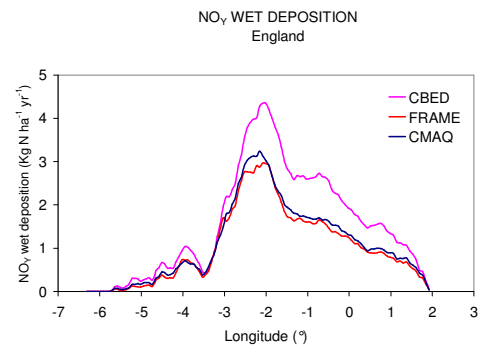
NH_X
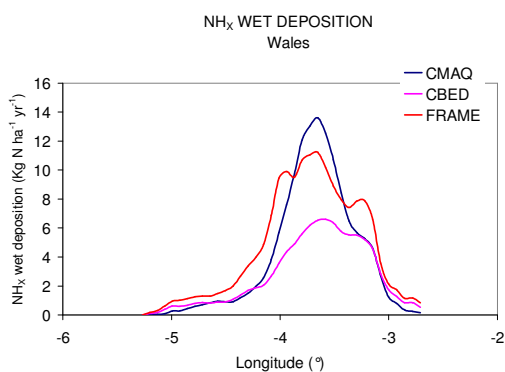
i)   j)
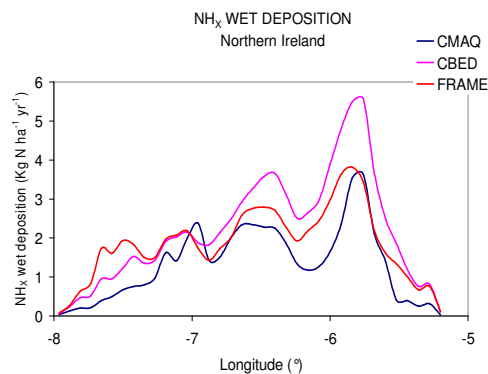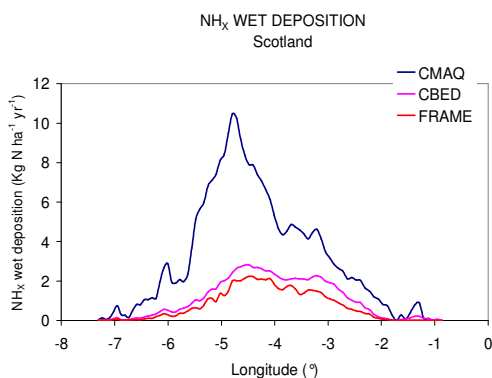
k)   m)
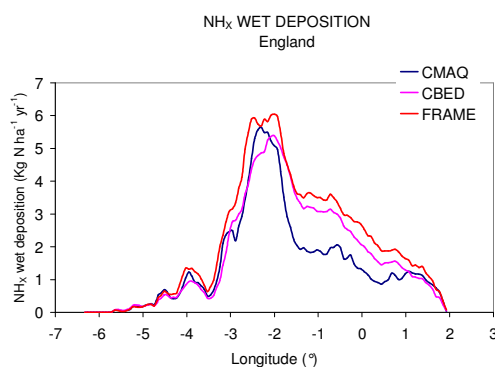
Figure 6-7. Directional wet deposition as a function of longitude (degrees) from West to East in the UK, as provided by FRAME (red), CMAQ (blue) and CBED (pink). Units are kg N ha^{-1} yr^{-1} for NH$_X$ and NO$_Y$ and kg S ha^{-1} yr^{-1} for SO$_X$.

6.3.3   Statistics

The Normalized Mean Bias (NMB) (equation 5.6) for the UK is positive for NH$_X$ (+10%) and negative for SO$_X$ and NO$_Y$ (-18% and -2% respectively) in FRAME

(Figure 6-8). In CMAQ NMB is around +43% for NH_X and SO_X and -15% for NO_Y. CMAQ overestimates NH_X over Scotland (180%) and Wales (+47%) and underestimates it in the rest of the country. FRAME underestimates NH_X in Scotland of about -50%. For SO_X CMAQ underestimates wet deposition of about -43%, whereas FRAME under-prediction is approximately -17% and this is due to a negative bias over Scotland (-50%). Finally for NO_Y the CMAQ bias is close to zero (between and -10% and +10%) for all regions but England (-28%). CMAQ performs better than FRAME which over-predicts NO_Y wet deposition over England, Northern Ireland and Isle of Man (+30%) and under-predicts it over Scotland (-58%). The Taylor diagram (Taylor, 2001) (Figure 6-9) shows a correlation coefficient between observed and modelled values of approximately 0.7 for FRAME and around 0.4 for CMAQ. Excluding NH_X, both models represent spatial variability accurately, with a standard deviation ratio between 0.6 and 1.
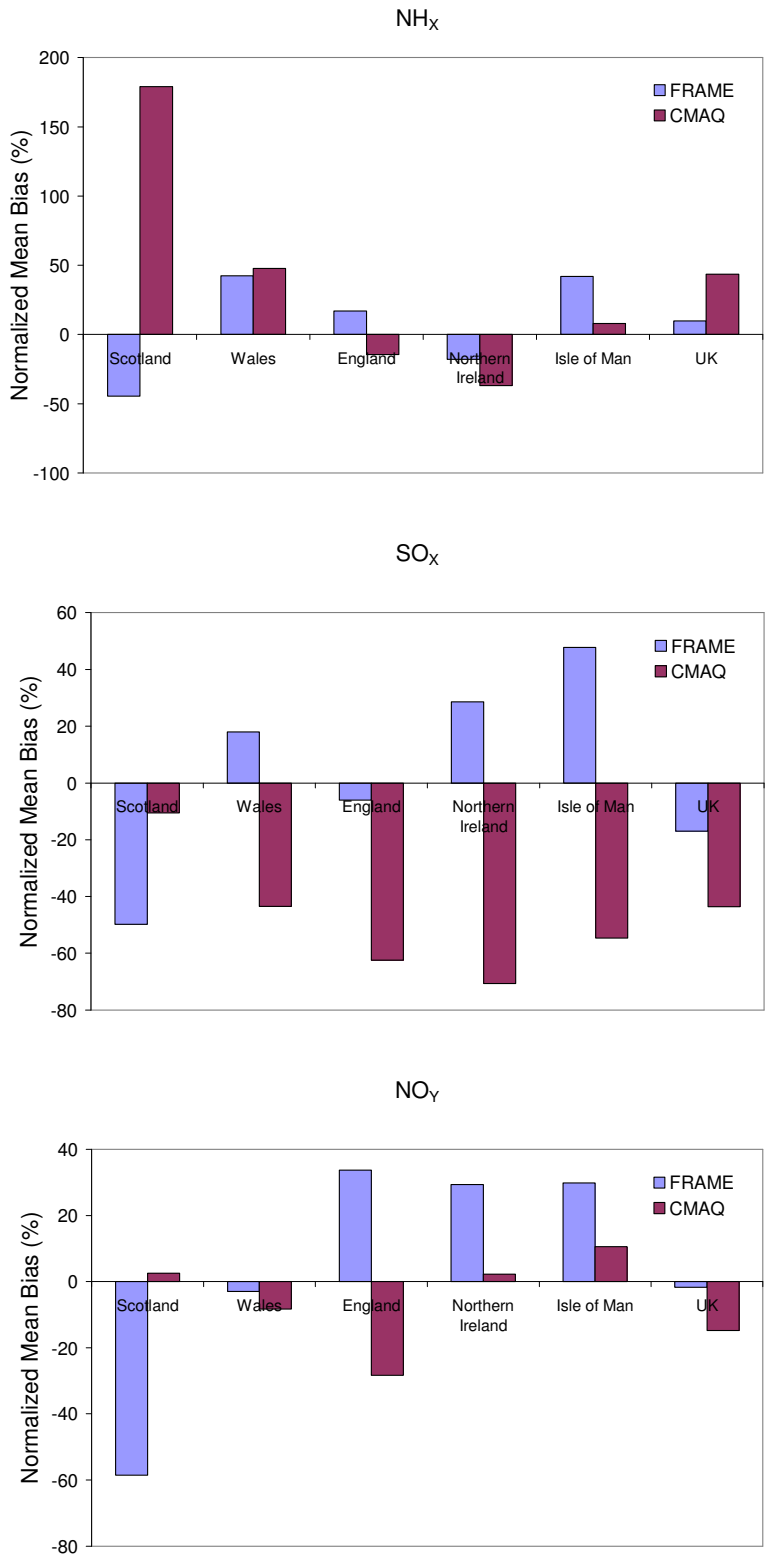
Figure 6-8. Normalized Mean Bias (%) for NH$_X$, SO$_X$ and NO$_Y$ for FRAME (blue) and CMAQ (red).
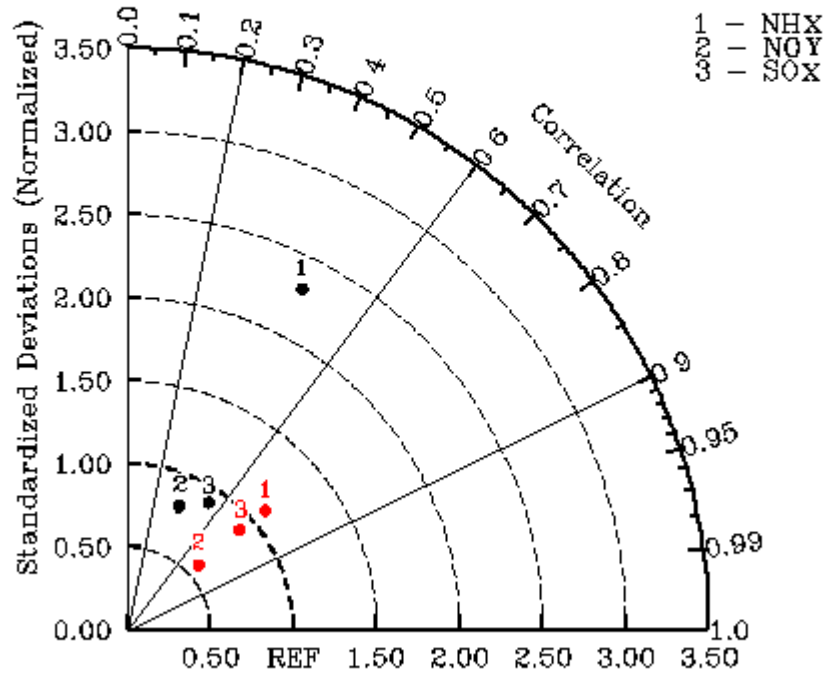
Figure 6-9. Normalized Taylor diagram of annual wet deposition for CMAQ (black dots) and FRAME (red dots).

6.4 CONCLUSIONS

An annual inter-comparison between two atmospheric dispersion models (FRAME and CMAQ) has been performed over the British Isles; the models have been applied on a national scale at 5 x 5 km^2 resolution. The study focuses on total wet deposition fluxes of oxidised nitrogen, oxidised sulphur and reduced nitrogen for year 1999. Results from both models have also been compared to values from CBED, the

official UK data set for estimation of exceedance of critical loads for acid deposition and nitrogen deposition. The inter-comparison shows that both models can simulate the orographic enhancement of wet deposition over the western regions of the UK. CMAQ estimates of NH_X total wet deposition are significantly higher than FRAME and CBED and the greatest differences are visible over Scotland and Wales. In the other areas of the country, the distribution patterns are very similar, with values slightly higher in FRAME compared to CMAQ and CBED. For NO_Y wet deposition, CMAQ performs better than FRAME in every area of the UK apart from England where CMAQ estimates are lower than FRAME and CBED. Finally, for sulphur CMAQ clearly under-predicts wet deposition almost everywhere in the UK. FRAME also under-predicts it over Scotland by about 50%. A possible explanation for the differences between the model results can be identified in the use of two different input datasets for both boundary concentrations and emissions.

The total estimate of NO_X input emissions and boundary concentrations over the UK in CMAQ differ from the one in FRAME (Table 6-2, Table 6-1). The CMAQ total import of NO_X from the boundaries is almost twice the one in FRAME. This means an increased concentration of nitric acid (reactions 1.7-1.10) which can be converted to ammonium nitrate (reaction 1.11). This may affect the amount of wet deposition of both NH_X and NO_Y as predicted by CMAQ. The future use of the same input datasets in both models is therefore recommended in order to reduce inter-model differences. A monthly comparison between the models is also suggested in order to understand how the under-prediction of rainfall by MM5, which is more consistent during the warm season (Figure 3-9), can influence the CMAQ wet deposition estimates.

CHAPTER 7
Summary, conclusions and future work

7.1 SUMMARY

Present-day numerical air quality models are considered essential tools for predicting future air pollutant concentrations and deposition fluxes, contributing to the development of new effective strategies for the control and the reduction of pollutant emissions. They simulate concentrations and deposition fluxes of pollutants on a wide range of scales (global, national, urban scale) and they are used for identifying critical areas, integrating measurements and achieving a deeper scientific understanding of the physical and chemical processes involving air pollutants in the atmosphere.

The use of comprehensive air quality models started in the late 1970s and since then their development has increased rapidly, hand in hand with the fast increase in computational resources. Today more and more complex and computationally expensive numerical models are available to the scientific community. One of these tools is the Community Multi-Scale Air Quality System (CMAQ), developed in the 1990s by the Environmental Protection Agency (EPA) and currently widely applied across the world for air pollution studies. This work focuses on the application of CMAQ to the United Kingdom, for estimating concentrations and deposition fluxes of acidifying pollutants (NO_X, NH_X, SO_X) on a national scale.

The work is divided into seven chapters, the first one describing the main issues related to the emission and dispersion in the atmosphere of acidifying species. It also includes a general overview of the main international policies signed in the last thirty years in order to reduce the problem of acidification in Europe, as well as a brief description of some models mentioned in this thesis.

The second chapter describes the main features of CMAQ and addresses some issues such as the use of a nesting process for achieving temporally and spatially resolved boundary concentrations, and the implementation of the model on parallel machines, essential for reducing the simulation computing time.

The third part of the thesis focuses on the application and evaluation over the United Kingdom of the 5th Generation Mesoscale Model MM5, used for providing 3D meteorological input fields to CMAQ. This study was performed assuming that an accurate representation of depositions and concentrations of chemical species cannot be achieved without a good estimate of the meteorological parameters involved in most of the atmospheric processes (transport, photochemistry, aerosol processes, cloud processes etc.). The evaluation study mainly focuses on three meteorological variables: rainfall, wind speed and surface temperature.

The fourth part of the thesis describes the preliminary implementation of the Sparse Matrix Operational Kernel Emission System (SMOKE) in the United Kingdom. The use of SMOKE is usually avoided in the applications of CMAQ outside America, and CMAQ input emission files are prepared by the application of other emission processors. The reason is that the model requires radical changes for being applied outside Northern and Central America. Some of these changes have been made in this study, such as the adaptation of the European emission inventory EMEP and the UK National Inventory NAEI to the modelling system for area and point sources respectively, the introduction of new European emission temporal profiles in substitution of the American ones and the introduction of new geographical references for the spatial allocation of emissions.

In the fifth chapter the results of CMAQ application in two specific months (June and February 1999) over the UK are discussed. The study mainly focuses on NO_X, SO_2 and NH_X. Maps of concentration are presented and modelled data are compared to measurements from two different air quality networks in the UK. An analysis of the performance of CMAQ over the UK is also performed.

In the final chapter an annual inter-comparison between CMAQ and the Lagrangian transport model FRAME is carried out. Maps of annual wet deposition fluxes of NO_X, SO_X and NH_X for year 1999 are presented. The results of both models are

compared to one another and they are also compared to observations from the UK dataset CBED.

The following sections summarize the conclusions achieved in each one of these chapters (Section 7.2) and suggest the work which has to be done in the future with CMAQ (Section 7.3).

7.2   CONCLUSIONS ABOUT THIS WORK

MM5 is evaluated for the year 1999, and two periods covering June 1999 and February 1999 are analysed in detail. Simulations of precipitation, wind speed and surface temperature are performed. Modelled values in single grid cells are extracted and compared to observations from several meteorological stations across the UK. The results show a general tendency of MM5 in overestimating wind speed (+30%), underestimating precipitation in summer (between -10% and -20%) and overestimating it in winter (+30%), whereas there is generally a good agreement with observations for surface temperature even if the model tends to overestimate it for low values (below ~14 ºC) and underestimate it for high values (above ~20 ºC). The evaluation study shows MM5 generally performs better than ECMWF re-analysis in terms of standard deviation and correlation coefficient. A 1-year simulation with MM5 was also performed in order to confirm or disprove the monthly results. The annual trends confirm the good agreement as observed in the monthly analysis with a correlation coefficient between 0.7 and 0.9 for temperature temporal series and between 0.6 and 0.9 for wind speed temporal series. MM5 generally performs better than ECMWF. The long term run also confirms the tendency of MM5 in overestimating temperature for low values and underestimating it for high values. The surface temperature spatial distribution is generally well reproduced by MM5. Regions of under-prediction (between 1 ºC and 2 ºC) are visible in England and Ireland. The study shows that the spatial distribution of total rainfall is also underestimated. The areas of larger under-prediction (between 120 and 200 cm) mainly involve the western area of the UK and Ireland.

The preliminary implementation of SMOKE is also performed. Maps of emissions have been produced by SMOKE for NO_X, NH_3, SO_2 and PM_{10}. The application of

SMOKE makes a positive contribution to the improvement of the distribution of emissions over the UK compared to the original emission dataset EMEP. Even if this is a preliminary work limited to point and area sources, it can be considered as a first step towards a more comprehensive implementation of the model in Europe.

In the fifth chapter two monthly simulations with CMAQ are performed and results are presented and discussed. June and February 1999 are selected for running the model. Modelled concentrations of NO_X, NH_X and SO_2 are compared to observations provided by two air quality monitoring networks in the UK (The UK Air Quality Monitoring Network and the Ammonia Monitoring Network). The results indicate a better performance of CMAQ in June rather than in February for almost all pollutants. Significant over-predictions of SO_2 occur at rural sites. The model under-predicts NO_X concentration in the urban areas of London, Manchester, Bolton and Glasgow in both months. The difference between modelled monthly ammonia concentrations and monthly measurements varies approximately between -3 μg m^{-3} and 1 μg m^{-3}. The model reproduces ammonium concentration well in June, with differences between modelled and measured data varying approximately between -0.2 and +0.2 μg m^{-3}. In both months the model cannot reproduce the diurnal cycle of SO_2 and NO_X concentrations, with a correlation coefficient between measured and modelled data less than 0.5. This is probably due to the uncertainty affecting the temporal profiles used for disaggregating annual NO_x and SO_2 emissions into hourly emissions. Another possible reason may be that the model's vertical resolution is not high enough to resolve the night time boundary layer. The Normalized Mean Error (NME) in June is assessed around 50% for NO_X, NH_3 and SO_2. In February NME is around 36% for SO_2 and NO_2 and 50% for NH_3. In terms of systematic error the Normalized Mean Bias (NMB) is negative for NH_4^+ (-10%), NO_X (-25% and -40% in February and June respectively) and NH_3 (around -20%) and positive for SO_2 (4% and 27%).

Annual maps of NH_X, NO_Y and SO_X wet deposition fluxes by CMAQ and FRAME are presented in Chapter 6. The orographic enhancement of wet deposition is clearly visible over hill regions in the western UK, due to the seeder-feeder effect.

CMAQ estimates of NH_X total wet deposition are significantly higher than FRAME and CBED and the greatest differences are visible over Scotland and Wales. In the

other areas of the country, the distribution patterns are very similar, with values slightly higher in FRAME compared to CMAQ and CBED. FOR NO_X wet deposition, CMAQ performs better than FRAME in every area of the UK apart from England where CMAQ estimates are lower than FRAME and CBED. Finally, for sulphur CMAQ clearly under-predicts wet deposition almost everywhere in the UK. FRAME also under-predicts it over Scotland of about 50%. A possible explanation for the differences between the results provided by the two models can be identified in the use of two different datasets for both boundary concentrations and emissions. The CMAQ total estimate of NO_X import from the boundaries is about twice the one in FRAME. This means an increased concentration of nitric acid (reactions 1.7-1.10) which can be converted in ammonium nitrate (reaction 1.11). This may affect the amount of wet deposition of both NH_X and NO_X as predicted by CMAQ.

The results achieved in chapters 5 and 6 indicate that CMAQ can actually be considered as a valid tool for modelling atmospheric pollutant concentrations and depositions in the United Kingdom and its future application should be taken into account, even if the long execution time may represent a limitation for policy and regulatory purposes.

Compared to many recently developed models, CMAQ has the advantage of a very large user community as well as a vast documentation which make the application of the model easier for new users. The experience achieved in the last 20 years in the United States also represents a valid support.

This study also shows that even if several alternative options have been recently taken into account, the meteorological driver MM5 is still one of the best tools for providing meteorological input data to CMAQ. On the contrary, the emission processor SMOKE represents an obstacle for the application of CMAQ outside America and it still requires a considerable amount of work for being adapted to the UK case.

7.3   FUTURE WORK

In the future a series of sensitivity studies needs to be performed in order to quantify the response of the model to changes in specific parameters. These parameters should include meteorological variables such as boundary layer height, wind speed, relative humidity and rainfall. Other parameters need to be considered because they may have strong influence on depositions, like roughness lengths, deposition velocities and wet scavenging coefficients.

A deeper understanding of the influence of meteorology on modelled concentrations and deposition fluxes is also important. The use of other meteorological drivers including the UK Met Office Unified Model (UM) and the Weather Research and Forecasting model (WRF) is therefore suggested. A comparison of the results achieved with CMAQ using three different sets of meteorological inputs (MM5, WRF and UM) should be performed. The tendency of MM5 in overestimating wind speed and underestimating rainfall require further investigation, because it may affects the processes of transport (advection) and removal of atmospheric pollutants, resulting in a systematic error in concentrations and deposition fluxes estimates.

Different simulations should be performed using different sets of emission temporal profiles. This will give the chance to identify the set of profiles which makes the model capable to reproduce the hourly and daily variation of pollutant concentrations best.

The future implementation of a specific module for on road mobile emissions (MOBILE6), which takes into account details such as type of vehicle and type of fuel, will provide more detailed emissions from the traffic sector, improving the quality of the results and reducing the uncertainty in air quality studies with CMAQ.

Using the same meteorology, different simulations assuming reductions of emissions should also be performed in order to ascertain the sensitivity of concentrations to specific changes in emissions.

The study of CMAQ concerning concentrations must be extended to a 1-year simulation. This needs to be done in order to confirm or disprove the monthly results and for achieving more solid conclusions in CMAQ evaluation. It will also allow the comparison of CMAQ results with annual concentrations provided by FRAME.

The future use of the same input sets in FRAME and CMAQ will help to reduce inter-model differences in the study of wet deposition fluxes over the UK. A monthly comparison between the models will also help to understand how the under-prediction of rainfall by MM5, which is more consistent during the warm season, influences the CMAQ wet deposition estimates.

An inter-comparison with another Eulerian model currently applied in the UK (EMEP4UK) is also strongly suggested in order to identify which is the model more suitable for modelling acidifying species in the UK.

APPENDIX A

CMAQ GOVERING EQUATIONS IN GENERALIZED COORDINATES

Modules inside the CMAQ Chemical Transport Model (CCTM) are not specific to any coordinate system. This means that CCTM can be adapted to any of the coordinates used in the meteorological models, making CMAQ extremely flexible. This generality is achieved using generalized coordinates inside CCTM. A full description if the generalized coordinate system can be found in Byun et al. (1999). The governing conservation equation in generalized coordinates can be written as:

$$
\frac{\partial(\overline{\varphi}_i J_\xi)}{\partial t} + m^2 \nabla_\xi \bullet \left(\frac{\overline{\varphi}_i \overline{\hat{V}}_\xi J_\xi}{m^2} \right) + \frac{\partial(\overline{\varphi}_i \overline{\hat{v}}^3 J_\xi)}{\partial \hat{x}^3} - m^2 \frac{\partial}{\partial \hat{x}^1}\left[\frac{\overline{\rho} J_\xi}{m^2}\left(\hat{K}^{11} \frac{\partial \overline{q}_i}{\partial \hat{x}^1} \right) \right] - m^2 \frac{\partial}{\partial \hat{x}^2}\left[\frac{\overline{\rho} J_\xi}{m^2}\left(\hat{K}^{22} \frac{\partial \overline{q}_i}{\partial \hat{x}^2} \right) \right]
$$

$$
(a) \qquad\qquad (b) \qquad\qquad (c) \qquad\qquad\qquad (d)
$$

$$
- \frac{\partial}{\partial \hat{x}^3}\left[\overline{\rho} J_\xi\left(\hat{K}^{33} \frac{\partial \overline{q}_i}{\partial \hat{x}^3} \right) \right] - m^2 \frac{\partial}{\partial \hat{x}^1}\left[\frac{\overline{\rho} J_\xi}{m^2}\left(\hat{K}^{13} \frac{\partial \overline{q}_i}{\partial \hat{x}^3} \right) \right] - m^2 \frac{\partial}{\partial \hat{x}^2}\left[\frac{\overline{\rho} J_\xi}{m^2}\left(\hat{K}^{23} \frac{\partial \overline{q}_i}{\partial \hat{x}^3} \right) \right] -
$$

$$
(e) \qquad\qquad\qquad\qquad (f)
$$

$$
\frac{\partial}{\partial \hat{x}^3}\left[\overline{\rho} J_\xi\left(\hat{K}^{31} \frac{\partial \overline{q}_i}{\partial \hat{x}^1} + \hat{K}^{32} \frac{\partial \overline{q}_i}{\partial \hat{x}^2} \right) \right] = J_\xi R_{\varphi_i}(\overline{\varphi}_i,....,\overline{\varphi}_N) + J_\xi Q_{\varphi_i} + \frac{\partial(\overline{\varphi}_i J_\xi)}{\partial t}\bigg|_{cld} + \frac{\partial(\overline{\varphi}_i J_\xi)}{\partial t}\bigg|_{ae} + \frac{\partial(\overline{\varphi}_i J_\xi)}{\partial t}\bigg|_{ping}
$$

$$
(g) \qquad\qquad (h)\qquad (i)\qquad\qquad (j)\qquad (k)\qquad (l)
$$

h)   Time rate of change of change of pollutant concentration

i)   Horizontal advection

j)   Vertical advection

k)   Diagonal term for horizontal eddy diffusion

l)   Diagonal term for vertical eddy diffusion

m)   Off diagonal horizontal diffusion

n)   Off diagonal vertical diffusion

o)   Production or loss from chemical reactions

p) emissions

q) Cloud mixing and aqueous phase chemical production or loss

r) Aerosol process

s) Plume in grid process

$\overline{\varphi_i}$ = mean concentration in density units (e.g., kg m^{-3})

J_ξ = vertical Jacobian of the coordinate ξ

m = map scale factor

$\overline{q_i}$ = mean mass mixing ratio

$\overline{\hat{v}}^{\,3}$ = vertical velocity

$\hat{K}$ = eddy diffusivity tensor in the Cartesian coordinate

Q_{φ_i} = emission term

R_{φ_i} = chemical reaction term

REFERENCES LIST

Altshuler S.L., Arcado T.D., Lawson D.R. (1995) Weekday vs. weekend ambient ozone concentrations: discussion and hypotheses with focus on Northern California. Journal of the Air and Waste Management Association 45, 967–972.

Anthes, R.A., Warner T.T. (1978) Development of hydrodynamic models suitable for air pollution and other mesometeorological studies. *Mon. Weather. Rev*., **106**: 1045-1078.

ApSimon H.M., Barker B.M., Kayin S. (1994) Modelling studies of the atmospheric release and transport of ammonia—applications of the TERN model to an EMEP site in eastern England in anticyclonic episodes. *Atmos Environ* **28**: 665–678.

Baek B. H., Eyth A., Holland A. (2006) Recent Updates to the SMOKE Modeling System Presented at the 15th International Emission Inventory Conference "*Reinventing Inventories - New Ideas in New Orleans.* New Orleans, May 15 - 18, 2006

Barrett K., Seland Ø., Foss A., Mylona S., Sandnes H., Styve H., Tarrason F. (1995) European transboundary acidifiying air pollution: Ten years calculated fields and budgets to the end of the first Sulphur Protocol. EMEP/MSC-W Report 1/95, DNMI, Oslo.

Barrett M., Protheroe R. (1995). Sulphur emission from large point sources in Europe. Air pollution and climate series, **3**. Published by the Swedish NGO Secretariat on Acid Rain. Available at http://www.acidrain.org.

Barrett M. (2000). Atmospheric emissions from Large Point Sources in Europe. Air pollution and climate series, **15**. Published by the Swedish NGO Secretariat on Acid Rain. Available at http://www.acidrain.org.

Bergeron T. (1965) On the low-level redistribution of atmospheric water caused by orography. In: Proceedings of the International Conference on Cloud Physics, Tokyo, May 1965, pp. 96–100.

Binkowski F.S (1999), Aerosols in models-3 CMAQ, Science documentation of the Community Multi-Scale air quality System, EPA/600/R-99/030 Chapter 10

Blackadar A. K. (1978) Modelling pollutant transfer during daytime convection, *Preprints, Fourth Symposium on Atmospheric Turbulence, Diffusion, and Air Quality*, Reno, Am. Meteor. Soc., 443-447.

Blanchard C.L., Tanenbaum S.J. (2003) Differences between weekday and weekend air pollutant levels in Southern California, *Journal of the Air and Waste Management Association* **53** (2003), pp. 816–828.

Borge R., Lumbreras J., Rodriguez M.E. (2003) Preparation of Emission Data for Modeling with CMAQ from Spanish Emission Inventories and Emission Projections. 12th International Emission Inventory Conference - "*Emission Inventories - Applying New Technologies*" San Diego, April 29 - May 1, 2003

Bresnahan P. A., Miller D. R., Bash J. O. (2005) Estimating atmospheric deposition of nitrogen into the CT River Basin using CMAQ, abstract from the 4th Annual CMAS Models-3 Users' Conference September 26-28, 2005 Friday Center, UNC-Chapel Hill

Brink J.C., Kroeze C., Klimont Z. (2001a) Ammonia abatement and its impact on emissions of nitrous oxide and methane – Part 1: method. *Atmos. Environ.* **35**: 6299-6312.

Brink C., Kroeze C., Klimont Z. (2001b) Ammonia abatement and its impact on emissions of nitrous oxide and methane - Part 2: application for Europe. *Atmos. Environ.* **35**: 6313–6325.

Bronnimann S., Neu U. (1997) Weekend - weekday differences of near-surface ozone concentrations in Switzerland for different meteorological conditions. *Atmos. Environ*. **31**, 1127–1135.

Bullock, O. R., Brehme K. A. (2002) Atmospheric mercury simulation using the CMAQ model: formulation description and analysis of wet deposition results. *Atmos. Environ.*, **36**, 2135-2146.

Byun W.D., Young J., Pleim J. (1990) Numerical transport algorithms for the Community Multi-scale Air Quality transport model (CMAQ) in generalized coordinates. Eds. EPA-600/R-99/030.

Carmichael G.R., Peters L.K. (1984a) An Eulerian/transport/transformation/removal model for SO_2 and sulfate – I. Model development. *Atmos. Environ.* **18** (1984): 937–952.

Carmichael G.R., Peters L.K. (1984b) An Eulerian/transport/transformation/removal model for SO_2 and sulfate – II. Model calculation of SO_x transport in the Eastern in the United States. *Atmos. Environ.* **20**: 173–188.

Carmichael G.R., Peters L.K., Saylor R.D. (1991) The STEM-II regional scale acid deposition and photochemical oxidant model – I. An overview of model development and applications. *Atmos. Environ.* **25A**: 2077–2090.

Carnevale C., Gabusi V., Volta M. (2004) POEM-PM: an emission model for secondary pollution control scenarios**,** Environmental Modelling & Software, Volume 21, Issue 3, March 2006, Pages 320-329

Causley M.C.; Fieber, J.L.; Jimenez M.; Gardner L. (1990) The Emissions Preporocessor System version 2.5 (EPS2.5) User`s guide for the Urban Airshed Model. Volume 4. User`s manual for the Emissions Preprocessor System Jun 01 PB-91-131250/XAB Technical Report

Chang J. S., Binkowski F. S., Seaman N. L., Byun D. W McHenry., J. N., Samson P. J., Stockwell W. R., Walcek C. J., Madronich S., Middleton P. B., Pleim J. E., Landsford H. L. (1990) The regional acid deposition model and engineering model, *NAPAP SOS/T Report 4, in National Acid Precipitation Assessment Program, Acidic Deposition: State of Science and Technology*, *Volume I*., National Acid Precipitation Assessment Program, Washington, DC, 1990.

Chang, J.S., Brost R.A., Isaksen I.S.A., Madronich S., Middleton P., Stockwell W.R., and Walcek C.J. (1987) A three-dimensional Eulerian acid deposition model: Physical concepts and formulation. *J. Geophy. Res.* **92**: 14681-14700.

Chang, J.S., Middleton P.B., Stockwell W.R., Walcek C.J., Pleim J.E., Lansford H.H., Binkowski F.S., Madronich S., Seaman N.L., Stauffer D.R., Byun D., McHenry J.N., Samson P.J., Hass H. (1990) The regional acid deposition model and engineering model, *Acidic Deposition: State of Science and Technology,* Report 4, National Acid Precipitation Assessment Program.

Ching J., Byun D. (1999) Introduction to the models-3 framework and the community multiscale air quality model (CMAQ), Science documentation of the Community Multi-Scale Air Quality System, EPA/600/R-99/030 Chapt. 1

Ching, J.K.S., Byun D.W., Young J., Binkowski F., Pleim J., Roselle S., Godowitch J., Benjey W. and Gipson G. (1998) Science features in Models-3 Community multiscale air quality system. Proceedings of the American Meteorological Society 78th Annual Meeting, Phoenix, AZ, Jan. 11-16, 1998: 269-273

Cleveland W.S., Graedel T.E., Kleiner B., Warner J.L., (1974).Sundayand workday variation s in photochemical air pollutants in New Jerseyand New York. Science 186, 1037–1038.

CMAQ Model Performance Evaluation for 2001: Updated March 2005 (2005). 2001 CMAQ statistical assessment based on IMPROVE, STN, CASTnet, NADP, and AIRS monitoring networks. Conducted by US EPA Office of Air Quality Planning and standards Emissions Analysis and Monitoring Division. Air Quality Group, Research triangle Park, NC 27711.

Coats C.J. Jr. (1996) High-performance algorithms in the Sparse Matrix Operator Kernel Emissions (SMOKE) modeling system. *Proceedings of the 9th AMS Joint Conference on Applications of Air Pollution Meteorology with A&WMA*, American Meteorological Society, Atlanta, GA, 584-588.

Courant R., Friedrichs K., Lewy H. (1967) On the partial difference equations of mathematical physics. IBM journal pp. 215-234.

Colella P. and Woodward P.L. (1984) The Piecewise Parabolic Method (PPM) for gasdynamical simulations, *J. Comput. Phys*. **54**: 174-201.

Collins, W. J, Stevenson D. S., Johnson C. E., Derwent R. G. (1997) Tropospheric ozone in a global-scale three-dimensional Lagrangian model and its response to NO_x emission controls*, J. Atmos. Chem.*, 26, 223-274, 1997.

DEFRA (2006) Provisional 2005 UK climate change sustainable develoment indicator and 2004 air pollutant emissions. Available at http://www.defra.gov.uk/news/2006/060330a.htm

Dennis, R.L., McHenry J.N., Barchet W.R., Binkowski F.S., and Byun D.W. (1993) Correcting RADM's sulfate underprediction: Discovery and correction of model errors and testing the corrections through comparisons against field data, *Atmos. Environ.*, **26A**(6), 975-997.

Derwent R. G., Jenkin M. E., Saunders, S. M. (1996) Photochemical ozone creation potentials for a large number of reactive hydrocarbons under European conditions, *Atmos. Environ.* **30**, 181–199.

Derwent R. G., Jenkin M. E., Saunders S. M., Pilling M. J. (1998) Photochemical ozone creation potentials for organic compounds in northwest Europe calculated with a master chemical mechanism, *Atmos. Environ.* **32**, 2429–2441.

Derwent R.G., Simmonds P.G., O'Doherty S., **Stevenson D.S.**, Collins W.J., Sanderson M.G., Johnson C.E., Dentener F., Cofala J., Mechler R., Amann M. (2006) External influences on Europe's air quality: Baseline methane, carbon monoxide and ozone from 1990 to 2030 at Mace Head, Ireland, *Atmos. Environ.*, **40**, 844-855

Dore A.J, Choularton T.W., Fowler D. (1992) An improved wet deposition map of the United Kingdom incorporating the seeder-feeder effect over mountainous terrain. *Atmos Environ* **26A**: 1375–1381.

Dore A.J., McDougall M., Vieno M., Smith R.I., Sutton M.A. (2005) Modelling the deposition and concentration of long range air pollution, annual report to Department for Environment, Food and Rural Affairs (Air and Environment Quality Division) 2004-2005, Interim report under project EPG 1/3/202, CEH Edinburgh

Dore A.J., Vieno M., Fournier N., Weston K.J., Sutton M.A. (2006) Development of a new wind rose for the British Isles using radiosonde data and application to an atmospheric transport model. Quarterly Journal of the Royal Meteorological Society (2006), 132, pp. 2769-2784.

Dragosits U., Sutton M.A., Place C.J., Bayley A. (1998) Modelling the spatial distribution of ammonia emissions in the United Kingdom. *Environmental Pollution* **102** S1 (1998), pp. 195–203.

Dudhia, J. (1989) Numerical study of convection observed during winter monsoon experiment using a mesoscale two-dimensional model. *J. Atmos. Sci*., **46**: 3077-3107.

Dudhia, J. (1993) A nonhydrostatic version of the Penn State/NCAR mesoscale model: Validation tests and simulation of an Atlantic cyclone and cold front. *Mon. Weather. Rev*., **121**, 1493-1513.

Dudhia, J. (1996) A multi-layer soil temperature model for MM5. Preprints, The Sixth PSU/NCAR Mesoscale Model Users' Workshop, 22-24 July 1996, Boulder, Colorado, 49-50. Available at http://www.mmm.ucar.edu/mm5/mm5v2/whatisnewinv2.html.

Dudhia, J., Gill D., Guo Y.R., Hansen D., Manning K., and Wang W. (1998) PSU/NCAR mesoscale modeling system tutorial class notes (MM5 modeling system version 2). [Available from the National Center for Atmospheric Research, P. O. Box 3000, Boulder, CO 80307.]

EC (1996) Council Directive 96/62/EC of 27 September 1996 on ambient air quality assessment and management. *Official Journal L 296 , 21/11/1996 P. 0055 – 0063.* Available at http://eurlex.europa.eu/LexUriServ/LexUriServ.do?uri=CELEX:31996L0062:EN:HTML

EC (2001) Commission of the European Communities Decision of 17 October 2001 amending the Annexes to Council Decision 97/101/EC establishing a reciprocal exchange of information and data from networks and individual stations measuring ambient air pollution within the Member States. Available at http://eur-lex.europa.eu/LexUriServ/LexUriServ.do?uri=CELEX:32001D0752:EN:HTML

Eder B.K, Yu S., Dennis R., Gillinand A., Howard S., Torian A. (2005) An annual evaluation of Models-3 CMAQ using a 2001 simulation. Presented at European Modeling and Monitoring organization (EMEP) workshop on particulatre matter monitoring and modelling, 20-23 April 2005, New Orlaeans (USA)

Eder, B.K, Yu S., Dennis R., Pleim J., Schere K. (2002) Preliminary Evaluation of the June 2002 Version of CMAQ. CMAS Models-3 User's Workshop, Oct. 21-23, RTP, NC

EEA (1999) Ambient air quality, pollutant dispersion and transport models, appendix A1. Prepared by the European Environment Agency. Available at http://reports.eea.europa.eu/92-9167-028-6/en

EU NECD (2001) Directive 2001/81/EC of the European Parliament and the Council on National Emission Ceilings for certain pollutants. Available at http://ec.europa.eu/environment/air/ceilings.htm

Eyth A., Hanisak K. (2003) The MIMS spatial allocator: a tool for generating emissions surrogates without a geographic information system, *Proceedings, 12th*

International Emission Inventory Conference, San Diego, April 29–May 1, 2003 (2003) (available at http://www.epa.gov/ttn/chief/conference/ei12/).

Fournier N. (2002) Development of an Atmospheric Transport model simulating concentration and deposition of reduced nitrogen over the British Isles. PhD thesis, University of Edinburgh.

Fournier N., Pais V.A., Sutton M.A., Weston K.J., Dragosits U., Tang S.Y., Aherne J. (2002) Parallelisation and application of an atmospheric transport model simulating dispersion and deposition of ammonia over the British Isles. *Environmental Pollution* **116** 1 (2002), pp. 95–107.

Fournier N. (2003) Development of an atmospheric transport model simulating concentration and deposition of reduced nitrogen over the British Isles. Ph.D. Thesis, University of Edinburgh.

Fowler D., Leith I.D., Binnie J., Crossley A., Inglis D.W.F., Choularton T.W., Gay M., Longhurst J.W.S., Conland D.E (1995) Orographic enhancement of wet deposition in the United Kingdom: continuous monitoring. *Water, Air and Soil Pollution* **85**: 2107–2112.

Fragkou E. (2005) Application of a mesoscale model to analyse the meteorology of urban air pollution episodes. Ph.D. thesis, University of Hertfordshire, UK

Gal-Chen T., Somerville R. (1975) On the use of a coordinate transformation for the solution of the Navier–Stokes equations. *J. Comput. Phys.,* **17,** 209–228.

Gallus W. A., Jr. 1999: Eta simulations of three extreme rainfall events: Impact of resolution and choice of convective scheme. *Wea. Forecasting*, **14**, 405-426.

Gear C. W. (1971a) Numerical Initial Value Problems in Ordinary Differential Equations.Prentice-Hall, Englewood Cliffs, NJ.

Gear C. W. (1971b) The automatic integration of ordinary differential equations. *Comm. ACM* **14**, 176-179.

Gilliam R., Bhave P., Pleim J.A., Otte T.L. (2004) A year-long MM5 evaluation using a model evaluation toolkit. Presented at 2004 Models-3 Conference, Chapel Hill, NC, October 18-20, 2004.

Gilliland A.B., Appel K.W., Pinder R., Roselle S.J., Dennis R.L. (2006) Seasonal NH_3 emissions for an annual 2001 CMAQ simulation: inverse model estimation and evaluation, *Atmos. Environ.* **40:** 4986-4998. 2006.

Gipson G. L. (1998) The initial concentration and boundary condition processors, Science documentation of the Community Multi-Scale air quality system, EPA/600/R-99/030 Chapter 13.

Gipson G. L., Young J.O (1999) Gas phase chemistry, Science documentation of the Community Multi-Scale air quality system, EPA/600/R-99/030 Chapter 8

Grell G. (1993) Prognostic evaluation of assumptions used by cumulus parameterizations. *Mon. Weather. Rev*., **121**: 764-787.

Grell G., Kuo Y.H., Pasch R.J. (1991) Semi-prognostic tests of cumulus parameterization schemes in the middle latitudes. *Mon. Weather. Rev*., **119**: 5-31.

Grell, G., Dudhia J., Stauffer D.R. (1994) A description of the fifth-generation Penn State/NCAR mesoscale model (MM5). NCAR Technical Note, NCAR/TN-398+STR, 117 pp.

Grell G.A., Stefan E., Stockwell W.R., Schoenemeyer T., Forkel R., Michalakes J., Knoche R., Seidl W (2000) Application of a multiscale, coupled MM5/chemistry model to the complex terrain of the VOTALP valley campaign. *Atmos. Env.* Volume 34, Issue 9, 2000, Pages 1435-1453

Gyldenkaerne S., C.A. Skjoth, Hertel O., Ellerman T. (2005) A dynamical ammonia emission parameterization for use in air pollution models, *Journal of Geophysical Research* **110** (2005), p. D07108.

Hall G., Cratchley R. (2005a) Modelling frontal and convective rainfall distributions over North Wales. Proceedings of the 2005 WRF/MM5 User's Workshop, National Centre for Atmospheric Research, Boulder, Colorado.

Hanna S.R., Yang R (2000) Evaluations of Mesoscale Models' Simulations of Near-Surface Winds, Temperature Gradients, and Mixing Depths - Journal of Applied Meteorology pp. 1095–1104

Hayes P.S., Rasmussen A., Conway H. (2002) Estimating precipitation on the Central Cascades of Washington, Journal of Hydrometeorology, vol. **3** , no. 3: 335-346

Hertel O., Berkowicz R., Christensen J., Hov O.(1993) Test of two numerical schemes for use in atmospheric transport-chemistry models. *Atmos. Environ.* **27A**, 2591-2611.

Heuss J.M., Kahlbaum D.F., Wolff G.T. (2003) Weekday/weekend ozone differences: what can we learn from them?, *Journal of the Air and Waste Management Association* **53** (2003), pp. 772–788.

Holtslag A.A.M., Van Meijgaard E., de Rooij W.C. (1995) A Comparison of Boundary Layer Diffusion Schemes in Unstable Conditions over Land *Boundary-Layer Meteorol.* **76**: 69–95.

Hong S.Y., Pan H.L. (1996) Non local boundary layer vertical diffusion in a medium-range forecast model. *Mon. Weather. Rev*., **124:** 2322-2339.

Houyoux, M., Vukovich J. M, (1999) Updates to the Sparse Matrix Operator Kernel Emissions (SMOKE) Modeling System and Integration with Models-3. Presented at the Emission Inventory: Regional Strategies for the Future, 26-28 October, Raleigh, North Carolina (USA)

Houyoux, M., Vukovich J., Seppanen C, Brandmeyer J.E. (2002) SMOKE User Manual, Available at http://www.smoke-model.org/documentation.cfm

Hov Ø., Hjøllo B.A., Eliassen A. (1994) Transport distance of ammonia and ammonium in Northern Europe 1. Model description. *Journal of Geophysical Research* **99**, 18735–18748.

Huang H.-C., Chang J. S. (2001) On the performance of numerical solvers for a chemistry submodel in three-dimensional air quality models, Part1 Box-model simulations, *J. Geophy. Res*.**106**: No. D17, 20175-20188.

IPCC (2007), Fourth Assessment Report of the Intergovernmental Panel on Climate Change. Working Group I: the physical science basis of climate change. Summary for Policymakers. Available at http://ipcc-wg1.ucar.edu/wg1/

Jacobson M., Turco R.P. (1994) SMVGEAR: A Sparse-Matrix, vectorized Gear code for atmospheric models. *Atmos. Environ.***28**, 273-284

Jenkin M.E., Davies T.J., Stedman J.R. (2002) The origin and day-of-week dependence of photochemical ozone episodes in the UK. *Atmos. Envrion.* **36**, 999–1012

Jiménez, P., Parra R., Gassó S., Baldasano J.M. (2005) Modeling the ozone weekend effect in very complex terrains: a case study in the northeastern Iberian Peninsula. *Atmos. Environ.*, **39**: 429-444.

Joseph, J.H., Wiscombe W.J., and Weinman J.A. (1976) The delta-Eddington approximation for radiative flux transfer, *J. Atmos. Sci.*, **33**, 2452-2459.

Judson G., Janssen M. (2001) *EMS-2001* Presented at the 10th International Emission Inventory Conference "*One Atmosphere, One Inventory, Many Challenges*"May 1 - 3, 2001Denver, CO, April 30, 2001.

Kain J. S., Fritsch J.M. (1992) The role of the convective ''trigger function'' in numerical forecasts of mesoscale convective systems. *Meteor. Atmos. Phys.,* **49,** 93–106.

Kirchstetter T.W., Maser C.M., Brown. N.J. (2004) Ammonia Emission Inventory for the State of Wyoming. Final report prepared for Bureau of Land Management, Department of Interior, 2004. LBNL Report No. 54219.

Kitwiroon N. (2006). Treatment of surface boundary layer parameters for modelling air quality in urban regions. Ph.D. thesis, University of Hertfordshire, UK.

Kukkonen J., Pohjola M., Sokhi R.S., Luhana L., Kitwiroon N., Fragkou L., Rantamäki M., Berge E., Odegaard V., Slordal L.H., Denby B., Finardi S. (2005). Analysis and evaluation of selected local-scale PM_{10} air pollution episodes in four European cities: Helsinki, London, Milan and Oslo. *Atmos. Environ.* **39**: 2759-2773.

Kulmala, M., Laaksonen A., and Pirjola L. (1998) Parameterization for sulfuric acid/water nucleation rates. *J. Geophys. Res.* **103**, 8301-8307

Lamb R.G. (1983a) A regional scale (1000 km) Model of Photochemical Air Pollution, Part I: Theoretical Formulation. EPA 600/3-83-035, U.S. Environmental Protection Agency, Research Triangle Park, NC.

Lamb R.G. (1983b) A regional scale (1000 km) Model of Photochemical Air Pollution, Part II: Input Processor Network Design. EPA 600/3-84-085, U.S. Environmental Protection Agency, Research Triangle Park, NC.

Lawson D.R. (2003) Forum—the weekend ozone effect—the weekly ambient emissions control experiment. Environmental Management, 17–25 July.

Lebron F. (1975) A comparison of weekend-weekday ozone and hydrocarbon concentrations in the Baltimore–Washington metropolitan area. *Atmos. Environ*. **9**, 861–863.

Lee D.S., Kingdom R.D., Jenkin M.E., Garland J.A. (2000) Modelling the atmospheric oxidised and reduced nitrogen budgets for the UK with a Lagrangian multi-layer long-range transport model, *Environmental Modelling and Assessment* **5** (2000), pp. 83–104.

Lennard R. J., Griffiths S. J. (2005) Optimising the performance of Models-3 using MM5 input meteorological data. Joint Environmental Programme (JEP) report, 2005.

Ludwig E. L., Johnson W. B., Moon A. E., Mancuso R. L. (1970) A Practical Multipurpose Urban Diffusion Model for Carbon Monoxide', *Stanford Research Institute Report* Contract CAPA-3-68.

Madronich S. (1987) Photodissociation in the Atmosphere: 1. Actinic flux and the effects of ground reflections and clouds, *J. Geophys. Res.* **92 (D8)**: 9740-9752.

Maffeis G., Longoni M. G., Bossi E. (2002) Spatial, temporal and chemical disaggregation of Lombardy 1997 gas inventory, proceedings of Workshop of the CITY – DELTA European Modelling Exercise, June 24-25, 2002, at IIASA, Laxenburg, Austria.

Marr L.C., Harley R.A. (2002a) Spectral analysis of weekday-weekend differences in ambient ozone, nitrogen dioxide, and non-methane hydrocarbon time series in California, *Atmos. Environ.* **36** (2002), pp. 2327–2335

Metcalfe S.E., Whyatt J.D., Broughton R., Derwent R.G., Finnegan D., Hall J., Mineter M., O'Donoghue M., Sutton M.A. (2001) Developing the hull acid rain model: its validation and implications for policy makers, *Journal of Environmental Science and Policy* **4** (2001), pp. 25–37.

Metcalfe S.E., Whyatt J.D., Nicholson J.P.G., Derwent R.G., Heywood E. (2005) Issues in model validation: assessing the performance of a regional-scale acid deposition model using measured and modelled data *Atmos Env* (**39**), Issue 4, pp 587-598

Miao, J., Chen D., Wyser K., Borne K., Lindgren J., M. K. Svensson, Thorsson S., Achberger C., Almkvist E., (2007) Evaluation of MM5 mesoscale model at local scale for air quality applications over the Swedish west coast: Influence of PBL and LSM parameterizations, Meteorology and Atmospheric Physics (in press).

Middleton, P., Stockwell,W. R. and Carter W. P. L (1990) Aggregation and analysis of volatile organic compound emissions for regional modeling. *Atmos. Environ.*, **24A**, 1107-1133.

Mol-Dijkstra J.P., Kros H. (2001) Modelling effects of acid deposition and climate change on soil and run-off chemistry at Risdalsheia, Norway, *Hydrology and Earth System Sciences* **5** (2001): 487–498

Moller D., Schieferdecker H. (1989) Ammonia emission and deposition in the G.D.R. *Atmos. Environ.* **23** 1187-1193.

Monforti F., Pederzoli A. (2004) THOSCANE: a tool to detail CORINAIR emission inventories, Environmental Modelling & Software**,** Volume 20, Issue 5, May 2005, Pages 505-508

Morris R.E., Myers T.C. (1990) User's guide for the Urban Airshed Model. Vol.I: Users manual for UAM (CB-IV). EPA-450/4-90-007A. US Environmental Protection Agency, Research Triangle Park, NC.

NEGTAP (2001) Transboundary air pollution: acidification, eutrophication and ground level Ozone in the UK. Prepared by the National Expert Group on Transboundary Air Pollution, on behalf of the Department for Environment, Food and Rural Affairs (DEFRA).

New M., Hulme M., Jones P.D. (1999) Representing twentieth century space-time climate variability. Part 1: development of a 1961–90 mean monthly terrestrial climatology. Journal of Climate 12, 829–856

New M., Hulme M, Jones P.D. (2000) Representing twentieth century space-time climate variability. Part 2: development of 1901–96 monthly grids of terrestrial surface climate. Journal of Climate 13, 2217-2238

Nowak J.B., Huey L.G., Russell A.G., Neuman J. A., Orsini D., Sjostedt S.J., Sullivan A.P., Tanner D.J., Weber R.J., Nenes A., Edgerton E., Fehsenfeld F.C. (2006) Analysis of Urban Gas-phase Ammonia Measurements from the 2002 Atlanta

Aerosol Nucleation and Real-time Characterization Experiment (ANARChE), *J.Geoph.Res.*, **111**, D17308, doi:10.1029/2006JD007113.

Novak, J., Young J., Byun D.W., Coats C., Walter G., Benjey W., Gipson G., LeDuc S. (1998) Models-3: A unifying framework for environmental modeling and assessments. Preprint Volume, 10th Joint AMS and A&WMA Conference on the Applications of Air Pollution Meteorology, Phoenix, AZ, Jan 11-16, 1998: 259-263.

Otte T. L.**,** Byun D. W., Ching J. K. S. (1999) Developing meteorological fields. Science Algorithms of the EPA Models-3 Community Multiscale Air Quality (CMAQ) Modeling System., Eds. EPA-600/R-99/030, March 1999, 3-1 – 3-17.

Pandis S. N., Harley R. A., Cass G. R. and Seinfeld J. H (1992) Secondary aerosol formation and transport. *Atmos. Environ.* **26A**, 2,269-2,282.

Parra R (2004). Development of the EMICAT 2000 Model for the Estimation of air Pollutants Emissions in Catalonia and Its Use in Photochemical Dispersion Models. Ph.D. Dissertation (in Spanish), Polytechnic University of Catalonia, Catalonia, Spain, July 2004. Available at http://www.tdx.cesca.es/TDX-0803104–102139

Parrish D. D. (2005) Critical evaluation of US on-road vehicle emission inventories. *Atmos. Environ*., **40**: 2288-2300

Perry M.C., Hollis D.M. (2005) The generation of monthly gridded datasets for a range of climatic variables over the UK. International Journal of Climatology, 25, 1,041-1,054.

Phillips N. A. (1957) A coordinate system having some special advantages for numerical forecasting. Journal of the Atmospheric Sciences **14, pp.** 184–185

Phillips S.B., Arya S., Aneja V.P. (2004) Measurement and modelling of Ammonia flux and deposition velocity over natural surfaces in eastern North Carolina. 13th

Joint Conference on the Application of Air Pollution Meteorology with the Air and Waste Management Association (A&WMA), Vancouver, British Columbia, Canada, 23-27 August 2004.

Pinder R. W., Pekney N.J., Davidson C.I., Adams P.J.. (2004). A process-based model of ammonia emissions from dairy cows: improved temporal and spatial resolution. *Atmos. Environ.* **38 (9)**:1357-1365.

Pleim J.E., Chang J.S. (1992) A non-local closure model in the convective boundary layer. *Atm Environ.*, **26A**: 965-981.

Pleim, J. E., Clarke J. F., Finkelstein P.L., Cooter E. J., Ellestad T. G, Xiu A., Angevine W.M. (1996) Comparison of measured and modeled surface fluxes of heat, moisture and chemical dry deposition. *Air Pollution Modeling and Its Application XI*, Gryning and Schiermeier, Eds, Plenum Press, New York.

Pun B.K., Seigneur C., White W. (2003) Day-of-week behaviour of atmospheric ozone in three US cities. Journal of the Air and Waste Management Association 53, 789–801.

Rakesh V., Pal P.K., Joshi P.C. (2006) Quantitative evaluation of PSU-NCAR MM5 forecasts over Indian region during monsoon 1998. *The international society for optical engineering, 2006*

Rantamaki, M., Pohjola, Ødegaard V., M., Kukkonen, J., Karppinen, A., Berge E. (2004) Evaluation of various versions of HIRLAM and MM5 models against meteorological data during a wintertime air pollution episode in Helsinki. Proceedings from the 9th Int. Conf. on Harmonisation within Atmospheric Dispersion Modelling for Regulatory Purposes, Garmish 2004

Roselle S. J., Binkowski F.S. (1999), Cloud dynamics and chemistry, Science documentation of the Community Multi-Scale air quality System EPA/600/R-99/030 Chapter 11

Sanderson M. G., Collins W. J., Johnson C. E., Derwent R. G. (2006) Present and future acid deposition to ecosystems: The effect of climate change, *Atmos. Environ.* **40** (2006): 1275–1283.

Sandu, A., Verwer J. G., Blom J. G., Spee E. J., Carmichael G. R., and Potra F. A.(1997) Benchmarking stiff ODE solvers for atmospheric chemistry problems II: Rosenbrock solvers Atmos. Environ.**31**, 3459-3472.

Schell B., Ackermann I.J., Hass H., Ebel A. (1998b) Modelling secondary organic aerosol with MADE: a 3D application to study the formation, transport, and impact on aerosol properties, *Abstracts of the 17th Annual AAAR Conference,*, Cincinnati, OH, pp.220.

Seinfeld J. H. and Pandis S. N. (1998) Atmospheric Chemistry and Physics: From Air Pollution to Climate Change, J. Wiley&Sons, New York.

Seinfeld, J. H. (1986) Atmospheric Chemistry and Physics of Air Pollution, Wiley, New York, 1986.

Seppanen C. (2005) Recent Updates to the SMOKE Modeling System, 4th Annual CMAS Models-3 Users's Conference, Chapel Hill, NC, September 26-28, 2005.

Shafran P.C., Seaman N.L., Gayno G.A. (2000) Evaluation of Numerical Predictions of Boundary Layer Structure during the Lake Michigan Ozone - Journal of Applied Meteorology Volume **39** pp. 412–426

Singles R.J., (1996) Fine resolution modelling of ammonia dry deposition over Great Britain. PhD thesis, University of Edinburgh.

Singles, R.J., Sutton, M.A., Weston, K.J., (1998) A multi-layer model to describe the atmospheric transport and deposition of ammonia in Great Britain. Atmos Environ **32(3)**, (Ammonia Special Issue): 393–399.

Smith R.I., Fowler D. (2001) Uncertainty in wet deposition of sulphur, *Water, Air and Soil Pollution: Focus* **1**, pp. 341–354.

Smith R.I., Fowler D., Sutton M.A., Flechard C., Coyle M. (2000) Regional estimation of pollutant gas deposition in the UK: model description, sensitivity analyses and outputs, *Atmos. Environ.* **34**, pp. 3757–3777.

Smith, R.I., Fowler, D., Sutton, M.A., Cape, J.N., Nemitz, E., Coyle, M., Muller, J. (2004) Acid Deposition Processes. Final Report to the Department for Environment, Food and Rural Affairs, Rep. No. EPG 1/3/166. Centre for Ecology and Hydrology, Edinburgh.

Sokhi R.S, San José R., Kitwiroon N., Fragkou E., Pérez J.L., Middleton D R (2006) Prediction of ozone levels in London using the MM5-CMAQ modelling system. Environmental Modelling and Software Journal, **21(4)**, pp 566-576.

Spencer P.L., Stensrud D.J. (1998) Simulating flash flood events: Importance of the sub-grid representation of convection. *Mon. Wea. Rev.*, **126**, 2884-2912.

Stauffer, D. R., Seaman N. L. (1990) Use of four-dimensional data assimilation in a limitedarea forecast model. Part I: Experiments with synoptic-scale data. *Mon. Wea. Rev.*,**118**, 1250–1277.

Stauffer, D. R., Seaman N. L., Binkowski F. S. (1991) Use of four-dimensional data assimilation in a limited-area mesoscale model. Part II: Effects of data assimilation within the planetary boundary layer. *Mon. Wea. Rev.*, **119**, 734–754.

Stella G. (2002) Temporal Allocation of Annual Emissions Using EMCH Temporal Profiles Available at http://www.epa.gov/ttn/chief/emch/temporal

Stensrud D.J., Fritsch J.M. (1994b) Mesoscale convective systems in weakly forced large-scale environments. Part III: Numerical simulations and implications for operational forecasting. *Mon. Wea. Rev.*, **122**, 2084-2104.

Stephens G.L. (1978) Radiation profiles in extended water clouds. II.: Parameterization schemes, *J. Atmos. Sci.* **35**: 2123-2132.

Stevenson D. S., Johnson C.E., Collins W.J., Derwent R.G. (1998) Intercomparison and evaluation of atmospheric transport in a Lagrangian model (STOCHEM) and an Eulerian model (UM) using ^{222}Rn as a short-lived tracer, *Quarterly Journal of the Royal Meteorological Society,* **124**, 2477–2491.

Stevenson D.S., Dentener F. and 39 others (2006) Multi-model ensemble simulations of present-day and near-future tropospheric ozone, *J. Geophys. Res.*, 111, D08301, doi:10.1029/2005JD006338

Stevenson D.S., Doherty R.M., Sanderson M.G., Collins W.J., Johnson C.E., Derwent R.G. (2004) Radiative forcing from aircraft NO_x emissions: mechanisms and seasonal dependence, *J. Geophys. Res*. 109, D17307

Stevenson D.S., Doherty R.M., Sanderson M.G., Johnson C.E., Collins W.J., Derwent R.G. (2005) Impacts of climate change and variability on tropospheric ozone and its precursors, *Faraday Discuss.,* 130, 41-57, DOI:10.1039/b417412g

Stevenson D.S., Johnson C.E., Collins W.J., Derwent R.G. (1998) Intercomparison and evaluation of atmospheric transport in a Lagrangian model (STOCHEM) and an Eulerian model (UM) using ^{222}Rn as a short-lived tracer, *Quarterly Journal of the Royal Meteorological Society,* **124**, 2477–2491.

Stockwell W. R., Middleton P. and Chang J. S. (1990) The second generation regional acid deposition model chemical mechanism for regional air quality modeling. *J. geophys. Res.* **95** (d10), 16,343-16,367.

Stockwell W.R. (1986) A homogeneous gas phase mechanism for use in a regional acid deposition model. *Atmos. Environ.*, **20**, 1,615-1,632.

Sutton M.A., Fowler D., Moncrieff J.B. (1993a) The exchange of atmospheric ammonia with vegetated surfaces. I: Unfertilized vegetation. *Quarterly Journal of the Royal Meteorological Society,* **119**, 1023–1045.

Sutton M.A., Miners B., Tang Y.S., Milford C., Wyers G.P., Duyzer J.H., Fowler D. (2001) Comparison of low-cost measurement techniques for long-term monitoring of atmospheric ammonia. J. Environ. Monit. **3**, 446-453.

Sutton M.A., Schjørring J.K., Wyers G.P. (1995b) Plant-atmosphere exchange of ammonia Phil. Trans. Roy. Soc., London. Series A.**351**, 261–278.

Sutton, M.A., Pitcairn C.E.R., Fowler, D. (1993b) The exchange of ammonia between the atmosphere and plant communities. *Adv. Ecol. Research.***24**, 301–393.

Symeonidis P., Ziomas I., Proyou A. (2004) Development of an emission inventory system from transport in Greece, Environmental Modelling & Software Volume 19, Issue 4, April 2004, Pages 413-421

Tang Y.S., Cape J.N., Sutton M.A. (2001) Development and types of passive samplers for monitoring atmospheric NO_2 and NH_3 concentrations. *The Scientific World*, 1, 513-529

Tarrasòn L., Schaug J. (1999) Transboundary acid deposition in Europe, EMEP report 1/1999, EMEP –CCC/MSC-W

Taylor K.E. (2001) Summarizing multiple aspects of model performance in a single diagram Journal of geophysical research. **106**, no D7: 7183-7192

The US EPA Draft Visibility Monitoring Guidance Document (1999) available at http://www.epa.gov/ttn/amtic/files/ambient/visible/r-99-003.pdf

Tonse S. R. (2006) A timing and scalability analysis of the parallel performance of cmaq v4.5 on a beowulf linux cluster, Abstract from the 5th Annual CMAS Conference October 16-18, 2006 Chapel Hill, NC

Toon O.B., Mckay C.P., and Ackerman T.P. (1989) Rapid calculation of radiative heating rates and photodissociation rates in inhomogeneous multiple scattering atmospheres, *J. Geophys. Res.* **94**, 16287-16301.

Troen I., Mahrt L. (1986) A simple model of the atmospheric boundary layer: Sensitivity to surface evaporation. *Boundary-Layer Meteorol.* **37**:129-148

UN 1994. Protocol to the 1979 Convention on Long-range Transboundary Air Pollution on Further Reductions of Sulphur Emissions. Oslo: United Stations. 32 p.

UN/ECE: 1999. Protocol to the 1979 Convention on Long-Range Transboundary Air Pollution to Abate Acidification, Eutrophication and Ground-level Ozone. United Nations Economic Commission for Europe, Geneva, Switzerland.

United Kingdom Review Group of Acid Rain (1990). Acid deposition in the United Kingdom 1986-1988, 3rd report

Vallack H., Rypdal K. (2007) The Global Atmospheric Pollution Forum Air Pollutant Emissions Inventory Manual Version 1.3. Available at www.sei.se/editable/pages/sections/**atmospheric/Forum_emissions_manual_v1.3**.doc

Venkatram A., Karamchandani P.K., Misra P.K. (1988) Testing a comprehensive acid deposition model. *Atmos. Environ*. **22**:737–747.

Vieno M. (2005). The use of an atmospheric chemistry-transport model (FRAME) over the UK and the development of its numerical and physical schemes. PhD thesis, University of Edinburgh

Vieno M., Dore A.J., Wind P., Tarrason L., Sutton M. (2007) Application of the EMEP model to the UK with a resolution of 5 km^2 grid – EMEP4UK. Final project report to the Department for Environment, Food and Rural Affairs.

Vieno M., Wind P., Weston K.J., Dore A.J., Tarrason L., Sutton M. (2006) Fine scale application of the EMEP Unified Air Pollution model to the United Kingdom. Proceedings of the 10th International Conference on Harmonisation within Atmospheric Dispersion Modelling for Regulatory Purposes

Vijayaraghavan K., Hu J., Zhang Y., Liu X., Chance K., Snell H.E. (2006) Evaluation of CMAQ using Satellite Remote Sensing Measurement, CMAS Conference, Oct 16-18, 2006. Chapel Hill, NC

Walcek, C.J. and Taylor G.R. (1986) A theoretical method for computing vertical distributions of acidity and sulfate production within cumulus clouds, *J. Atmos. Sci* **43**, 339-355.

Weber R.J., Marti J.J., McMurry P.H., Eisele F.L., Tanner D.J., Jefferson A., Measurements of new particle formation and ultrafine partilce growth rates at a clean continental site. *J. Geophys. Res.*,102, 4375-4385, 1997.

Wesely, M. L. (1989) Parameterization of surface resistances to gaseous dry deposition in regional-scale numerical models, *Atmos.Environ.*, **23**, 1293-1304.

Whitby, K. T. (1978) The physical characteristics of sulfur aerosols, *Atmos. Environ.*, **12**, 135-159

Whitby, E. R., McMurry P. H., Shankar U., and Binkowski F. S. (1991) Modal Aerosol Dynamics Modeling, Rep. 600/3-91/020, Atmospheric Research and Exposure Assessment Laboratory, U.S. Environmental Protection Agency, Research Triangle Park, N.C., (NTIS PB91- 161729/AS).

Wu, S.-Y., S. Krishnan, J.-L. Hu, C. Misenis, Y. Zhang, V. P. Aneja, and R. Mathur, (2005) Simulating the Atmospheric Fate of Ammonia in Southeast U.S. using CMAQ with a 4-km Resolution, *Proceedings of the 2005 Models-3 Workshop*, September 26-28, Chapel Hill , NC , 5 pages.

Yang M.J., Tung Q.C. (2003) Evaluation of Rainfall Forecasts over Taiwan by Four Cumulus Parameterization Schemes. **Journal of the Meteorological Society of Japan,** Vol. 81, No. 5 pp.1163-1183

Yu S., Eder B.K., Dennis R., Chu S.H., Schwartz S. (2006) New unbiased symmetric metrics for evaluation of air quality models. Atmospheric Science Letters, accepted for publication.

Zhang M., Uno I., Zhang R., Han Z., Wang Z., Pu Y. (2006) Evaluation of the Models-3 Community Multi-scale Air Quality (CMAQ) modeling system with observations obtained during the TRACE-P experiment: Comparison of ozone and its related species. *Atmos. Environ.* **40:** 4874-4882

Zilitinkevich S. S. (1989) Velocity profiles, the resistance law and the dissipation rate of mean flow kinetic energy in a neutrally and stably stratified planetary boundary layer. *Bound. Layer Met.*, **46**, 367-387.